The Role of the Hendra Virus and Nipah Virus Attachment Glycoproteins in Receptor

Binding and Antibody Neutralization

by

Deborah Lynn Fusco

Dissertation submitted to the Faculty of the
Emerging Infectious Diseases Graduate Program
Uniformed Services University of the Health Sciences
In partial fulfillment of the requirements for the degree of
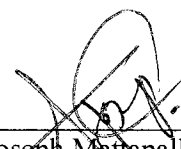Doctor of Philosophy 2014

DISSERTATION APPROVAL FOR THE DEGREE OF DOCTOR OF PHILOSOPHY IN THE EMERGING INFECTIOUS DISEASES GRADUATE PROGRAM

Title of Dissertation: "The Role of Hedra and Nipah Virus Attachment Glycoproteins in Receptor Binding and Antibody Neutralization"

Name of Candidate: Deborah Fusco
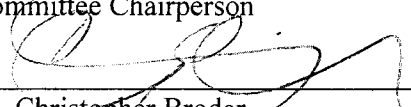Doctor of Philosophy Degree
January 31, 2014

DISSERTATION AND ABSTRACT APPROVED:

DATE:

_____   1/31/14
Dr. Joseph Mattapallil
DEPARTMENT OF MICROBIOLOGY AND IMMUNOLOGY
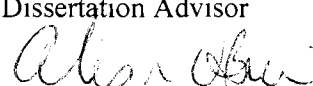Committee Chairperson

_____   1/21/2014
Dr. Christopher Broder
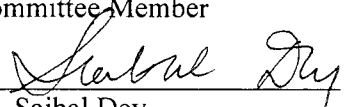DEPARTMENT OF MICROBIOLOGY AND IMMUNOLOGY
Dissertation Advisor
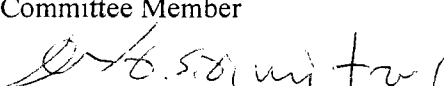
_____   1/31/2014
Dr. Alison O'Brien
DEPARTMENT OF Microbiology & Immunology
Committee Member

_____   1/31/2014
Dr. Saibal Dey
DEPARTMENT OF BIOCHEMISTRY AND MOLECULAR BIOLOGY
Committee Member

_____   1/31 2014
Dr. Dimiter Dimitrov
CCRNP SENIOR INVESTIGATOR, NCI – NATIONAL INSTITUTES OF HEALTH
Committee Member

PREFACE

Portions of this manuscript have been published as:

Steffen DL, Xu K, Nikolov DB, Broder CC. 2012. Henipavirus mediated membrane fusion, virus entry and targeted therapeutics. *Viruses* 4:280-308.

and

Bossart KN, **Fusco DL**, Broder CC. 2013. Paramyxovirus entry. *Advances in experimental medicine and biology* 790:95-127.

and

Xu K, Rockx B, Xie Y, Debuysscher BL, **Fusco DL**, et al. 2013. Crystal structure of the hendra virus attachment G glycoprotein bound to a potent cross-reactive neutralizing human monoclonal antibody. *PLoS pathogens* 9:e1003684.

ACKNOWLEDGMENTS

DEDICATION

To my Mom and Dad, who envisioned me attaining this degree long before I did and provided the love, support and encouragement I needed to achieve it.

To my husband Tony, who patiently stood by me through all the ups and downs of research. I can't thank you enough for all your love and understanding as you listened, learned and believed in me throughout this process.

To my Grandma Kehoe and Uncle Dave, who watched me begin this program, proudly supported me through it and knew I would succeed, even though they didn't get to see it.

COPYRIGHT STATEMENT

ABSTRACT

The Role of the Hendra Virus and Nipah Virus Attachment Glycoproteins in Receptor Binding and Antibody Neutralization:

Deborah Lynn Fusco, Doctor of Philosophy, 2014

Thesis directed by: Dr. Christopher C. Broder, Professor and Director of the Emerging Infectious Diseases Graduate Program

Recently identified as members of the family *Paramyxoviridae*, Hendra virus (HeV) and Nipah virus (NiV) are newly emerged agents capable of causing severe respiratory and encephalitic illness with high mortality in both animals and humans. Both viruses infect cells using a highly conserved attachment glycoprotein (G) that engages host cellular receptors ephrin-B2 or ephrin-B3 and a fusion glycoprotein (F) that mediates membrane merger. Passive immunization with the henipavirus G glycoprotein-specific human monoclonal antibody m102.4 has been shown to neutralize HeV and NiV infection. Recent findings have revealed that both receptors and m102.4 bind the same ectodomain of G. In order to improve the efficacy of m102.4 we constructed variants of m102.4 in which the binding residues were replaced with the corresponding residues of ephrin-B2/B3. Using soluble, tetrameric forms of HeV/NiV-G (wt-G) and m102.4 escape mutants of G (esc-G), which were generated *in vitro*, m102.4 variants were tested for their ability to bind G, block G-receptor interaction and inhibit cell-cell fusion. Variants with a single mutation bound G,

inhibited G-receptor interactions and decreased cell-cell fusion better than multiple mutation variants, but none of the variants were able to bind or inhibit interactions and fusion at the level of m102.4, indicating that manipulation of m102.4 to resemble receptors decreases the potency of m102.4 neutralization. Additionally m102.4 and m102.4 variants were able to bind G-escape variants (esc-G) but had little effect on inhibiting fusion mediated by these esc-Gs, suggesting that m102.4 neutralization does not solely rely on blocking G-receptor binding. New escape variants of HeV/NiV were generated using m102.4 variants and resulted in the same or similar mutations as were seen previously. The HeV and NiV esc-Gs were also used to further characterize m102.4-G interactions in order to determine the mechanism of m102.4 neutralization. Due to the oligomeric nature of G, we hypothesize that m102.4 potentially uses two neutralization mechanisms – blocking G-receptor engagement and inhibition of receptor-induced conformational change in G. Competition binding assays revealed that HeV wt-G, NiV wt-G and NiV esc-G were able to simultaneously bind receptor and m102.4, whereas HeV esc-G only bound receptor. Additionally, m102.4 bound to G could be displaced by ephrin-B2 on the esc-G mutants but not wt-G, whereas bound ephrin-B2 inhibited binding of m102.4 to esc-G but not wt-G. We also demonstrated an increased G-F association in the presence of receptor which did not occur in the presence of m102.4, implying m102.4 may inhibit conformational changes in G required for F association presumed to lead to fusion triggering. These studies provide novel insight on the mechanisms of antibody neutralization of HeV and NiV and further our understanding of the steps required for henipavirus fusion.

TABLE OF CONTENTS

LIST OF TABLES

LIST OF FIGURES

List of Abbreviations

Co-IP – co-immunoprecipitation

HeV – Hendra virus

HeV-F – fusion glycoprotein of Hendra

HeV-G – attachment glycoprotein of HeV

HeV-sG – soluble HeV-G

HeV-G-D582N – m102.4 escape variant of HeV-G

IP – immunoprecipitation

NiV – Nipah virus

NiV-F – fusion glycoprotein of Nipah

NiV-G – attachment glycoprotein of NiV

NiV-sG – soluble NiV-G

NiV-G-V507I – m102.4 escape variant of NiV-G

SPR – surface Plasmon resonance

Tet-HeV-sG – soluble, tetrameric HeV-G

Tet-NiV-sG – soluble, tetrameric NiV-G

Tet-HeV/NiV-sGs – Tet-HeV-sG and Tet-NiV-sG

Tet-D582N-sG – soluble, tetrameric HeV-G-D582N

Tet-V507I-sG – soluble, tetrameric NiV-G-V507I

Tet-D582N/V507I-sGs – Tet-D582N-sG and Tet-V507I-sG

Tet-sGs – Tet-HeV-sG, Tet-NiV-sG, Tet-D582N-sG and Tet-V507I-sG

Tri-HeV-sF – soluble, trimeric HeV-F

Tri-NiV-sF – soluble, trimeric NiV-F

Tri-sFs – Tri-HeV-sF and Tri-NiV-sF

CHAPTER 1: Introduction

PARAMYXOVIRUSES

Paramyxoviruses, belonging to the order *Monengavirale*, are enveloped, non-segmented negative-stranded RNA viruses that include a number of important human (measles (MeV), mumps, human parainfluenza and respiratory syncytial virus (RSV)) and animal (canine distemper virus (CDV), Newcastle disease virus (NDV), rinderpest and parainfluenza virus type 5 (PIV5)) viruses. Virions, while generally spherical in shape, are classified as pleomorphic with nucleocapsids surrounded by a cell-derived lipid envelope and a genome size ranging from 13,280 nucleotides (human metapneumovirus) to 19,212 nucleotides (Beilong virus) (86). Viruses encode six essential proteins: nucleocapsid (N), phosphoprotein (P), matrix (M), fusion (F), attachment (HN/H/G) and large polymerase (L) (86).

Subfamilies – *Paramyxovirinae* and *Pneumovirinae*

Based on several distinguishing characteristics, including transcriptional elements, genome size and amino acid sequence, paramyxoviruses are classified into two subfamilies – *Paramyxovirinae* and *Pneumovirinae* (86; 96).

Genera in the subfamily *Paramyxovirinae* include *Rubulavirus* (mumps and parainfluenza viruses), *Avulavirus* (NDV), *Respirovirus* (Sendai virus), *Henipavirus* (Hendra (HeV) and Nipah (NiV)) and *Morbillivirus* (MeV). These genera are divided based on antigenic cross-reactivity and the presence or absence of neuraminidase activity on the attachment glycoprotein (96). These viruses encode 6-7 transcriptional elements that express 7-10 proteins and have a genome length that is a multiple of six (known as

the "rule of 6") (86; 96). *Henipavirus*, the newest genus in this subfamily, contains HeV and NiV as well as the recently emerged, non-pathogenic Cedar virus (113; 193).

The subfamily *Penumovirinae* contains 2 genera – *Pneumovirus* (RSV) and *Metapneumovirus* (metapneumovirus). These viruses encode 8-10 transcriptional units that express 9-11 proteins and do not follow the "rule of 6" as seen with the subfamily *paramyxovirinae*. These viruses encode and express an additional nucleocapsid-associated protein called M2-1 and an RNA regulatory and immune suppressant protein, M2-2 (86; 160). Also in contrast to viruses in *Paramyxovirinae*, *Pneumovirinae* viruses only encode one open reading frame (ORF) in the P gene (discussed below).

In addition to the viruses in these two subfamilies, there are a number of paramyxoviruses that have not yet been classified. Some of these viruses are J-virus, Beilong virus and Mossman virus.

Viral proteins

The complete RNA genome consists of 6-10 genes flanked by a 3' extracistronic leader sequence (~50 nucleotides) and a 5' extracistronic trailer sequence (50-161 nucleotides) that are critical for transcription and replication. Each gene is flanked by transcriptional control sequences and intergenic regions that contain 1-56 nucleotides (96). Gene transcription occurs in a gradient manner as genes closer to the 3' end are transcribed in more abundance than proteins at the 5' end due to failure of the RNA polymerase to reinitiate transcription at downstream genes (96). The majority of paramyxoviruses have three non-structural proteins – N, P and L – and three structural proteins – M, F and either a hemagglutinin-neruaminidase (HN), hemagglutinin (H) or attachment (G) glycoprotein.

Non-Structural proteins

N and P are typically the first and second gene in the genome (3' – 5') and are transcribed in great abundance in comparison to L, which is the 5' gene and is transcribed in low amounts (95). The combined binding of RNA genome, N, P and L form the riconucleoprotein (RNP) or nucleocapsid core (reviewed in (67)). The N, or nucleocapsid protein, is approximately 500 amino acids and is responsible for binding the RNA genome, forming a protective helical structure that also serves as the template for RNA synthesis. Interestingly, one nucleoprotein binds six nucleotides, explaining why the genome of paramyxoviruses needs to be a multiple of six (31; 32; 175). While the N-terminus of N is responsible for binding the RNA genome, the C-terminus binds the L-P transcription complex (30; 87).

While most paramyxovirus genes express a single protein, due to RNA editing and multiple open reading frames (ORFs) the phosphoprotein (P) gene expresses 3-7 different proteins (P, V, W, I, D, Y and C). A straight transcriptional read-through of the P gene by the RNA polymerase results in expression of the phosphoprotein, but transcriptional insertion of one or two G residues at a specific insertion site leads to the expression of V and W/I/D proteins, respectively (96; 104). The only exception to this occurs among rubulaviruses in which straight transcriptional read-through of the P gene results in expression of the V protein, and one or two G insertions results in the expression of W/I and P proteins, respectively.

The phosphoprotein is responsible for associating with L to form the RNA-dependent RNA polymerase (homotetramer of P with a single L protein). Additionally, it serves to anchor the nucleocapsid and L proteins, making it essential for RNA synthesis

(46). Expressed through transcriptional insertion of G residues, the V and W/I/D proteins share the same N-terminus end as the P protein but have different C-terminal tails. Involved in viral pathogenesis, V has been shown to inhibit cellular anti-viral responses, such as type I interferon pathway, and negatively regulate RNA synthesis (76; 82; 102; 147). The W/I/D proteins are expressed with the addition of two G nucleotides during transcription, and while W inhibits the immune response, it remains unclear how I and D proteins affect viral pathogenesis. C proteins are expressed using an alternative translation initiation codon in the P gene and have multiple functions during viral pathogenesis, including control of viral synthesis, inhibition of anti-viral measures and facilitation of viral release from infected cells (45; 83; 92; 111; 171).

Expressed in low amounts, L contains the catalytic activity of the RNP complex, having all the necessary enzymatic activities required to create fully functional mRNA (5' capping and 3' polyadenylation) (96). L is also involved in the replication of viral genomic and anti-genomic RNA.

Structural proteins

All paramyxoviruses express three main structural proteins – M, F and HN/H/G. The matrix protein, M, is the most abundant protein in the virion and lies just underneath the lipid bilayer membrane. It has been suggested that M associates with the cytoplasmic tails of the fusion and attachment glycoproteins and that self-association and association with the nucleocapsid is the driving force for formation of new virions (164-166).

The F and attachment (HN/H/G) glycoproteins are the two main surface glycoproteins expressed by all paramyxoviruses. The fusion glycoprotein is activated via interactions with the attachment glycoprotein and mediates the merger of the viral and

5

cellular membranes through a class I fusion mechanism. The attachment glycoprotein binds the cellular receptor and activates the fusion glycoprotein. Three different types of attachment glycoproteins exist among paramyxoviruses and are classified based on their hemagglutinin and neuraminidase abilities. As the fusion and attachment glycoproteins are critical for cellular infection they will both be discussed in greater detail below.

In addition to the three structural proteins discussed above, some viruses encode additional structural glycoproteins. Rubulaviruses and pneumoviruses express an additional type II membrane protein called SH (small hydrophobic glycoprotein) that is believed to prevent virus-induced apoptosis by decreasing levels of TNF-α (53; 71; 101). J-virus and Beilong virus also express a TM protein, which is a glycosylated type II integral membrane protein with an as yet unknown function (80; 101).

Viral Replication and Tissue Tropism

All paramyxoviruses bind to cell-surface receptors, fuse with the cellular membrane at neutral pH and replicate in the cytoplasm of the cell using virion encoded RNA-dependent RNA polymerase (P and L). Following receptor binding and fusion with the cellular membrane, the M protein shell is disassembled, allowing primary transcription to occur. When the viral proteins, particularly N, are expressed at high enough levels, viral transcription switches to viral replication and the production of anti-genome, which in turn is replicated into genome (reviewed in (96)).

Viral proteins HN/H/G and F are expressed and processed, eventually clustering on the cellular membrane, most likely in lipid rafts. Assembly and budding of new virions occurs at the envelope and is dependent upon M, which interacts with the cytoplasmic tails of the viral surface glycoproteins as well as the nucleoprotein core (156;

6

167; 168). Additional N, P and L proteins are included in the new virion, and the virion

buds from the cellular membrane, expressing HN/H/G and F on the membrane surface.

Henipavirus antigen has been identified in arterial endothelial cells, neurons,

smooth muscle cells and some epithelial cells (12; 132). The formation of giant syncytia,

multi-nucleated cells, is a hallmark feature of paramyxovirus infection, and these cells

can be found in the blood vessels of HeV/NiV infected humans (201). While HeV/NiV

can affect a majority of organs, the brain, lung, heart and kidney are most susceptible to

HeV/NiV-mediated pathology (38; 202).

EMERGENCE OF HENIPAVIRUSES

The first reported outbreak of HeV occurred in Queensland, Australia in 1994 as

an equine respiratory disease (126; 169). The disease quickly spread, ultimately infecting

20 horses, 14 of which died of the infection and 6 were euthanized. During this outbreak,

two individuals who had close contact with infected horses also developed an influenza-

like illness (ILI) - respiratory distress, myalgia and fever - that ultimately resulted in the

death of one individual. Comparison of viral genetic material isolated from the deceased

individual and one of the infected horses verified that both the horses and humans were

infected with the same virus. Sequencing of the M protein revealed 50% homology to

morbilliviruses, and therefore the virus was given the name equine morbillivirus (126). It

was quickly determined, however, that the isolated virus was not a morbillivirus as it was

not neutralized by anti-morbillivirus serum, had surface glycoproteins of two different

lengths and had low sequence homology with known morbilliviruses (79; 127; 192). The

virus was then renamed Hendra virus after the suburb in Australia where the first reported

case originated.

In reality the first case of Hendra virus infection occurred a month before the 1994 Hendra outbreak. In this case a male was exposed and infected with Hendra virus after treating a horse with a respiratory illness. The man developed acute encephalitis from which he recovered only to succumb 13 months later when it recurred (137). This case along with further equine outbreaks revealed that HeV is capable of presenting as either a respiratory and/or neurological disease in humans and equines (148).

Outbreaks of HeV were rare until 2004 when they started to become an annual occurrence between the months of May and October (178). Most of these outbreaks were isolated and involved a small number of equines with rarely any human involvement. However, in the summer of 2011 18 separate outbreaks were reported, which resulted in 22 equine cases, monitoring of approximately 70 individuals at risk for HeV infection and the first occurrence of a natural canine infection (6; 7). Since the emergence of HeV there have been a total of 86 horse fatalities, 2 canine infections and 7 human infections of which 4 were fatal.

The first outbreak of Nipah virus (NiV) occurred in Malaysia in 1998-1999 among abbatoir workers. The total case fatality rate was approximately 40% (265 infections), and over 1 million pigs were culled in an attempt to contain the spread of the virus (37; 38). Infection was characterized by an ILI that quickly progressed into neurological symptoms that were often recurring. Since the initial outbreak, the virus has not reemerged in Malaysia but has spread to southern Asia, causing outbreaks in India and Bangladesh. Yearly outbreaks have occurred in Bangladesh since 2001, routinely occurring along what is now known as the "Nipah belt" (51; 61; 66; 78). Strikingly, the Bangladesh strain of Nipah virus has more respiratory involvement then Nipah-Malaysia

and is also more lethal with case fatalities ranging from 75-100% (77). Since 2001 there have been a total of 290 infections in Bangladesh and India with 211 fatalities.

Bat reservoir and Transmission

Following the initial HeV outbreak, 46 animal species were screened in an attempt to determine the reservoir for HeV. Isolation of HeV antibodies in frugivorous bats quickly led to the identification of Pteropus bats (flying foxes) as the natural reservoir for both HeV and NiV (39; 63; 212; 214). To date HeV transmission to humans has only been observed through the intermediate equine host, and it is believed that transmission from bats to equines occurs via contaminated fruit and water (199). Halpin *et al.* determined that bat excretion of HeV is extremely low, which accounts for the sporadic outbreaks of HeV (62). However, during the summer of 2011, the high number of spillover events was accredited to environmental stressors that increased the number of HeV-excreting bats (10% to 60%) (7).

Similar to HeV transmission, NiV was originally transmitted from bats to humans via an intermediate host (pigs) during the Malaysian outbreak (reviewed in (40)). Since the initial outbreak the mode of NiV transmission in Bangladesh has expanded to include direct bat-human and human-human spread (60; 78; 108). The transmission of NiV from bat-to-human is thought to occur through indirect methods, and consumption of NiV-contaminated raw date palm sap is a leading factor (109; 124). NiV spillover from bats to humans via date palm sap occurs during the collection period, when open containers are left uncovered overnight in trees, and bats have been observed contaminating these collection pots with bodily fluids, shedding the virus into the sap (85). Consumption of the raw sap can then result in NiV infection.

The ability of NiV to transmit directly from human-to-human is believed to occur through contact with contaminated respiratory secretions (reviewed in (106)). Individuals most at risk are care-givers of NiV-infected patients, particularly those individuals who are present during the last few days of the illness when respiratory symptoms are most severe (74; 108). While NiV transmission appears to terminate after 5 generations, a single index case can result in a large number of secondary infections, which occurred when one religious leader managed to infect 22 followers who came to tend him while he was ill (60; 107).

Although Pteropus bats serve as the reservoir for henipaviruses, they do not develop any clinical disease (122). How bats are able to maintain a healthy clinical state while being infected with HeV/NiV is not understood, but recent studies have focused on the bat immune response. Bats express Type I and III interferons (IFN), and it was determined that HeV/NiV infection results in decreased expression and inhibition of IFN signaling pathways, suggesting there is another, as yet unknown, mechanism for controlling infection (189; 217). Given the difficulties in isolating virus from bats it is possible that the bat immune response also restricts henipavirus replication to low levels that allow persistence without causing clinical disease (reviewed in (158)).

It was originally assumed that henipaviruses were limited to Australia and southern Asia, following the geographic range of Pteropus bats. However, recent studies indicate henipaviruses have a much broader geographic spread. Research in various regions of Africa have isolated henipavirus RNA from *E. helvum* bats, which are populous in Africa but not Asia, and henipavirus antibodies have been detected in pigs in Ghana (48; 70). Additionally, evidence of antibodies to NiV or NiV-like viruses have

also been detected in bats from China (100).   There are currently no reports of HeV/NiV

infections in either Africa or China, but given the presence of henipaviruses in the bat

populations of those areas, it may only be a matter of time.

Illness and Immune Response

Since the 1994 outbreak, only 7 cases of HeV infection in humans have occurred,

resulting in 4 fatalities. Each of the infected individuals had close contact with a HeV-

infected horse and developed an ILI approximately one to two weeks after exposure

(reviewed in (162)). The four individuals who succumbed to infection had progressively

declining health leading to pneumonitis and multi-organ failure or encephalitis and

seizures.

Similar to HeV infection, the incubation period for NiV is on average 10 days, but

can range from less than a week to more than 4 weeks (36). Individuals infected with

NiV present with fevers, headaches, chills, myalgia and rigors (36; 56). Interestingly,

outbreaks of NiV in Bangladesh involve more respiratory symptoms than the initial

Malaysian outbreak, which had respiratory distress in approximately 25% of infections

(77). This could also explain why human-human transmission has been observed for

outbreaks in Bangladesh but not Malaysia. In the Malaysian outbreak, disease

progression led to neurological manifestations, such as encephalitis and seizures, while

outbreaks in Bangladesh progress to atypical respiratory distress syndrome ((9; 77),

reviewed in (162)). Neurological manifestations can recrudesce, and relapse or late-onset

encephalitis occurred in victims of the Malaysian outbreak as late as 22 months after the

initial disease (183; 203).

The human immune response to henipavirus infection involves both innate and adaptive components. Upon infection, IFN responses are activated, but the virally expressed V and W proteins inhibit IFN production. There are conflicting reports as to whether IFN signaling can still occur in HeV/NiV infected cells, but it appears that with high enough concentrations of V, P and W proteins, the Signal Transducer and Activator of Transcription (STAT) protein can be sequestered into high molecular weight complexes in both the cytoplasm and nucleus (163; 172; 173; 190). Inhibition of IFN production, and possibly IFN signaling, is vital for henipavirus infection as a reverse engineered NiV lacking the P, V, W and C proteins failed to infect hamsters (213).

Antibodies to the attachment and fusion glycoproteins of HeV/NiV can be detected in sera from convalescent-patients, indicative of an adaptive immune response (57; 182). Both IgM and IgG antibodies can be isolated and are found more often in sera than cerebral spine fluid (CSF), although isolation of NiV antibodies in the CSF is associated with more severe disease outcome (38; 201). This finding confirms that viremia occurs before infection of the central nervous system. Additionally, the immune response may help disseminate disease as the virus can be carried and released by monocytes and lymphocytes without needing to infect these cells (114).

A study involving Syrian hamsters focused on the different immune responses to NiV-Malaysia and NiV-Bangladesh infections to ascertain differences in pathogenesis. They found that NiV-Malaysia induced an earlier and more robust immune response than NiV-Bangladesh, including greater IL-6 and IL-4 expression, leading to increased T-cell and B-cell involvement (47). However, despite B-cell activation, disease progression occurred rapidly, disallowing time for a robust antibody response. The delayed immune

response seen with NiV-Bangladesh infection may help explain the high mortality of outbreaks in Bangladesh compared to Malaysia.

ATTACHMENT GLYCOPROTEIN (G)

All paramyxoviruses have a receptor binding protein– HN, H or G – that is classified based on the characteristics of the protein. The HN or hemagglutinin-neuramindase glycoprotein (PIV5, NDV, mumps and hPIV1-4) is multifunctional in that it binds sialic acids and also cleaves neuraminic acids, removing receptor from the surface of a cell. Glycoproteins lacking the neuraminidase activity but retaining the hemagglutinin ability are classified as H, and several viruses, notably the morbilliviruses such as MeV, express this glycoprotein. The attachment glycoproteins of HeV and NiV, classified as G, are somewhat unique among paramyxoviruses as they have neither hemagglutinin nor neuraminidase activity and bind proteinaceous receptors rather than sialic acids (reviewed in (16; 97)).

Like the HN and H glycoproteins, the henipavirus attachment G glycoprotein is a type II transmembrane protein that consists of an N-terminus cytoplasmic tail, a transmembrane domain, a stalk domain and a globular head. The globular head folds as a β-propeller with a central cavity surrounded by six blades, which themselves are composed of four anti-parallel beta sheets (23; 25; 206). The β-propeller shape is maintained by disulfide bonds between beta sheets in each blade as well as two additional disulfide bonds between blades three and four and between the N- and C-termini of the globular head. Five potential N-linked glycosylation sites (N306, N378, N417, N481 and N529) have been identified in the globular head of NiV and evidence has verified that four of the five sites are glycosylated with one site, N417, yielding variable reports likely

owing to alternative expression methods (24; 25; 206). Likewise, the HeV-G head domain also has all of the same five predicted and conserved N-linked glycosylation sites occupied by carbohydrate moieties (205). Detailed glycan composition and site occupancy analysis of the entire ectodomain of HeV-G has recently been performed and has also revealed O-linked glycosylation sites in the protein (41). (Portions of this section published in (179)).

Oligomerization of G glycoprotein

The native conformation of G when expressed on the virion or the surface of an infected cell is a tetramer, which is comprised of a dimer of dimers (1; 15). Residues responsible for the oligomerization of G are isolated to the stalk domain as expression of the globular head alone results only in monomeric species (24). Further investigation determined that two disulfide bonds in the stalk domain of G enable dimer formation, and a third disulfide bond between the stalk domains of homodimers is responsible for tetramer formation (15; 110). Additionally, Bowden *et al.* proposed that one surface of dimer-dimer interface occurs across the β1- and β6-propellers of the globular head (24; 25). This suggestion is supported by the lack of both structural divergence and N-glycosylation sites, which would interfere with oligomerization, along this section of the protein. The recently reported structure and model of a tetrameric NDV-HN has provided further information on the organization and oligomeric structure of a paramyxovirus attachment glycoprotein. The stalk domains of NDV-HN form a four-helix bundle (4HB) with a hydrophobic core that is the result of an 11-residue repeat domain in the stalk (215). Similarly to NDV-HN, HeV and NiV-G stalks contain alpha helices with a predicted break from amino acids 95-98, and the modeled juxtaposition of

14

these stalks with the globular heads of HeV and NiV-G resembles the tetrameric structure

of NDV-HN (Figure 1).

A model of a tetrameric parainfluenza 5 (PIV5) HN previously reported suggested

a tetramer formation in which the globular heads of the two dimers were in contact (216),

which contrasts with the more recent structural data of the NDV tetramer in which the

globular heads of the dimers are separated (215). Although the globular head dimer of

NDV and PIV5 can be superimposed with a low 1.5 Å root mean square deviation

(rmsd), the earlier PIV5 tetramer model is not in accord with the recent NDV dimer and

stalk configurations. Given the characteristics of HeV and NiV-G, specifically the

location of the N-linked glycosylation sites and the predicted stalk helices, it seems

reasonable that the tetrameric form of the henipavirus G glycoprotein would also

resemble the NDV-HN structural model.

Recent work with PIV5-HN reveals that the globular heads adopt a conformation

referred to as "4-heads-down" in which the heads block the upper portion of the stalk, the

region implicated in F interaction. The opposite "4-heads-up" conformation positions the

globular heads away from the stalk, presumably allowing F interaction, and is considered

a post-receptor binding state (215). While all 4 heads can be in the same conformation,

the dimer pairs can act independently with one pair being up and one pair being down in

what is referred to as a "2-heads-up and 2-heads-down" conformation (195). In this state

it appears that only one dimer pair is required to be in a "heads-up" conformation to

trigger fusion. Similarly for MeV-H, it has been proposed that changing from a heads-

down to a heads-up conformation is responsible for fusion activation (68; 128). (Portions

of this section previously published in (179))

Figure 1. Model of the Hendra virus attachment G glycoprotein.
The HeV-G ectodomain is shown in its dimer conformation. The secondary structure elements of the two globular head domains, colored in green and blue, are derived from the crystal structure, which also revealed the five predicted N-linked glycosylation sites (N306, N378, N417, N481 and N529) occupied by carbohydrate moieties (gray spheres) (41; 205). However, N378 was not modeled in the figure due to weak electron density. The G glycoprotein head domain folds as a six-blade β-propeller with disulfide bonds illustrated as yellow sticks. The residues of the ephrin-B2 G-H loop are shown in yellow. While the entire structure of the HeV-G stalk domain (residues 71-173) has not been determined, residues 77-136 are modeled in green, suggesting this region forms a discontinuous helix (84). The position of the HeV-sG head dimer and stalks are oriented based on the alignment with the NDV structure and the receptor binding face of the red monomer is facing out and the blue monomer is facing left. Despite having two helical ranges, Thr-77 to Lys-95 and Thr-98 to Ser-135, the HeV-sG stalk residues 98-135 appear equivalent to the HN glycoprotein stalk helix domain of the recently reported NDV structure (215). Additionally, the Ile residues in the HeV-G stalk domain that can modulate conformational changes associated with receptor binding are indicated and are located in the alpha helical region of the HeV-G stalk domain that aligns with the NDV-HN stalk (10). (Figure from (179))

Ile131

Ile124

Ile112

Ile105

Ile101

Helix Break
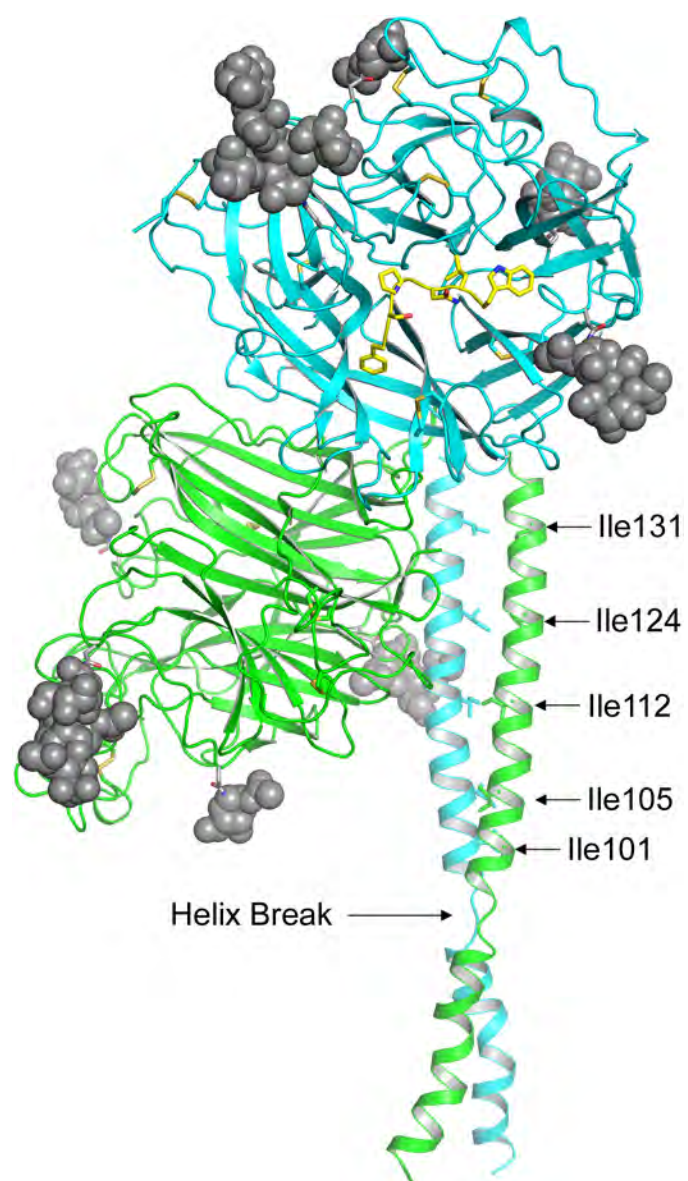
RECEPTORS EPHRIN-B2 AND EPHRIN-B3

The henipaviruses are the most recently recognized paramyxoviruses that also use host cell membrane proteins as virus entry receptors, and both HeV and NiV bind to ephrin-B2 and ephrin-B3 via their G glycoproteins (11; 12; 132; 133). Human ephrin-B2 and ephrin-B3 are 39% identical in amino acid sequence and are members of a large family of surface expressed glycoprotein ligands that bind to Eph receptor tyrosine kinases and mediate bi-directional cell-cell signaling events within the nervous, skeletal and vascular systems (93; 145). The ephrin-B2 and -B3 molecules are highly conserved proteins across species with amino acid identities ranging from 95-96% and 95-98%, respectively, including those hosts susceptible to henipavirus infection such as human, horse, pig, cat, dog and flying foxes (20).

Ephrin-B2 is found in arteries, arterioles and capillaries in multiple organs and tissues including arterial smooth muscle and human bronchiolar epithelial cells (181) but appears absent from venous components of the vasculature (54), whereas ephrin-B3 is found predominantly in the nervous system and the vasculature (144). The identification of ephrin-B2 and ephrin-B3 as functional receptors for the henipaviruses in cultured cells provides some explanation for both the broad species tropisms of the viruses, owing to their highly conserved nature, and the observed distribution of viral antigen in arterial endothelial cells, smooth muscle, neurons, and some epithelial cells (reviewed in (75; 200)).

While it is unclear how many ephrin molecules are required to bind oligomeric G to activate the henipavirus membrane fusion process, recent structural data have revealed that a G glycoprotein head domain (monomeric) binds an ephrin molecule in a 1:1 ratio

(23; 205; 206). Both ephrin-B2 and ephrin-B3 are able to support productive infection of

HeV and NiV, but the binding affinities of HeV and NiV-G for ephrin-B2 and -B3 are

uncertain, and this is also complicated by the oligomeric nature of both the G

glycoprotein and the ephrins. One report has suggested HeV and NiV-G have the same

binding affinity for ephrin-B3 while NiV-G has a higher affinity for ephrin-B2 than HeV-

G; however another study indicated that HeV and NiV-G bound ephrin-B2 similarly

while NiV-G engaged ephrin-B3 with a higher affinity in comparison to HeV-G (18; 20;

131). One possible explanation to explain these different findings is that two different

HeV-G sequences were used. Negrete *et al.* determined that the sequences of two HeV-G

strains currently used in research contain one amino acid change at position 507, having

either a Ser or a Thr (131). A Thr at position 507 confers ephrin-B3 affinity similar to

that of NiV-G, but a Ser at position 507 reduces the affinity of HeV-G for ephrin-B3

while having no effect on ephrin-B2 affinity. Given the physiological locations of

ephrin-B2 and -B3, the observed differences in the transmissibility of HeV and NiV and

the differences in HeV and NiV disease course in susceptible hosts upon infection,

additional study of the henipavirus G glycoproteins and their interaction with the ephrin

receptors will further our understanding of the biology and pathology of these important

zoonotic agents. (This section previously published in (179))

Interaction of henipavirus G with ephrin receptors

B-class ephrins contain a globular domain that is comprised of eight β-strands

(identified as A-D, F-H and K) surrounding a hydrophobic core (187). Although there

are three B-class ephrins (B1-B3) with high levels of similarity, only ephrin-B2 and

ephrin-B3 are able to serve as functional receptors for HeV and NiV. The major

structural divergence between these ephrins occurs in the respective G-H loop, which is a 15 amino acid linker region between β-strands G and H that is also primarily responsible for the binding between ephrins and their cognate Eph receptors (88).

Despite the 15-amino acid length of the G-H loop, only a short stretch of conserved amino acids ($F/Y_{117/120}SPNLW_{122/125}$) binds in the groove of the globular head of HeV and NiV-G with the only difference between ephrin-B2 and ephrin-B3 being F117 and Y120, respectively (23; 88; 206). (To avoid confusion, we will use the ephrin-B3 numerical designation for the G-H loop residues, identified as $F/Y_{120}-W_{125}$). Preceding the solution structures of the henipavirus G glycoproteins in complex with ephrin-B2 and -B3, the importance of the ephrin G-H loop was first hypothesized by Negrete *et al.* and confirmed by mutagenesis that involved the conversion of two residues in the G-H loop of ephrin-B1 to the residues in ephrin-B2, making ephrin-B1 a functional NiV receptor (133). The ephrin-B1 amino acid replacements L124 Y and W125 M would result in steric clashes and converting these residues to match the ephrin-B3 sequence eliminates this hindrance (133). The overall conformation and flexibility of the ephrin-B2 and ephrin-B3 G-H loops might also influence receptor selectivity of the henipavirus G glycoproteins. Indeed, both ephrin-B2 and -B3 appear to have G-H loops with extended and relatively rigid conformations, whereas ephrin-B1 has a more flexible G-H loop, which may not be compatible with the apparent lock-and-key ephrin/G glycoprotein binding mechanism (134).

Binding between ephrin-B2 and HeV and NiV-G is entirely through protein-protein interaction and occurs in two domains that have approximately $2,700 Å^2$ surface area of interaction (23; 206). The first domain, the ephrin-docking site, occurs along a

mostly polar region of the outer rim of the globular head of the henipavirus G and requires 24 hydrogen bonds, four salt bridges and multiple hydrophobic interactions (23; 206). The second domain primarily involves interaction through van der Waals forces of the ephrin G-H loop residues F/Y120, P122, L124 and W125 with binding pockets in the central groove of the globular head of G (23; 206). The four binding pockets in HeV and NiV-G for the residues in the ephrin-B2 and -B3 G-H loop are highly conserved with the only four differences with the most notable being a Val (NiV) to Thr (HeV) change at position 507 (23) (Table 1).

The crystal structures of both HeV and NiV-G in complex with ephrin-B2 have provided much information on the specific interaction between these attachment glycoproteins and receptor, but whether relevant conformational changes must occur for G/ephrin-B2 binding is not completely clear. It is generally accepted that the G-H loop of ephrin-B2 and -B3 does not undergo major conformational change, except for rearrangements of W125 upon G engagement that are suggested to "latch" ephrin-B2 into a stronger association (205).

While there is debate as to whether major or minor conformational changes occur in the monomeric henipavirus G head domain upon receptor binding, it is clear that some limited structural rearrangements do occur but appear restricted to a specific region (23; 206). Three of the binding pockets in the HeV and NiV-G head domain (pockets for ephrin-B2 and -B3 residues P122, L124 and W125) undergo little conformational change, while the G glycoprotein D579-P590 loop (binding pocket for ephrin-B2 and -B3 F117 and Y120, respectively) appears to have the greatest structural alteration upon receptor

binding (25). Interestingly, this region is the one binding pocket that must accommodate

two different residues, suggesting ephrin-B2 and -B3 bind to HeV and NiV-G by an

Table 1: Henipavirus G glycoprotein receptor binding pockets.
The residues in HeV-G and NiV-G that form the binding pockets for the residues of the ephrin-B2 and ephrin-B3 G-H loop are shown. The residues are highly conserved with the only difference occurring at position 507, which is involved in forming the binding pocket for residue P_{122} of ephrin-B2 and ephrin-B3. Residues in bold are the four amino acids that are different between the HeV-G and NiV-G binding pockets for eprhin-B2 and -B3 P122, L124 and W125. (Table previously published in (179))

Binding Pocket for loop residues	HeV-G glycoprotein residues	NiV-G glycoprotein residues
F/Y	C240, N557, A558, Q559, E579, I580, Y581, I588, R589	C240, N557, A558, Q559, E579, I580, Y581, I588, R589
P	P488, G489, Q490, E505, G506, **T507**, Q530, T531, A532	P488, G489, Q490, E505, G506, **V507**, Q530, T531, A532
L	**Y458**, W504, E505, G506	**F458**, W504, E505, G506
W	L305, **V401**, **N402**, W504	L305, **I401**, **R402**, W504

induced-fit model as the F residue binding pockets in each henipavirus G glycoprotein must conform in a way to accommodate the different residues in the G-H loops of ephrin-B2 and ephrin-B3 (24; 25). Other more recent data suggest that ephrin-B2 binding to HeV G supports a "lock, key and latch" model for the association between the G glycoprotein and its receptors with the W122 residue of ephrin-B2 serving as the "latch" (205). Finally, it should also be recognized that the available structural data of a henipavirus G glycoprotein complexed with an ephrin receptor is from monomeric proteins and do not take into account the possibility of broader oligomeric changes that may occur following receptor engagement. For example, in case of MeV-H, it was recently reported that following receptor binding, the two heads of a MeV-H dimer move in relation to each other. This movement stabilizes the H-dimer interface through inter-molecular disulfide bonds and blocks fusion, suggesting that oligomeric H conformational changes (dimer separation or movement) are linked to fusion triggering (129). (This section previously published in (179))

Fusion glycoprotein (F)

While the G glycoprotein is required for attachment of the henipavirus virion to the target cell, the F glycoprotein is responsible for the merger of the viral membrane envelope with the target cell plasma membrane. The F glycoprotein is initially expressed as a 546 amino acid precursor (F_0) which forms an oligomeric trimer that is cleaved into two subunits (F_1 and F_2) by the endosomal protease cathepsin L (139). Unique to the henipaviruses, the processing of F_0 into its biologically active form is a multi-step process requiring recycling of F_0 from the cell surface into an endosomal compartment, mediated by an enodcytosis motif present in the cytoplasmic tail of F (120; 191). Interestingly,

HeV and NiV-F glycoproteins contain no specific cleavage sequence, and cleavage is only inhibited by the deletion of six residues upstream of the cleavage site (123). After cleavage, the homotrimer of disulfide bond linked F_1 and F_2 subunits is trafficked back to the cell surface.

The F_1 subunit contains several important structural characteristics that include an N-terminal hydrophobic fusion peptide domain, two heptad repeat (HR) domains, a transmembrane domain and cytoplasmic tail. The two α-helical heptad repeat domains reside immediately downstream of the fusion peptide (HR1 or HRA) and upstream (HR2 or HRB) of the transmembrane domain and are the shortest HR domains among paramyxoviruses (105). The C-terminal cytoplasmic tail and the transmembrane domain have also recently been implicated in modulating virus-mediated fusion as tyrosine residues in the tail have been shown to increase fusion activity and aid in the proper trafficking of F in polarized epithelial cells (152; 194). (This section previously published in (179))

The fusion mechanism

The crystal structures of the paramyxovirus F glycoproteins (SV5/PIV5 and human parainfluenza virus 3 (hPIV3)) have provided significant insight into the mechanism of the fusion process and the structural transition that occurs between the pre- and post-fusion conformations of F (210; 211). Although the paramyxovirus F glycoproteins resemble other Class I viral fusion glycoproteins, they are distinctly structurally different in comparison to other pre- and post-fusion Class I viral fusion glycoprotein structures, and the hPIV3-F and PIV5-F structures are the only available models for making good comparisons of the paramyxovirus F structural transition (94).

Prior to receptor binding, the hydrophobic fusion peptide located at the N-terminus of the F_1 subunit is concealed in the protein. Upon receptor binding, the paramyxovirus attachment glycoprotein promotes F fusion activity by an as yet ill-defined mechanism, triggering irreversible conformational changes in F that 1) exposes the fusion peptide, allowing it to be inserted into the opposing target cell membrane and 2) rearranges the HR domains, leading to the formation of the hallmark feature of Class I fusion – the six helix bundle (6HB) (recently reviewed (97; 176)). This process is a multi-step event that results in the elongation of F as well as the merger of the viral and cellular membranes. The assembly of the 6HB is believed to provide the energy required for the membrane destabilization and merger event as the three HR2 domains within the F trimer are rearranged to bind via hydrophobic interactions in the grooves of the trimeric core composed of the HR1 domains (105). However, the number of F homotrimers required for fusion pore formation and membrane merger is unknown. (This section previously published in (179))

G AND F GLYCOPROTEIN INTERACTION

While hRSV and PIV5 are able to mediate fusion without a corresponding attachment glycoprotein, the majority of paramyxoviruses, including HeV and NiV, require G and F interaction on the virion surface for viral fusion, in which G is required for F activation and the initiation of the fusion cascade (49; 81; 185). Despite the requirement of receptor engagement by G to initiate fusion, the interaction of G and F appears independent of receptor binding as G and F can be co-precipitated in the absence of receptor (1; 2; 11; 15). It has been shown that several paramyxovirus F and attachment glycoprotein pairs, including those from MeV, NDV and hPIV2, first interact

in the endoplasmic reticulum (ER); however, the henipavirus G and F glycoproteins have different and more complex trafficking patterns in comparison to other paramyxoviruses (150; 180; 186; 198). HeV/NiV-Gs have been shown to take longer than their partner F glycoproteins to traffic through the ER and Golgi, and this longer trafficking time of G and the complex pattern of F maturation suggests that G-F interaction does not occur until both glycoproteins are expressed on the cell membrane (197; 198).

Although most evidence indicates that the G and F glycoproteins interact prior to G-ephrin receptor binding, the exact nature of this interaction and the domain(s) of G and F that associate are not well defined, although recent studies have highlighted the importance of the G stalk domain. Bishop *et al.* found that mutations at specific sites in the stalk domain of HeV-G inhibited HeV fusion due to an apparent loss of interaction with F (10). These particular isoleucine residues are located in an alpha helical domain that resembles a heptad repeat that is highly conserved among paramyxoviruses (10). Interestingly, the nine Ile → Ala mutations that abolished the fusion promotion activity of HeV-G are located near the region that Yuan *et al.* have implicated as important for the tetramer formation of NDV-HN (Figure 1 and discussed above) (10; 215). Monoclonal antibody (mAb) binding analysis, with several mAbs that preferentially recognize G in complex with ephrin receptor, revealed that these HeV-G stalk domain mutants appeared to adopt a receptor-bound conformation in the absence of receptor binding and thus were unable to trigger F fusion activation even upon any subsequent ephrin receptor binding. These observations suggest that G must be in some correct pre-receptor bound tetrameric conformation in order to properly trigger F fusion activity and also indicate that receptor binding and fusion triggering by G can be uncoupled.

Recent work by Bose *et al*. on the stalk domain of PIV5-HN has continued to promote the stalk of the attachment glycoprotein as the F-activating domain. A headless PIV5-HN expressed with its cognate F glycoprotein is able to mediate fusion (13). Furthermore, expression of HN-Stalk and F resulted in F adopting a post-fusion conformation, which is not the conformation adopted when F is solely expressed. Similar results have also been reported for MeV and NiV, again indicating that the stalk domains of the attachment glycoproteins are responsible for F activation (26; 103). Combining this information with the "heads-up" and "heads-down" conformations previously discussed suggests that the globular heads regulate G-F association and prevent F activation until receptor has been engaged. (Portions of this section previously published in (179))

MODEL OF HENIPAVIRUS FUSION

Two principal models of paramyxovirus glycoprotein-mediated membrane fusion have been postulated (170) (recently reviewed (176)) (Figure 2). In the first model, the F glycoprotein and the attachment glycoprotein are not physically associated in the membrane, but following receptor engagement there is an alteration in the attachment protein, possibly a switch from heads-down to heads-up, which facilitates its association with F and in so doing imparts or triggers/induces the F glycoprotein conformational changes leading to membrane fusion (Figure 2A). This association or provocateur scenario has been supported by extensive functional and structural studies on the HN and F glycoproteins of hPIV3, NDV and PIV5 (42; 99; 118; 146; 215). In the second dissociation or clamp model, the F and attachment glycoproteins are pre-associated and a conformational alteration in the latter following receptor engagement alters or releases F

Figure 2: Models of paramyxovirus membrane fusion involving heads-up and heads-down conformations.

Initial expression of the tetrameric attachment (HN/H/G) glycoprotein (dimers colored red and blue) and the fusion (F) glycoprotein (green) is depicted in the **(A)** heads-down, non-F-associated or **(B)** heads-up, F-associated conformations. In both models, HN/H/G binds receptor (maroon) and undergoes receptor-induced conformational changes, switching from heads-up to heads-down or vice versa. The change in the position of the globular heads allows for (A) association (provocateur model) or (B) dissociation (clamp model) with F, leading to the fusion activation of F and the beginning membrane fusion by the insertion of the fusion peptide (yellow) into the target cell membrane. (Figure previously published in (16))

A.

Host Cell Plasma Membrane

Viral receptors

Heads-down

Virion surface

B.

Heads-up

Receptor binding

HN/H/G conformational change

Heads-up
Associates with F

Heads-down and rotational change
Dissociates from F

F activation

Insertion of fusion peptide

Insertion of fusion peptide

29
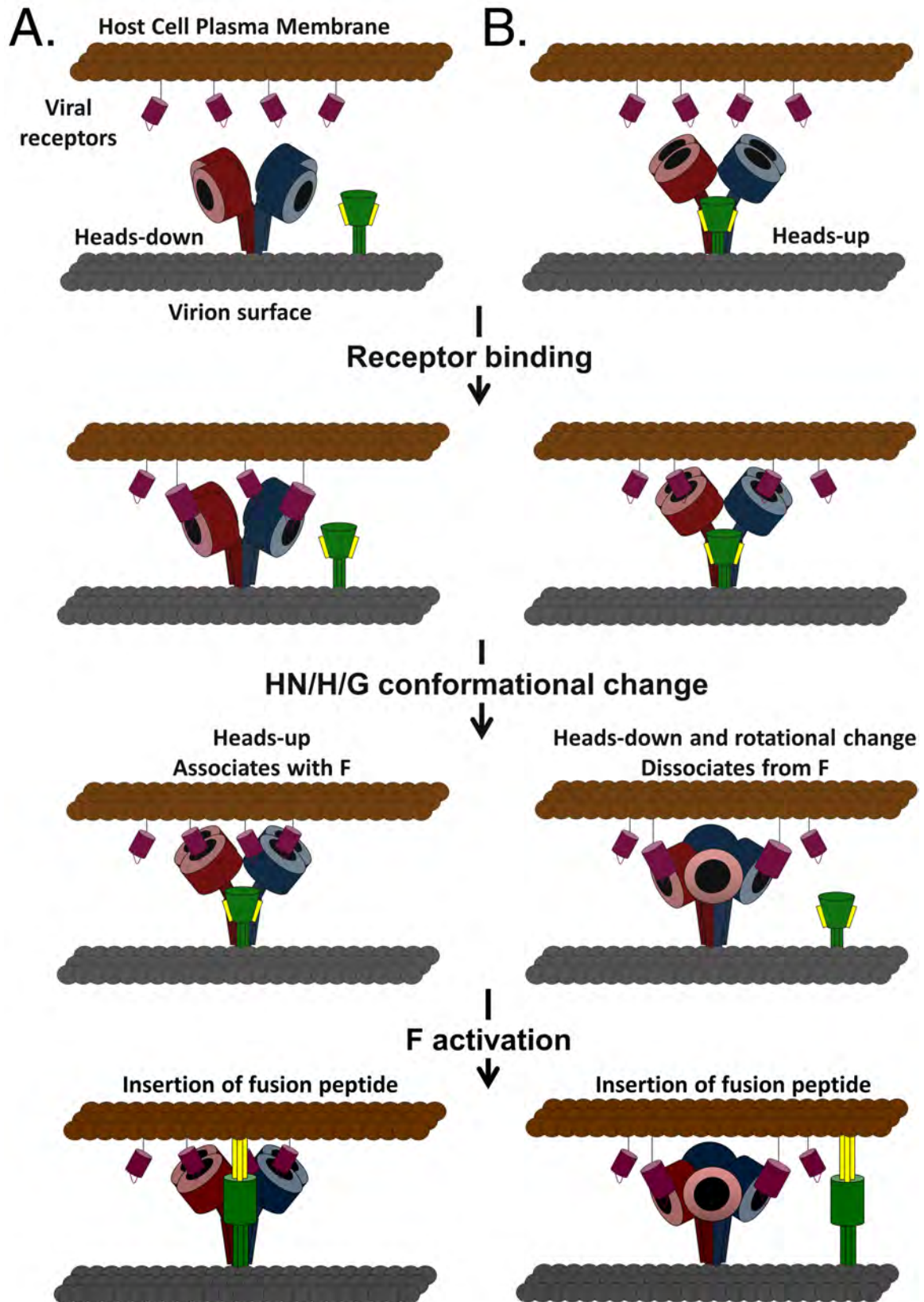
allowing it to proceed towards the fusion active state and 6HB formation, supported by studies with the MeV H and F glycoproteins (43; 150; 151) (Figure 2B).

For the henipaviruses, several studies suggest that HeV and NiV initiate fusion via a clamp model. In this scenario F could be stabilized in some manner by interaction with G, perhaps maintaining F in a pre-fusion state, or it could just simply be that G and F have some propensity to specifically interact until receptor binding to G initiates some specific interaction with F triggering fusion activity and then followed by dissociation, much like a provocateur model.

In support of a general clamp model for henipavirus fusion, it has been observed that the strength of G-F interaction is inversely proportional to fusion activity as stronger G-F interaction results in decreased fusion due to the inability of F to disassociate from G (2; 3; 11). These observations are in agreement with the earlier suggestion that the henipavirus-mediated fusion mechanism is similar to MeV, which also exhibits an inverse relationship between the attachment glycoprotein (H) and F (151). Also in accord with this fusion model are the observations that both MeV and HeV possess attachment glycoproteins that with certain mutations decrease their receptor binding activity while strengthening the interactions with their respective F glycoprotein partner (11; 44).

Indirect support for the provocateur model also comes from data indicating that F expressed in the absence of G can be recognized by a conformation-dependent mouse mAb specific for the pre-fusion form of NiV-F (33). These conflicting data suggest that neither a clamp model nor a provocateur model alone can fully account for all the experimental observations to date on the mechanism of henipavirus-mediated fusion. In fact, a recent report by Porotto *et al.* details a new, third fusion mechanism that is based

on both the clamp and provocateur models (153). Their new model is based on the need

for continuous receptor engagement by hPIV3-HN to activate F for membrane fusion

(153). In this study, fusion intermediates were captured by using HR2 peptides localized

in the target cell membrane by a cholesterol tag. It was determined that if interaction

between hPIV3-HN and its receptor was interrupted during F activation and insertion into

the target membrane, fusion would not occur. Most recently, a further study by Porotto *et

al.*, examined the hPIV3 fusion system using a bimolecular fluorescence

complementation approach to follow the dynamics of the viral HN and F in living cells

(155). The authors were able to demonstrate that in this system the HN and F

glycoproteins do associate prior to receptor engagement, HN drives the formation of HN

and F interacting clusters at the site of membrane fusion and the interaction of the HN-F

pairs of oliogmers modulate the viral glycoprotein pairs fusogenicity (155). This

requirement of continual receptor engagement and interaction between the attachment

and fusion glycoproteins is hypothesized to be applicable to all paramyxoviruses,

including HeV and NiV (153). Further research regarding this proposed mechanism in

respect to HeV/NiV may be able to resolve the conflicting data supporting the two

current models and clarify the mechanism of henipavirus-mediated fusion. (Section

previously published in (179))

THERAPEUTICS

Licensed and efficacious human antiviral therapeutics for the henipaviruses are

currently not available. Ribavirin was used to treat 140 patients during the NiV outbreak

in Malaysia in 1998/99, lessening the mortality rate by 35% from 54% in the control

group to 32% in the treated group (35). Without any other currently available therapeutic

options, ribavirin is still considered an option for treatment, but its impact on disease progression is questionable as two HeV infected patients in 2008 showed no discernable benefit after treatment with ribavirin (148). Additionally, chloroquine, an anti-malarial drug first demonstrated to block the proteolytic processing of HeV-F (140), was later shown to inhibit henipavirus infection *in vitro* (154). However, treatment with chloroquine and ribavirin proved ineffective for one HeV-infected individual in 2009 as no clinical benefit was observed (4).

In subsequent animal challenge models with henipaviruses, ribavirin only delayed NiV disease and death and had no therapeutic effect against HeV infection in hamsters (52; 55). Ribavirin also only delayed HeV disease by 1 or 2 days in African green monkeys and did not prevent disease outcome (161). Chloroquine, either alone or in combination with ribavirin, also had no therapeutic benefit in ferrets challenged with NiV or hamsters challenged with either NiV or HeV (52; 141). Thus, due to the extreme pathogenic capacity of HeV and NiV infection in people, considerable effort has been spent in developing and exploring new therapeutic options against the henipaviruses, and these treatments have primarily focused on targeting the fusion and entry step of the virus infection process and include subunit vaccines, F glycoprotein-targeted peptide fusion inhibitors and passive immunotherapy with virus neutralizing mAbs targeting the G and F glycoproteins.

The development of a soluble form of HeV-G that maintained many of the characteristics of full-length G led to its testing as a possible subunit vaccine. It was quickly determined that immunization with soluble G (sG) resulted in antibody protection and that HeV-sG rather than NiV-sG resulted in higher cross neutralization (125).

Multiple animal studies in cats, ferrets and non-human primates have verified that vaccination with HeV-sG protects against both lethal NiV and HeV challenge ((115; 125; 142), reviewed in (29)). The continual success of HeV-sG as a subunit vaccine in animal studies led to its development, licensure and release in the fall of 2012 as a Hendra virus equine vaccine in Australia. The vaccine, Equivac® HeV, appears to be well received in Australia, and many veterinarians may require horse owners to vaccinate their horses before receiving treatment (91; 119).

Monoclonal antibodies (mAbs)

For paramyxoviruses, antibodies specific for either the F or attachment glycoproteins can neutralize virus with antibodies directed against attachment glycoproteins typically being the more predominant (reviewed in (28)). The first evidence of passive protection against a NiV challenge was demonstrated using hamsters with monospecific polyclonal antiserums against F and G (57). Passive immune plasma therapy was also successful in the post-exposure treatment of African green monkeys infected with NiV (Geisbert & Broder, unpublished). However, the development of virus neutralizing mAbs has made passive antibody therapy development a major focus of current research. Another passive immunotherapy study in the hamster model using two murine mAbs against NiV-F and two against G was shown to completely protect the challenged animals if animals received mAbs before and immediately following challenge, and again, mAbs targeting the G glycoprotein proved more effective than mAbs targeting the F glycoprotein (58). Similar results were also obtained in a HeV challenge model in the hamster (59).

A major advance in the development of specific mAbs has been the use of recombinant antibody technologies (69; 159). Earlier, recombinant HeV-sG was used to isolate human mAbs. One particular human mAb (m102.4) was HeV and NiV cross-reactive and possessed extremely potent virus neutralizing activity (218; 219). *In vivo* studies have since demonstrated that m102.4 can protect animals from a lethal challenge with henipaviruses as a post-exposure application in the ferret model with NiV (22) or HeV (Pallister, Middleton & Broder, unpublished work). Most recently, mAb m102.4 was tested in the African green monkey model against HeV, and again all animals could be protected from lethal disease by m102.4 when it was administered from 12 to as late as 72 hours after a lethal high dose intratracheal challenge (17). In August 2009, m102.4 was used on a compassionate basis to save the life of a HeV-infected individual while in a coma (149). Unfortunately, delivery and intravenous administration of only 100mg of available antibody occurred after the onset of encephalitis and the individual died shortly thereafter. However, during the 2010 HeV emergence, prior to HeV diagnosis or the onset of clinical disease, two individuals that were considered as high risk cases of possible infection received m102.4 antibody at doses sufficient to achieve a high serum concentration, and both individuals have remained healthy (5). Together, these findings highlight the therapeutic potential of mAb-based passive transfer modalities for treating henipavirus exposure. Presently, m102.4 is being developed further for clinical use in people.

The mechanism and efficacy of m102.4-mediated neutralization is likely due to its ability to directly compete with ephrin-B2 and -B3 receptors for binding to the HeV and NiV-G glycoprotein. Indeed, this seems born out when a comparison of the G

glycoprotein binding pockets used by m102.4 and ephrin-B2 and -B3 is made, which

shows a remarkable series of identical contacting residues in G that are important for

engaging the ephrins as well as mAb m102.4 (Figure 3) (204). Substituting for the G-H

loop of ephrin-B2 and -B3, m102.4 has a stretch of amino acid residues (L_{105}APHPS$_{110}$)

that bind the henipavirus G glycoprotein with four residues considered critical for binding

(L105, P107, H108 and P109). (Portions of this section previously published in (179))

m102.4 escape variants of HeV/NiV-G

To gain a better understanding of the neutralizing ability of m102.4 and the

escape potential of HeV/NiV, m102.4 escape variants of HeV/NiV were generated *in*

vitro by serially passaging virus in the presence of low levels of m102.4. HeV/NiV

escape variants were isolated and tested for viral fitness and genomic mutation.

Surprisingly, the escape variants maintained levels of viral fitness similar to wild type

HeV/NiV, and both HeV and NiV had a single amino acid mutation in G that was

responsible for m102.4 escape (207). Despite the high level of similarity between

HeV/NiV-G, each virus had developed a unique mutation: HeV-G had a mutation in

residue 582 from aspartic acid (D) to asparagine (N) and NiV-G had a mutation in

residue 507 from valine (V) to isoleucine (I) (Figure 4).

The mutation in HeV-G lies outside of the binding pocket for receptor and

m102.4, and it has been speculated that this mutation prevents the formation of a salt

bridge near the binding pocket for receptors and m102.4 (207). The V507I mutation in

NiV-G lies inside the binding pocket of the conserved proline, but it is not fully

understood how this mutation affects m102.4 but not receptor binding.
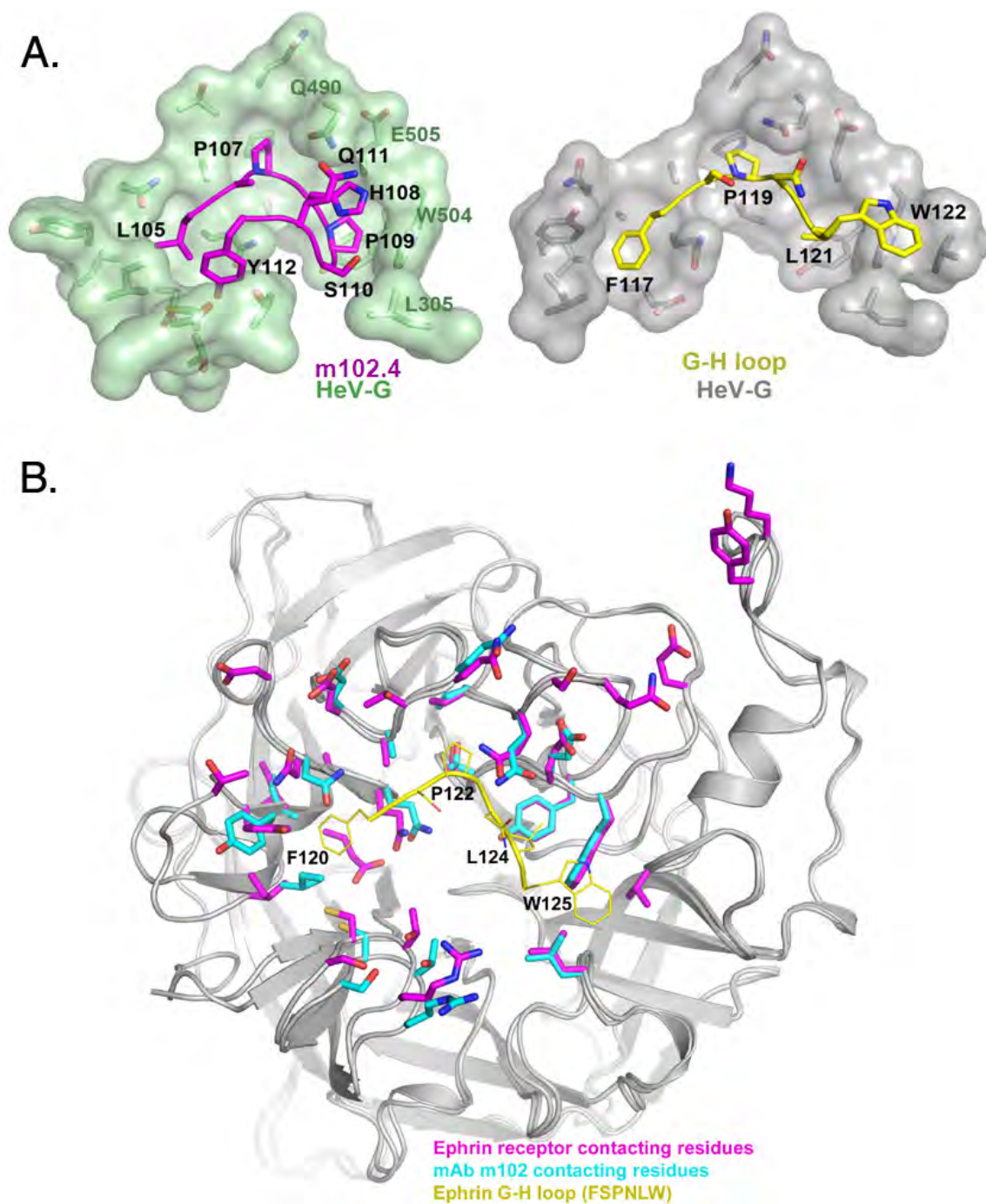
Figure 3. HeV-G residues that bind ephrin and mAb m102.4.

(A) Portions of the globular head of HeV-G (green and gray) are shown bound to m102.4 (purple) and the ephrin G-H loop (yellow). (B) The globular head of HeV-G (gray) is shown with residues important for ephrin-B2 and -B3 binding highlighted in purple, residues required for binding mAb m102.4 shown in blue and the residues of the ephrin-B2 G-H loop in yellow. While the conformations of the residues may be slightly different, most residues involved in binding ephrin G-H loop are also required for binding m102.4. (Figure published in (179))
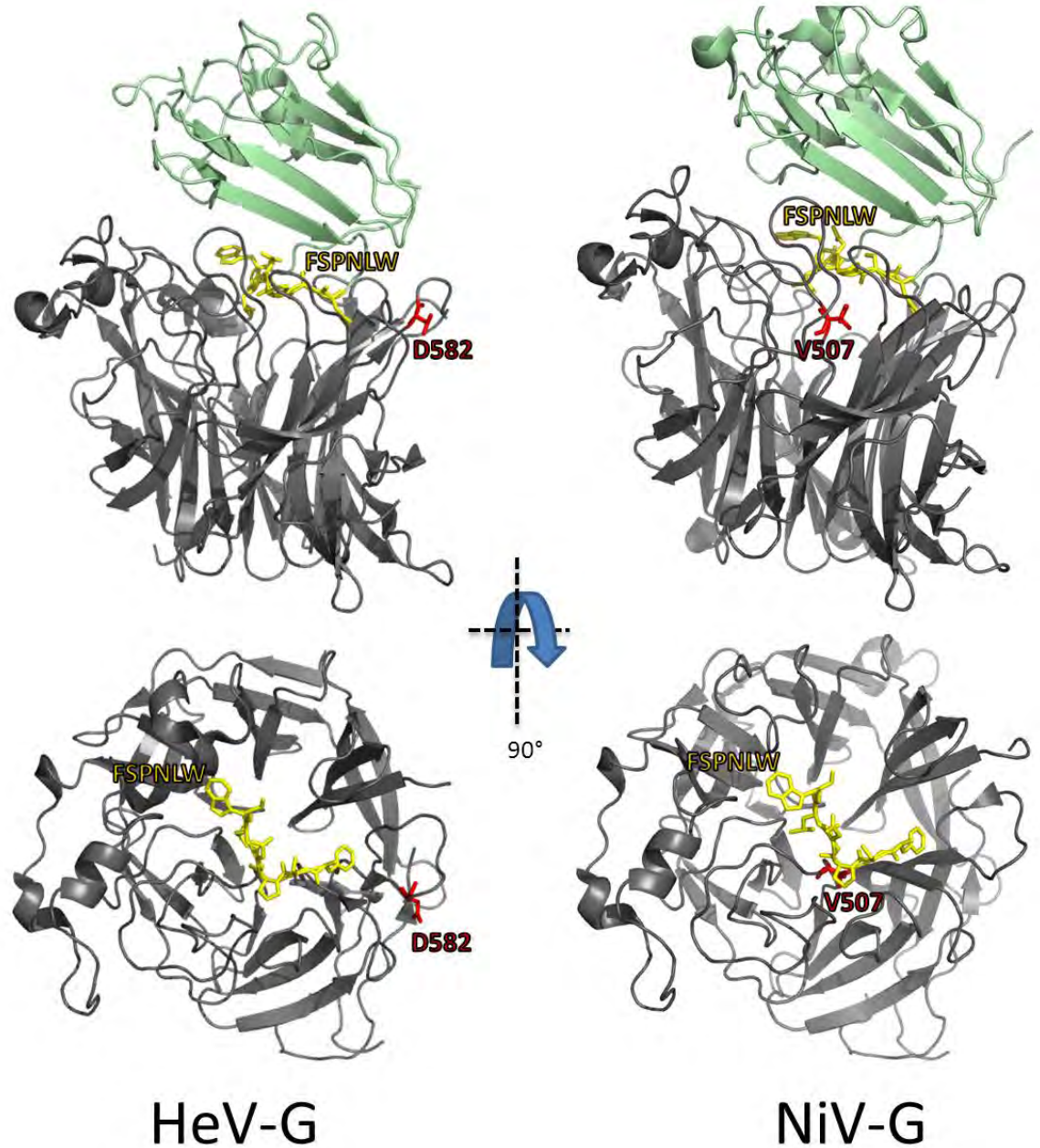
Figure 4: HeV/NiV m102.4 escape mutants.
HeV-G and NiV-G (gray) are shown in complex with ephrin-B2 (pale green) with the G-H loop residues FSPNLW shown in yellow. The positions of D582 (HeV-G) and V507 (NiV-G) are shown in red. HeV-G and ephrin-B2 structure – PDB ID: 2VSK (23), NiV-G and ephrin-B2 structure – PDB ID: 2VSM (23).

The attachment glycoprotein is critical for henipavirus infection as G binds receptor, triggering a cascading series of events that ultimately leads to viral-cell membrane merger. The human mAb m102.4 specifically binds G and inhibits infection most likely through competitive binding of G. Despite a lack of viral escape mutants *in vivo*, m102.4 escape mutants have been generated *in vitro* and show no loss of viral fitness. My work seeks to enhance the neutralizing ability of m102.4 to prevent future escape variants from being generated. Concurrently, we seek to describe the molecular events of G-receptor binding, G-F interaction and the possible mechanism of m102.4 neutralization.

Specific Aim 1 - Develop second-generation m102.4 variants that bind and inhibit wildtype and m102.4 escape variants of HeV and NiV.

> *Subaim 1* - Mutate m102.4 HeV/NiV-G binding region to more closely resemble ephrin-B2 and -B3 G-H loop
>
> - Variants of m102.4 that more closely resemble the G-H loop of ephrin-B2 and -B3 will prove more efficacious at inhibiting HeV/NiV-G binding to receptor than m102.4
>
> - m102.4 variants will be able to bind soluble, tetrameric versions of HeV/NiV-G and prevent receptor binding and fusion
>
> *Subaim 2* - Test binding of m102.4 variants to m102.4 escape variants of HeV/NiV-G
>
> - m102.4 escape variants of HeV- and NiV-G will be bound and inhibited by m102.4 variants resembling ephrin-B2 and -B3 G-H loop

Specific Aim 2 - Characterize the interactions of ephrin-B2, ephrin-B3 and m102.4 with the attachment glycoproteins of wild type and m102.4 escape variants of HeV and NiV.

Subaim 1 - Identify conformational changes that occur in HeV/NiV-G upon receptor or m102.4 binding

- Receptor binding induces conformational changes in HeV/NiV-G

- m102.4 binding to HeV/NiV-G mimics receptor binding, also causing conformational changes in HeV/NiV-G

Subaim 2 - Determine the interaction between HeV/NiV-G and HeV/NiV-F

- Given the two current models of G/F interaction (clamp and provocateur), the addition of receptor and/or m102.4 will cause an increase or decrease in G-F association

Subaim 3 - Determine how m102.4 neutralizes HeV/NiV infection and how escape variants escape m102.4 neutralization

- Mechanism of m102.4 neutralization is likely to be through competitive inhibition or preventing or inducing conformational changes in HeV/NiV-G associated with receptor binding. m102.4 escape variants of HeV/NiV-G will react differently to m102.4 binding than their wild type counterparts

Chapter 2: Materials and Methods

CELLS

HeLa cells (#CCL 2) were provided by the American Type Culture Collection (Manassas, VA), 293T cells were provided by G. Quinnan (USUHS), HeLa-USU cells were supplied by A. Maurelli (USUHS), Free Style 293-F (293Free) cells were obtained from Invitrogen (Carlsbad, CA) and Vero 76 cells were used for escape studies (12). These cell lines were cultured in Dulbecco's Modified Media (DMEM) supplemented with L-glutamine, penicillin/streptomycin and either 5% or 10% cosmic calf serum (Quality Biologicals, Gaithersburg, MD). 293Free cells were initially grown as an adherent cell line in DMEM-10 but then grown in suspension using 293 FreeStyle media (Invitrogen) without any additional reagents. All cells were incubated at 37°C with 5% CO_2.

PLASMIDS AND EPHRINS

The expression plasmid pCOMB3X-m102.4 expresses m102.4 as a flag-tagged Fab and was used as the template for m102.4 variant generation (8). Full-length and soluble, tetrameric HeV/NiV-G along with their m102.4 escape variants (HeV-G-D582N/NiV-G-V507I) were expressed in a modified pcDNA3.1 vector (34; 135). Recombinant soluble ephrin-B2 (mouse) and ephrin-B3 (human) fused with the Fc domain of IgG were purchased from R&D Systems (Minneapolis, MN). Additionally, Y. Feng (USUHS) supplied soluble ephrin-B2 that was S-tagged.

ANTIBODIES AND PROTEINS

Flag-tagged Fabs of m102.4 and m106.3 were expressed and purified from E. coli HB2151 cells and purified by Ni-NTA columns (Qiagen, Germantown, MD) (72; 218).

Along with m102.4 and m106.3, G-specific and F-specific rabbit polyclonal sera and goat-α-rabbit-HRP antibodies were used to detect both HeV/NiV-G and HeV/NiV-F, respectively. The rabbit α-S-tag, HRP-conjugated antibody (Bethyl Laboratories, Inc., Montgomery, TX) was also used to detect HeV/NiV-G.

IgG constructs of m102.4 were provided by Y. Feng (USUHS), and the α-ephrin-B2 antibody, m150.8, was supplied by V. Choudhry (USUHS). m150.8 and m102.4 IgG were biotinylated with EZ-Link biotin (Pierce, Rockford, IL, manufacturer's protocol). Fluorophores α-Flag-FITC antibody and Streptavidin-Pacific Blue antibody were purchased from Invitrogen.

Soluble trimeric fusion glycoproteins of HeV/NiV-F that were either S-tagged or untagged were provided by YP. Chan (USUHS).

GENERATION OF SOLUBLE, TETRAMERIC HENDRA/NIPAH-G

GCN4 addition

Sense and anti-sense oligomers containing the GCN4 sequence flanked by SalI restriction sites were synthesized (5'-GG GCG GTC GAC ATG AAG CAG ATC GAG GAC AAG CTG GAG GAG ATC GAG AGC AAG CTG AAG AAG ATC GAG AAC GAG CTG GCC AGG ATC AAG AAG GTC GAC CGC GC -3'). Equal concentrations of both oligomers were mixed, incubated at 94°C for 2 minutes (min), annealed on ice for 5 min and then digested with SalI-HF (New England Biolabs, Ipswich, MA, manufacturer's protocol). Plasmid pcDNA3.1-HeV-sG was digested using SalI-HF, ligated with SalI-HF digested GCN4 using T4 DNA ligase (Roche, Pleasanton, CA) and transformed in Top10 cells (Invitrogen). Correct insertion of the GCN4 motif was verified by sequencing, and the construct was designated pcDNA-GCN(tet)-HeV-sG.

Addition of the GCN4 motif to pcDNA3.1-NiV-sG was performed using overlapping PCR (Figure 5) (98). The GCN4 motif was amplified using forward and reverse primers that also contained portions of the NiV-sG sequence on the 5' ends (**c**: 5'-CGG AAG CTG ATG AAG CAG ATC GAG GAC-3' , **d**: 5'-CTG GTG TAC TT CTT GAT CCT GGC CAG-3'). The leader sequence and S-tag were amplified using primers **a** and **b** in which primer **b** contained a portion of the 5' end of the GCN4 sequence (**a**: 5'-TAA TAC GAC TCA CTA TAG GG-3', **b**: 5'-CTG CTT CAT CAG CTT CCG GCC CTC GAT GC-3'). NiV-sG sequence was amplified using primers **e** and **f**, and primer **e** contained a portion of the GCN4 sequence at the 5' end (**e**: 5'-GGA TCA AGA AGT ACA CCA GAA GCA CCG AC-3', **f**: 5'-TAG AAG GCA CAG TCG AGG C-3'). PCR products from all three reactions were mixed and amplified using primers **a** and **f**. Correct insertion of the GCN4 motif was verified by sequencing, and the construct was named pcDNA-GCN(tet)-NiV-sG.

Escape variants of tetrameric (Tet) HeV-sG and NiV-sG, Tet-HeV-sG-D582N and Tet-NiV-sG-V507I, respectively, were generated using quick change mutagenesis (Agilent technologies, Santa Clara, CA, manufacturer's protocol). For Tet-HeV-sG-D582N: starting template-pcDNA-GCN(tet)-HeV-sG, forward primer: 5'- GTG GAG ATC TAC AAC ACC GGC GAC TC-3' and reverse primer: 5'- GAG TCG CCG GTG TTG TAG ATC TCC AC-3.' For Tet-NiV-sG-V507I: starting template-pcDNA-GCN(tet)-NiV-sG, forward primer: 5'- GAG ATC TGC TGG AGG GGC ATC TAC AAC GAC GCC TTC C-3' and reverse primer: 5'- GGA AGG CGT CGT TGT AGA TGC CCT CCC AGC AGA TCT C-3.' Correct mutation was confirmed by mutagenesis,
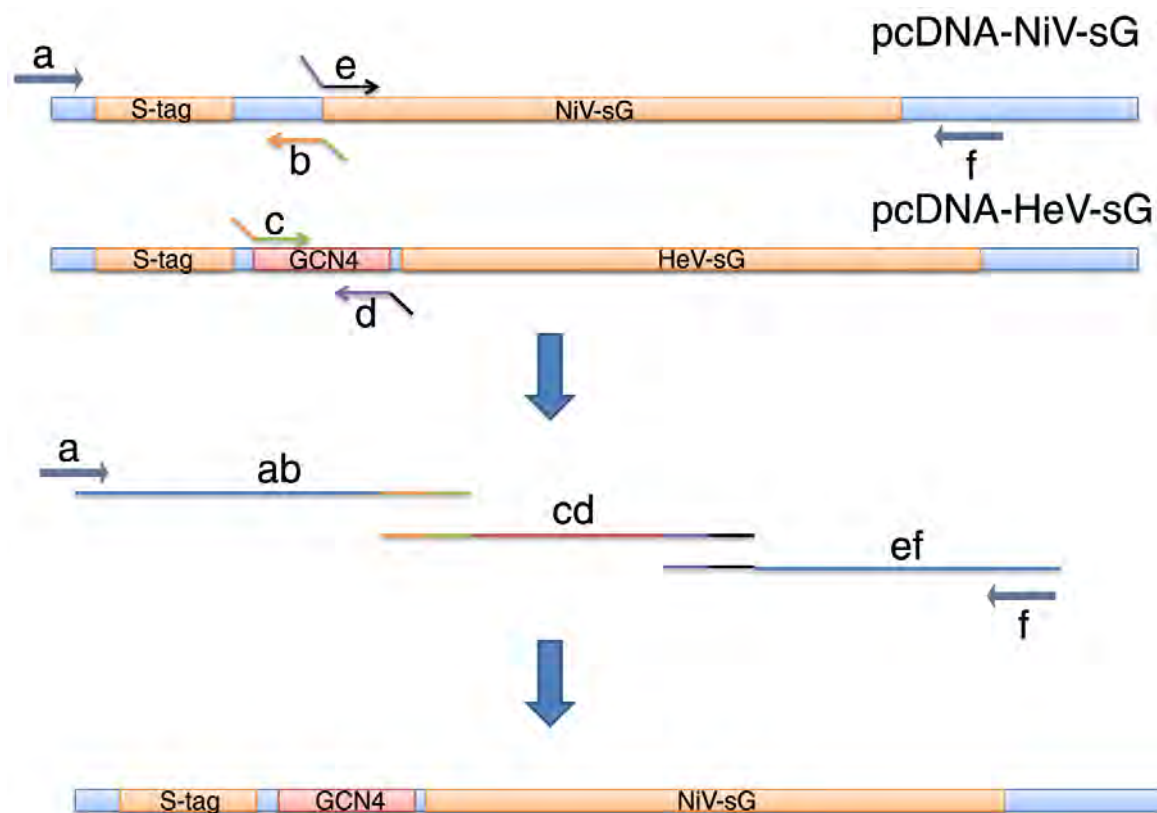
Figure 5: Schematic of overlapping-PCR protocol for GCN4 insertion.
The first round of PCR had three reactions: pcDNA-NiV-sG with primers **a** and **b**, pcDNA-NiV-sG with primers **e** and **f** and pcDNA-HeV-sG with primers **c** and **d**. Primers **b** and **c** share 5' GCN4 (green) and upstream NiV-sG (orange) sequences. Primers **d** and **e** share 3' GCN4 (purple) and 5' NiV-sG (black) sequences. The products from the 3 reactions were mixed and amplified using primers **a** and **f**, resulting in a NiV-sG product that contained the GCN4 sequence.

and the resulting constructs were designated pcDNA-GCN(tet)-HeV-sG-D582N and pcDNA-GCN(tet)-NiV-sG-V507I.

Expression of pcDNA-GCN(tet)-sG constructs

Expression of sG constructs was verified by transient transfections in 293Free cells using xTremegene 9 (Roche, manufacturer's protocol). Lysates and supernatants were collected 48 hours post transfection (hpt) and mixed with S-agarose overnight at 4°C, rotating end-over-end. S-agarose was collected by centrifugation and washed three times with lysis buffer (100mM Tris-HCl, pH 8.0, 100mM NaCl, 1% Triton X-100) before the addition of 2X NuPage LDS Sample Buffer (Invitrogen) containing 5% β-mercaptoethanol (Sigma-Aldrich, St. Louis, MO). Samples were heated at 100°C for 10 min, centrifuged briefly and loaded on a NuPAGE Novex 4-12% Bis-Tris gel (Invitrogen). Following transfer to nitrocellulose, membranes were blocked overnight at 4°C in PBS containing 3% milk (PBS-M) then incubated one hour with α-S-HRP antibody in blocking buffer. Following multiple washes with PBS containing 0.05% Tween (PBS-T) and PBS, membranes were incubated 5 min in SuperSignal West Pico Chemiluminescent substrate (Pierce) and imaged.

Verification of tetrameric oligomerization

Upon determination that the sG constructs were being expressed and secreted, verification of the oligomeric status of these constructs was confirmed by Native-PAGE and cross-linking western blots.

Native-PAGE western blot

Supernatants from 293Free cells transfected with pcDNA3.1-GCN(tet)-HeV/NiV-sG or their respective escape variants were collected 48 hpt mixed with NativePAGE sample buffer and G-250 before being run on a NativePAGE Novex 3-12% Bis-Tris gel (Invitrogen). Controls of 2 µg dimeric HeV/NiV-sG proteins were also tested for comparison. Proteins were transferred to PVDF membrane, fixed, dried and then blocked overnight in PBS-M prior to immunoblotting with 1:15,000 α-S-HRP antibody.

Cross-linking western blot

Supernatants from 293Free cells expressing Tet-HeV/NiV-sG or Tet-D582N/V507I-sG were collected, concentrated with Amicon Ultra 30k filters (4,000 rpm for 10 min) in conjugation buffer (20mM HEPES) and mixed with BS^3 (Pierce) on ice for 1 h with gentle shaking every 15 min (final concentration BS^3 2.17mM).   The reaction was quenched by the addition of 36mM Tris-HCl, pH 7.5 on ice for 15 min followed by overnight incubation with S-agarose at 4°C, rotating end-over-end. S-agarose was washed with lysis buffer prior to the addition of 2X LDS Sample buffer. Samples were boiled, centrifuged and then run on a NuPAGE Novex 3-8% Tris-Acetate gel (Invitrogen) followed by transfer to nitrocellulose membrane and immunoblotting with α-S-HRP antibody.

Western blots – Receptor, m102.4 and m106.3 binding by Tet-sGs

293Free supernatants containing Tet-sG constructs were collected 48 hpt and incubated overnight at 4°C with 2 µg ephrin-B2, ephrin-B3 or m102.4 IgG. The following day G-beads or S-agarose were added to the samples and incubated at room temperature (RT), end-over-end for 45 min. Beads were collected by centrifugation,

washed three times with lysis buffer, and heated with 2X LDS Sample buffer. Samples

were then briefly centrifuged and run on a NuPAGE Novex 4-12% Bis-Tris gel followed

by transfer to nitrocellulose membrane and immunoblotting with α-S-HRP antibody.

For co-immunoprecipitations involving m106.3 the above protocol was followed

with minor modifications. Overnight incubation occurred in the presence of 2 µg m106.3

and 4 µg ephrin-B2 (S-tagged), and m106.3 was precipitated using G-beads.

Stable Cell Line Generation

Stable cell lines expressing Tet-HeV/NiV-sG or their escape variants were

constructed using 293Free cells. In a 6-well plate, cells were transfected with 2 µg

soluble construct (e.g. pcDNA-GCN(tet)-HeV-sG) using xTremegene 9 (Roche,

manufacturer's protocol). Beginning 48 hpt, media was replaced daily with DMEM

containing 5% calf serum and 180 µg/ml hygromycin (DMEM-5/Hygro) (Invitrogen).

When a population of non-transfected cells died while transfected cells survived and

propagated, the cells were transferred to a T-75 flask in DMEM-5/Hygro. After the cells

reached confluency, limiting dilutions were performed to select colonies with high

expression levels of Tet-sG. Briefly, 400 cells were added to a 35 mm well containing 3

ml media. From this well 1ml was transferred to another 35 mm well containing 5 ml

media. Finally 1 ml was transferred from this well to two 35 mm wells containing 9 ml

media. The cells/media in these final two wells were combined and 100 µl was aliquoted

per well into three 96-well plates. These plates were then placed in a 37°C, 5% CO_2

incubator for approximately 2 weeks. Wells containing single-cell colonies were

expanded by transferring the cells to a 24-well plate and allowing them to grow to

confluency. Supernatants were collected and tested for the expression of Tet-sG, and

populations with high levels of expression were expanded into T-75 flasks. Once the cells were confluent, the limiting dilution was repeated. Upon the completion of two limiting dilution steps, cells were grown to confluency and then either used or stored in liquid nitrogen.

Large scale expression and purification of Tet-sGs

Stable cell lines expressing Tet-sGs were grown in shaker flasks in serum free 293 FreeStyle media at a cell density of $1x10^6$ cells/ml for 5 days. Media was collected and centrifuged twice at 3,900 rpm and 10,000 rpm. Supernatant was filtered through 0.2 µm filter and then incubated with S-agarose for 2-3 days at 4°C. Tet- sGs were purified by affinity chromatography with S-agarose (Binding/Wash buffer: 100mM Tris-HCl, pH 7.5, 500mM NaCl, 0.1% Triton X-100) and eluted multiple times using 0.2 M citric acid, pH 2.0. Eluates were neutralized to pH 7.0 with 1M Tris-HCl, pH 8.0 and concentrated and buffer exchanged into PBS using Amicon Ultra 30k filter units at 4,000 rpm for 10min. Concentrate was further filtered through a 0.22 µm filter and then underwent size-exclusion chromatography using a calibrated HiLoad 16/60 Superdex 200 Gel filtration column. Fractions of 1 ml were collected and tested by Native-PAGE coomassie and western blot. Fractions containing Tet-sG were pooled, concentrated using Amicon Ultra 30k filters and stored at -80°C.

Tet-sGs binding receptors and m102.4

A number of different assays were used to determine the binding characteristics of ephrin-B2, ephrin-B3, m102.4 and the conformation-dependent antibody m106.3 to all four Tet-sGs.

Enzyme linked immunosorbent assays (ELISAs)

Tet-sGs were coated overnight at 4°C on a ½-well ELISA plate at 50 ng/well in 50 µl coating buffer (18.2mM Na_2Co_3, 45.3mM $NaHCO_3$ in PBS). Wells were blocked with PBS-M, washed three times with PBS-T and then incubated for 1 h at RT with increasing concentration of ephrin-B2, ephrin-B3 or m102.4. Following three more washes with PBS-T, 1:5000 α-Fc-HRP (ephrins) or 1:1000 α-Flag (m102.4) antibodies were added and incubated for 1h at RT. Wells were washed three times with PBS-T and then 50 µl/well ABTS substrate was added and incubated for 30 min RT. Colorimetric change was measured using a VersaMAX plate reader (Molecular Devices, Sunyvale, CA) at 405 nm.

Conversely, some ELISAs had 50 ng/well ephrin-B2 or ephrin-B3 coated on the plate. Increasing concentrations of Tet-sGs were added following the protocol outlined above, and bound Tet-sGs were detected using 1:5000 α-S-HRP antibody.

Additionally, ELISAs measuring m106.3 binding to Tet-sGs followed the protocol above with the following modifications: (a) constant concentration of m106.3 Fab was added with increasing concentrations of ephrin-B2 and (b) bound m106.3 was determined using 1:1000 α-Flag-HRP antibody.

Surface Plasmon Resonance

The binding kinetics of the Tet-sGs to m102.4 and ephrin-B2 were measured by bio-layer interferometry on a BLItz instrument (ForteBio, Menlo Park, CA). Ni-NTA biosensors were used to immobilize the hexa-Histidine fused m102.4 and ephrin-B2 proteins. Kinetic parameters (k_{on} and k_{off}) and binding affinities (KD) were calculated

from a non-linear fit of the BLItz instrument data using the BLItz software. (Method modified from (207))

m102.4 VARIANTS

m102.4 variant generation and Fab expression

Variants of m102.4 were constructed with multiple mutagenic primer sets (Table 2) with pCOMB3X-m102.4 as the starting template using Quick-Change mutagenesis (Agilent Technologies, manufacturer's protocol). Mutation of variants was confirmed by sequencing. Variant Fabs were expressed by transforming plasmids into HB2151 E. coli cells. Colonies were cultured in 1 ml 2YT media containing 0.2% glucose and 50 μg/ml carbenicillin until log phase growth was reached. Then 500 μl of the culture was used to inoculate 200 ml 2YT/carbenicillin/glucose, and cells were grown until $OD_{600} = 0.6$-0.8, at which point IPTG (600 μM) was added and cultures were incubated overnight in 30°C shaking incubator.

The following day, cultures were collected, centrifuged at 1500 rpm for 15 min and resuspended in 25 ml PBS containing 0.1 mg polymixin B (Invitrogen) and complete anti-protease tablet (Roche) for 1 h at room temperature with rotation. Suspensions were then centrifuged for 30 min at 10,000 rpm, and supernatants were collected. Ni-NTA columns were prepared by adding PBS and 0.5 ml Ni-NTA beads to the column followed by a PBS wash. Imidazole (10 mM) and NaCl (0.3 M) were added to the supernatants containing m102.4/variant Fabs, which were then added to the prepared Ni-NTA column. The column was then washed with PBS, followed by three washes with washing buffer (10 mM Imidazole and 0.3 M NaCl in PBS) before Fabs were eluted by the addition of 200 mM Imidazole. Fabs were then concentrated and PBS buffer exchanged using

Table 2: m102.4 variants and primers.
 The amino acid sequence for m102.4 is shown with the variants' mutations highlighted in red. The corresponding forward mutagenic primers are also shown with the mutation also shown in red. The variants are classified as "single mutation" or "multiple mutation" variants.

Abbreviation	A.A. Sequence	Forward Primer
m102.4	LAPHPS	n/a
Ephrin-B2	FSPNLW	n/a
Ephrin-B3	YSPNLW	n/a
Single Mutation		
LD	**D**APHPS	GGG AGG GAG CAG **GAC** GCC CCC CAT CC
LF	**F**APHPS	GGG AGG GAG CAG **TTC** GCC CCC CAT C
LA	**A**APHPS	GGG AGG GAG CAG **GCC** GCC CCC CAT CC
PA	LA**A**HPS	GAG CAG CTC GCC **GCC** CAT CCG TCC C
HA	LAP**A**PS	GAG CAG CTC GCC CCC **GCT** CCG TCC CAA TAT TAC
HN	LAP**N**PS	GGA GCA GCT CGC CCC C**AA T**CC GTC CCA ATA TTA C
LY	**Y**APHPS	GGG AGG GAG CAG **TAC** GCC CCC CAT C
Multiple Mutation		
F&L	**F**APH**L**S	G**TT C**GC CCC CCA T**CT G**TC CCA ATA TTA C
FP	**F**A**A**HPS	GAG CAG **TTC** GCC **GCC** CAT CCG TCC C
YP	**Y**AP**A**PS	GAG CAG **TAC** GCC CCC **GCT** CCG TCC CAA TAT TAC
AW	LAP**A**P**W**	GCT CGC CCC C**GC T**CC G**TG G**CA ATA TTA CTA CTA C
YA	**Y**A**A**HPS	GAG CAG **TAC** GCC **GCC** CAT CCG TCC C
F/L/W	**F**APH**LW**	G **TTC** GCC CCC CAT **CTG TGG** CAA TAT TAC TAC TAC

FA	**F**A**A**HP**W**	G**TT** **C**GC C**GC** **C**CA TCC G**TG** **G**CA ATA TTA CTA CTA C
YW	**Y**AP**A**P**W**	G**TA** **C**GC CCC C**GC** **T**CC G**TG** **G**CA ATA TTA CTA CTA C
FW	**F**AP**A**P**W**	GGG AGG GAG CAG **TTC** GCC CCC **GCT** C
F_PNLW	**F**AP**NLW**	GGA GCA G**TT** **C**GC CCC C**AA TCT GTG G**
SLP	**F**S**P**N**P**W	GCA G**TT CTC C**CC C**AA** T**CC** G**TG** **G**CA ATA TTA CTA CT
FSPNLW	**FSPNLW**	GGA GCA G**TT CTC C**CC C**AA TCT GTG G**

51

Amicon Ultra 10k filter units, centrifuging 4000 rpm for 10 min. Concentrated Fab was collected, quantitated and stored -80°C.

ELISAs

Binding ELISAs

Half-well ELISA plates were coated overnight at 4°C with 50 ng/well Tet-sG in 50 μl coating buffer. The next day, wells were washed three times with 0.05% PBS-T and blocked with 3% PBS-M at room temperature for 2-3 h. Wells were washed again and then increasing concentrations of m102.4/variant Fabs were added in triplicate, 50 μl per well, and incubated at room temperature for 1 h, followed by washing with PBS-T. Bound variants were detected by incubating wells with 1:1000 α-Flag-HRP for 1 h, followed by washing and incubation with ABTS for 30 min. Colorimetric change was measured using a VersaMAX plate reader at 405 nm.

Competition ELISAs

Half-well ELISA plates were coated overnight at 4°C with 50 ng/well ephrin-B2 or ephrin-B3 in coating buffer. Plates were washed with PBS-T, blocked with PBS-M and then incubated for one hour with 0.5 ng/μl Tet-sG in the presence of increasing concentrations of m102.4 variants (Fabs). The amount of Tet-sG bound to ephrin-B2/B3 was determined by the addition of 1:5000 α-S-HRP antibody or 1:5000 polyclonal rabbit α-G and 1:10,000 Goat-α-rabbit-HRP antibodies. The substrate ABTS was added for 30 min at room temperature, and colorimetric change was measured using a VersaMAX plate reader at 405 nm.

Cell-Cell Fusion Assays

Cell-cell fusion assays were performed as previously described (14). HeLa-USU effector cells were transfected with 2 μg pcDNA-HeV/NiV-G and 2 μg pcDNA-HeV/NiV-F (or the respective m102.4 escape variants) using xTremegene 9 (Roche, manufacturer's protocol). At 24 hpt cells were infected with recombinant vaccinia encoding bacteriophage T7 RNA polymerase (vTF7.3) at a multiplicity of infection (MOI) of 10 and placed in 37°C incubator for approximately 6 h. HeLa-ATCC target cells were seeded in a 6-well plate and grown 24 h at 37°C before being infected at a MOI of 10 with recombinant vaccinia encoding *E. coli*. *Lac*Z gene (β-galactosidase) under the control of a T7 promoter (vCB21R). Cells were incubated at 37°C for 6 h. Following 37°C incubation, all cells were washed, supplied with fresh media and incubated overnight at 31°C.

The next day, cells were washed, counted and resuspended at 2×10^6 cells/ml in DMEM-10 containing cytosine arabinoside (AraC) to reduce background β-galactosidase expression by preventing vaccinia superinfection. Effector and target cells were combined in a 96-well plate at a ratio of 1:1 (total 200,000 cells/well). Prior to the addition of target cells, m102.4, m102.4 variants and ephrins were added in duplicate at a final concentration of 50 μg/ml. Cells were incubated at 37°C for 3 h, lysed with 20 μl NP-40 and stored overnight at -80°C. The following day, lysates were thawed and 50 μl lysate was combined with 50 μl 2X chlorophenol red-ß-D-galactopyranoside (CPRG). Kinetic analysis of colorimetric change was measured using a VersaMAX plate reader at 570 nm for 15 min with readings every 20seconds.

For cell-cell fusion assays comparing m102.4 IgG and Fab with HeV-G and HeV-G-D582N, the above protocol was followed except various concentrations of m102.4 IgG and Fab were added in duplicate to the effector cells prior to the addition of target cells.

Identification of new escape variants using LF, LD, HA and SLP

The protocol used to generate the original m102.4 escape variants of HeV/NiV-G was followed with modifications to generate escape variants to m102.4 variants LF, LD, HA and SLP (207). Briefly, 50,000 PFU of NiV Malaysia (NiV$_M$) or HeV were incubated with 10 µg of each Fab in 100 µl of total volume for 1 h at 37°C with rocking every 15 min. The volume of the virus-Fab mixture was then raised to 200 µl by addition of DMEM-10 and incubated on Vero 76 cells in a 35 mm well, rocking every 15 min for 1 h at 37°C. After the inoculum was removed, DMEM-10 containing the same concentration of Fab as the final of the inoculum (100 µg in 2000 µl) was added and supernatants were collected 72 hours post infection (hpi).

For the second and third passages, 5,000 PFU of NiV$_M$ or HeV from the previous passages were used, following the protocol for the first passage. Supernatant titers were determined after all passages by plaque assays with Vero 76 cells. Second passage supernatants were titered by plaque assay with Vero 76 cells. Briefly, increasing 10-fold dilutions of the samples were adsorbed to Vero cell monolayers in duplicate wells (200 µl).

Virus from the third passage was diluted to approximately 100 PFU and incubated with 10 µg of each Fab in 100 µl of total volume for 1 h at 37°C with rocking every 15 min. The volume of the virus-Fab mixture was then raised to 200 µl by addition of DMEM-10 and incubated on Vero 76 cells in a 35 mm well, rocking every 15 min for 1 h

at 37°C. Cells were then overlayed with 0.9% agarose EMEM and observed for plaque

formation 24 to 48 hours post-overlay. Five plaques per Fab, per virus were picked using

a P1000 pipette tip and placed into 500 µl of DMEM-10 and allowed to diffuse for 10

min at room temperature and then placed at -80°C.

Plaque purified virus preparations were used to inoculate Vero 76 cells by rocking

every 15 min for an hour at 37°C. After the inoculum was removed, DMEM-10 was

added and supernatants were collected 72 hpi, and 200 µl of supernatants were placed

into 1ml of Trizol LS for RNA extraction (Life Technologies, manufacturer's

instructions). RNA was reconstituted into 30 µl of nuclease-free dH$_2$O.

This RNA was converted to cDNA using One-Step RT-PCR kit (Qiagen,

manufacturer's protocol) and HeV/NiV-G specific primers (HeV Forward: 5'-

GCTTCTTCAAGAGCCTGTCTC-3,' HeV Reverse: 5'-

GCACTTTTGGTCAATCAACTC-3,' NiV Forward: 5'-

CGTACTGATTGATCTGCTTG-3,' NiV Reverse: 5'-CATCACATGTCTTTGTACG-

3'). RT-PCR products were run on a 1% agarose gel, and in some cases re-amplified

with the same primers used for RT-PCR. Products were cloned into Blunt-TOPO

(Invitrogen) and transformed in Top 10 cells (Invitrogen). Individual colonies were

grown in culture, mini-prepped and sequenced using M13F and M13R primers.

EFFECT OF EPHRIN-B2 AND M102.4 ON TET-SGS

Binding ELISAs

Tri-HeV/NiV-sF and Tet-sGs

Half-well ELISA plates were coated with 125 ng/well Tri-HeV/NiV-sF in coating

buffer and incubated overnight at 4°C. Plates were then blocked with PBS-M for 2 h at

RT followed by washing with PBS-T. Tet-sGs were added at 1 μg/well with or without

the addition of increasing concentrations of ephrin-B2, ephrin-B3 or m102.4 (Fab or

IgG), incubated at RT for 1 h followed by PBS-T wash. Detection of bound Tet-sG was

determined by incubation with either 1:5000 α-S-HRP antibody or 1:5000 polyclonal

rabbit α-G Abs and 1:10,000 Goat-α-Rabbit-HRP antibody. Substrate ABTS was added

for 30 min, and colorimetric change was measured at 405 nm using a VersaMAX plate

reader.

m102.4 and Tet-HeV/D582N-sG

ELISA plates were coated with 50 ng/μl m102.4 IgG and incubated overnight at

4°C. The next day, solution was removed, and wells were blocked with PBS-M,

followed by PBS-T wash. Tet-HeV/D582N-sGs were added at 0.5 ng/μl, incubated RT 1

h and then washed with PBS-T. The wells were then incubated 1 h RT with 0.08 ng/ul

m106.3 Fab in the absence or presence of 8 ng/ul ephrin-B2. Following PBS-T wash,

bound m106.3 was determined using 1:1000 α-Flag-HRP antibody and ABTS substrate

as described for ELISAs mentioned previously.

m102.4 and ephrin-B2 binding Tet-sGs – Sequential

Tet-sGs were coated at 50 ng/well in 96 ½-well ELISA plate in 50 μl coating

buffer and incubated overnight at 4°C. The next day wells were blocked with PBS-M,

washed with PBS-T and then incubated 1 h RT with either 8 ng/μl ephrin-B2 or 8 ng/μl

m102.4 Fab. Wells were then washed with PBS-T and incubated 1 h RT with the

opposite ligand or PBS. Bound ephrin-B2 was determined using 0.3 ng/μl biotinyalted

α-B2 antibody (m150.8) and 1:5000 Streptavidin-HRP, and bound m102.4 was

determined using 1:1000 a-Flag-HRP antibody.

m102.4 and ephrin-B2 binding Tet-sGs – Simultaneous

The protocol for measuring sequential binding of ephrin-B2 and m102.4 was followed with the following exceptions. After the blocking and first wash, Tet-sGs were incubated with either (a) 8 ng/μl ephrin-B2, (b) 8 ng/μl m102.4 Fab, (c) 8 ng/μl ephrin-B2 and 8 ng/μl m102.4 Fab, (d) 6 ng/μl ephrin-B2 and 2 ng/μl m102.4 Fab or (e) 2 ng/μl ephrin-B2 and 6 ng/μl m102.4 Fab. Bound ephrin-B2 and m102.4 were determined as indicated above.

Chapter 3: Generation of Soluble, Tetrameric Versions of HeV/NiV-G

INTRODUCTION

The generation of recombinant soluble Hendra and Nipah G glycoproteins has greatly aided our understanding of henipavirus attachment and fusion and has led to the development of therapeutics that prevent and constrain viral infection. Soluble HeV-G (HeV-sG) has been shown to retain receptor binding abilities, induce an antibody response in rabbits and protect ferrets, African green monkeys and horses from infection as a subunit vaccine (recently licensed and released in Australia as Equivac HeV®) (15; 19; 29; 142). Despite these accomplishments, HeV-sG and NiV-sG lack an important characteristic of their native full-length counterparts – expression and oligomerization into a stable tetrameric conformation.

The construction of HeV/NiV-sGs required the deletion and replacement of the cytoplasmic and transmembrane domains with an Igκ leader sequence (secretion) and a S-tag (detection and purification) (Figure 6A). However, unlike native HeV/NiV-Gs, which are expressed on viral/cell membranes exclusively as tetramers, the majority of HeV/NiV-sGs are expressed as dimers (15). This lack of complete physiological resemblance to full-length HeV/NiV-Gs limits the full potential of HeV/NiV-sGs. A study by McGinnes *et al*. demonstrated that mutation of the transmembrane domain of NDV-HN resulted in a loss of tetrameric conformation and a decrease in fusion promotion (116). Similarly, the tetrameric conformation of HeV/NiV-Gs may be essential for viral infectivity, and critical components of receptor attachment and fusion may be missed by studying non-tetrameric HeV/NiV-sGs.

The expression of HeV/NiV-sGs occurs primarily as dimers, but tetrameric

conformations are detected, suggesting that the bonds required for maintaining a

Figure 6. Models of full-length and soluble attachment glycoproteins of HeV.
(**A**) Full-length schematic of HeV-G monomer with cytoplasmic tail,
transmembrane domain, stalk and globular head indicated. Beta sheets in the
globular head are color-coded with disulfide bonds in both the globular head and
stalk shown as dashed lines. Transformation of full-length HeV-G monomer to
soluble HeV-G monomer occurs by replacement of the cytoplasmic tail and
transmembrane domains with Igκ leader sequence and S-tag, respectively. The
genetic layout for soluble HeV-G is shown below the figures. (**B**) The difference
between soluble HeV-sG and soluble, tetrameric HeV-G is the GCN4 motif at the
5' end of the stalk, which is represented by a blue column. The genetic layout,
including the sequence of GCN4, is shown below the figure. Figure modified
from (15; 72).

A.

β3 β4

β2

β6S4 β1 β5 β6

Globular Head

C-term

Disulfide bonds

Stalk

Transmembrane

Cytoplasmic Tail

N-term

C-term

Disulfide bonds

Stalk

S-tag

IgK Leader Sequence

XhoI

ApaI

HeV/NiV-sG

Ig κ-chain Leader Sequence – METDTLLLWVLLLWVPGSTGD (21aa)

2 aa linker – AA

S-tag – KETAAAKFERQHMDS (15aa)

B.

C-term

Disulfide bonds

Stalk

GCN4

S-tag

IgK Leader Sequence

XhoI

ApaI

HeV/NiV-sG

Ig κ-chain Leader Sequence – METDTLLLWVLLLWVPGSTGD (21aa)

2 aa linker – AA

S-tag – KETAAAKFERQHMDS (15aa)

GCN4 – MKQIEDKLEEIESKLKKIENELARIKK (27aa)

60

tetrameric conformation are not stable. Therefore, a motif needed to be added that would strengthen or substitute for any interactions that have been lost or weakened by converting HeV/NiV-Gs to soluble constructs. A review of current soluble viral glycoproteins reveals two primary motifs that are used for stabilizing and/or forming soluble oligomeric structures – *S. cerevisiae* transcription factor GCN4 and T4 bacteriophage Fibritin (89; 174; 208; 209).

Bacteriophage T4 Fibritin is a structural chaperone protein that contains a coiled-coil motif that results in trimerization (184). While T4 Fibritin has been useful for stabilizing several different soluble viral glycoproteins, such as HIV gp140 and Rabies glycoprotein, its ability to form trimers but not tetramers makes it ineffective for correct oligomerization of HeV/NiV-sGs. The transcription factor GCN4, however, contains a dimeric leucine zipper motif that upon expression creates stable coiled-coil structures (136). These dimeric coiled-coil structures consist of two 7-mer alpha-helices that associate due to interactions between non-polar residues on one side of each alpha-helix, which can be seen in the helical wheel schematics (Figure 7A-C). Harbury *et al*. determined that specific non-polar residues in the 'a' and 'd' positions of the helical wheel influence the oligomerization of the alpha helices, allowing for dimeric, trimeric or tetrameric conformations (64; 65). The specific residues required for each oligomerization state are shown in Figure 7D.

Given that the tetrameric structure of HeV/NiV-Gs may be essential for receptor-induced conformational change that leads to F activation and fusion, we constructed and characterized soluble, tetrameric versions of HeV/NiV-Gs by inserting the GCN4(tet) motif immediately upstream of the HeV/NiV-sG sequence. These tetrameric soluble

constructs were then characterized for oligomeric expression, receptor binding, m102.4

binding and receptor-induced conformational changes.

A.

B.

C.

D.

GCN4 Residue	Dimer (pIL)	Trimer (pII)	Tetramer (pLI)
Residue at a	I	I	L
Residue at d	L	I	I
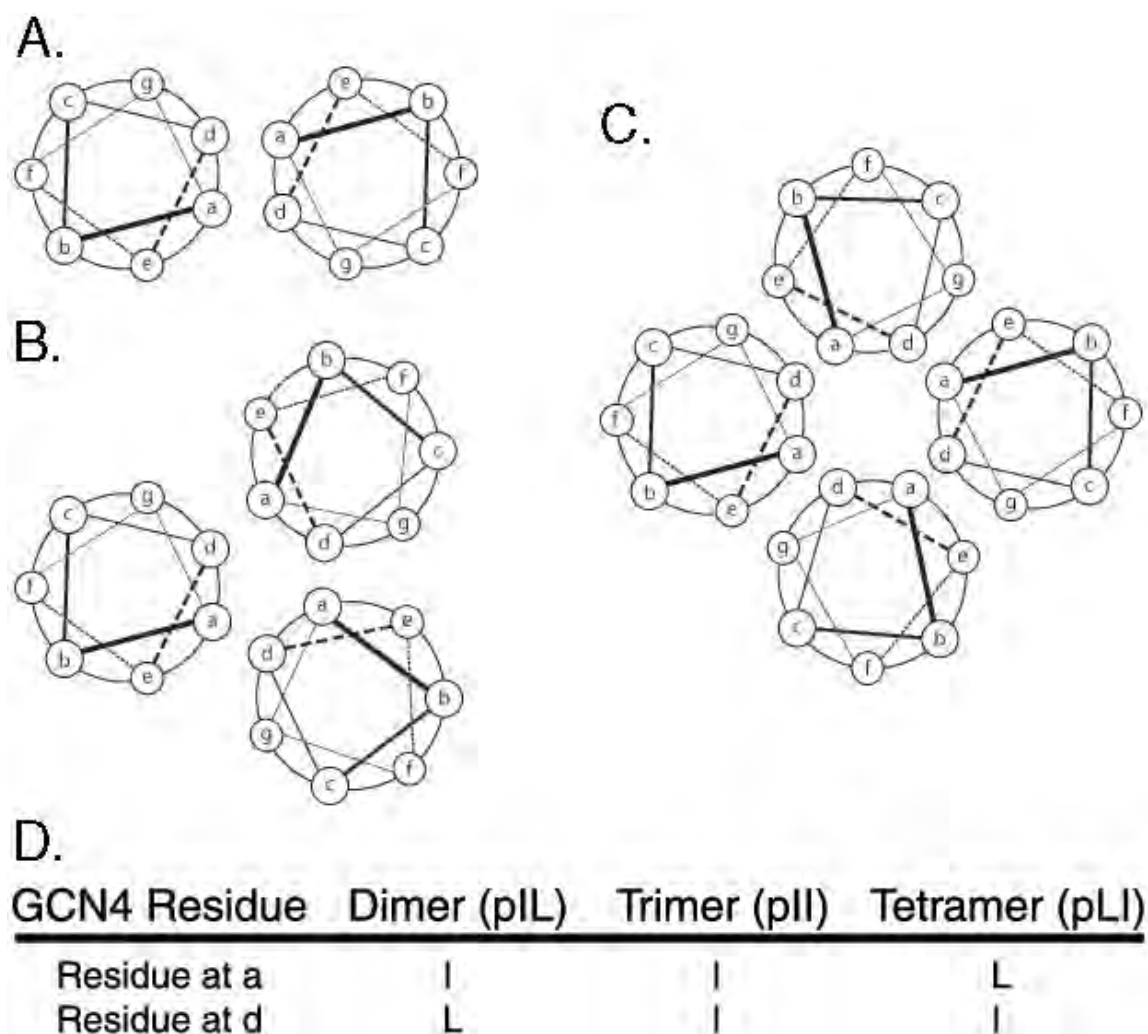
Figure 7. Configuration of GCN4 motif variations.
Helical wheel representations of GCN4 motif, showing the association between the non-polar 'a' and 'd' residues in **(A)** dimer, **(B)** trimer or **(C)** tetramer conformations. **(D)** Table of the required 'a' and 'd' residues for each of the oligomeric conformations. I – isoleucine. L – leucine.

RESULTS

Addition of GCN4 motif

To improve the efficiency of HeV/NiV-sGs' tetrameric oligomerization the GCN4(tet) motif was inserted into pcDNA-HeV/NiV-sGs immediately upstream of the sG sequence but downstream of the Igκ leader sequence and S-tag (Figure 6B). The GCN4(tet) motif was first added to pcDNA-HeV-sG by restriction enzyme digestion and ligation, and the resulting plasmid pcDNA-GCN(tet)-HeV-sG served as a template for overlapping PCR insertion of the GCN4(tet) motif into pcDNA-NiV-sG. Plasmids were sequenced to verify correct insertion of GCN4, and the resulting constructs were identified as pcDNA-GCN(tet)-HeV/NiV-sG. Proteins expressed from these two constructs will be referred to as Tet-HeV-sG and Tet-NiV-sG.

Expression and verification of tetrameric structure

In order to verify expression of the GCN4 constructs, both plasmids were transiently transfected into 293Free cells, and cellular lysates and supernatants were collected and incubated with S-agarose. Immunoprecipitated (IP'd) Tet-HeV/NiV-sGs were detected by western blots, which revealed bands of approximately 65 kDa in both the lysates and supernatants (Figure 8 A&B). While the size of Tet-HeV-sG appears to be slightly larger than Tet-NiV-sG, both bands are near the predicted molecular weight of a monomeric unit of Tet-HeV/NiV-sG (67 kDa). While protein was detected in both the lysate and supernatant, the presence of higher amounts of Tet-HeV/NiV-sGs in the supernatants indicates that Tet-HeV/NiV-sGs are being expressed and efficiently secreted from the cells.
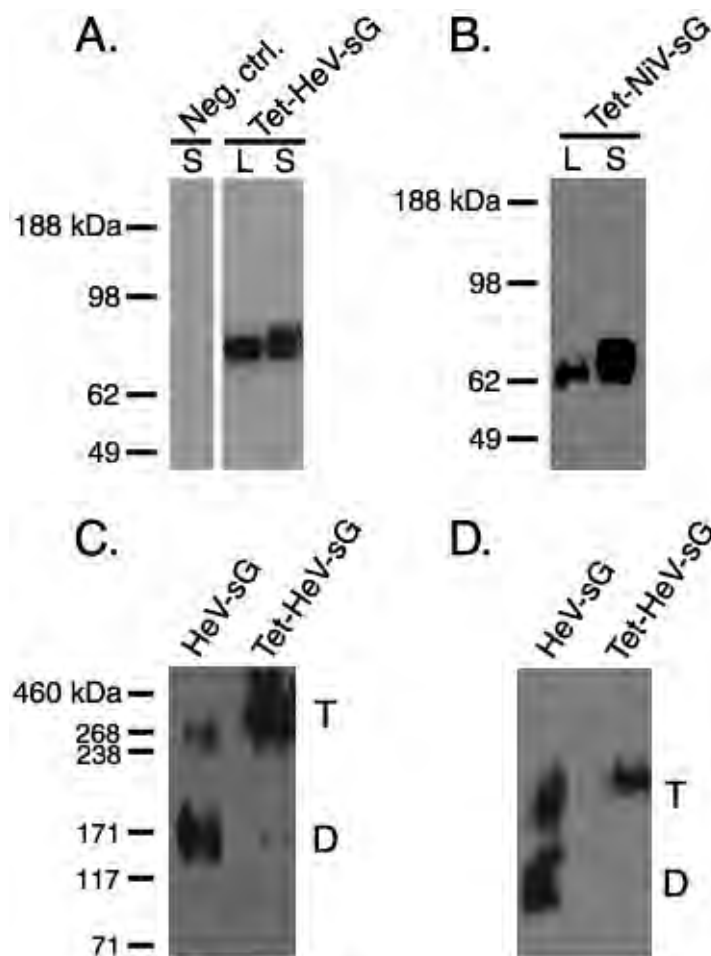
Figure 8: Expression of Tet-HeV/NiV-sGs.
Supernatants and lysates were collected from 293Free cells transfected with **(A)** pcDNA-GCN(tet)-HeV-sG or **(B)** pcDNA-GCN(tet)-NiV-sG. Samples were immunoprecipitated with S-agarose and western blotted using α-S-HRP antibody. **(C)** Supernatants collected from 293Free cells expressing Tet-HeV-sG were cross-linked with BS^3, immunoprecipitated with S-agarose and western blotted using α-S-HRP antibody and compared to cross-linked HeV-sG. **(D)** Native-PAGE analysis of supernatants collected in (C). L-lysate, S-supernatant, T-tetramer and D-dimer.

Cross-linking experiments using BS^3 were then used to verify the oligomerization of Tet-HeV-sG (Figure 8C). A comparison of Tet-HeV-sG to HeV-sG reveals expression of two molecular weight species, which represent dimer (~171 kDa) and tetrameric (~300 kDa) oligomerizations. In contrast to HeV-sG, which is expressed predominantly as a dimer, the vast majority of Tet-HeV-sG is expressed as a tetramer. Additionally, the inability to detect any Tet-HeV-sG between the tetrameric and dimeric bands suggests that Tet-HeV-sG is stable with little to no degradation. The levels of dimeric and tetrameric expression were further confirmed by NativePAGE analysis, which again indicates that HeV-sG is expressed as both a tetramer and dimer while Tet-HeV-sG is expressed almost exclusively as a tetramer (Figure 8D).

Binding Characteristics of Tet-HeV/NiV-sGs

While the addition of the GCN4(tet) motif to HeV/NiV-sGs resulted in expression of tetrameric protein, it needed to be confirmed that Tet-HeV/NiV-sGs retained their abilities to bind receptors ephrin-B2 and ephrin-B3. Tet-HeV/NiV-sGs collected from the supernatants of 293Free cells were co-immunoprecipitated (co-IP'd) with recombinant soluble ephrin-B2 and -B3 (Figure 9 A&C). Both receptors were able to bind and precipitate Tet-HeV/NiV-sGs, verifying that these proteins retain their natural binding abilities.

The human neutralizing antibody m102.4 also binds HeV/NiV-Gs using the same epitope as ephrin-B2 and -B3. Since Tet-HeV/NiV-sGs will be used to further study the neutralizing mechanism of m102.4, it was crucial to demonstrate that Tet-HeV/NiV-sGs maintained their abilities to bind m102.4. Again, co-IPs were used to confirm
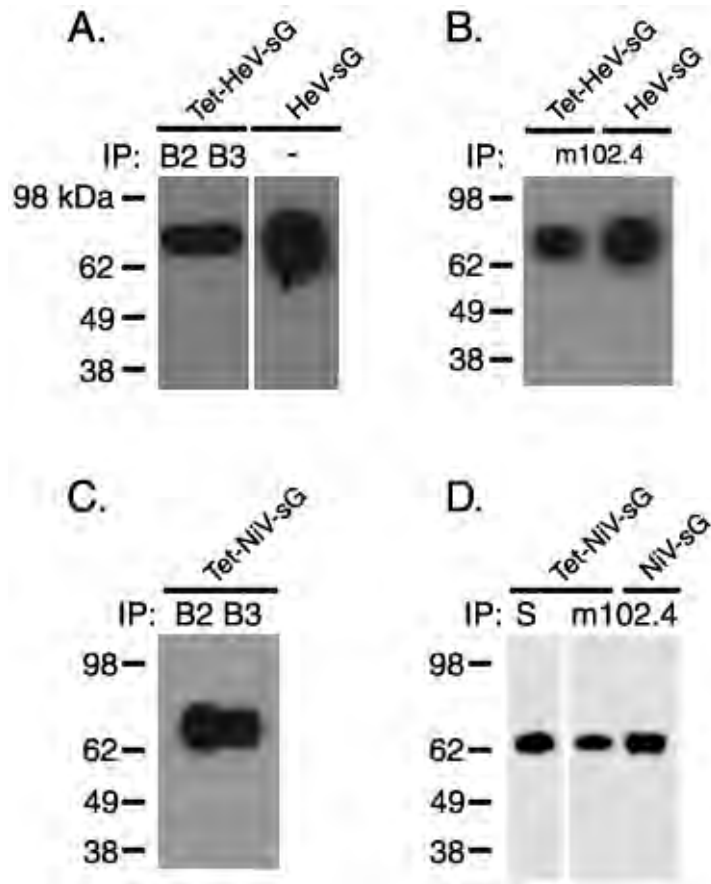
Figure 9: Immunoprecipitation of Tet-HeV/NiV-sGs by receptors and m102.4.
Supernatants from 293Free cells expressing Tet-HeV-sG were
immunoprecipitated alongside HeV-sG with **(A)** ephrin-B2 and ephrin-B3 or **(B)**
m102.4 and then immunoblotted using α-S-HRP antibody. Tet-NiV-sG
supernatants were also immunoprecipitated with **(C)** ephrin-B2, ephrin-B3 and
(D) m102.4 followed by detection with α-S-HRP antibody. Tet-NiV-sG
expression was verified by immunoprecipitation with S-agarose (S).

Tet-HeV/NiV-sGs bind m102.4 similarly to their non-tetrameric counterparts (Figure 9 B&D).

Large scale production of Tet-HeV/NiV-sGs

As Tet-HeV/NiV-sGs are expressed as tetramers and maintain receptor and m102.4 binding, large scale production and purification of Tet-HeV/NiV-sGs was commenced. During this production 293Free cells expressing Tet-HeV/NiV-sGs were grown in shaker flasks for 3-5 days, at which point supernatants were collected and purified by centrifugation and filtration. Following 2-3 day incubation with S-agarose, Tet-HeV/NiV-sGs were first purified by ion-exchange chromatography and then size exclusion chromatography. Fractions of Tet-HeV/NiV-sGs were collected during the size exclusion chromatography and re-tested for tetrameric conformation using Native-PAGE coomassie and western blots.

For example, the diffusion range of Tet-HeV-sG during size exclusion chromatography was narrow (fractions 13-27), and while higher order oligomeric conformations were detected, the majority of Tet-HeV-sG eluted as a tetramer, fractions 19-26 (Figure 10 A&B). Additionally, a comparison of protein samples taken throughout the large-scale production and purification process revealed that a vast majority of the expressed Tet-HeV-sG was collected with little protein loss or degradation during the purification steps (Figure 10C).

Stocks of purified Tet-HeV/NiV-sGs were made and stored at -80°C, and all further experiments involving Tet-HeV/NiV-sGs were performed using purified protein unless otherwise noted.
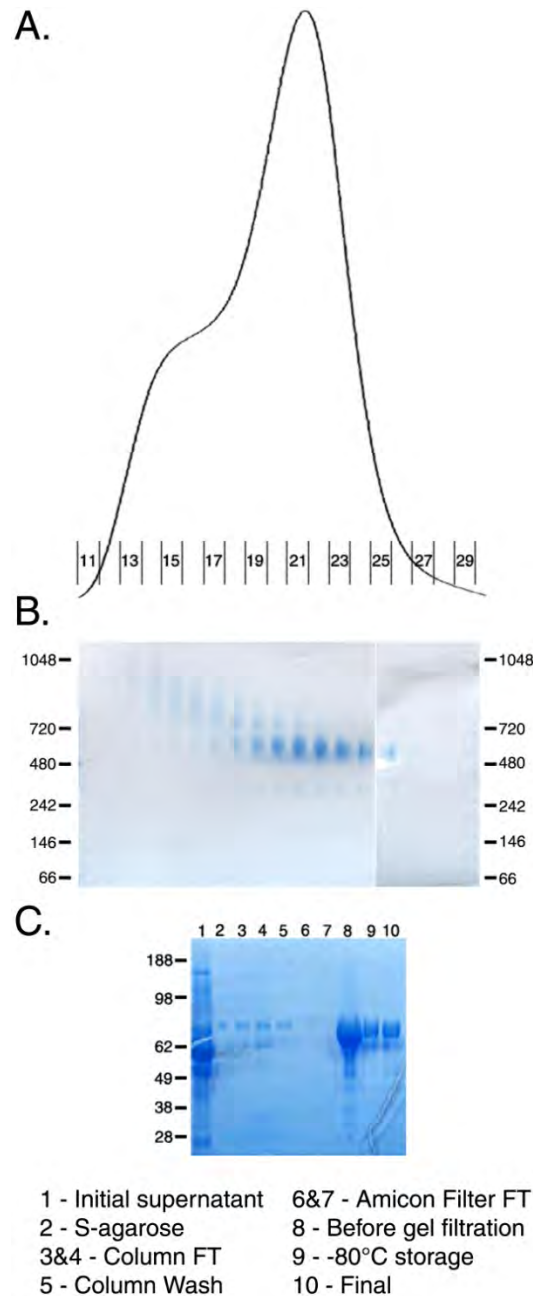
Figure 10: Purification of Tet-HeV-sG.
(A) Size exclusion chromatography analysis of Tet-HeV-sG purified from 293Free cells. Protein was run on a calibrated HiLoad 16/60 Superdex 200 Gel filtration column, and 1ml fractions were collected. UV detection indicates that Tet-HeV-sG was eluted in fractions 12-27. (B) Fractions collected in (A) were run on a Native-PAGE coomassie gel, and Tet-HeV-sG is the band at approximately 520 kDa. (C) Fractions collected throughout the expression and purification of Tet-HeV-sG were run on a denatured coomassie gel, showing that expression, isolation and purification of Tet-HeV-sG yielded a clean, stable final product. FT – flow-through

Binding affinities of Tet-HeV/NiV-sGs to receptors and m102.4

Binding of Tet-HeV/NiV-sGs to receptors and m102.4 was confirmed by testing supernatants containing Tet-HeV/NiV-sGs, but purified Tet-HeV/NiV-sGs allowed us to more quantitatively determine binding affinities of Tet-HeV/NiV-sGs to receptors and m102.4. Surface Plasmon Resonance (SPR) was used to calculate the affinity constants of Tet-HeV/NiV-sGs with ephrin-B2 and m102.4, in which a smaller affinity constant is indicative of stronger binding affinity. The affinity constants for ephrin-B2 and Tet-HeV/NiV-sGs were 17.3 nM and 8.88 nM, respectively, indicating that both Tet-HeV/NiV-sGs have high binding affinities for ephrin-B2 (Table 3).

While both Tet-HeV/NiV-sGs bound ephrin-B2 strongly, they exhibited different binding affinities for m102.4, having affinity constants of 111 nM and 25.5 nM, respectively (Table 3). This difference in binding affinity for m102.4 may explain why m102.4 appears to be more effective at neutralizing NiV rather than HeV infections (218). While the affinity constant for Tet-NiV-sG and m102.4 is three fold greater than for ephrin-B2, it is still extremely low, indicating that there is a strong binding affinity between Tet-NiV-sG and m102.4. The affinity constant for Tet-HeV-sG and m102.4 is 6.5 fold greater than with ephrin-B2, suggesting that Tet-HeV-sG has stronger binding with receptor than with m102.4. Again, it should be noted that despite the difference in affinity constants for Tet-HeV-sG with ephrin-B2 and m102.4, both affinity constants are in the nanomolar range, indicating there is strong binding between Tet-HeV-sG and the two ligands.

Table 3: Binding affinities of Tet-sGs to ephrin-B2 and m102.4.

      Surface plasmon resonance was used to determine the binding affinities between Tet-sGs and ephrin-B2 and m102.4. Graphical representation of the affinity constants is shown below the graph.

		K_{D*} (M)	k_{on} (1/Ms)	k_{on} error	k_{off} (1/s)	k_{off} error
m102.4	NiV-sG	2.55E-08	1.37E+05	3.09E+03	3.49E-03	1.25E-04
	NiV-sG-V507I	7.31E-09	1.61E+05	3.56E+03	1.18E-03	6.81E-05
	HeV-sG	1.11E-07	2.75E+04	6.84E+02	3.05E-03	9.48E-05
	HeV-sG-D582N	3.00E-07	1.43E+04	4.50E+02	4.29E-03	1.37E-04
Ephrin-B2	NiV-sG	8.88E-09	1.66E+05	2.24E+03	1.48E-03	4.37E-05
	NiV-sG-V507I	3.62E-09	1.59E+05	2.05E+03	5.76E-04	3.61E-05
	HeV-sG	1.73E-08	7.22E+04	9.04E+02	1.25E-03	3.73E-05
	HeV-sG-D582N	2.36E-08	4.42E+04	5.15E+02	1.04E-03	3.28E-05

* $K_D = k_{off}/k_{on}$
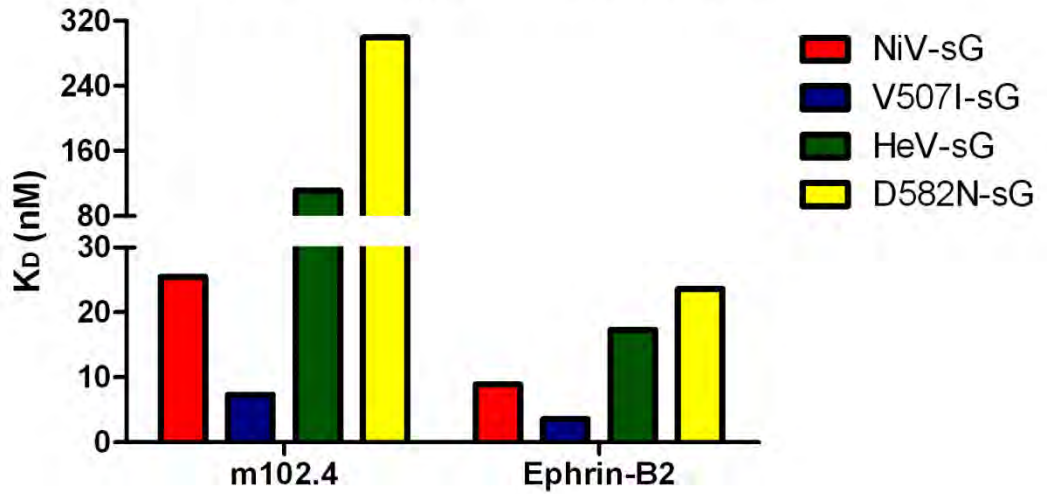
Conformational change associated with receptor binding

It was previously shown that the conformation-dependent human mAb m106.3 is only able to bind full-length HeV/NiV-Gs in the presence of receptor, meaning the epitope of m106.3 is exposed on HeV/NiV-Gs only after receptor-induced conformational changes occur (72). To further verify the correct expression and conformation of Tet-HeV/NiV-sGs, ELISAs and IPs were used to determine the binding pattern of m106.3 Fab (Flag-tagged) to Tet-HeV/NiV-sGs in the presence and absence of ephrin-B2. To serve as a control for Tet-HeV-sG, full-length HeV-G was also tested, having been expressed in USU cells, lysed and IP'd with m106.3 in the presence and absence of ephrin-B2. Very little to no HeV-G bound m106.3 in the absence of receptor, but upon addition of ephrin-B2, a large band representing m106.3-bound-HeV-G can be detected (Figure 11A). In comparison to full-length HeV-G, Tet-HeV-sG bound m106.3 in the absence of receptor, but the level of IP'd Tet-HeV-sG increased upon addition of ephrin-B2.

To obtain more quantitative results and to test both Tet-HeV/NiV-sGs, binding ELISAs were used. Tet-HeV/NiV-sGs coated on an ELISA plate were incubated with a constant concentration of m106.3 Fab mixed with increasing amounts of ephrin-B2, and bound m106.3 was measured using α-Flag antibody (Figure 11B). Corroborating the IP data, m106.3 demonstrated an ability to bind Tet-HeV/NiV-sGs even in the absence of ephrin-B2. Although the level of bound m106.3 remained relatively constant, there was a significant increase in the amount of m106.3 bound to Tet-HeV/NiV-sGs when increasing concentrations of ephrin-B2 were added.
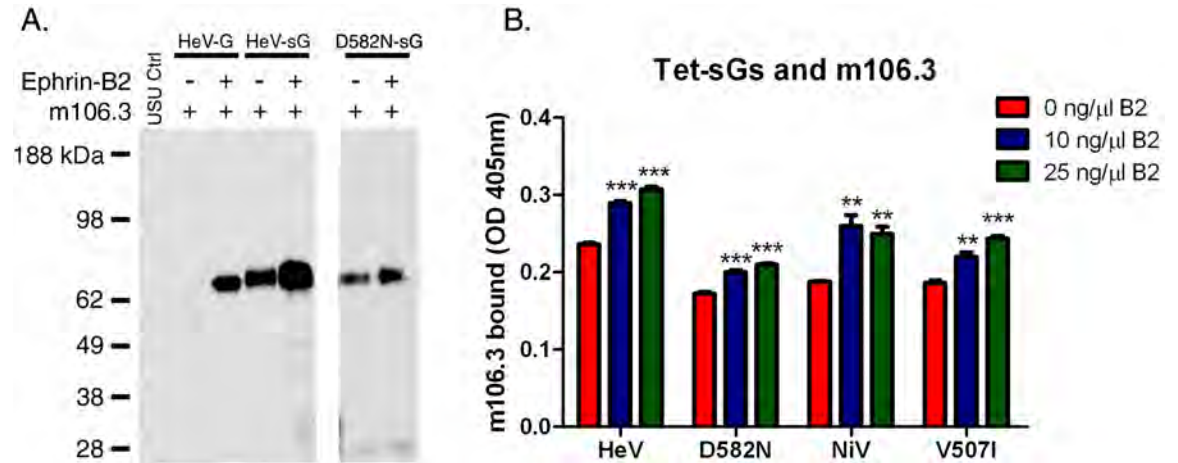
Figure 11: Pattern of m106.3 binding to Tet-sGs.
(A) Purified Tet-HeV-sG and Tet-D582N-sG along with lysate of USU cells expressing HeV-G were immunoprecipitated with m106.3 in the absence and presence of ephrin-B2. Levels of G/sG bound to m106.3 were determined by SDS-PAGE followed by western blotting with various α-G antibodies.
(B) Levels of m106.3 bound to all 4 Tet-sGs as determined by ELISA with Tet-sGs bound to the plate and incubated with m106.3 in the presence of increasing concentrations of ephrin-B2. One-way Anova statistics, **<0.005, ***<0.0001

Escape variants of Tet-HeV/NiV-sG: Tet-HeV-sG-D582N and Tet-NiV-sG-V507I

HeV/NiV m102.4 escape variants were generated by serially passaging virus in sub-neutralizing concentrations of m102.4. Upon sequencing of HeV/NiV-Gs, it was determined that a single amino acid mutation in HeV/NiV-Gs enabled these variants to escape m102.4 neutralization without any concomitant loss of viral fitness (207). It was decided to construct recombinant soluble, tetrameric versions of these escape glycoproteins to study how the single amino acid changes resulted in m102.4 escape.

The escape variant of HeV-G and NiV-G, HeV-G-D582N and NiV-G-V507I, respectively, were constructed by mutating pcDNA-GCN(tet)-HeV-sG and pcDNA-GCN(tet)-NiV-sG. Upon sequence verification, these constructs were expressed in 293Free cells, and Tet-D582N-sG and Tet-V507I-sG were collected from the supernatants (Figure 12A). Similar to their wild type counterparts, Tet-D582N/V507I-sGs are expressed as ~65 kDa monomeric units that readily oligomerize into tetramers as confirmed by cross-linking experiments with BS^3 (Figure 12B).

Receptor binding

Binding of Tet-D582N-sG and Tet-V507I-sG to receptors ephrin-B2 and ephrin-B3 was confirmed by co-IP and ELISA. Supernatants containing Tet-D582N-sG and Tet-V507I-sG were collected and precipitated with ephrin-B2 and -B3, and Tet-D582/V507I-sGs were detected by western blot, confirming the ability of Tet-D582N/V507I-sGs to bind receptors (Figure 13 A&B). Stocks of purified Tet-D582N/V507I-sGs were then produced and used for subsequent testing.
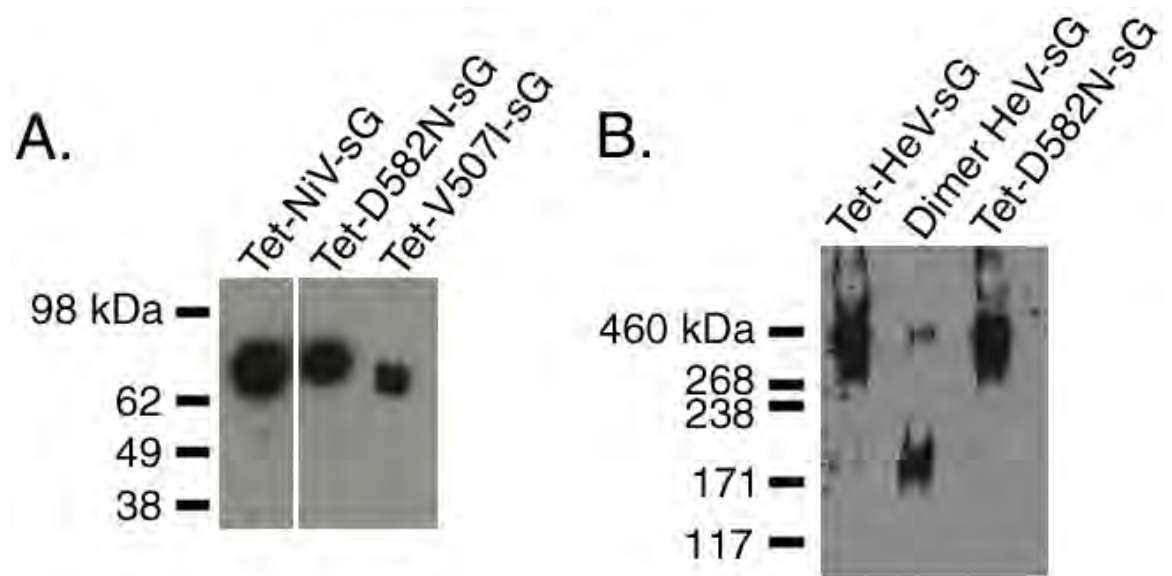
Figure 12: Expression and tetrameric status of Tet-D582N-sG and Tet-V507I-sG.
(A) Supernatants collected from 293Free cells expressing Tet-NiV-sG, Tet-D582N-sG and Tet-V507I-sG were immunoprecipitated with S-agarose, run on a denaturing gel and then immunoblotted using α-S-HRP antibody.
(B) Supernatants containing Tet-HeV-sG and Tet-D582N-sG along with purified Dimer HeV-sG were cross-linked with BS³, immunoprecipitated with S-agarose, run on a non-denaturing gel and detected with α-S-HRP antibody.
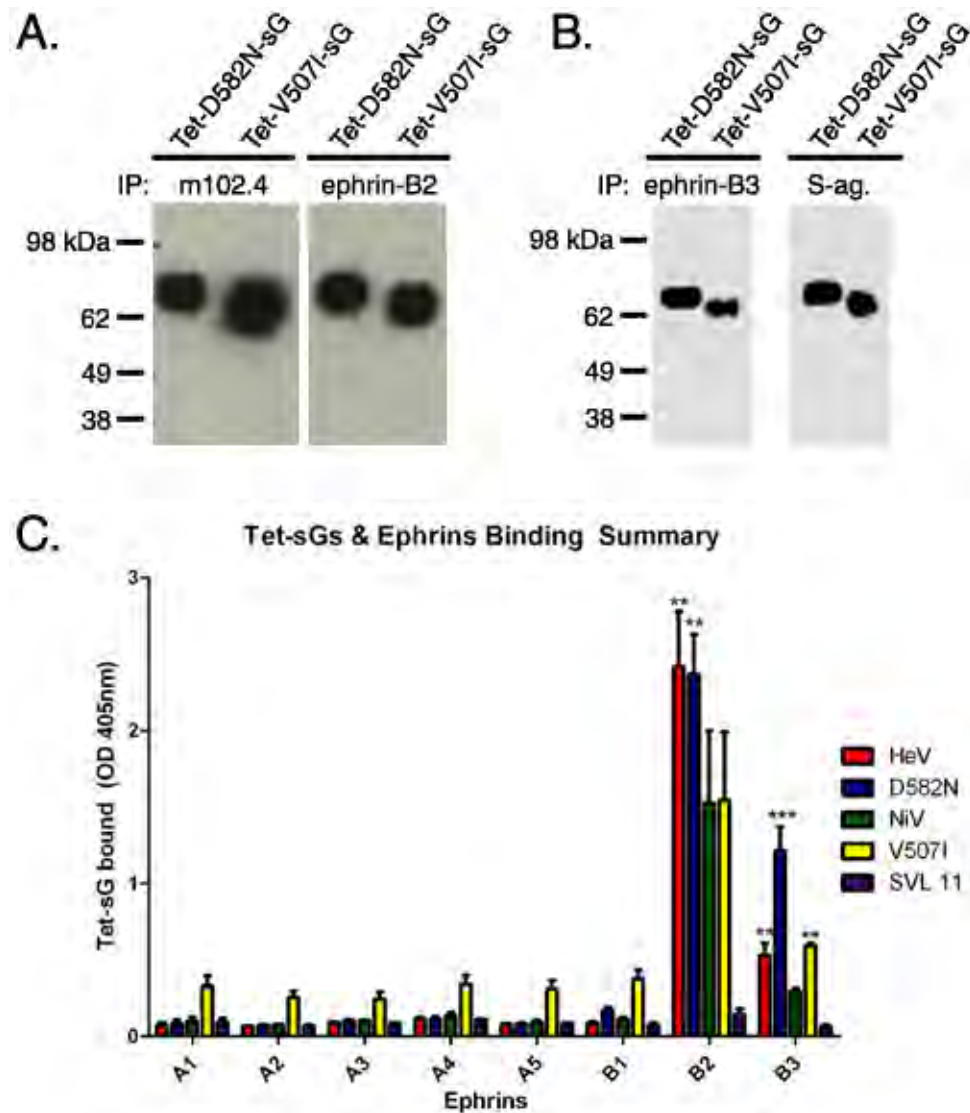
Figure 13: Tet-D582N-sG and Tet-V507I-sG bind ephrin-B2 and m102.4.
Supernatants collected from 293Free cells expressing Tet-D582N-sG and Tet-V507I-sG were immunoprecipitated with **(A)** ephrin-B2, m102.4, **(B)** ephrin-B3 and S-agarose, run on a denaturing gel and detected using α-S-HRP antibody. (S-ag. – S-agarose). **(C)** ELISA plates were coated with all 8 ephrins and incubated with 8 ng/μl Tet-sGs. The levels of bound Tet-sGs were measured using α-S-HRP antibody.

Since Tet-D582N/V507I-sGs contain mutations in or near the ephrin binding site, there existed the possibility that the mutations altered receptor tropism. Purified Tet-D582N/V507I-sGs alongside Tet-HeV/NiV-sGs were added to ELISA plates coated with all eight ephrins and tested for bound Tet-sGs. These ELISAs confirmed the IP data that Tet-D582N/V507I-sGs, along with Tet-HeV/NiV-sGs, only bind ephrin-B2 and ephrin-B3 with a preference for ephrin-B2 binding (Figure 13C). Interestingly, Tet-V507I-sG displayed low levels of binding to all ephrins tested. It was later determined that the low levels of Tet-V507I-sG binding to ephrins was not due to enhanced binding affinity but rather mucilaginous properties of Tet-V507I-sG (data not shown).

Additional ELISAs comparing the binding of Tet-HeV/NiV-sGs and Tet-D582N/V507I-sGs to receptors were performed, using various concentrations of either Tet-sGs or ephrins (Figure 14 A&B). Little difference in the binding patterns of wildtype (wt) and m102.4 escape variants to receptors was detected, indicating the mutations in Tet-D582N/V507I-sGs have no significant impact on receptor binding. The ELISAs further confirmed the preference of Tet-sGs to bind ephrin-B2 over ephrin-B3.

While these ELISAs revealed similar binding affinities between Tet-HeV/NiV-sGs and Tet-D582N/V507I-sGs to receptor ephrin-B2, we wanted to more quantitatively compare the binding affinities. Using SPR we determined the affinity constant for ephrin-B2 was lower with Tet-V507I-sG than with Tet-NiV-sG, 3.62 nM compared to 8.88 nM, while Tet-D582N-sG had a higher affinity constant with ephrin-B2 than Tet-HeV-sG, 23.6 nM vs. 17.3 nM, respectively (Table 3). Despite these slight differences, the low values of all four affinity constants indicate that all four Tet-sGs are able to bind
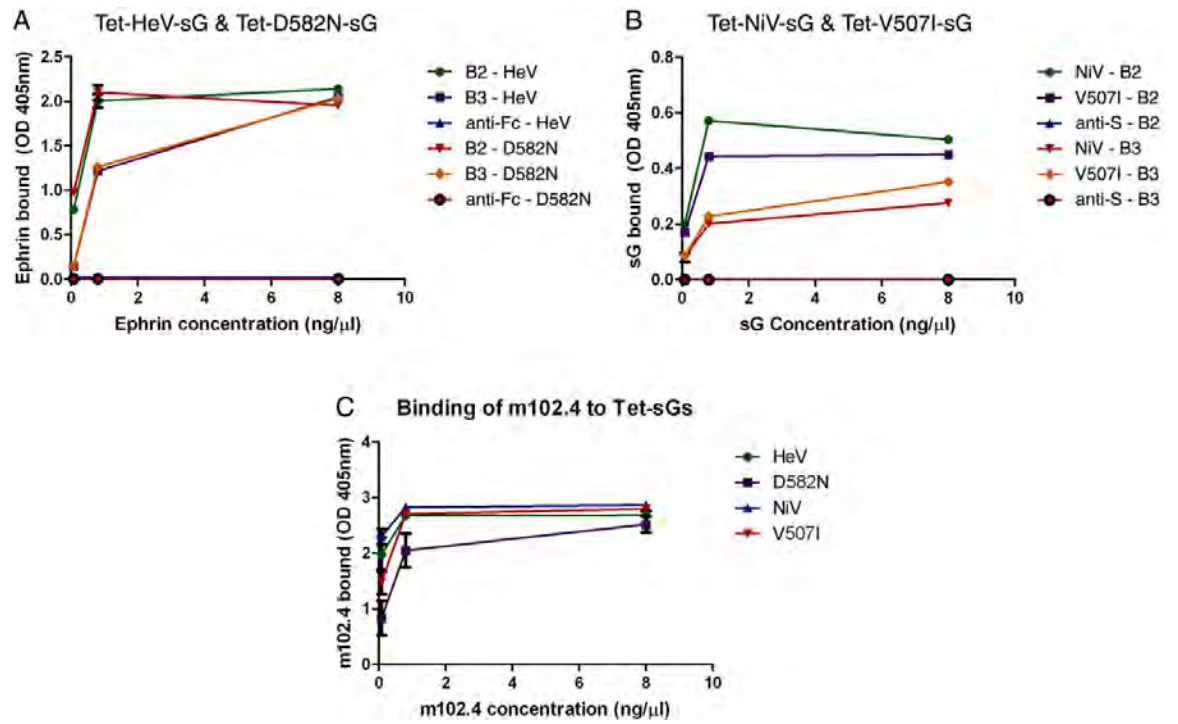
Figure 14: Receptor and m102.4 binding by Tet-sGs.
ELISAs were used to compare the abilities of wild-type and escape-variant Tet-sGs to bind ephrin receptors and m102.4. **(A)** Increasing concentrations of ephrin-B2 and ephrin-B3 were added to immobilized Tet-HeV-sG and Tet-D582N-sG, and bound ephrins were detected using α-Fc-HRP antibody. **(B)** Similar to (A), increasing concentrations of Tet-NiV-sG and Tet-V507I-sG were added to immobilized ephrin-B2 and ephrin-B3. Bound Tet-sGs were detected using α-S-HRP antibody. **(C)** All 4 Tet-sGs were coated on a plate and incubated with increasing concentrations of m102.4, and levels of bound m102.4 were determined using α-Flag-HRP antibody.

ephrin-B2 with high affinity, and the lack of any great discrepancy between the escape variants and wt confirms the hypothesis that the mutations have little impact on receptor binding.

Binding m102.4

Since HeV-G-D582N and NiV-G-V507I are able to escape m102.4 neutralization it was assumed that the amino acid changes in HeV/NiV-Gs inhibited m102.4 binding. However, this assumption was shown to be incorrect when Tet-D582N/V507I-sGs were tested for m102.4 binding. Co-IPs of Tet-D582N/V507I-sGs with m102.4 and receptors revealed that Tet-D582N/V507I-sGs bind m102.4 at levels similar to receptor binding (Figure 13A). Furthermore, when binding ELISAs were used to compare m102.4 binding with Tet-D582N/V507I-sGs and Tet-HeV/NiV-sGs, m102.4 was able to bind all four Tet-sGs to similar levels (Figure 14C). In fact, there was no noticeable difference in the level of m102.4 binding for Tet-V507I-sG and Tet-NiV-sG. Tet-D582N-sG did exhibit lower levels of m102.4 binding than Tet-HeV-sG, suggesting that m102.4 may not bind Tet-D582N-sG as strongly as it does Tet-HeV-sG. To investigate this slight difference further, SPR was used to determine affinity constants for all four Tet-sGs with m102.4. Somewhat surprisingly, Tet-V507I-sG displayed a higher binding affinity to m102.4 than Tet-NiV-sG with affinity constants of 7.31nM and 25.5nM, respectively (Table 3). Supporting the earlier ELISA data, Tet-D582N-sG had an affinity constant of 300nM, which is 3 fold greater than the affinity constant for Tet-HeV-sG, 111nM.

Overall, Tet-HeV-sG and Tet-D582N-sG had lower binding affinities to m102.4 than Tet-NiV-sG and Tet-V507I-sG, and Tet-D582N-sG binds m102.4 with less affinity than Tet-HeV-sG. The different affinity constants of Tet-HeV-sG and Tet-D582N-sG

suggest that Tet-D582N-sG may be able to escape m102.4 neutralization due to a decreased affinity for m102.4 compared to receptor.

Conformational Change – m106.3 binding

So far it has been shown that Tet-D582N/V507I-sGs are expressed as tetramers, bind receptors and bind m102.4, but it also needed to be verified that they undergo conformational change upon receptor binding. Again IPs and ELISAs were used to determine the pattern of m106.3 binding. Co-IP of Tet-D582N-sG with m106.3 in the presence and absence of ephrin-B2 reveals a similar pattern as that seen with Tet-HeV-sG (Figure 11A). Tet-D582N-sG can bind m106.3 in the absence of receptor, but the level of bound Tet-D582N-sG increases with the addition of ephrin-B2, indicating that the conformation of Tet-D582N-sG is not in complete alignment with full-length HeV-G. In the ELISA format, Tet-D582N/V507I-sGs had increased levels of m106.3 binding when incubated with increasing concentrations of ephrin-B2, although m106.3 was still able to bind Tet-D582N/V507I-sGs in the absence of receptor (Figure 11B). Overall Tet-D582N/V507I-sGs exhibit a conformation similar to Tet-HeV/NiV-sGs in that m106.3 is able to bind in the absence of receptor but still undergo conformational changes upon receptor binding that allow for increased m106.3 binding.

DISCUSSION

Here we have successfully shown that recombinant soluble HeV/NiV-Gs can be expressed as stable tetramers, the natural oligomeric state of full-length HeV/NiV-Gs, with little to no expression as dimers or monomers. These tetrameric HeV/NiV-sGs (Tet-sGs) are capable of binding receptors ephrin-B2 and ephrin-B3 as well as the neutralizing human mAb m102.4. Large scale production, purification and storage of Tet-sGs can be

performed quickly and easily, allowing for rapid, safe and detailed studies of these glycoproteins.

Requirement of the GCN4 motif

The ability of Tet-HeV/NiV-sGs to maintain a tetrameric state is due to the addition of the GCN4 motif on the N-terminus end of the stalk region. Why this tetrameric motif is required for efficient tetramer formation is not fully understood, but Pratap *et al.* suggests that certain helical bundles cannot maintain an oligomeric conformation based solely on the interactions of the hydrophobic core and that additional bonds are required (157). Transmembrane domains of other paramyxovirus glycoproteins, such as PIV5-HN, HeV-F and PIV5-F, have been shown to help stabilize the proteins in higher order oligomeric conformations (143; 177). It is possible, therefore, that the cytoplasmic tail and/or transmembrane domains may have a stabilizing effect on G conformation, and when these domains are removed the interactions of the 4-helix bundle are not strong enough to maintain the tetrameric conformation.

Another point to note is that the stalk domains of HeV/NiV-Gs contain three cysteine residues capable of forming disulfide bonds that aid in the stabilization of higher order oligomers. All three of these residues (C146, C158 and C162) are towards the C-terminus of the stalk, past the four helix bundle. C158 and C162 form inter-subunit disulfide bonds that result in dimer formation, while C146 is involved in cross-dimer disulfide bonds that aid tetramer formation. Interestingly, mutation of either C158 or C162 results in only monomeric expression of full-length NiV-G, while mutation of C146 results in monomeric or dimeric expression (110). This suggests that two disulfide bonds (C158 and C162) are required to maintain a dimeric conformation. Given that

HeV/NiV-sGs without the GCN4 motif results in dimer formation it appears that these two disulfide bonds are sufficient to maintain a dimeric conformation without any additional stabilizing factors. It would be interesting to determine the resulting oligomeric conformation of HeV/NiV-sGs if either C162 or C158 were mutated. One would expect that only monomeric HeV/NiV-Gs would be detected. Contrastingly, it appears that a sole disulfide bond (C146) is required but not sufficient to maintain a tetrameric conformation in HeV/NiV-sGs without an additional stabilizing factor (e.g. transmembrane domain or GCN4 motif).

Receptor binding and conformational change

The ability of Tet-HeV/NiV-sGs and Tet-D582N/V507I-sGs to bind m106.3 in the absence of receptor suggests the conformation of Tet-sGs is not completely in alignment with full-length HeV/NiV-Gs. The tetrameric GCN4 motif provides stability and support for maintaining a tetrameric structure as evidenced by tetramers being the predominant species expressed, but it appears that the addition of the GCN4 motif only partially compensates for any additional structural support required for Tet-sGs to adopt the correct pre-fusion conformation.

It is known that HeV/NiV-Gs undergo conformational changes upon receptor binding, and it is these conformational changes that result in the exposure of the m106.3 epitope. Since the Tet-sGs are able to bind m106.3 in the absence of receptor, they may resemble an intermediate of HeV/NiV-Gs that occurs during the transition from pre-receptor-bound to post-receptor-bound stages. In this intermediate conformation the epitope of m106.3 may be slightly, but not completely, exposed as the addition of receptor does enhance m106.3 binding. Therefore, while Tet-sGs may not completely

resemble the pre-receptor-bound conformation, neither do they completely resemble the

post-receptor-bound conformation.

Furthermore, the true importance of the conformational change in HeV/NiV-Gs is

the resulting interaction and triggering of F. Data presented in Chapter 5 will discuss the

nature of the interaction between Tet-sGs and soluble trimeric HeV/NiV-F in more detail,

but the two soluble glycoproteins, sG and sF, are able to associate. This further confirms

that the conformation of Tet-sGs closely resembles full-length HeV/NiV-Gs, and any

slight variations in the Tet-sGs conformations do not inhibit interactions with receptors or

their cognate F glycoproteins.

Tet-D582N/V507I-sGs

When HeV and NiV were passaged in sub-neutralizing concentrations of m102.4,

two m102.4 escape variants were identified. These variants each had a single amino acid

mutation in (NiV – V507I) or near (HeV – D582N) the binding pocket of G.

Surprisingly, unlike most viral escape variants, HeV-G-D582N and NiV-G-V507I

displayed no growth defects (207). Purified Tet-D582N/V507I-sGs were used to verify

receptor tropism, and it was determined that the mutations did not broaden ephrin binding

as Tet-D582N/V507I-sGs only bound ephrin-B2 and ephrin-B3. Furthermore, these

mutations do not appear to have a drastic effect on receptor binding since the escape

variants and Tet-HeV/NiV-sGs demonstrated similar receptor binding patterns.

Prior to this work it was assumed that m102.4 escape occurred due to an inability

of m102.4 to bind the escape variants, but the data presented here suggest otherwise.

Multiple assays verified the ability of Tet-D582N/V507I-sGs to bind m102.4, and Tet-

V507I-sG was shown to have the greatest binding affinity for m102.4. Conversely, Tet-

D582N-sG has the lowest binding affinity for m102.4. We determined that Tet-V507I-sG does have increased non-specific interactions that slightly enhanced binding to multiple ephrins. While this mucilaginous property may have slightly inflated the binding affinity of Tet-V507I-sG to receptors and m102.4, multiple assays confirmed that Tet-V507I-sG has strong binding affinity for receptors and m102.4 at levels similar to Tet-NiV-sG. The extreme difference in binding affinity to m102.4 between Tet-D582N-sG and Tet-V507I-sG suggests that these two variants may employ different mechanisms for m102.4 escape. Possible escape mechanisms will be discussed in more detail in Chapters 4 and 5, but it appears that at least for HeV-G-D582N, decreased binding affinity for m102.4 may aid HeV escape.

Summary and Future Directions

HeV/NiV-Gs can be expressed, purified and studied as tetrameric, soluble constructs that can be produced with relative ease and demonstrate a high level of stability. These Tet-sGs maintain receptor binding, m102.4 binding, receptor-induced conformational change and association with soluble HeV/NiV-F.   The only possible drawback is that Tet-sGs do not adopt a completely pre-receptor-bound conformation.

Numerous possibilities exist for creating a Tet-sG conformation that would more closely resemble full-length HeV/NiV-G. The addition of another cysteine residue to the upper region of the stalk in the vicinity of C146 might strengthen the tetrameric conformation and remove the requirement for the GCN4 motif. Or, single residues in the GCN4 motif could be added or deleted, resulting in a slightly different alignment of the GCN4 motif with the two different α-helices in the stalk domain (7-mer and 11-mer).

Another possibility would be to lengthen the GCN4 motif, having it express as an α-helix with four or five complete turns as opposed to three.

The ability to construct stable Tet-sGs provides a great platform for studying the interactions of HeV/NiV-Gs with receptors, m102.4 and HeV/NiV-F. Tet-sGs can be used to further clarify the steps of viral attachment, activation and fusion in BSL-2 conditions, providing opportunities to generate more advanced and specific therapeutics. When variants of HeV/NiV-Gs are isolated and identified either *in vivo* or *in vitro*, they can easily be constructed as Tet-sGs and studied to determine binding properties and potential neutralizing mechanisms. The four Tet-sGs created here (Tet-HeV/NiV-sGs and Tet-D582N/V507I-sGs) were all used for further study (Chapters 4 and 5) and provided much insight into the mechanism of HeV/NiV infection and m102.4 neutralization.

Chapter 4: Characterization of m102.4 Variants

INTRODUCTION

Since their emergence in the mid-1990s, HeV and NiV have caused over 500 infections and 300 fatalities, resulting in their classification as BSL-4 and CDC Category C Bioterrorism agents. The recent release of Equivac® HeV presents the first successful commercial therapeutic designed to prevent henipavirus infections. The vaccine, however, was specifically designed to prevent human HeV infections by stopping transmission of HeV from infected bats to horses, but the vaccine has little to no therapeutic potential for individuals already infected with HeV or NiV.

Since known antiviral drugs have minimal effect on human infection, alternative therapeutics, including mAbs, were investigated. Working with a naïve human phage library, Zhu *et al.* identified a human mAb capable of binding and neutralizing both HeV and NiV (218; 219). The efficacy of this antibody, designated m102.4, has been shown in ferret and African green monkey trials with both HeV and NiV (reviewed in (29)), and has also been administered numerous times as compassionate drug use. The most recent use of m102.4 occurred in the summer of 2013 when a researcher was bitten by a Nipah (Bangladesh strain) infected non-human primate. Multiple doses of m102.4 were administered to the patient beginning approximately 24 hours after exposure, and the patient suffered no adverse reaction to the antibody and remained free of any NiV-induced symptomatology (C.C. Broder, Personal communication).

Crystal structures of HeV/NiV-Gs with ephrin-B2 indicate that a "channel" in the head domains of HeV/NiV-Gs is responsible for receptor binding (23; 205). Examination of the recently solved crystal structure of HeV-G and the antibody m102.3 reveals that

this same channel is used for m102.3 binding (207). Since, the human antibody m102.3 is closely related to m102.4 in both sequence and structure, having identical heavy chains and few amino acid differences in the light chain, it has generally been accepted that the binding of m102.3 and m102.4 to HeV/NiV-Gs is identical.

The main region of ephrin-B2 and -B3 responsible for binding HeV/NiV-Gs is the G-H loop, which is highly conserved between ephrin-B2 and -B3. When ephrin-B2/B3 bind HeV/NiV-Gs, the G-H loop buries a stretch of six amino acids ($F/Y_{120}SPNLW_{125}$, ephrin-B3 numeric designations) in the head domains of HeV/NiV-G. Of these six amino acids, four are considered critical for binding (F/Y_{120}, P_{121}, L_{124} and W_{125}), and only the first residue F/Y_{120} differs between ephrin-B2 and ephrin-B3, with ephrin-B2 having a phenylalanine (F) and ephrin-B3 a tyrosine (Y).

Binding studies with m102.4 suggest that a stretch of amino acids in the CDRH3 region of m102.4 is responsible for binding to HeV/NiV-Gs. Similar to the ephrin G-H loop, m102.4 contains a stretch of six amino acids in the CDRH3 region ($L_{105}APHPS_{110}$) that is buried in the head domains of HeV/NiV-G. Among those amino acids four are also considered critical for binding (L_{105}, P_{107}, H_{108} and P_{109}). Interestingly, a majority of these amino acids are not conserved between m102.4 and the ephrin receptors, the lone exception being the first proline in both m102.4 (P_{107}) and ephrin-B2/B3 (P_{122}).

As it was hypothesized that m102.4 neutralizes HeV/NiV by binding and blocking receptor, m102.4 escape variants of HeV/NiV would therefore likely have mutations in the G binding pocket that would prevent m102.4 but not receptor from binding. However, as the studies with Tet-D582N/V507I-sGs in Chapter 3 demonstrate, these m102.4 escape variants maintain their ability to bind m102.4 without being neutralized.

This suggests that there is enough dissimilarity in the binding of receptor and m102.4 to HeV/NiV-Gs that a single residue mutation in HeV/NiV-Gs can render one interaction functional (receptor) and one ineffectual (m102.4).

In order to improve the efficacy of m102.4 against both wild type and escape variants of HeV/NiV we modified the binding region of m102.4 ($L_{105}APHPS_{110}$) to resemble the binding region of ephrin-B2/B3 ($F/Y_{120}SPNLW_{125}$). We predicted that variants of m102.4 that more closely resembled ephrin-B2/B3 would retain the properties of m102.4 (binding and neutralization of HeV/NiV-Gs) while also preventing the formation of new, fully functional HeV/NiV escape variants as mutations in HeV/NiV-Gs required to escape the modified m102.4 would also disrupt receptor interaction. Multiple variants of m102.4 were therefore constructed and tested to determine their ability to bind and neutralize wild type and m102.4 escape variants of HeV/NiV-Gs.

RESULTS

Generation and expression of m102.4 variants

Variants of m102.4 were generated by quick-change mutagenesis, changing 1-5 residues in the 6-amino acid CDRH3 binding region ($L_{105}APHPS_{110}$). The mutations in m102.4 replaced the m102.4 residues with either the corresponding amino acid in the G-H loop of ephrin-B2/B3 or alanine, which would remove any contribution to binding provided by that residue. Single and multiple mutation variants were constructed with the most mutated variant completely resembling the 6-residue binding region of the ephrin-B2/B3 G-H loop. In total 19 variants were constructed and considered representative of the array of variants that could be generated (Figure 15).

m102.4 Variants

m102.4 L_{105} A **P H** P S_{110}

Ephrin-B2/3 F/Y_{120} S P N **L** W_{125}

1 Mutation	2 Mutation	3 Mutation	4 Mutation	5 Mutation
FAPHPS (LF)	FAPHLS (F&L)	FAPHLW (F/L/W)	FAPNLW	FSPNLW
DAPHPS (LD)	FAAHPS (FP)	FAAHPW (FA)	(F_PNLW)	
AAPHPS (LA)	YAPAPS (YP)	YAPAPW (YW)	FSPNPW	
LAAHPS (PA)	LAPAPW (AW)	FAPAPW (FW)	(SLP)	
LAPAPS (HA)	YAAHPS (YA)			
LAPNPS (HN)				
YAPHPS (LY)				

Figure 15: m102.4 Variants.
> The amino acid sequences for m102.4 and ephrin-B2/B3 are shown on top with the 4 critical residues for each ligand highlighted in red. The m102.4 variants, whose mutations are also highlighted in red, are separated based on the number of mutations from the parent m102.4 sequence. Abbreviations for the variants are shown in parentheses to the right or below the variant sequence. The m102.4 variants have 1-5 amino acid changes and are classified as "single mutation" (1 change) or "multiple mutation" (2-5 changes) variants.

These variants were expressed and purified as Fabs and tested alongside m102.4 Fab to determine their abilities to bind Tet-HeV/NiV-sGs and Tet-D582N/V507I-sGs.

Binding of m102.4 Variants to Tet-HeV/NiV-sGs and Tet-D582N/ V507I-sGs

Binding ELISAs were used to test the ability of m102.4 variants to bind Tet-HeV/NiV-sGs and Tet-D582N/V507I-sGs. Increasing concentrations of m102.4 and m102.4 variants were added to plates coated with Tet-sGs, and bound Fab was detected using an anti-Flag antibody (Figures 16-19). As expected, m102.4 bound all four Tet-sGs with relatively high affinity. In fact for Tet-HeV/NiV-sGs and Tet-V507I-sG, m102.4 binding appeared to be saturated at 0.8 ng/µl. Tet-D582N-sG bound m102.4 less efficiently, but binding of m102.4 increased at higher concentrations to levels similar to those seen with the other Tet-sGs. A comparison of all 19 m102.4 variants reveals a clear distinction between the abilities of the single mutation and multiple mutation variants to bind Tet-sGs.

Single mutation variants

A majority of the single mutation variants were able to bind the Tet-sGs with varying levels of intensity. At the lowest concentration tested, 0.08 ng/µl, the majority of single mutation variants had no to low levels of binding for Tet-HeV-sG, Tet-D582N-sG and Tet-V507I-sG, but these variants demonstrated slightly stronger binding for Tet-NiV-sG. While the level of binding was low for these variants at 0.08 ng/µl, their binding increased with increasing concentrations, and several single mutation variants had binding levels similar to m102.4 at 8 ng/µl. Interestingly, the m102.4 variants bound best to Tet-NiV-sG, while binding less well to Tet-HeV-sG and Tet-V507I-sG.

Figure 16: Binding pattern of m102.4 variants to Tet-HeV-sG.
Binding ability of m102.4 and 19 m102.4 variants to Tet-HeV-sG were determined by ELISA using three concentrations of antibody. **(A)** Representative sample of individual ELISA binding data for all 19 variants. **(B)** Summary of ELISA binding data. Each variant was tested at three different concentrations on three separate ELISAs. Results were averaged and compared to the level of m102.4 binding at 8 ng/µl (100%). The five antibodies of interest – m102.4, LD, LF, HA and SLP – are color-coded to distinguish them from the other variants.

A

Tet-HeV-sG and m102.4 Variants

Tet-HeV-sG and m102.4 Variants

Tet-HeV-sG and m102.4 Variants

B.

Tet-HeV-sG Variant Binding Summary
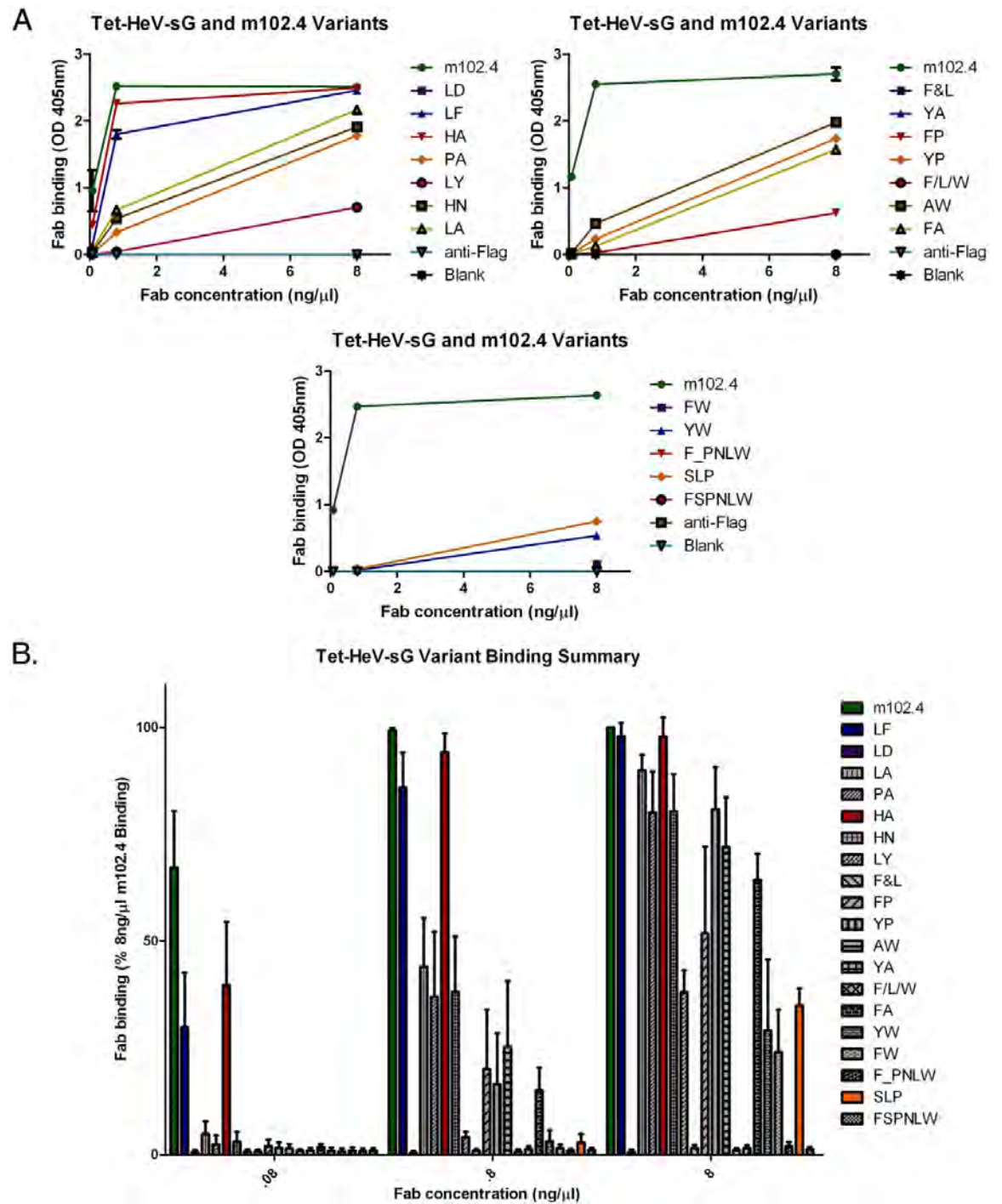
Figure 17: Binding pattern of m102.4 variants to Tet-NiV-sG.

Binding ability of m102.4 and 19 m102.4 variants to Tet-NiV-sG were determined by ELISA using three concentrations of antibody. **(A)** Representative sample of individual ELISA binding data for all 19 variants. **(B)** Summary of ELISA binding data. Each variant was tested at three different concentrations on three separate ELISAs. Results were averaged and compared to the level of m102.4 binding at 8 ng/µl (100%). The five antibodies of interest – m102.4, LD, LF, HA and SLP – are color-coded to distinguish them from the other variants.

A

Tet-NiV-sG and m102.4 variants

Tet-NiV-sG and m102.4 variants

Tet-NiV-sG and m102.4 variants

B.

Tet-NiV-sG Variant Binding Summary
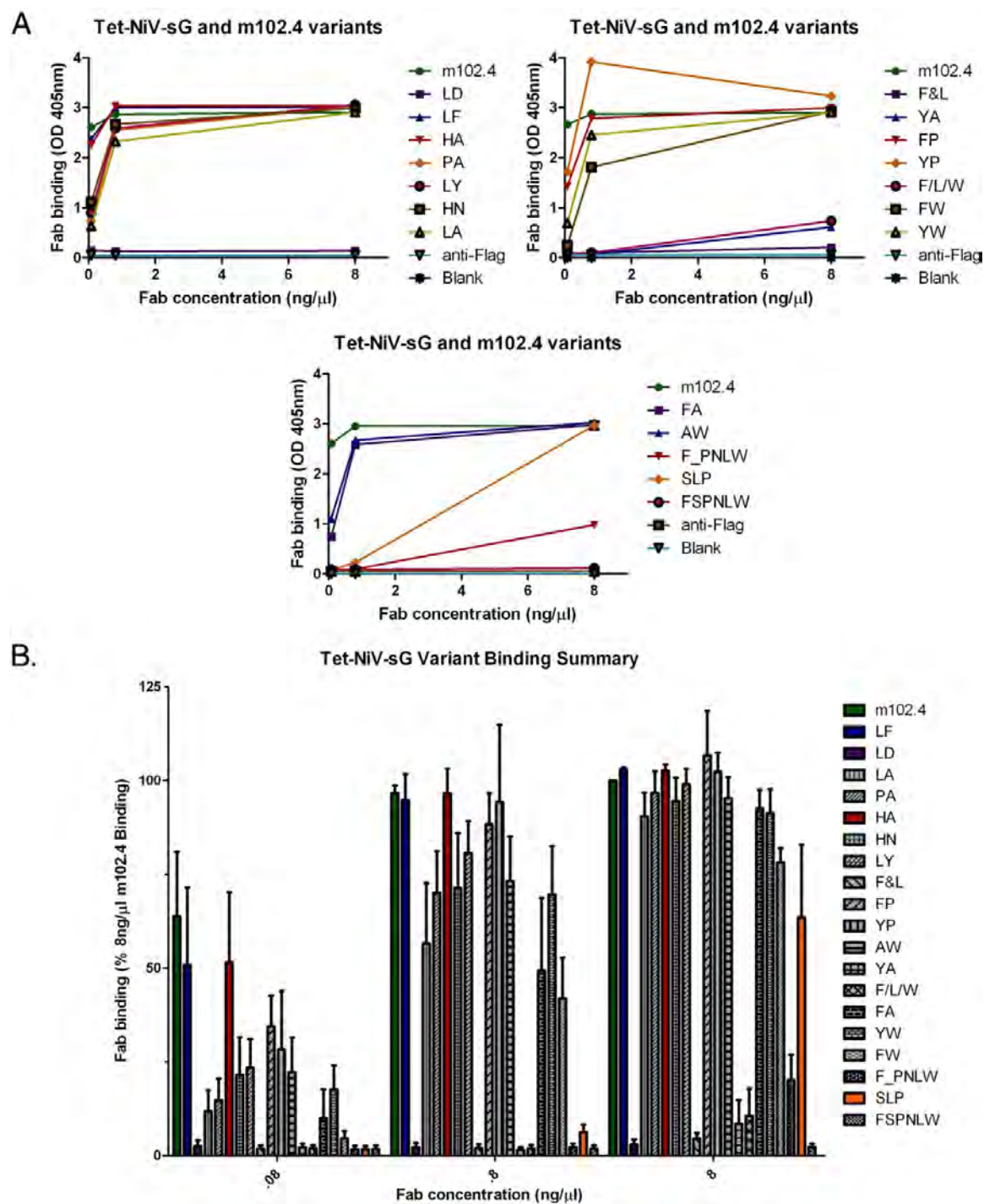
Figure 18: Binding pattern of m102.4 variants to Tet-D582N-sG.
Binding ability of m102.4 and 19 m102.4 variants to Tet-D582N-sG were determined by ELISA using three concentrations of antibody. **(A)** Representative sample of individual ELISA binding data for all 19 variants. **(B)** Summary of ELISA binding data. Each variant was tested at three different concentrations on three separate ELISAs. Results were averaged and compared to the level of m102.4 binding at 8 ng/µl (100%). The five antibodies of interest – m102.4, LD, LF, HA and SLP – are color-coded to distinguish them from the other variants.

A

Tet-HeV-sG-D582N and m102.4 Variants

Tet-HeV-sG-D582N and m102.4 Variants

Tet-HeV-sG-D582N and m102.4 Variants

B.

Tet-HeV-sG-D582N Variant Binding Summary
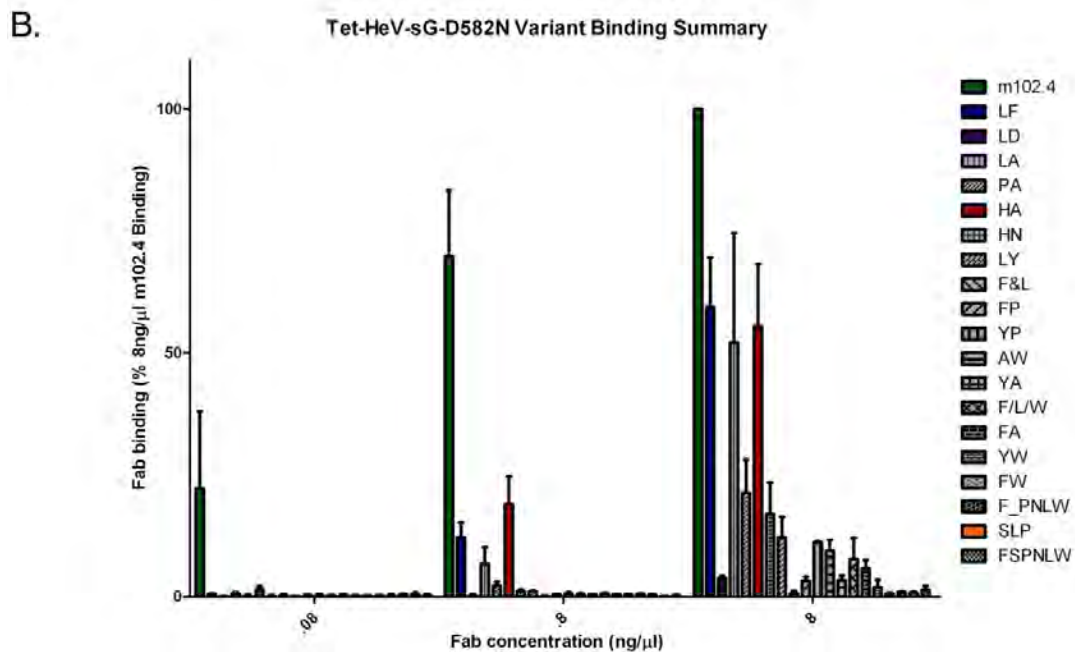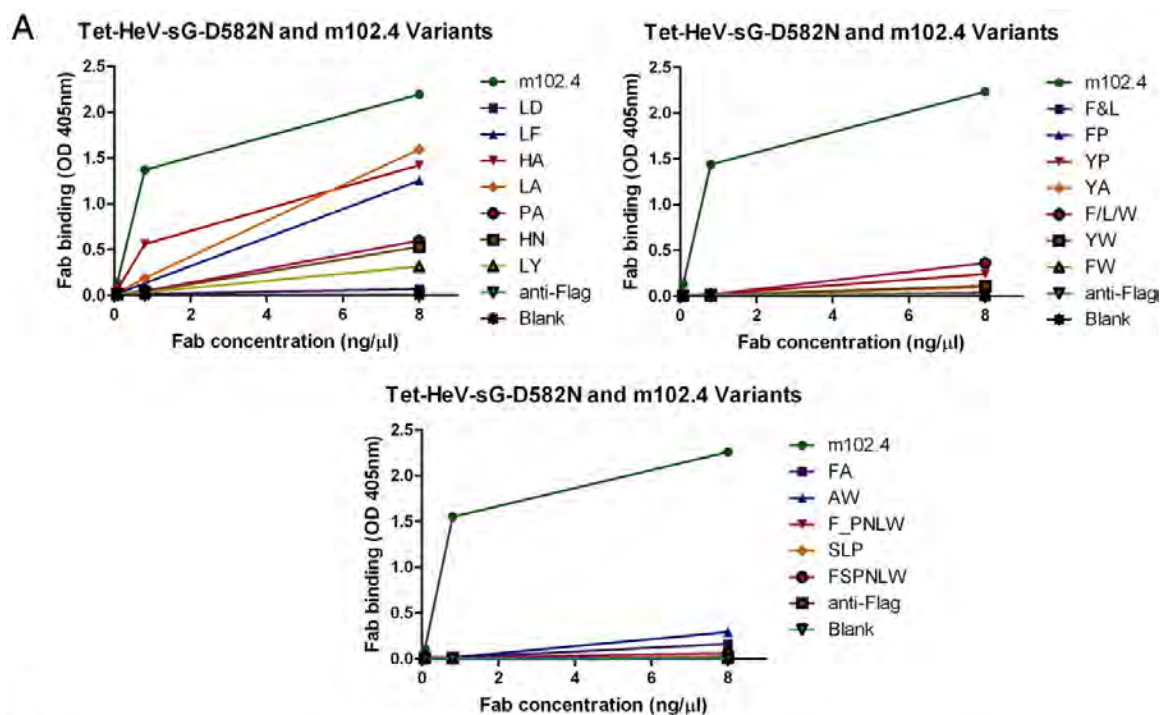
Figure 19: Binding pattern of m102.4 variants to Tet-V507I-sG.

Binding ability of m102.4 and 19 m102.4 variants to Tet-V507I-sG were determined by ELISA using three concentrations of antibody. (A) Representative sample of individual ELISA binding data for all 19 variants. (B) Summary of ELISA binding data. Each variant was tested at three different concentrations on three separate ELISAs. Results were averaged and compared to the level of m102.4 binding at 8 ng/µl (100%). The five antibodies of interest – m102.4, LD, LF, HA and SLP – are color-coded to distinguish them from the other variants.

A Tet-NiV-sG-V507I and m102.4 variants

B. Tet-NiV-sG-V507I Variant Binding Summary
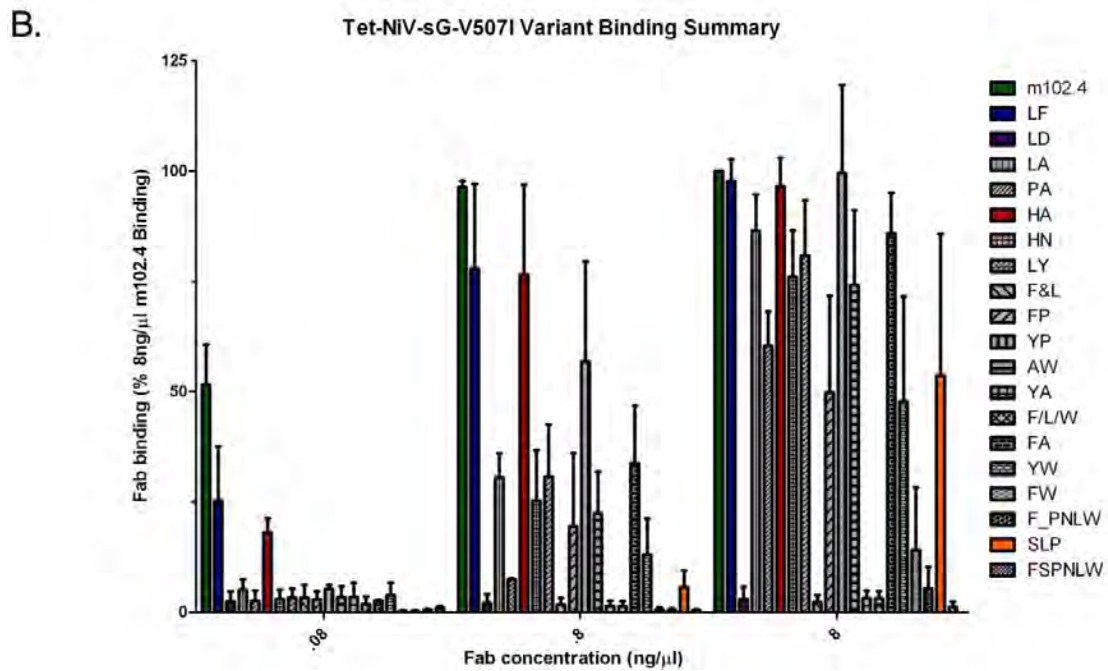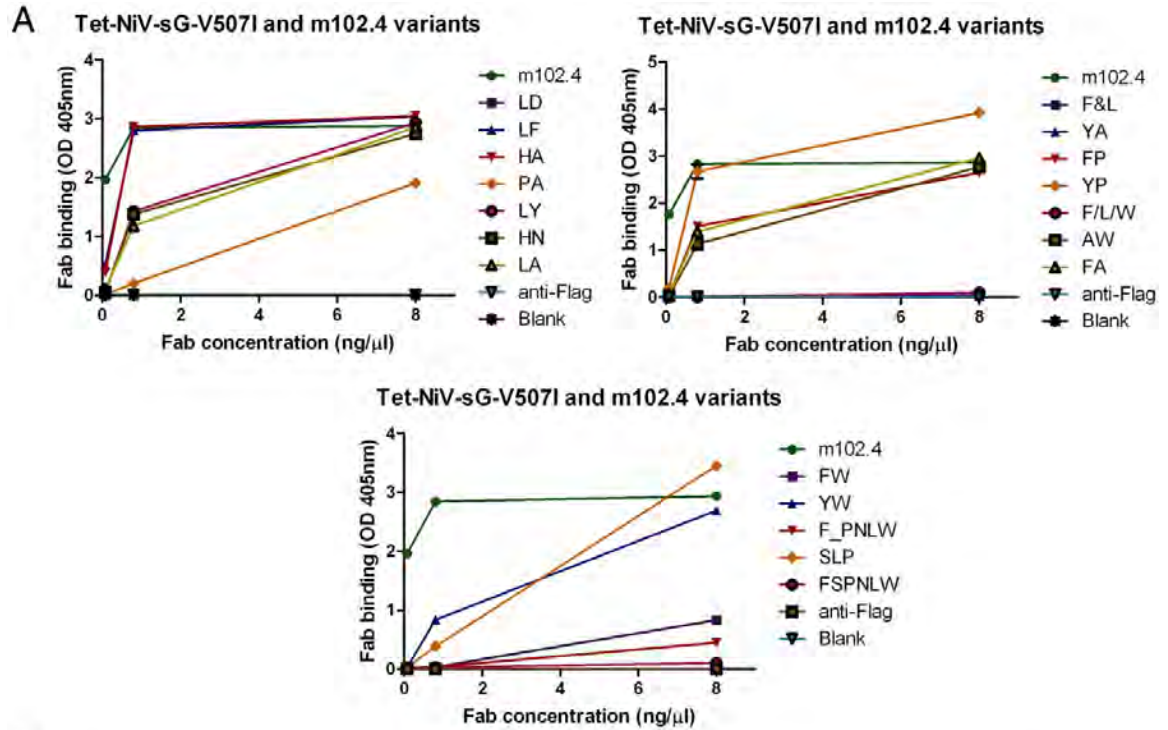
Tet-D582N-sG had the lowest levels of single mutation variant binding, which is unsurprising given the lower binding affinity between Tet-D582N-sG and m102.4 (Chapter 2).

The two single mutation variants that demonstrated the highest levels of binding to all Tet-sGs were variants LF and HA, which both have a single amino acid mutation in the CDRH3 region of m102.4 (**F**APHPS and LAP**A**PS, respectively). These two variants were the strongest binders and even bound Tet-sGs, except Tet-D582N-sG, at 0.08 ng/µl.

While most single mutation variants demonstrated moderate binding to Tet-sGs, the variant LD (**D**APHPS) was unable to bind any Tet-sG at any concentration tested. The mutation in the LD variant replaces the first hydrophobic leucine (L) in the binding region with a charged aspartic acid (D). As this mutation completely destroyed any ability of this variant to bind Tet-sGs, LD was frequently used as a negative control in future studies.

Multiple mutation variants

While binding of the single mutation variants to Tet-sGs was relatively straightforward, the multiple mutation variants showed varying degrees of binding to Tet-sGs compared to m102.4 (Figures 16-19). At first it appears that there is no pattern in which m102.4 variants bind or do not bind as variants with the same number of mutations differ in binding abilities. However, a comparison of the variants that bind with those that do not bind begins to reveal the importance of the second proline in the binding sequence (LAPH**P**S). The multiple mutation variants that retain the second proline are able to bind most Tet-sGs at higher concentrations, while those variants with a mutated P109 have limited binding ability.

99

Interestingly, the fully mutated m102.4 variant FSPNLW, which completely resembles the binding region in the G-H loop of ephrin-B2, had little to no ability to bind any of the Tet-sGs. However, the variant SLP, which retains the second proline (**FS**P**NPW**) was able to bind Tet-sGs, although at levels lower than the single mutation variants or m102.4. This highlights the importance of the second proline in m102.4 as it appears to be critical for m102.4 binding.

As seen with the single mutation variants, multiple mutation variants that were able to bind, bound better to Tet-NiV-sG than Tet-HeV-sG or Tet-V507I-sG. Few multiple mutation variants were able to bind Tet-D582N-sG, and those that did bind had extremely low binding ability, even at higher concentrations.

m102.4 and m102.4 variants selectively inhibit receptor binding

While no variant was able to bind to all Tet-sGs as efficiently as m102.4, a number of them were able to bind Tet-sGs to levels similar to m102.4. The next step was to determine how effective the m102.4 variants were at blocking Tet-sG-receptor interaction. Competition ELISAs were used in which the receptors ephrin-B2 and -B3 were coated on an ELISA plate and a constant concentration of Tet-sG along with increasing concentrations of m102.4 and m102.4 variants were added. The amount of Tet-sG capable of binding receptor was determined in the absence of m102.4 and m102.4 variants and designated as the maximal level of Tet-sG binding. Levels of bound Tet-sG in the presence of m102.4 and m102.4 variants was determined and compared to the maximal Tet-sG binding level. All 19 m102.4 variants were tested in competition ELISAs and compared with m102.4 for their ability to inhibit Tet-sG interaction with receptor (Table 4, showing inhibitory ability at highest m102.4 variant concentration

tested), and based on this information four variants – LF, LD, HA and SLP – were chosen

for further investigation (Figure 20). Comprehensive competition ELISA data for all 19

variants can be found in Appendix A.

Table 4: Competition ELISAs with Tet-sGs, receptors and m102.4 variants.

Tet-sGs mixed with 100 ng/µl m102.4 variants were added to receptors ephrin-B2 and ephrin-B3. Levels of bound Tet-sGs in the presence of m102.4 variants were compared to bound Tet-sGs in the absence of variants. The ability of each m102.4 variant to inhibit Tet-sG from binding receptors is indicated.

	Ephrin-B2				Ephrin-B3			
	HeV	NiV	D582N	V507I	HeV	NiV	D582N	V507I
m102.4	++	+	+	-	+++	++	+++	++
LF	+	+	+	-	+++	++	+++	++
LD	-	-	-	-	-	-	-	-
LA	-	-	-	-	+++	+	-	-
PA	+	-	-	-	+++	++	++	-
HA	+	+	-	-	+++	++	+++	+
HN	+	-	-	-	+++	++	+	-
LY	+	-	-	-	+++	++	++	++
F&L	-	-	-	-	-	-	-	-
FP	-	-	-	-	+++	++	+	+
YP	-	-	-	-	+++	+++	+++	++
AW	-	-	-	-	+++	++	++	+
YA	-	-	-	-	-	-	-	-
F/L/W	-	-	-	-	-	+	-	-
FA	+	-	-	-	+++	++	++	+
YW	-	-	-	-	++	++	-	-
FW	+	-	-	-	++	++	+	-
F_PNLW	-	-	-	-	-	-	-	-
SLP	-	-	-	-	++	+	-	+
FSPNLW	-	-	-	-	-	-	+	-

+++ >80% inhibition
++ 80%-50% inhibition
+ 50%-20% inhibition
- <20% inhibition

Figure 20: Summary of competition ELISAs with Tet-sGs, ephrin-B2, ephrin-B3, m102.4 and m102.4 variants.

Increasing concentrations of m102.4 and variants LF, LD, HA and SLP were mixed with Tet-sGs and added to receptors. The bars represent the level of bound Tet-sGs to receptors with all values normalized to the level of Tet-sG bound in absence of antibody (100%). Green – m102.4, Blue – LF, Purple – LD, Red- HA, Orange – SLP and Black – Tet-sG. Each combination of Tet-sG and m102.4 variant was tested three separate times. Significance determined by one-way Anova. ***<0.0001, *<0.05

![Figure showing bar graphs of % sG Bound (no Fab) versus Fab concentration (ng/µl) for Ephrin-B2 and Ephrin-B3 across HeV, NiV, D582N, and V507I rows.]

Ephrin-B2 | Ephrin-B3

HeV

NiV

D582N

V507I

Fab concentration (ng/µl)

Legend:
- m102.4
- LF
- LD
- HA
- SLP
- Tet-sG
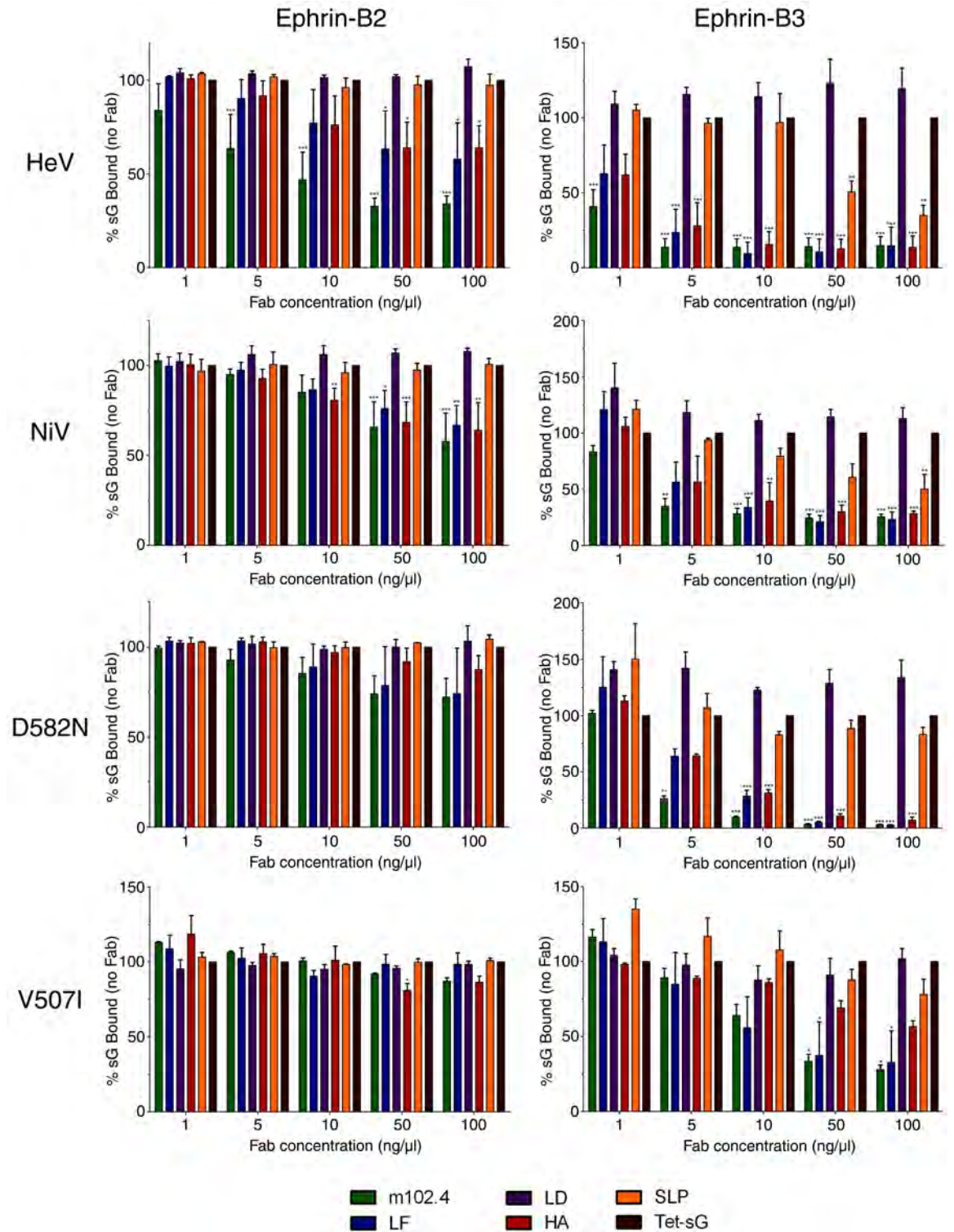
Ephrin-B2 and Tet-sGs

Starting with Tet-sGs and ephrin-B2 binding, it can be seen that the inhibitory ability of m102.4 and the m102.4 variants to prevent Tet-sGs from binding receptor varies among the Tet-sGs.

Tet-HeV-sG and Tet-NiV-sG

The ability of m102.4 to prevent Tet-HeV-sG from binding receptor is evident even at the lowest concentration of m102.4 tested, 1 ng/µl (Figure 20). The level of bound Tet-HeV-sG continues to significantly decrease with increasing m102.4 concentrations, reaching approximately 23% of maximal bound Tet-HeV-sG when 100 ng/µl of m102.4 is present. While all of the m102.4 variants were tested for their ability to inhibit Tet-HeV-sG and ephrin-B2 interaction, most of the variants had no inhibitory ability despite their ability to bind Tet-HeV-sG (Table 4). The single mutation variants had slightly more inhibitory ability than multiple mutation variants, but this ability was only observed at high concentrations and the differences were minimal. However, variants LF and HA, which had the best binding ability of the variants, also had the best inhibitory ability. While not as effective as m102.4, LF and HA were able to reduce the levels of bound Tet-HeV-sG to approximately 60% at 50 and 100 ng/µl.

m102.4 is less effective at preventing Tet-NiV-sG from binding ephrin-B2 than Tet-HeV-sG. Higher concentrations of m102.4 must be present to reduce the amount of bound Tet-NiV-sG with the first significant decrease requiring 50 ng/µl m102.4, and the highest level of m102.4 tested only resulted in approximately 40% reduction of bound Tet-NiV-sG. Similarly, m102.4 variants are less effective at inhibiting Tet-NiV-sG and ephrin-B2 interaction, although LF and HA are the two most effective variants. LF and

HA appear to be just as effective as m102.4 in reducing Tet-NiV-sG and receptor interaction. The LD and SLP variants have no effect on the levels of bound Tet-NiV-sG.

Tet-D582N-sG and Tet-V507I-sG

Unlike Tet-HeV-sG, Tet-D582N-sG binding ephrin-B2 appears to be almost completely unaffected by m102.4 or m102.4 variants. At all concentrations tested no significant decrease in the amount of Tet-D582N-sG bound to ephrin-B2 was detected, although m102.4, LF and HA do appear to slightly decrease the levels of bound Tet-D582N-sG. Except for m102.4, LF and HA, none of the variants had any effect on Tet-D582N-sG-receptor binding.

Tet-V507I-sG was the least effected by m102.4 and m102.4 variants in regards to binding ephrin-B2. Despite the ability of several variants to bind Tet-V507I-sG with relatively high affinity, there was no noticeable disruption in ephrin-B2 binding. Even variants LF and HA had little to no effect at any concentration tested.

Summary

All the m102.4 variants were tested for their ability to inhibit Tet-sGs and ephrin-B2 interaction, and despite the abilities of several variants to bind Tet-sGs, a majority, including both single and multiple mutation variants, had no inhibitory ability. The notable exceptions are m102.4 variants LF and HA, which were able to significantly reduce the ability of Tet-HeV/NiV-sGs but not Tet-D582N/V507I-sGs from binding ephrin-B2.

The variant LD had no effect on any Tet-sG's ability to bind ephrin-B2, which is unsurprising given the inability of LD to bind Tet-sGs. Interestingly, though, variant

SLP, which closely resembles ephrin-B2 and had some ability to bind Tet-sGs, also had no ability to inhibit Tet-sGs and ephrin-B2 association.

Ephrin-B3 and Tet-sGs

The competition results differed greatly when receptor ephrin-B3 was used in place of ephrin-B2. In contrast to ephrin-B2 competition ELISAs, m102.4 significantly inhibited Tet-sG-ephrin-B3 interaction for all four Tet-sGs.

Tet-HeV-sG and Tet-NiV-sG

Significant reductions in bound Tet-HeV-sG begin with m102.4 concentrations of 1 ng/µl, and the m102.4 variants LF and HA cause significant reduction in bound Tet-HeV-sG starting at 5 ng/µl (Figure 20). Beginning at 10 ng/µl there is no difference in the inhibitory ability between m102.4, LF and HA. Even the variant SLP, which had no inhibitory effect on Tet-HeV-sG and eprhin-B2 association, causes significant reduction beginning at 50 ng/µl. While most of the variants had little to no effect on blocking Tet-HeV-sG interaction with ephrin-B2, a majority of the variants are able to reduce the levels of Tet-HeV-sG bound to ephrin-B3. However, as expected, variant LD had no inhibitory ability.

Similar results are seen for Tet-NiV-sG and ephrin-B3. A majority of the m102.4 variants inhibit Tet-NiV-sG and ephrin-B3 interaction with significant reductions requiring only 10 ng/µl for the more potent variants. Again, variants LF and HA reduce the level of Tet-NiV-sG-ephrin-B3 association to levels similar to m102.4, and variant SLP causes a steady decrease in association with increasing concentration. Variant LD again had no effect on the levels of Tet-NiV-sG binding.

Tet-D582N-sG and Tet-V507I-sG

While none of the variants were able to significantly reduce the levels of Tet-D582N-sG association with ephrin-B2, the variants were able to inhibit Tet-D582N-sG association with ephrin-B3. m102.4 markedly reduced the levels of bound Tet-D582N-sG at 5 ng/µl, and variants LF and HA caused an approximate 40% decrease in bound Tet-D582N-sG at that same concentration. With increasing levels of m102.4 and variants LF and HA, the amount of bound Tet-D582N-sG decreased to almost undetectable levels at 100 ng/µl. Interestingly, the variant SLP, which inhibited Tet-HeV-sG and ephrin-B3 association, had little effect on Tet-D582N-sG and ephrin-B3 association. Another point of note is that at 1 ng/µl, the m102.4 variants appear to increase the levels of Tet-D582N-sG bound to ephrin-B3, although these levels rapidly decrease with increasing concentrations of the variants.

Of all the Tet-sGs tested, Tet-V507I-sG was the least inhibited by m102.4 and m102.4 variants from binding ephrin-B3. m102.4 did cause significant reductions in the levels of Tet-V507I-sG bound to ephrin-B3, but it required at least 50 ng/µl m102.4, a concentration much higher than that required to inhibit ephrin-B3 interaction with the three other Tet-sGs. Variants LF and HA were able to reduce the association between Tet-V507I-sG and ephrin-B3 with LF being slightly more effective than HA. As was seen with Tet-D582N-sG, variant SLP had minimal impact on Tet-V507I-sG and ephrin-B3 association.

Summary

The ability of m102.4 and the m102.4 variants to inhibit interaction between Tet-sGs and ephrin-B3 is strikingly different than their ability to inhibit interaction between

the Tet-sGs and ephrin-B2. In the majority of cases, variants LF and HA behaved

similarly to m102.4, being able to inhibit the interactions inhibited by m102.4, although

usually requiring higher concentrations to achieve the same level of inhibition.

Interestingly, Tet-HeV/NiV-sGs were inhibited from binding ephrin-B2 by m102.4, LF

and HA, but these variants had little ability to block Tet-D582N/V507I-sG from binding

ephrin-B2. Additionally, variant SLP acted similar to variant LD, showing no inhibitory

ability in preventing Tet-sGs from binding with ephrin-B2.

Contrastingly, m102.4 and variants LF and HA were very successful at inhibiting

Tet-sG interaction with ephrin-B3, usually at relatively low concentrations of m102.4 and

m102.4 variants. The only possible exception is Tet-V507I-sG, which was less effected

by m102.4, LF and HA than the three other Tet-sGs. Variant SLP prevented Tet-

HeV/NiV-sGs from interacting with ephrin-B3 but was largely unable to prevent Tet-

D582N/V507I-sGs from associating with ephrin-B3.

Cell-Cell Fusion Assays

It has now been shown that m102.4 variants are able to bind and inhibit some Tet-

sG-receptor interactions, but it needs to be determined if the ability to block this

interaction results in fusion inhibition. In order to verify the ability of the m102.4

variants to inhibit fusion, cell-cell fusion assays were used in which m102.4 variants LD,

LF, HA and SLP were tested alongside soluble ephrin-B2 and m102.4. These four

variants represent variants that have no binding or inhibitory ability (LD), strong binding

and inhibitory ability (LF and HA) and weak binding but moderate inhibitory ability

(SLP).

HeLa-USU cells transfected with HeV-G and -F or NiV-G and -F and infected with vaccinia virus encoding T7 polymerase were mixed with 50 µg/ml ephrin-B2, m102.4 Fab and m102.4 variants prior to the addition of Hela-ATCC cells infected with a vaccinia virus encoding β-galactosidase under the control of a T7 promoter. Cells were allowed to fuse for 3 h at 37°C before being lysed and frozen at -80°C. Fusion rate was determined by adding CPRG substrate and measuring colorimetric change at 570 nm with 46 readings taken every 20 seconds. For each cell-cell fusion assay, fusion levels of HeV and NiV in the absence of additional ligands were normalized to 100% and used as the basis for comparison.

Results obtained for HeV and NiV were similar in that fusion levels in the presence of ephrin-B2 and m102.4 were significantly reduced (HeV fusion reduced to 18% and 14%, respectively, and NiV fusion reduced to 9% and 17%, respectively) (Figure 21 A&B). The variants LF and HA also had significant inhibitory ability on both HeV and NiV fusion, although neither inhibited fusion to the levels of m102.4 or ephrin-B2. As expected the variant LD had no effect on HeV or NiV fusion as the rate of fusion was similar to the rate of fusion in the absence of additional ligands. Surprisingly, variant SLP seemed to slightly, but significantly, increase fusion compared to wild type levels, 169% for HeV and 118% for NiV.

Cell-cell fusion assays were repeated with effector cells expressing HeV-G-D582N and HeV-F or NiV-G-V507I and NiV-F (Figure 21 C&D). For fusion with HeV-G-D582N, ephrin-B2 was able to reduce fusion to background levels (~17%), and surprisingly, m102.4 Fab was also able to significantly reduce fusion to about 45% maximal fusion. Variants LF and HA also had a moderate ability to decrease

110
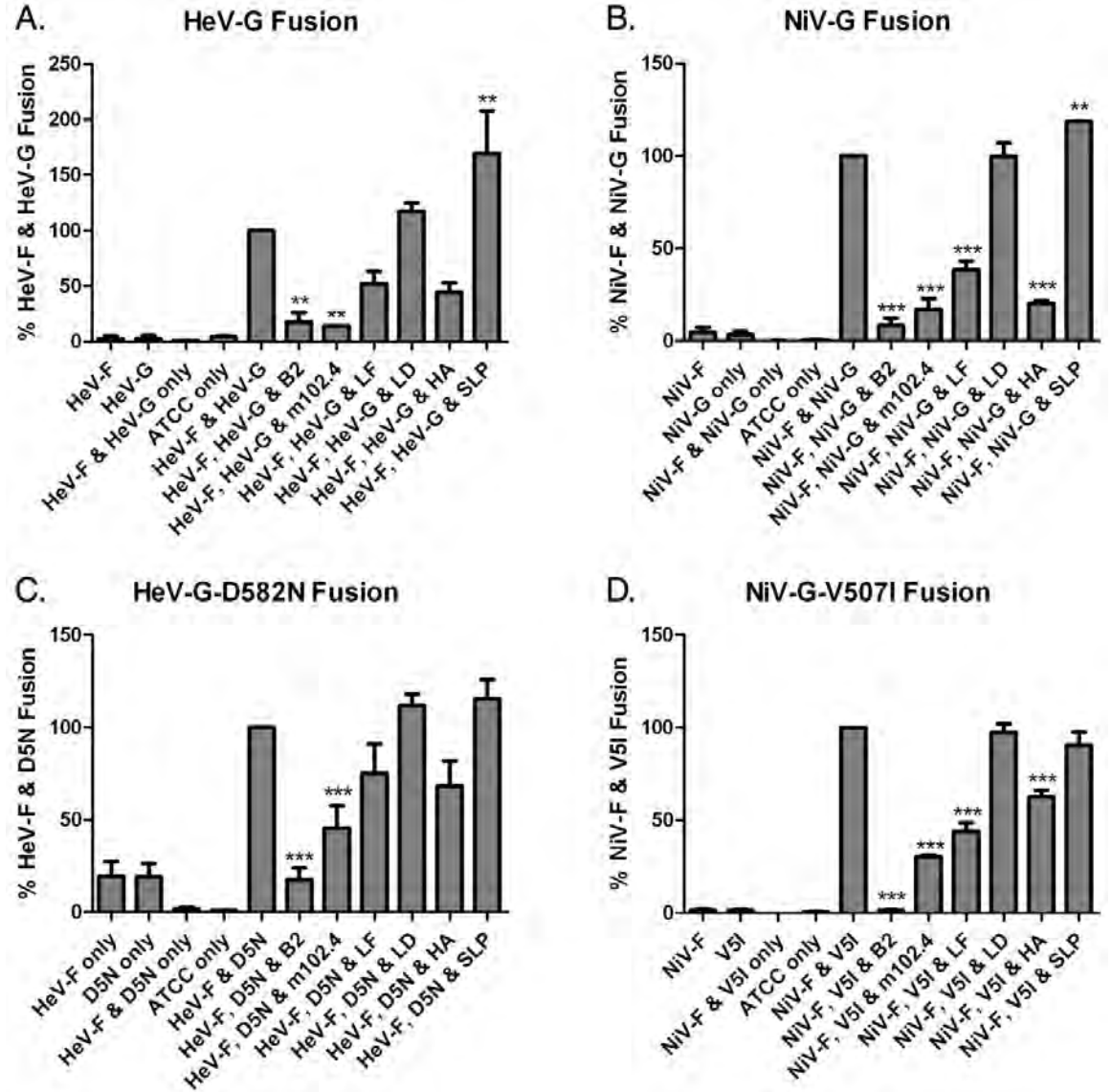
Figure 21: Cell-cell fusion assays with ephrin-B2, m102.4 and m102.4 variants.
Cells expressing (**A**) HeV-G, (**B**) NiV-G, (**C**) HeV-G-D582N or (**D**) NiV-G-V507I with their respective F glycoproteins were mixed with receptor-expressing target cells in the presence of 50 µg/ml ephrin-B2, m102.4 or m102.4 variants LF, LD, HA and SLP. Fusion values were normalized to the level of fusion obtained with G/F expressing cells without any additional ligands. Significance determined by one-way Anova. ***<0.0001, **<0.001

HeV-G-D582N fusion to 75% and 68%, respectively. However, the ability of LF and HA to inhibit HeV-G-D582N was reduced compared to their ability to inhibit HeV-G fusion.

Similar results were obtained with NiV-G-V507I cell-cell fusion assays. The addition of soluble ephrin-B2 reduced fusion levels to background levels, and m102.4 Fab managed to reduce fusion by approximately 60%. Variants LF and HA were also able to significantly reduce NiV-G-V507I fusion, although the levels of reduction were less than those seen with NiV-G. The LD and SLP variants had no impact on fusion levels.

The ability of m102.4 to inhibit fusion of m102.4 escape variants HeV-G-D582N and NiV-G-V507I was rather surprising as HeV-G-D582N and NiV-G-V507I were generated to escape m102.4 neutralization. To compare the effect of m102.4 on wild type vs. escape mutants of HeV/NiV-Gs, cell-cell fusion assays were performed in the presence of decreasing concentrations of m102.4 Fab and IgG (Figure 22). Two concentrations of m102.4 Fab were used for each concentration of m102.4 IgG to control for equal molar concentrations as well as equal total concentrations (e.g. 50 µg/ml IgG has an equal molar ratio with 17 µg/ml Fab). HeV/NiV-G mediated fusion are inhibited by m102.4 IgG at all concentrations tested, but interestingly, m102.4 Fab has a clear dose-dependent effect on fusion with HeV-G. It also appears that Fab is less effective at neutralizing NiV-G mediated fusion than m102.4 IgG. HeV-G-D582N fusion, however, is inhibited in a dose-dependent manner by both m102.4 IgG and Fab with very little difference between IgG and Fab. NiV-G-V507I fusion appears to be more sensitive to m102.4 neutralization than HeV-G-D582N as m102.4 IgG is able to reduce fusion levels

112
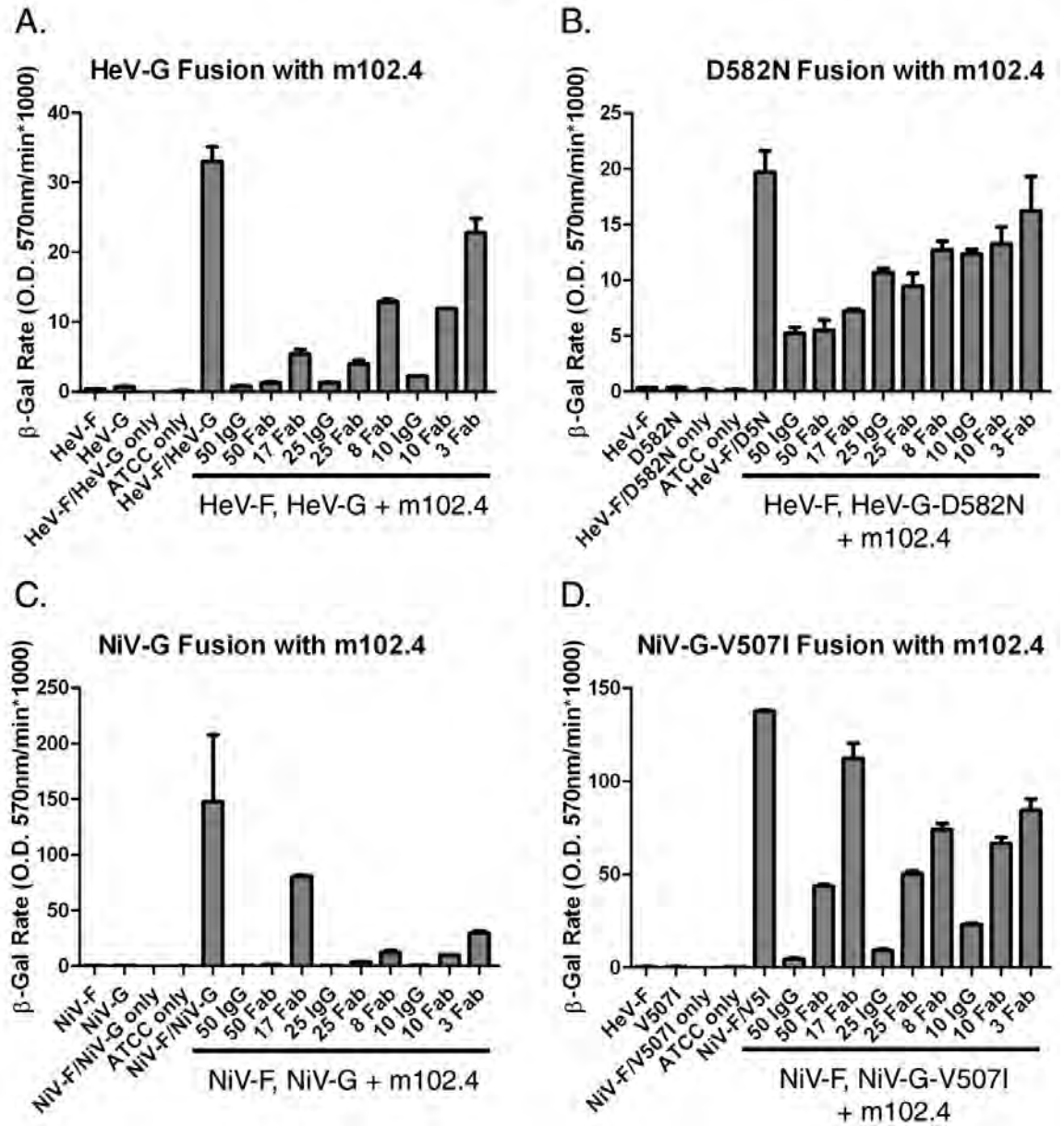
Figure 22: Comparison of wildtype and escape fusion with m102.4 IgG and Fab.
Cells expressing **(A)** HeV-G, **(B)** HeV-G-D582N, **(C)** NiV-G or **(D)** NiV-G-V507I with HeV-F or NiV-F glycoproteins were mixed with receptor-expressing target cells in the presence of three different concentrations of m102.4 IgG and Fab, 50 µg/ml, 25 µg/ml and 10 µg/ml. At each concentration tested, equal concentrations and equal molar concentrations of IgG and Fab were used. Fusion levels are shown as rate of β-galactosidase production.

by greater than 60% for all three concentrations tested. However, it appears that m102.4 Fab is less effective against NiV-G-V507I than m102.4 IgG. For both HeV-G-D582N and NiV-G-V507I high enough concentrations of m102.4 are able to compromise but not completely abolish fusion, and it appears that m102.4 IgG may be more effective at neutralizing fusion than m102.4 Fab.

Generation of new escape variants of HeV/NiV-Gs with m102.4 Variants

Of the 19 m102.4 variants constructed and tested variants LF and HA show the most promise for neutralizing HeV/NiV infection. The variant SLP is also worth further consideration as it seems to decrease some G-receptor interactions but ultimately increases cell-cell mediated fusion. To better understand the effect of these variants on HeV/NiV, they along with variant LD and m102.4 were used to generate a new round of HeV/NiV escape variants. HeV and NiV were serially passaged three times in sub-optimal concentrations of m102.4 Fab, LF, LD, HA and SLP as well as in the absence of any Fab.

Viral titers were measured after each passage and show a steady increase in HeV/NiV production (Table 5). HeV passaged in the presence of m102.4 had the lowest viral titer after three passages at 1.15×10^7 pfu/ml compared to a viral titer of 5.0×10^7 pfu/ml when no Fab is present. Variants LF and HA had viral titers of 1.70×10^7 pfu/ml and 1.93×10^7 pfu/ml, respectively, and HeV titers in the presence of LD increased to 5.25×10^7 pfu/ml. These results support the previous data, verifying that m102.4 is the most efficient at neutralizing HeV, variants LF and HA also neutralize HeV but less effectively than m102.4 and variant LD has no effect on HeV fusion. Also in alignment with the cell-cell fusion data, variant SLP seems to increase the level of viral production

Table 5: Viral titers for HeV/NiV escape variants generated with m102.4 variants.
Viral titer was determined after 3 separate passages of HeV and NiV in the presence of m102.4, LD, LF, HA and no Fab. PFU – plaque forming units

Fab	Viral Titer (PFU/ml)		
	P. 1	P. 2	P. 3
HeV			
m102.4	6.75×10^6	4.0×10^6	1.15×10^7
LD	8.5×10^6	2.20×10^7	5.25×10^7
LF	7.0×10^6	9.0×10^6	1.70×10^7
HA	6.75×10^6	1.33×10^7	1.93×10^7
SLP	2.82×10^7	3.20×10^7	6.5×10^7
No Fab	1.55×10^7	1.75×10^7	5.0×10^7
NiV			
m102.4	1.5×10^6	1.30×10^7	5.0×10^7
LD	1.98×10^7	1.78×10^7	8.25×10^7
LF	2.33×10^7	1.53×10^7	7.75×10^7
HA	3.05×10^7	1.68×10^7	6.25×10^7
SLP	3.05×10^7	2.50×10^7	1.43×10^8
No Fab	1.38×10^7	1.78×10^7	4.75×10^7

as the resulting titer increased to 6.5×10^7 pfu/ml, which is higher than the viral titer in the absence of any Fab.

When NiV escape variants were generated a slightly different pattern emerges. After three rounds of passaging, the viral titer for NiV was less in the absence of Fab, 4.75×10^7 pfu/ml, than when passaged with m102.4, LF and HA, 5.0×10^7 pfu/ml, 7.75×10^7 pfu/ml and 6.25×10^7 pfu/ml, respectively. However, the titers of NiV are in alignment with the cell-cell fusion data in which HA reduced fusion more than LF but less than m102.4. Viral titer was also increased for LD (8.25×10^7 pfu/ml) and SLP (1.43×10^8 pfu/ml) compared to no Fab, which in the case of SLP also supports the cell-cell fusion data.

After the third passage, RNA samples were collected from plaque purified viruses, converted into cDNA, cloned into Blunt-TOPO, transformed and used for sequencing of the HeV/NiV-G genes. The presence of many random, non-repetitive mutations in each of the clones suggests that the method of G sequencing here may allow for the introduction of random mutations. Additionally, we were only able to provide 1X coverage of the majority of the G gene, so mutations identified during sequencing may be due to misreading of the sequence rather than an actual mutation in the gene. A summary of the mutations that were identified in at least two clones of HeV/NiV-Gs is shown in Table 6, and a full listing of the mutations in each clone can be found in Appendix B.

HeV-G strongly favored the formerly seen D582N mutation to escape from m102.4 as well as LF and HA, although it appears that D582 can be mutated to either asparagine (N), tyrosine (Y) or even serine (S). Interestingly, a T507I mutation appeared in 5 clones passaged in the presence of HA. The T507I mutation mimics the original

116

V507I mutation that was first identified in NiV-G m102.4 escape variants. The mutations identified in NiV-G were either D582E or N586T, which were identified in 9 and 3 clones, respectively. Again, the D582E mutation mimics the D582N mutation first identified for HeV-G m102.4 escape variants, but the N586T mutation is unique. The frequency and consistency of mutations at residues 507 and 582 highlight the importance of these two residues, and perhaps those binding pockets in general, for inhibiting m102.4 neutralization.

Table 6: Mutations in HeV/NiV-G that allow escape from m102.4 variants.

> Multiple G genes were sequenced for each condition as indicated. Mutations that were identified in at least 2 clones are shown below with the number of repetitions shown in parentheses. Clones that had no consistent mutation are indicated with a '-.'

	Fab	Mutations	Sequenced
HeV	No Fab	-	9
	m102.4	D582S, D582N (5)	6
	LD	-	7
	LF	Q93R (2), D423G (2), D582N (2), D582Y (2)	4
	HA	T507I (5), D582N (3)	10
	SLP	-	11

	Fab	Mutations	Sequenced
NiV	No Fab	-	5
	m102.4	D582E (5), N586T (2)	7
	LD	-	9
	LF	D582E (3)	4
	HA	D582E (6), N586T (2)	8
	SLP	-	7

DISCUSSION

The therapeutic potential of m102.4 is remarkable due to its strong neutralization of HeV/NiV infections. Animal studies have proven that administration of m102.4 to lethally infected animals can result in complete recovery, even when given as late as 72 hours post infection (17). To date m102.4 has only been administered to humans through compassionate drug use, but it was recently announced that human trials will begin in Australia in 2014, testing the safety of m102.4. No escape from m102.4 has occurred *in vivo*, but viral escape from neutralizing antibodies is a common occurrence among RNA viruses due to a high mutation rate. A better understanding of how HeV/NiV escape from m102.4 neutralization and how that escape can be prevented will further clarify the fusion process and may lead to the development of more targeted therapeutics.

As HeV and NiV infection requires binding ephrin-B2 or -B3, any HeV/NiV escape mutations must disable antibody neutralization without disrupting ephrin binding. Since m102.4 binds the same epitope as ephrin-B2/B3, we sought to create a modified m102.4 that resembled the binding region of ephrin-B2/B3 and would hopefully reduce the potential for viral escape.

A total of 19 m102.4 variants were generated that ranged from single amino acid mutations to complete mutation of the m102.4 binding region. These variants were tested and compared to m102.4 for G binding, inhibition of G-receptor interaction and prevention of HeV/NiV mediated cell-cell fusion, using both wild type HeV/NiV-Gs as well as the m102.4 escape variants HeV-G-D582N and NiV-G-V507I.

Binding ability

Binding ELISAs using Tet-sGs quickly determined that the single mutation

variants have binding characteristics similar to m102.4, although no variant had the same

level of binding as m102.4. The multiple mutation variants were divided on their ability

to bind Tet-sGs; variants that retained the second proline (LAPH<u>P</u>S) were able to bind

but those in which the second proline has been mutated had little to no binding.

The importance of the second proline is understandable upon examination of the

structure and binding of m102.4 (Figure 23). Prolines are unique among amino acids due

to their side chain being a part of the main chain of the peptide, creating what is termed

as a "proline kink" (reviewed in (188)). This kink causes the peptide backbone to change

directions. The first proline in m102.4 corresponds with the proline in the G-H loop of

ephrin-B2/B3, so both m102.4 and receptors have an identical kink in their respective

peptide structures.   The second proline, however, occurs only in m102.4 and is directly

upstream of a string of 6 tyrosine residues, which are large, bulky amino acids. The

proline kink in m102.4 likely allows these residues to be directed in such a way that they

do not cause steric hindrance when m102.4 is binding HeV/NiV-Gs, but when this

proline is removed, the peptide backbone alters, likely causing these tyrosines to come

into conflict with HeV/NiV-Gs, preventing the variants from binding. Notably, this

prevents the fully mutated FSPNLW variant from binding Tet-sGs, but the mostly

converted variant SLP (FSPNPW), which retains the second proline, does exhibit low

level binding to Tet-sGs.

Several attempts were made to construct a m102.4 variant that removed the

second proline (LAPH<u>A</u>S) in order to determine if the theory of the proline kink was

A. ephrin-B2 F₁₂₀SPNLW₁₂₅

m102.4   L₁₀₅APHPS₁₁₀
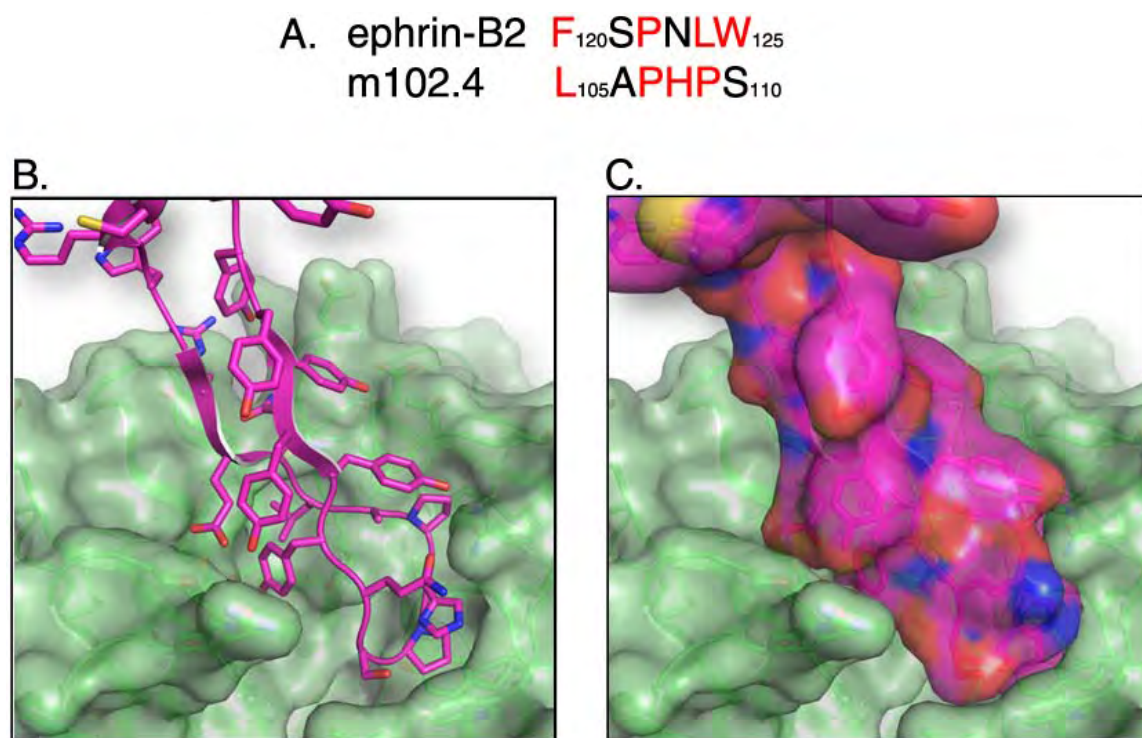
Figure 23: Space-filling model of m102.4 binding HeV-G.
(A) A portion of the ephrin-B2 G-H loop and the binding region of m102.4 are shown in alignment with residues critical for binding HeV/NiV-G highlighted in red. **(B)** Model of m102.4 (pink) binding the globular head of HeV-G (green). The residues HPS can be seen in the bottom right corner, followed by a string of tyrosine residues. **(C)** Space-filling model of model shown in (B). Model supplied by K. Xu.

accurate. However, these attempts were unsuccessful, and the second proline could only

be mutated when an additional mutation had already occurred in the binding region.

Difference between Tet-HeV/NiV-sGs and Tet-D582N/V507I-sGs

As expected from the binding data, m102.4 proved to be the most effective at

inhibiting interaction between Tet-sGs and receptor with variants LF and HA having

similar inhibitory abilities. Variant LD had no inhibitory ability, and variant SLP

inhibited interaction only between Tet-HeV/NiV-sGs and ephrin-B3.

Binding of Tet-sGs to ephrin-B3 was more sensitive to interference by m102.4

and m102.4 variants, which is unsurprising given that Tet-sGs appear to bind ephrin-B3

with less affinity than ephrin-B2 (Chapter 3). In fact, despite the high level of similarity

in the G-H loops of ephrin-B2 and ephrin-B3, Negrete *et al.* determined by SPR that

NiV-G has a greater binding affinity for ephrin-B2 than ephrin-B3 (133). Therefore it

seems that a weakened binding affinity allows for greater m102.4 inhibition.

Tet-HeV/NiV-sGs proved to be more susceptible to inhibition of receptor binding

and cell-cell fusion by m102.4 and m102.4 variants than Tet-D582N/V507I-sGs. At 50

μg/ml, m102.4, LF and HA significantly reduced both receptor binding and cell-cell

fusion for HeV-G and NiV-G. In contrast these variants were unable to significantly

reduce Tet-D582N/V507I-sGs' interaction with ephrin-B2. While variants LF and HA

had no significant impact on HeV-G-D582N cell-cell fusion, they did manage to

significantly reduce NiV-G-V507I fusion, despite the inability of LF and HA to inhibit

Tet-V507I-sG interaction with ephrin-B2. Therefore with respect to NiV-G, we see more

evidence that m102.4 neutralization must not solely depend on inhibiting G-receptor

association.

Variant SLP also managed to inhibit the interaction of Tet-HeV/NiV-sGs with ephrin-B3 but not ephrin-B2, but in cell-cell fusion assays, SLP increased fusion for HeV/NiV-Gs. Tet-D582N/V507I-sGs, however, were unaffected by SLP, either in receptor association or cell-cell fusion. Given the high similarity to receptor, it is possible that SLP may actually partially trigger G conformational change in HeV/NiV-Gs, which could aid fusion while decreasing receptor association. The different results with Tet-D582N/V507I-sGs suggest that Tet-D582N/V507I-sGs may bind receptor, and SLP, differently than wt.

Similarly, the competition ELISAs with Tet-D582N/V507I-sGs and ephrin-B3 seem to indicate that at lower concentrations, the m102.4 variants appear to enhance G-receptor association, highlighting again the different reactions of Tet-HeV/NiV-sGs and Tet-D582N/V507I-sGs to m102.4 variants binding. It is possible that the m102.4 variants are binding at low levels, causing slight conformational changes in Tet-D582N/V507I-sGs that favor receptor binding. As the concentration of variants increase, they are able to outcompete receptor binding to Tet-D582N/V507I-sGs and inhibit interaction. For the cell-cell fusion assays, only one concentration of variant was tested, and it would be interesting to note if lower concentrations of m102.4, LF, HA and SLP would increase cell-cell fusion due to increased receptor binding.

Variants LF, LD, HA and SLP

Of all the 19 variants constructed and characterized, variants LD, LF, HA and SLP were chosen for further study. Variants LF and HA bound all four Tet-sGs and had the greatest ability to inhibit Tet-sG-receptor interaction and cell-cell fusion. Variant LD had neither binding ability, inhibitory ability nor neutralizing activity, and variant SLP

was chosen because it most closely resembled the ephrin-B2/B3 G-H loop, bound Tet-sGs, demonstrated varying ability to inhibit Tet-sG's interaction with receptors and enhanced cell-cell fusion for wildtype HeV/NiV-Gs.

Variants LF, HA and LD each have a single residue change in the binding region of m102.4: **F**APHPS, LAP**A**PS and **D**APHPS, respectively. The mutations in LF and LD affect the first binding pocket of HeV/NiV-Gs (referred to as the L/F/Y pocket), which binds phenylalanine (F), tyrosine (Y) and leucine (L) residues from ephrin-B2, ephrin-B3 and m102.4, respectively. Interestingly, Bowden *et al*. showed that mutation of the ephrin-B2 F120 residue to alanine (A) or glutamic acid (E) prevented ephrin-B2 from binding, suggesting the hydrophobic interactions between F120 and HeV/NiV-G are critical for ephrin-B2 binding (23). Furthermore, the lack of variant LD (**D**APHPS) to bind or inhibit G-receptor interaction supports the importance of this first binding pocket as a non-conservative mutation can completely disrupt ligand binding. In comparison, L105 does not appear essential for binding as the variant LA (**A**APHPS) maintained a moderate level of binding to Tet-sGs. This suggests that the other residues of m102.4 compensate for a "weaker" bond with the L/F/Y hydrophobic pocket of HeV/NiV-Gs, and when L105 is mutated to F it may result in stronger binding in the L/F/Y pocket that strains the compensating factors of the other m102.4 residues. This would explain why variant LF maintains binding and inhibitory ability but not to the level as m102.4. It is somewhat surprising that LF does not have a greater binding and inhibitory ability with Tet-D582N-sG. The D582N mutation affects the L/F/Y binding pocket, and variant LF would be well suited to accommodate that mutation. However, the results presented here

suggest that additional factors beyond one binding residue must be considered in regards to binding m102.4 or m102.4 variants.

The mutation in the HA variant (LAP**A**PS) does not cause m102.4 to more closely resemble ephrin-B2/B3, but it does highlight the fact that H108 is not critical for binding. In the crystal structure of HeV-G with m102.3, the H residue was shown to be reaching towards but not filling the binding pocket occupied by W125 of ephrin-B2/B3 (FSPNL**W**). Given the importance of this binding pocket for helping to "latch" receptor binding to HeV/NiV-Gs, the inability of m102.4 to fill this pocket but maintain high binding affinity with G again highlights the differences between m102.4 and receptor binding.

Variant SLP, **FSPN**P**W**, is almost fully mutated to resemble ephrin-B2 but exhibits only weak binding ability and can only disrupt Tet-HeV/NiV-sG interaction with ephrin-B3. While the G-H loop of receptors and the CDRH3 region of m102.4 are the most critical components for binding to HeV/NiV-Gs, they cannot be the only interactions that determine binding. If they were the only factors influencing binding, then SLP should have similar properties as ephrin-B2. However, this is not the case, suggesting that additional factors outside of the G-H loop and CDRH3 region must influence binding.

HeV/NiV-G escape variants

In regard to m102.4 escape, HeV/NiV-G residues D582, T/V507 and N586 appear to be critical (Figure 24). Mutations in these residues were detected for both HeV and NiV when passaged in the presence of m102.4, LF and HA. It is not surprising that these mutations were detected for all three due to the high degree of similarity between

126
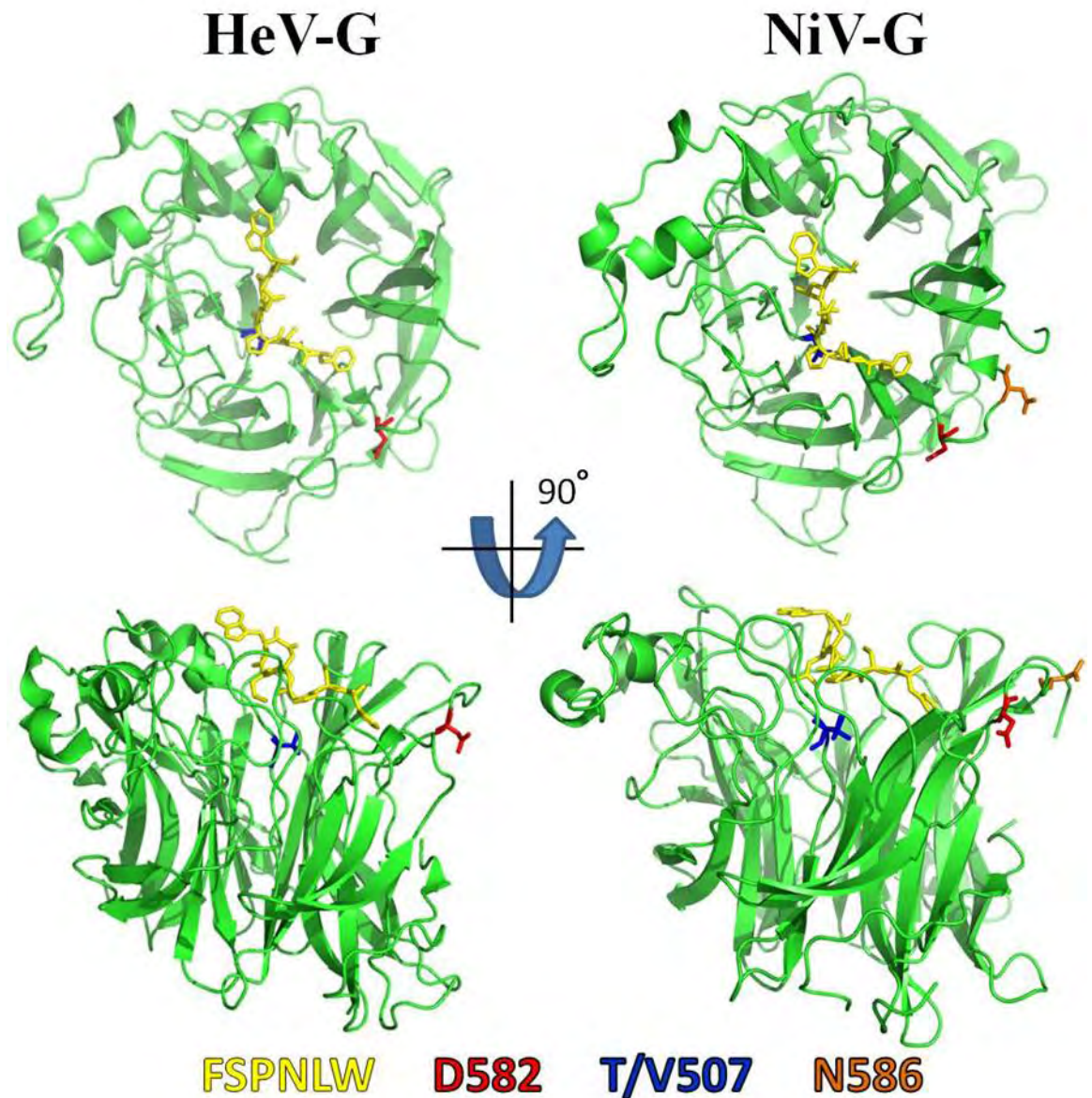
Figure 24: Mutations in HeV/NiV-G that allow for m102.4 escape.
Crystal structures of HeV/NiV-G monomers (green) bound to receptor ephrin-B2 are shown. The G-H loop residues FSPNLW of ephrin-B2 are shown in yellow bound to the top of the globular head. Mutations at residues D582 (red), T/V507 (blue) and N586 (orange) are indicated. HeV-G and ephrin-B2 structure – PDB ID: 2VSK (23), NiV-G and ephrin-B2 structure – PDB ID: 2VSM (23).

these three antibodies. Residue D582 in HeV can be changed to serine (S), asparagine

(N) or tyrosine (Y) to allow for m102.4 escape (Figure 25). The original mutation,

D582N, first seen with HeV escape changes the charged aspartic acid (D) to an

uncharged asparagine (N). Xu *et al.* predicted that this change in residue resulted in the

disruption of a salt bridge that resulted in the modification of the L/F/Y binding pocket,

preventing m102.4 neutralization (207). As previously mentioned, residues F and Y are

large, bulky residues that extend deep into this binding pocket while L is much smaller

and does not extend nearly as deep. Modification of the L/F/Y binding pocket could

therefore easily disrupt L but not F/Y binding. As can be seen in the crystal structure

residue D582 lies adjacent to a number of the residues involved in forming the L/F/Y

binding pocket, particularly those residues at the top of the pocket (Figure 25). A closer

examination of the mutations at residue D582 explains how each of the mutations may

disrupt the salt bridge. For D582N, one of the oxygen molecules on the side chain of D is

replaced with a nitrogen group in N, which cannot form a salt bridge with the nitrogen

groups on the side chains of R589 and K591. Similarly, the change of D582Y inserts a

tyrosine molecule, whose bulky phenyl ring likely prevents any association with R589 or

K591. Interestingly the mutation of D582S seems unlikely to disrupt the salt bridge, and

therefore may depend on other disrupted bonds to inhibit m102.4 neutralization.

Figure 25: Mutations of HeV-G D582.
The crystal structure of the globular head of HeV-G (green) is shown bound to the G-H loop FSPNLW residues (yellow) of ephrin-B2. Residue D582 (cyan) is shown mutated to D582N/Y/S (gray). The residues in HeV-G that form the L/F/Y binding pocket are indicated in magenta, and residues R589 and K591, which form a salt bridge with D582 are shown in tan. Oxygen (red) and nitrogen (blue) atoms on the side chains of D582, R589 and K591 are indicated. Crystal structures provided from PDB ID: 2VSK (23).

D582

D582N

D582Y

D582S

FSPNLW
D582
F pocket
R589
K591
Oxygen
nitrogen
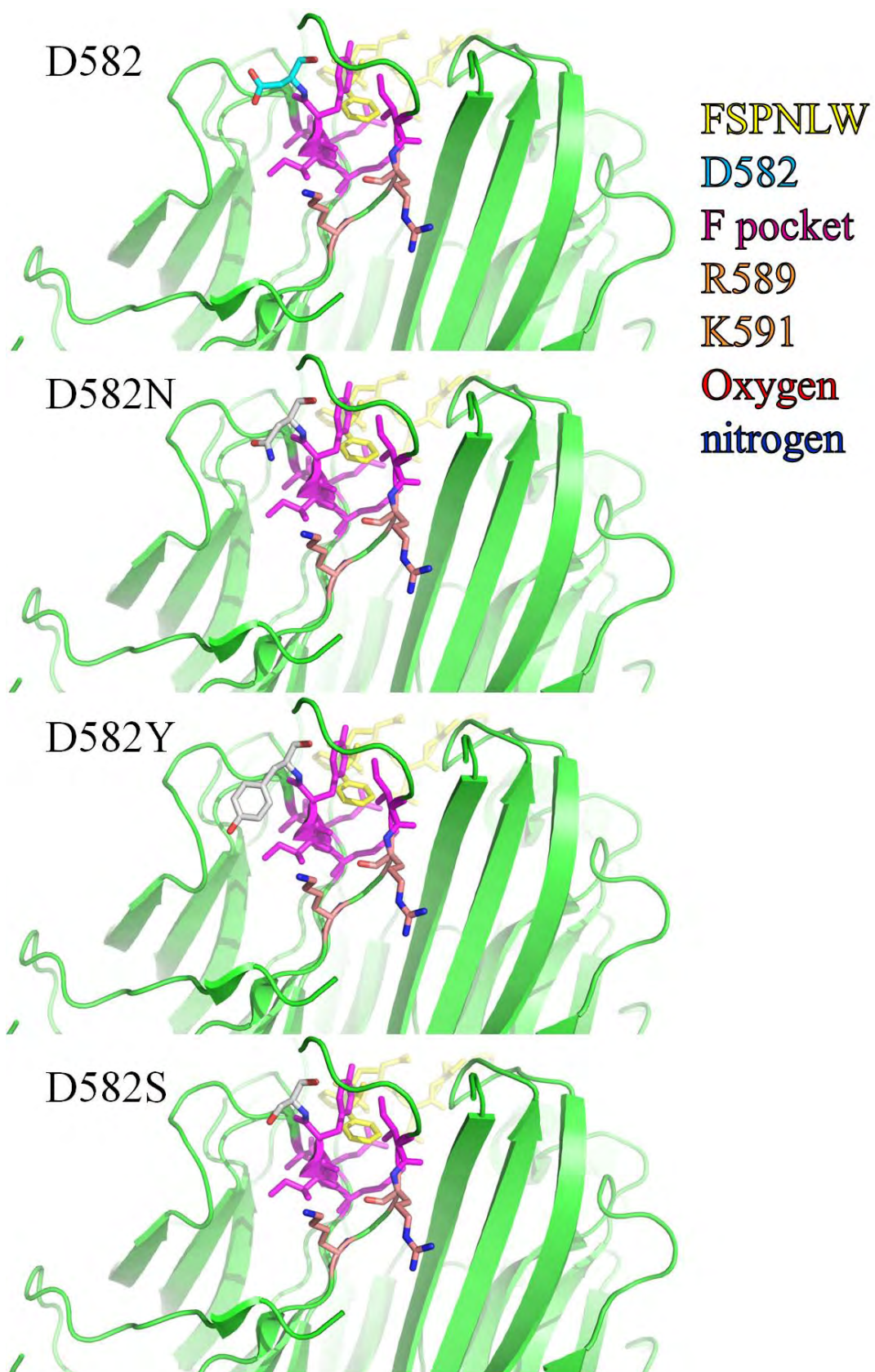
Five of the HeV-G HA escape variants had a T507I mutation, which resembles the original NiV-G escape mutation. This mutation lies directly underneath the conserved proline between receptors and m102.4. An examination of the crystal structure of HeV-G bound to ephrin-B2 reveals the close proximity of T507 to both P123 (ephrins) and the other HeV-G residues that form the P pocket (Figure 26). The mutation of T507I is not very drastic, resulting in a longer side chain with one less hydroxyl group. The longer side chain may result in steric hindrance with receptors and m102.4, but receptors, unlike m102.4, may be able to compensate for this strained binding through other interactions between receptor and HeV-G. Additionally, the loss of the hydroxyl group may prevent additional binding between T507 and surrounding residues, which could lead to the alteration of the P pocket residues.

NiV-G uses two mutations to escape m102.4, LF and HA neutralization. The D582 residue is mutated as in HeV-G, but the aspartic acid (D) is replaced with a very similar glutamic acid (E). An examination of the crystal structure of NiV-G shows that the two residues that form a salt bridge with D582 in HeV-G, R589 and K591, appear to be further away from D582 in NiV-G (Figure 27). However, residue T556 lies extremely close to D582, and the elongation of the side chain caused by the D582E mutation may bring the oxygen groups in D582E and T556 into close proximity, causing repulsion. This repulsion could then alter the L/F/Y binding pocket. The N586T mutation detected in NiV-G is similar to mutation of D582, being outside of the m102.4 and receptor binding area. However, an examination of the crystal structure of NiV-G with ephrin-B2 suggests that like D582, mutation of N586 may disrupt the L/F/Y binding pocket (Figure 28). The amino group in the asparagine (N) residue at position 586 appears to interact
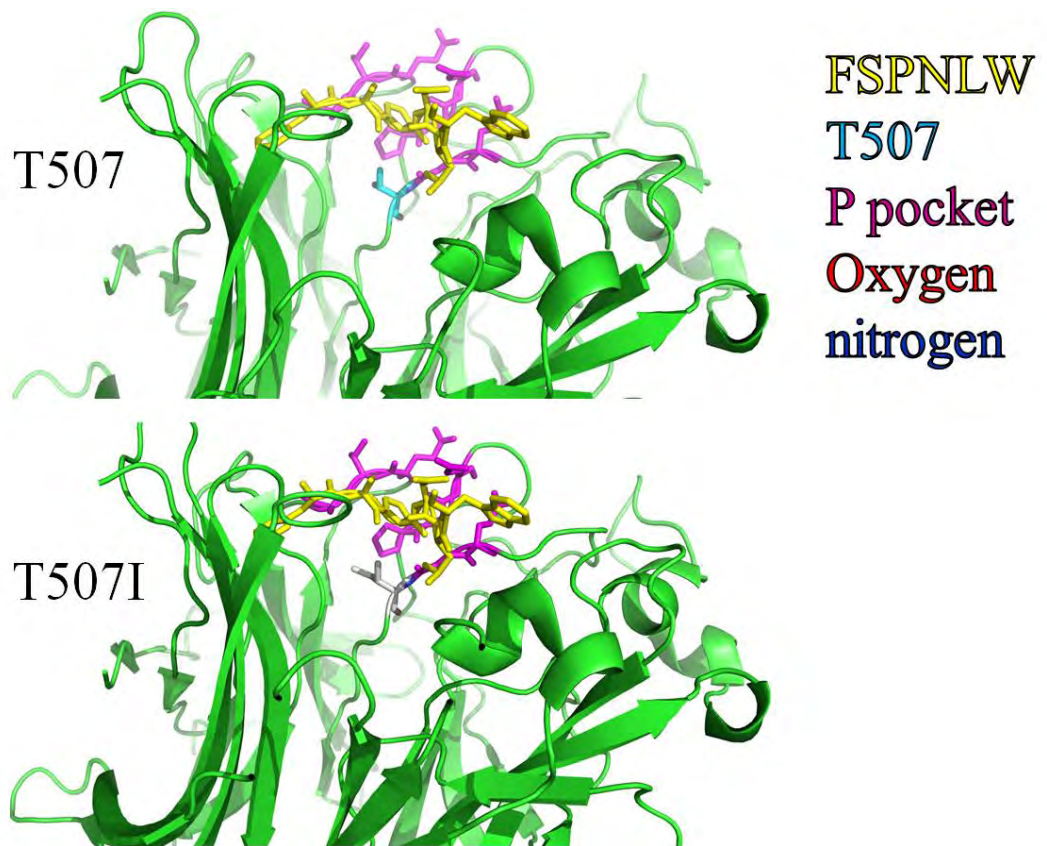
Figure 26: Mutations of HeV-G T507.
The crystal structure of the globular head of HeV-G (green) is shown with the FSPNLW (yellow) residues of ephrin-B2. Residue T507 (cyan) is shown mutated to T507I (gray). The residues in HeV-G that form the P binding pocket are indicated in magenta, and oxygen (red) and nitrogen (blue) atoms on the side chain of T507 are indicated. Crystal structures provided from PDB ID: 2VSK (23).
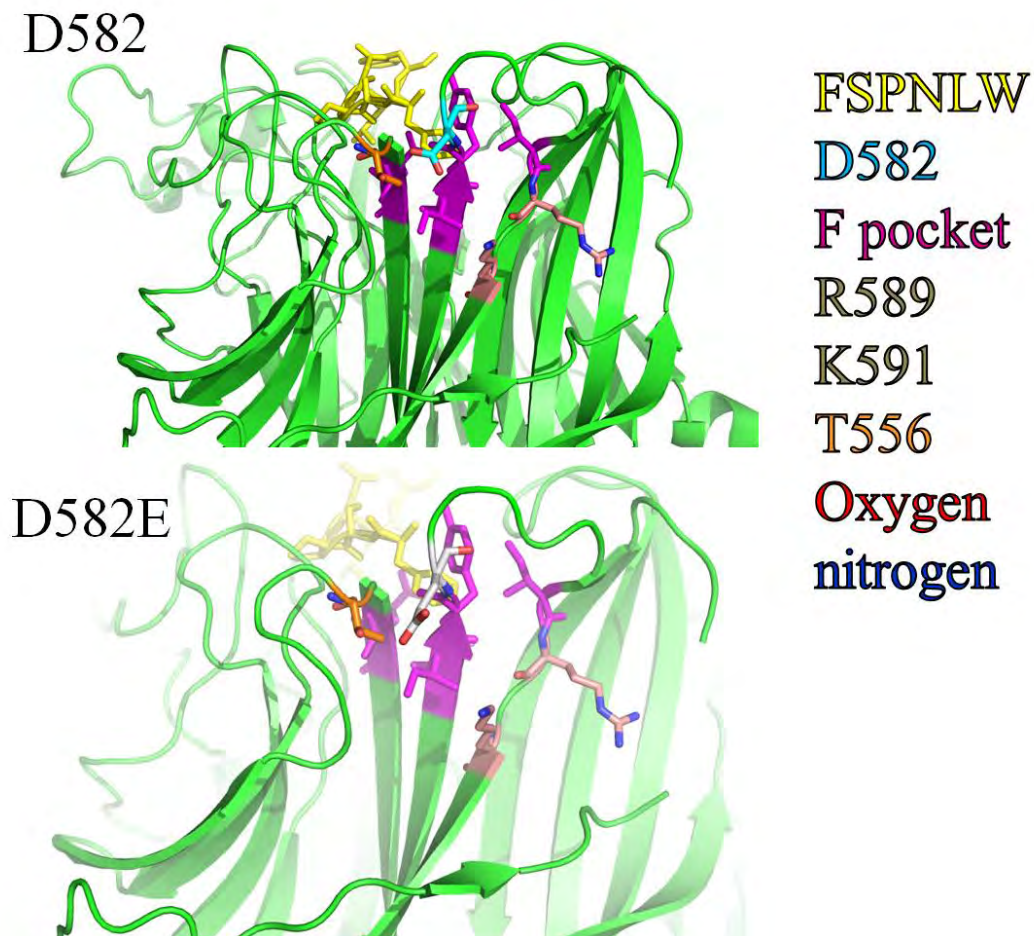
Figure 27: Mutation of NiV-G D582.
The crystal structure of the globular head of NiV-G (green) is shown with the FSPNLW (yellow) residues of ephrin-B2. Residue D582 (cyan) is shown mutated to D582E (gray). The residues in NiV-G that form the F binding pocket are indicated in magenta, and residues R589 and K591 are shown in tan, while residue T556 is shown in orange. Oxygen (red) and nitrogen (blue) atoms on the side chains of D582, R589, K591 and T556 are indicated. Crystal structures provided from PDB ID: 2VSM (23).
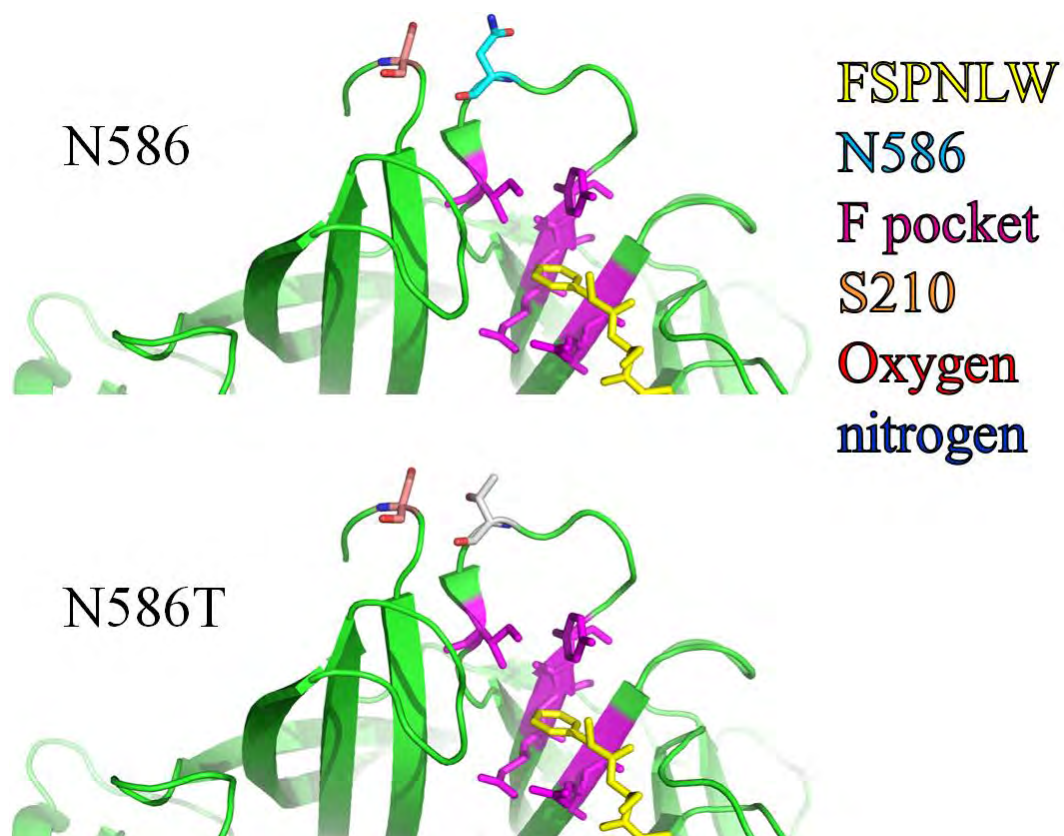
Figure 28: Mutation of NiV-G N586.
The crystal structure of the globular head of NiV-G (green) is shown bound to the ephrin-B2 G-H loop residues FSP (yellow). Residue N586 (cyan) is shown mutated to N586T (gray). The residues in NiV-G that form the F binding pocket are indicated in magenta, and residue S210 is shown in tan. Oxygen (red) and nitrogen (blue) atoms on the side chains of N586 and S210 are indicated. Crystal structures provided from PDB ID: 2VSM (23).

with the hydroxyl group of residue S210, likely creating a bond that helps stabilize the two beta sheets. When N586 is mutated to a threonine (T), the amino group is replaced with a hydroxyl group and likely results in repulsion with the hydroxyl group of S210, disrupting the L/F/Y binding pocket.

Limitations and Future Directions

One of the limitations of this work was that all the m102.4 variants were tested as Fabs rather than IgGs. The Fab constructs, while having a relatively high affinity to Tet-sGs, have lower binding affinities than their IgG counterparts. This can be clearly seen in Figure 23, where m102.4 IgG is able to inhibit HeV-G cell-cell fusion at a relatively constant level at all three concentrations used (50 μg/ml, 25 μg/ml and 10 μg/ml), but there is a steady increase in HeV fusion for the various Fab concentrations. It would be interesting to repeat the binding and competition ELISAs along with the cell-cell fusion assays using IgG constructs rather than Fabs to see if the results will repeat or if the IgG constructs would be more effective. Additionally, repetition of the cell-cell fusion assays with ephrin-B2 or ephrin-B3 expressing target cells would help determine how inhibition of G-receptor binding, or lack thereof, translates to fusion mediated by binding specific receptors.

We've seen evidence that mutation of D582 and V/T507 can occur in either HeV/NiV-G, while the N586T mutation has only been isolated from NiV-G. Variants of all the escape mutations should be made in both HeV/NiV-G to determine if they are effective for both HeV and NiV. Despite the high degree of similarity between HeV/NiV-G, mutations that work in one G may not be effective in the other or they may work through a different escape mechanism. Using different mutations in the same

residue to escape m102.4 through multiple mechanisms does appear to be possible as shown by the different mutations of D582. However, the crystal structures used to extrapolate the possible mechanisms of m102.4 escape for HeV/NiV escape are not easily manipulated and show G binding with receptor rather than m102.4. The interactions speculated to be effected by mutations in HeV/NiV-G may or may not be responsible for m102.4 escape. More work should be done to determine precisely how the mutations alter m102.4 neutralization without affecting receptor binding. This work can progress by making soluble Tet-sGs for each of the mutations and comparing receptor and m102.4 binding as was done for the original escape mutations. Furthermore, the F gene should be analyzed to verify that no mutation in F resulted in viral escape.

SUMMARY

A total of 19 m102.4 variants were constructed and tested for efficacy in binding Tet-sGs, inhibiting Tet-sG interaction with receptors and preventing cell-cell fusion. Of the 19 variants two, LF and HA, most closely mimicked the properties of m102.4 while ultimately being less effective than m102.4. We've determined that the CDRH3 binding region of m102.4 is critical for binding, but severe modification of this region, even to resemble receptor, inhibits its neutralizing potential. Any alteration to the binding region of m102.4 should also account for additional factors that aid m102.4 binding to HeV/NiV-G. It also appears that m102.4 binding may be slightly more dependent upon binding to the first two pockets of HeV/NiV-G (L/F/Y pocket and P pocket) as mutations near these two binding pockets results in viral escape from m102.4.

Chapter 5: Role of the Attachment Glycoprotein in Fusion and how m102.4 Neutralizes Infection

INTRODUCTION

Hendra and Nipah viruses are prototypical paramyxoviruses in that they require both an attachment (G) and fusion (F) glycoprotein to mediate viral entry. Both of these glycoproteins are expressed on the viral surface and interact during the fusion process, leading to two prevailing interaction models – clamp (dissociation) or provocateur (association). Several studies suggest that HeV/NiV follow a clamp model as G and F are associated prior to receptor binding and that strengthened G-F interaction results in decreased fusion (1; 3; 11). Other studies, however, indicate that HeV/NiV may follow more of a provocateur model as expression of HeV/NiV-F in the absence of G maintains a pre-fusion conformation (33). Furthermore the different trafficking patterns of G and F, along with the additional endocytosis and cleavage of F required for full maturation, align more with a provocateur model (138; 139; 197; 198). Given the contradictory data, it is likely that neither model is completely accurate and that true G-F interaction incorporates aspects of both models. In fact Porotto *et al.* recently proposed a third model in which G-F interaction occurs sporadically throughout the fusion process rather than through an absolute "on-off" association (153).

Regardless of the nature of G-F interaction, G-induced triggering of F requires conformational changes in G caused by receptor binding. These conformational changes in G are minor and are predicted to result in the movement of the globular heads between "heads-down" and "heads-up" conformations (195; 215; 216). In a heads-down conformation, residues in the globular head of G interact with the stalk domain, but in the heads-up conformation the globular heads are lifted away from the stalk. The interaction

of the globular heads with the stalk domain is critical as the stalk is responsible for F

association and presumably F activation (10; 13; 26; 103). Therefore, G and F

association can only occur when G is in a heads-up conformation. In relation to the

models of G-F interaction, it is unclear which conformation – heads-up or heads-down –

G adopts prior to receptor binding as a pre-receptor heads-up conformation would be

indicative of the clamp model and heads-down the provocateur model.

The change in F association with G leads to activation of F, which results in the

insertion of the fusion peptide into the target cell membrane, irreversible formation of a

six-helix bundle, hemifusion and ultimately pore formation. As m102.4 specifically

targets HeV/NiV-Gs, the neutralization mechanism of m102.4 most likely occurs prior to

F activation. While it was assumed that m102.4 neutralized HeV/NiV by preventing G

from binding receptor, the work here with the m102.4 escape variants (HeV-G-D582N

and NiV-G-V507I) indicate that binding alone cannot neutralize viral entry. It is

therefore easy to speculate that m102.4 may be affecting the conformational changes in G

that are required for F activation, either by prematurely inducing or preventing

conformational changes in G.

In order to further understand the interaction between HeV/NiV-G and -F and

how receptor and m102.4 may be altering this interaction, we used Tet-sGs with

Trimeric-HeV/NiV-sF to determine the effect of receptor and m102.4 binding on G-F

association. We also began to examine the possible neutralization mechanisms of

m102.4 by determining the impact of m102.4 on receptor binding to Tet-sGs.

Binding pattern of m106.3 to Tet-sGs in presence of ephrin-B2 and m102.4

In Chapter 3 it was shown in an ELISA format that the addition of increasing

concentrations of ephrin-B2 increased the level of bound m106.3 to Tet-sGs (Figure 11).

While it appears that ephrin-B2 induces conformational change in Tet-sGs that enhances

m106.3 binding, it was unknown what effect m102.4 would have on the ability of m106.3

to bind Tet-sGs and how this may relate to m102.4 neutralization. As done in Chapter 3,

an ELISA was prepared in which bound Tet-sGs were coated on an ELISA plate and then

incubated with a constant concentration of m106.3 in the presence of increasing levels of

m102.4 IgG. The results can be seen in Figure 29B with the previous data involving

ephrin-B2 reshown in part A.

Unlike ephrin-B2, m102.4 appears to have a deleterious effect on the ability of

m106.3 to bind Tet-sGs. At the lowest concentration of m102.4 tested, 10 ng/µl, the

level of m106.3 bound decreased for all four Tet-sGs. While there tended to be no

additional decrease when 25 ng/µl m102.4 was added, the level of bound m106.3

remained lower than the level of bound m106.3 in the absence of m102.4.

Association of Tet-sGs with Tri-HeV/NiV-sF

HeV/NiV-Gs have to trigger F to initiate membrane fusion, and we used binding

ELISAs to determine if G-F interaction increased or decreased in the presence of receptor

and m102.4. ELISA plates were coated with Tri-HeV/NiV-sFs, blocked and then

incubated with all four forms of Tet-sGs (HeV, NiV, D582N and V507I) in the presence

of increasing concentrations of ephrin-B2, ephrin-B3 or m102.4. The level of bound
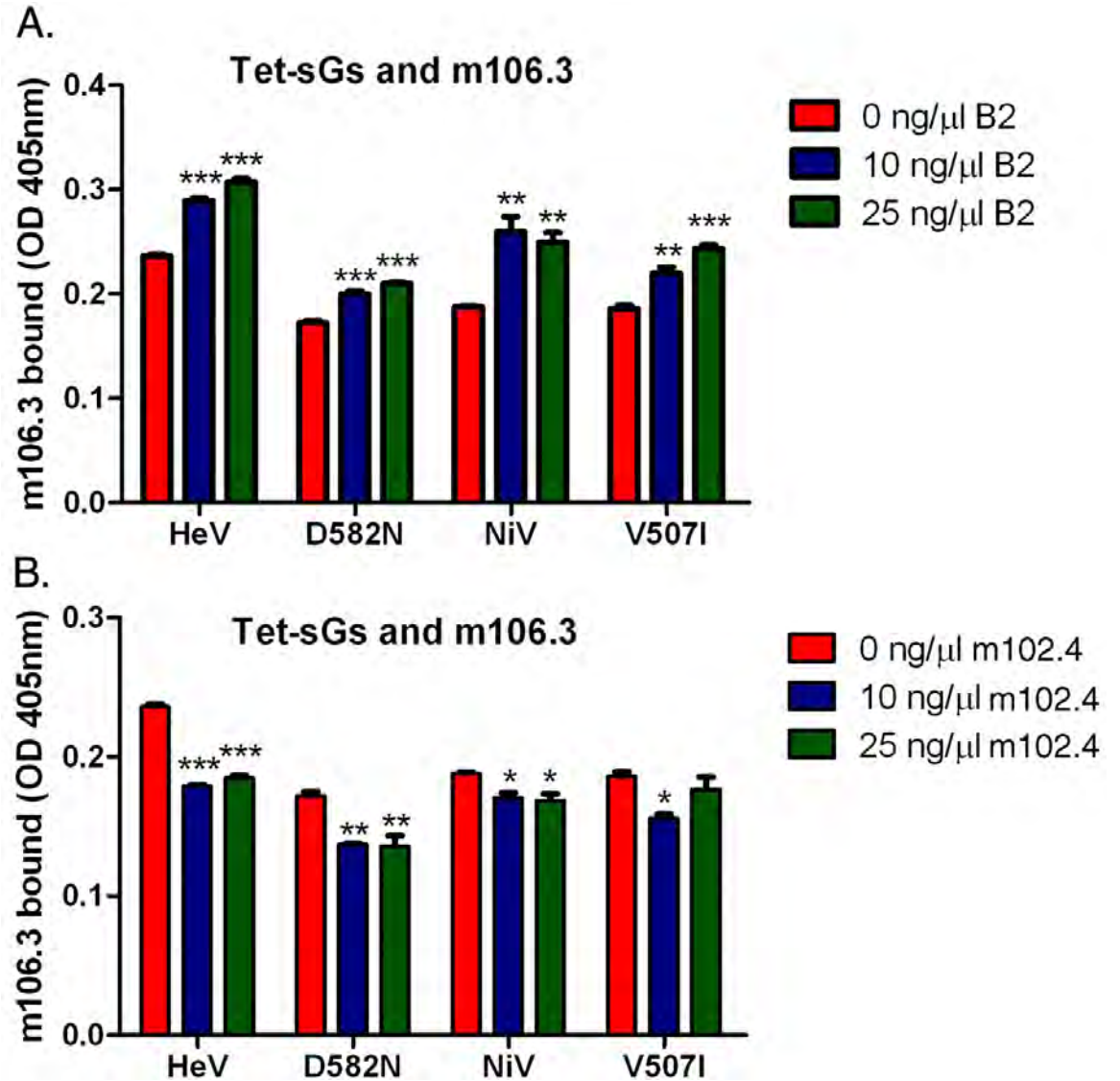
Figure 29: Binding pattern of m106.3 to Tet-sGs in presence of ephrin-B2 and m102.4.
Binding ELISA with Tet-sGs coated on a plate and incubated with m106.3 and increasing concentrations of (**A**) ephrin-B2 or (**B**) m102.4. Level of bound m106.3 was determined using α-Flag-HRP antibody. One-way Anova statistics, *<0.05, **<0.005, ***<0.0001

Tet-sGs was determined and compared to the binding of Tet-sGs to Tri-HeV/NiV-sFs in the absence of any additional ligands (Figure 30).

Tri-HeV-sF and Tet-sGs

The ability of Tet-sGs to bind Tri-HeV-sF in the absence of receptor or m102.4 was extremely low with levels at or barely above background. The notable exception is Tet-V507I-sG, which was able to bind to fairly high levels, although the heightened binding could be partly due to the mucilaginous properties of Tet-V507I-sG. Upon addition of ephrin-B2 the levels of bound Tet-sG increased for all four Tet-sGs. Interestingly, levels of bound Tet-HeV-sG and Tet-V507I-sG steadily increased with increasing levels of ephrin-B2, while Tet-D582N-sG and Tet-NiV-sG increased but then plateaued at 10 ng/μl ephrin-B2.

This steady increase in bound Tet-sGs was not observed when ephrin-B3 was incubated with Tet-sGs, except for Tet-V507I-sG. The three other Tet-sGs had little to no increased binding to Tri-HeV-sF until 50 ng/μl ephrin-B3 was added. At this concentration the levels of Tet-HeV-sG and Tet-D582N-sG doubled, and bound Tet-NiV-sG and Tet-V507I-sG also increased.

Ephrin-B2 and -B3 appear to increase association between Tet-sGs and Tri-HeV-sF, but the addition of m102.4 caused different results. Increasing concentration of m102.4 had no effect on Tet-HeV-sG, Tet-D582N-sG or Tet-NiV-sG as binding of these Tet-sGs never rose above background levels. However, Tet-V507I-sG, which binds Tri-HeV-sF in the absence of additional ligands, had decreased binding to Tri-HeV-sF in the presence of increasing concentrations of m102.4.

141
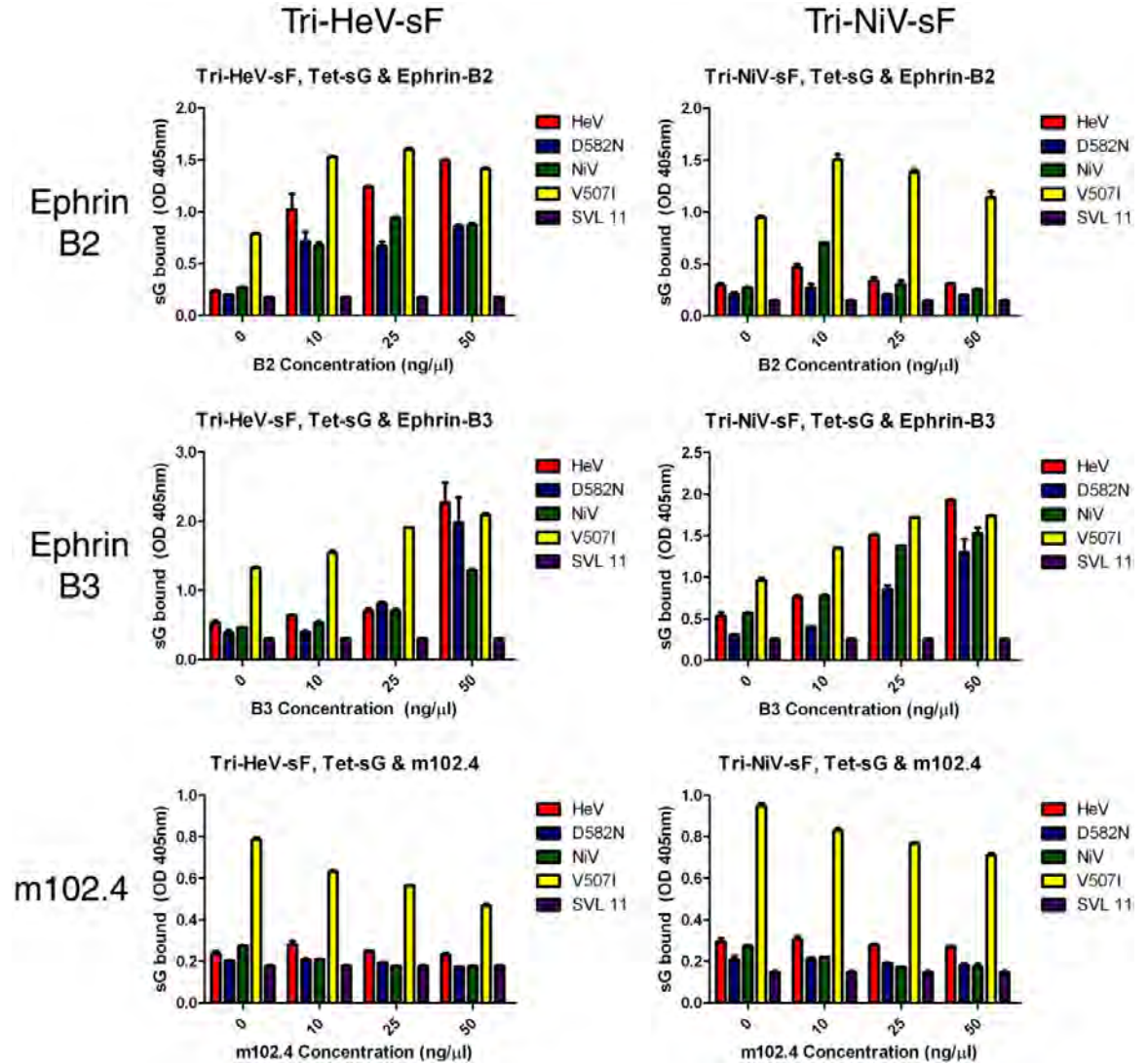
Figure 30: Tet-sG association with Tri-HeV/NiV-sF in presence of ephrin-B2, ephrin-B3 and m102.4.
Tri-HeV-sF (left) or Tri-NiV-sF (right) coated on an ELISA plate were incubated with Tet-HeV-sG, Tet-NiV-sG, Tet-D582N-sG or Tet-V507I-sG in the presence of increasing concentrations of ephrin-B2, ephrin-B3 or m102.4. Levels of bound Tet-sG were determined using a variety of G-specific antibodies.

Tri-NiV-sF and Tet-sGs

Similar, but not identical, results were obtained when Tri-NiV-sF was used in place of Tri-HeV-sF. The addition of ephrin-B2 at 10 ng/µl increased the levels of bound Tet-HeV-sG, Tet-NiV-sG and Tet-V507I-sG, although these increases were less than those seen with Tri-HeV-sF. Additionally, no increase was detected for Tet-D582N-sG, and the increased levels of the other Tet-sGs decreased with the addition of 25 ng/µl ephrin-B2.

The addition of ephrin-B3 resulted in increased association for all Tet-sGs similar to the pattern obtained with Tri-HeV-sF and ephrin-B2. Tet-D582N-sG had a slower increase than the other Tet-sGs, requiring the addition of 25 ng/µl ephrin-B3 to achieve a noticeable increase in binding Tri-NiV-sF.

As was seen with Tri-HeV-sF, the levels of Tet-sG association with Tri-NiV-sF remained constant or decreased with increasing concentration of m102.4. These results suggest that the neutralization ability of m102.4 is likely not due to an ability of m102.4 to mimic receptor as no increased association with Tri-sFs was detected.

Binding pattern of Tet-HeV/D582N-sGs to m102.4 in presence of ephrin-B2 and m106.3

Ephrin-B2/B3 and m102.4 use the same binding epitope on HeV/NiV-Gs, the top of the globular head. We know that the m102.4 escape variant of HeV-G (HeV-G-D582N) is still able to bind m102.4, so m102.4 escape cannot occur simply due to an inability of antibody to bind G. Another possible neutralization mechanism of m102.4 may be the ability of m102.4 to either induce or inhibit conformational changes in G required for F interaction (i.e. m102.4 mimics receptor or m102.4 prevent receptor-induced conformational change). To test this hypothesis, an ELISA assay was

143

constructed in which Tet-HeV/D582N-sGs were added to a plate coated with m102.4 IgG. After incubation and washing, m106.3 was added in the presence or absence of ephrin-B2, and bound m106.3 was measured. It was thought if m102.4 induces conformational change in G then no additional m106.3 binding would be detected with the addition of ephrin-B2. However, if ephrin-B2 increased the levels of bound m106.3 then that would suggest m102.4 is not inducing conformational change in HeV-G. The results between Tet-HeV-sG and Tet-D582N-sG would then be compared.

When Tet-HeV-sG was added to m102.4 followed by the addition of m106.3, high levels of bound m106.3 were detected (Figure 31). This result is not unexpected as it has been previously shown that Tet-sGs are able to bind m106.3 in the absence of receptor (Chapter 3). When m106.3 and ephrin-B2 were added simultaneously, the levels of bound m106.3 remained constant compared to the level of bound m106.3 in the absence of ephrin-B2. When Tet-D582N-sG was added to m102.4 followed by m106.3 addition, bound m106.3 was detected, albeit at lower levels than with Tet-HeV-sG. However, the level of bound m106.3 dropped significantly when ephrin-B2 was added along with m106.3.

Since the level of bound m106.3 changed for Tet-D582N-sG upon addition of ephrin-B2, it seems reasonable that ephrin-B2 disrupted the binding between Tet-D582N-sG and m102.4. Previous data indicated that Tet-D582N-sG has a lower binding affinity to m102.4 than Tet-HeV-sG (Chapter 3), allowing Tet-D582N-sG but not Tet-HeV-sG to dissociate from m102.4 in the presence of ephrin-B2. Thus any m106.3 bound to Tet-D582N-sG would be removed during subsequent washing steps, resulting in a lower level of detectable m106.3. The ability of Tet-D582N-sG but not Tet-HeV-sG to dissociate

144
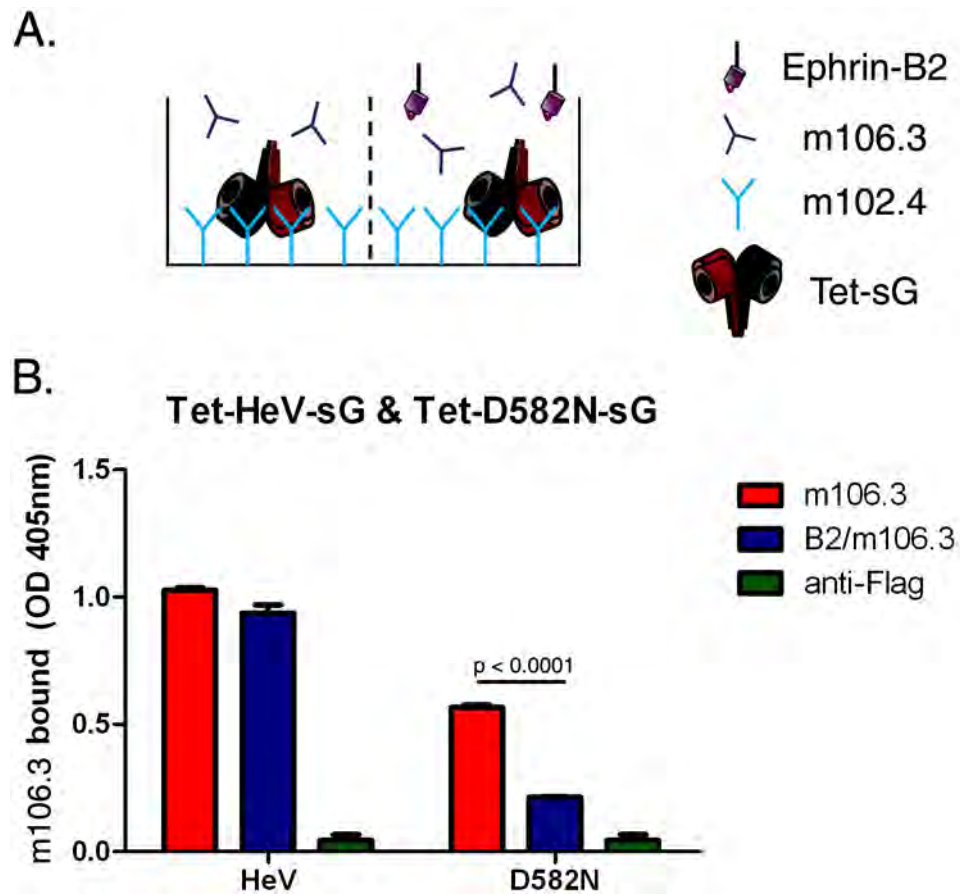
Figure 31: Tet-HeV-sG and Tet-D582N-sG bind m102.4 differently in presence of ephrin-B2.
(**A**) Schematic of the conditions tested in this binding ELISA. Tet-sG was added to an ELISA plate coated with m102.4 followed by the addition of m106.3 in the absence and presence of ephrin-B2. (**B**) Level of bound m106.3 to Tet-sG bound to m102.4 in absence and presence of ephrin-B2. The values of bound m106.3 were determined using α-Flag-HRP antibody.

from m102.4 suggests that the escape of HeV-G-D582N may be due to decreased binding affinity to m102.4.

Sequential binding of ephrin-B2 and m102.4 to Tet-sGs

HeV/NiV-Gs are tetramers comprised of four monomeric units, each containing a globular head. The stoichiometry of receptor and G binding is unknown, but Brindley *et al.* showed that only one dimer pair of the tetramer needs to be bound by receptor to induce conformational change in the attachment glycoprotein (27). Theoretically then, it is possible that receptor and antibody could simultaneously bind the same tetrameric unit. Given the results described above, it also seems plausible that bound m102.4, or perhaps even bound receptor, could be replaced by the other ligand. In order to further explore this possibility, all Tet-sGs were tested for their ability to bind m102.4 and ephrin-B2 when added in a sequential manner. A model of this assay is shown in Figure 32 A. Briefly, Tet-sGs were bound to ELISA plates followed by the addition of either m102.4 (Figure 32A, top row) or ephrin-B2 (bottom row). After this initial addition, wells were washed and the opposite ligand was added (ephrin-B2 to top row and m102.4 to bottom row). Levels of bound m102.4 and ephrin-B2 were measured and compared to wells in which only ephrin-B2 or m102.4 were added to determine if the addition of the opposite ligand had any effect on the initial ligand's binding to Tet-sGs.

The levels of bound m102.4 and ephrin-B2 without additional ligands were measured and considered as maximal binding for the two ligands (red and yellow bars, Figures 32B). Tet-D582N-sG had the lowest level of bound m102.4 (red bars), while the three remaining Tet-sGs bound m102.4 to similar levels. This again highlights the difference in binding affinity between Tet-HeV-sG and Tet-D582N-sG. Additionally, the

146
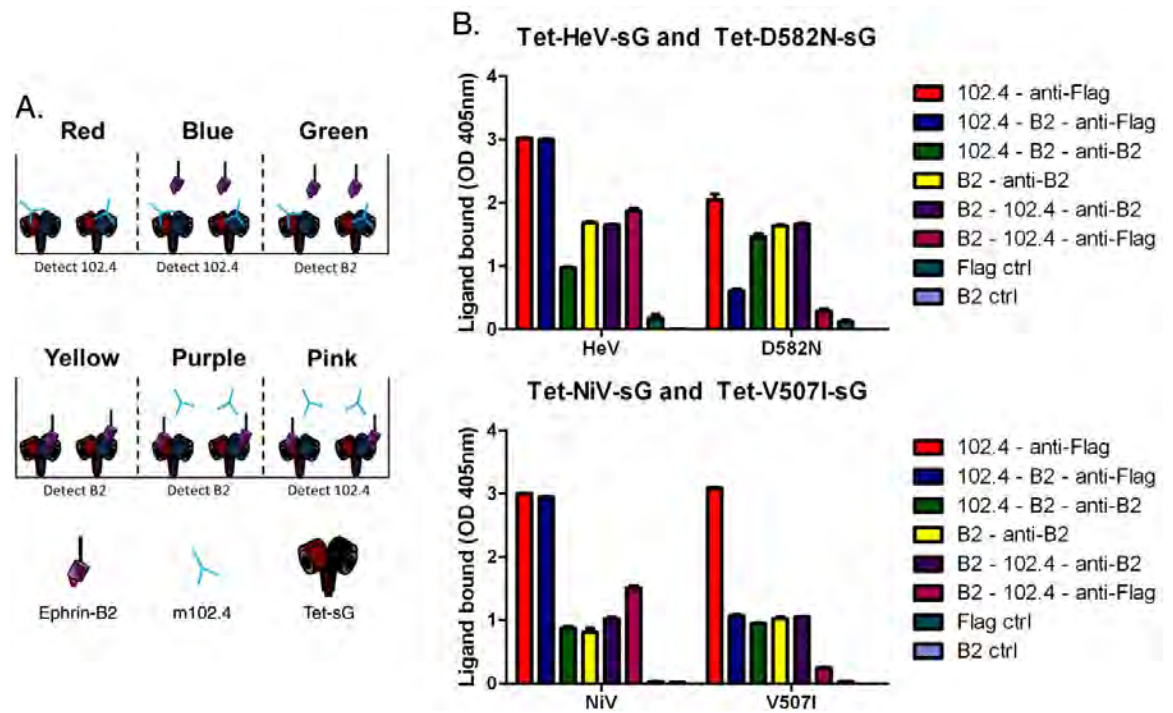
Figure 32: Sequential binding of m102.4 and ephrin-B2 to Tet-sGs.
(A) Representation of the binding ELISA conditions. Tet-sGs were bound to a plate, incubated with either m102.4 or ephrin-B2, washed and then incubated with the other ligand. The ligand detected for each well is indicated below the well, and the color listed above each well corresponds to the bar colors in (B). **(B)** Levels of m102.4 and ephrin-B2 bound to Tet-sGs were determined using ligand-specific antibodies.

levels of bound ephrin-B2 were similar for Tet-HeV-sG and Tet-D582N-sG, which were slightly higher than the levels observed for Tet-NiV-sG and Tet-V507I-sG (yellow bars).

The levels of bound m102.4 did not change with the addition of ephrin-B2 for Tet-HeV-sG and Tet-NiV-sG, but for the two escape variants, Tet-D582N-sG and Tet-V507I-sG, the levels of m102.4 dropped (blue bars). This suggests that ephrin-B2 can displace bound m102.4 on the globular heads of the two escape variants.

Interestingly, the detectable amount of bound ephrin-B2 added after m102.4 was similar to the maximal level of ephrin-B2 binding (green bars vs. yellow bars, respectively). The one exception is with Tet-HeV-sG, which had ephrin-B2 levels at about 60% of maximum. Since the level of m102.4 binding did not decrease after the addition of ephrin-B2 for Tet-HeV/NiV-sGs, even though ephrin-B2 bound to 60%-100% maximal levels, this suggests that m102.4 and ephrin-B2 binding do not require all four globular heads in the tetramer.

Conversely, for all Tet-sGs the level of bound ephrin-B2 did not change upon addition of m102.4 (purple bars), while the levels of m102.4 added after ephrin-B2 were higher for Tet-HeV/NiV-sGs than Tet-D582N/V507I-sGs (pink bars). Tet-HeV/NiV-sGs had levels of m102.4 binding that were approximately 50% of maximal m102.4 binding, but the levels for Tet-D582N/V507I-sGs were just above background. This suggests that m102.4 is unable to bind the globular heads of Tet-D582N/V507I-sGs when receptor is previously bound, which is not the case for Tet-HeV/NiV-sGs.

Simultaneous binding of m102.4 and ephrin-B2 to Tet-sGs

To further study the interplay of ephrin-B2 and m102.4 binding to Tet-sGs, the binding pattern of m102.4 and ephrin-B2 was determined when both ligands were added

simultaneously to Tet-sGs coated on an ELISA plate. Equal and unequal concentrations of m102.4 and ephrin-B2 were added to ELISA plates coated with Tet-sGs, and bound m102.4 and ephrin-B2 were detected (Figure 33). Maximal ephrin-B2 and m102.4 binding were again determined by adding each ligand separately to Tet-sGs.

Similar binding patterns were observed for both Tet-HeV/NiV-sGs. Regardless of the concentrations used, both m102.4 and ephrin-B2 could simultaneously bind Tet-HeV/NiV-sGs, although binding of m102.4 was more variable than ephrin-B2 compared to their maximal binding. For Tet-D582N-sG only bound ephrin-B2 could be detected regardless of the concentrations of m102.4 or ephrin-B2 added, again indicating that Tet-D582N-sG has a lower affinity for m102.4 than ephrin-B2. Interestingly, Tet-V507I-sG displayed a binding pattern more similar to wild type, binding both m102.4 and ephrin-B2 despite the concentrations used. While the escape mechanism of HeV-G-D582N appears to be due to binding affinity differences between m102.4 and receptor, NiV-G-V507I seems to require a different escape mechanism as m102.4 binding is not as inhibited as it is for HeV-G-D582N.
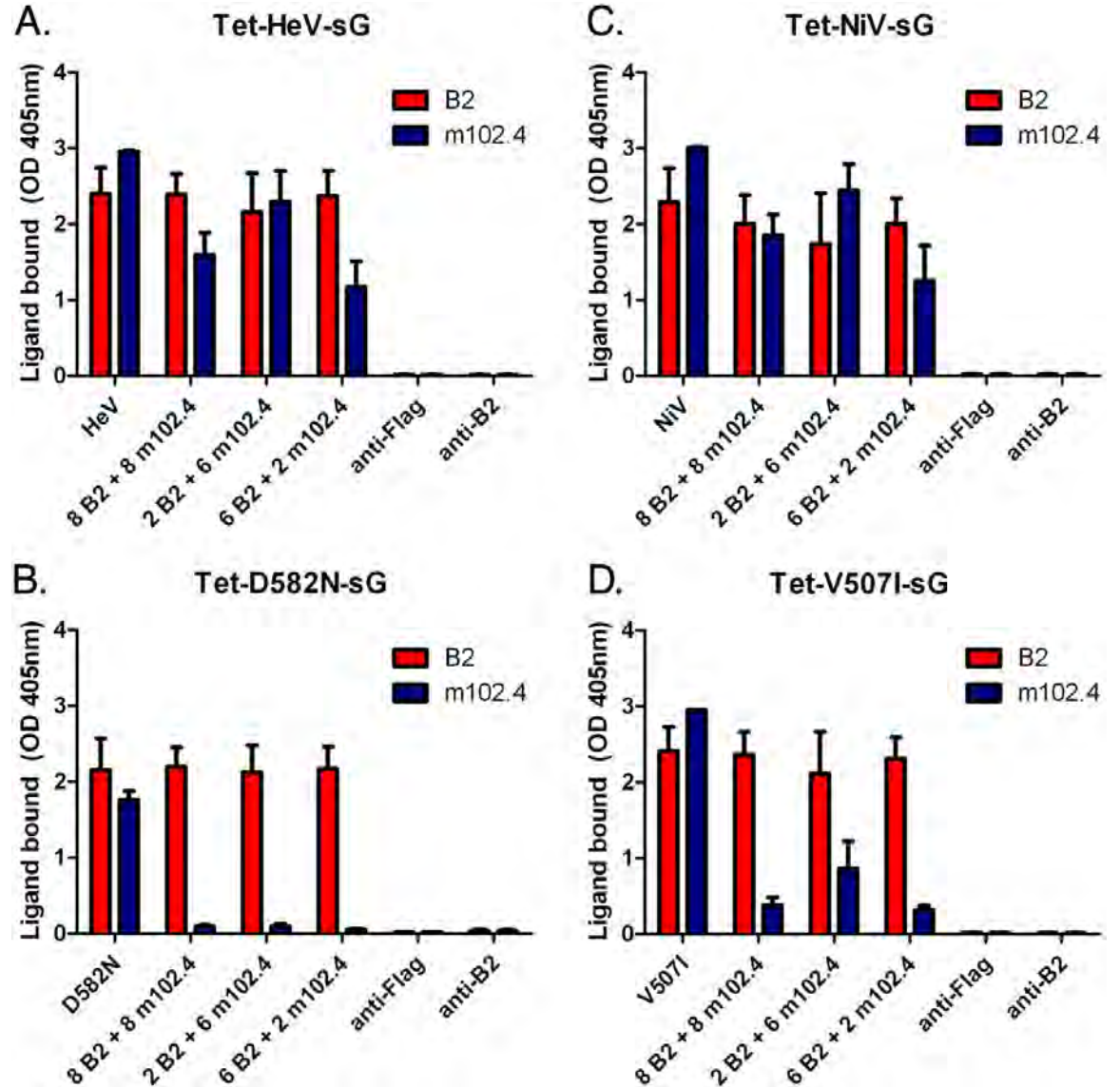
Figure 33: Simultaneous binding of m102.4 and ephrin-Be to Tet-sGs.
(**A**) Tet-HeV-sG, (**B**) Tet-D582N-sG, (**C**) Tet-NiV-sG and (**D**) Tet-V507I-sG
were bound to an ELISA plate and incubated with equal or biased concentrations
of ephrin-B2 and m102.4. Ligand-specific antibodies were used to determine the
levels of bound ephrin-B2 and m102.4 to each Tet-sG.

Viral fusion and infection are dependent upon the interactions of HeV/NiV-Gs and HeV/NiV-Fs. Binding of HeV/NiV-Gs to receptor triggers conformational changes in G that lead to the activation of F, either through association or dissociation from G. The data presented here suggest that receptor binding increases the association between G and F, while m102.4 prohibits any increased G-F interaction.

Tet-sGs and Tri-sFs associate according to provocateur model

Efficient heterotypic pairing between HeV/NiV-G/F has previously been shown (21), so it was expected that Tet-HeV/D582N-sGs would be able to bind Tri-NiV-sF and Tet-NiV/V507I-sGs could bind Tri-HeV-sF. The data here indicate that in the absence of receptor there is little to no sG-sF association, suggesting that the pre-receptor-bound state of sG is unable to interact with sF. The one exception is Tet-V507I-sG, which bound both Tri-HeV-sF and Tri-NiV-sF to fairly high levels in the absence of both ephrin-B2 and ephrin-B3. As previously stated, this increased association may be due to increased non-specific binding of Tet-V507I-sG. However, upon receptor addition, levels of Tet-V507I-sG steadily increased, making it seem unlikely that Tet-V507I-sG binding Tri-sF is completely due to artificial association. For all Tet-sGs, association with Tri-sF increased upon addition of receptor, suggesting that conformational changes in Tet-sGs induced by receptor binding allow for the stalk domain to associate with Tri-sF. This pattern of enhanced association upon receptor binding suggests that HeV/NiV-G/F interact through a provocateur model as opposed to a clamp model.

As stated previously, numerous studies indicate that enhanced G-F association results in decreased fusion, which suggests that the observed results here would result in

151

decreased fusion. While it is certain that receptor increases G-F association, how this interaction plays out in the broader context of viral attachment and fusion is unclear. Fluorescent studies involving m102.4 binding in the presence and absence of ephrin-B2 suggest that upon ephrin-B2 addition, HeV/NiV-Gs cluster on the membrane surface forming observable puncta (data not shown). One of the limitations of using Tet-sGs and Tet-sFs is that receptor-induced clustering would not be observed. Given Porotto *et al.*'s sporadic involvement model, it is easy to speculate that clustering of HeV/NiV-G/F might lead to disassociation due to steric hindrance caused by conflict between multiple large oligomers, but the unobstructed stalk domains of G would be the impetus for continued association, resulting in an association-disassociation pattern.

Interestingly, steady increases in bound Tet-sGs to Tri-HeV-sF occurred with the addition of ephrin-B2 but not ephrin-B3, while steady increases in binding of Tet-sGs to Tri-NiV-sF occurred with ephrin-B3 but not ephrin-B2. This suggests that F may also have a role in receptor preference or that conformational changes induced in G upon receptor binding may differ slightly depending upon the receptor engaged. Support for both of these hypotheses can be found in work by Bossart *et al.*, who showed that fusion potency in heterotypic pairing of HeV/NiV is dependent upon F (21), and Negrete *et al.*, who determined that the binding determinants of HeV/NiV-Gs for ephrin-B2 and ephrin-B3 are "distinct and dissociable" (131). Furthermore, clinical observation of NiV-induced death due to encephalitis suggests that NiV may prefer ephrin-B3 usage over ephrin-B2 as only ephrin-B3 is found in regions of the human brain stem (56; 181; 201). All together these data suggest that ephrin-B2 and ephrin-B3 binding may cause slightly different reactions in HeV/NiV-Gs that affect association with HeV/NiV-Fs. Additional

studies will need to be performed to determine the validity of this hypothesis, which could include studies of heterotypic fusion of cells expressing either ephrin-B2 or ephrin-B3.

Possible neutralization mechanisms of m102.4

We have already shown that the mechanism of m102.4 neutralization is not solely dependent upon binding and preventing HeV/NiV-Gs from binding receptor as HeV/NiV-G escape mutants still bind m102.4 (Chapters 3 and 4). It therefore seems likely that m102.4 may have multiple mechanisms for preventing HeV/NiV infection. The second mechanism of neutralization may be binding HeV/NiV-Gs and either (a) triggering conformational changes in HeV/NiV-Gs similar to receptor (referred to as m102.4-trigger) or (b) preventing conformational changes in HeV/NiV-Gs required for F interaction (m102.4-lock).

The first possibility would have m102.4 binding HeV/NiV-Gs, inducing conformational changes in G that then trigger the activation of F. This premature triggering of F is irreversible, and if it occurs in a time/location in which no target cell membrane is present would result in a non-infectious virus. The second possibility has m102.4 binding to HeV/NiV-Gs, possibly still allowing receptor binding, but locking HeV/NiV-Gs in a conformation that cannot be altered, thus F would never be triggered and fusion would not occur.

To investigate these two possibilities studies involving Tet-sGs, ephrin-B2 and m102.4 were performed. ELISAs with Tet-sGs revealed that ephrin-B2 is able to increase binding of m106.3, a conformational antibody that binds only after addition of receptor. Interestingly when m102.4 was added in place of ephrin-B2, binding of m106.3

153

remained relatively constant or even decreased, suggesting that m102.4 does not have the same effect on Tet-sGs as ephrin-B2. This result implies that the mechanism of m102.4 neutralization is the m102.4-lock rather than the m102.4-trigger.

Knowing that receptor induced conformational changes in G result in F activation, we next sought to determine the effect of m102.4 binding on Tet-sG and Tri-sF association, having already shown that receptor binding increases Tet-sG and Tri-sF association. Conversely, the addition of m102.4 had no effect or decreased the levels of Tet-sG-Tri-sF association. These results again suggest that m102.4 neutralizes henipavirus infection via a m102.4-lock mechanism, in which m102.4 binding prevents conformational changes in G required for F association. This is further supported by the lack of difference in Tri-sF association between Tet-HeV/NiV-sGs and Tet-D582N/V507I-sGs. If m102.4 neutralization occurs by the m102.4-trigger mechanism, m102.4 would have enhanced Tet-HeV/NiV-sGs association with Tri-sF while Tet-D582N/V507I-sGs would not have any increased association with Tri-sF.

Differences between wild type and escape mutants of HeV/NiV-Gs

We have previously seen that Tet-D582N-sG has reduced binding affinity for m102.4 compared to Tet-HeV-sG (Chapter 3), and this reduced affinity appears to allow Tet-D582N-sG to switch from m102.4 binding to ephrin-B2 binding. In two different ELISAs Tet-D582N-sG was able to displace bound m102.4 when ephrin-B2 was added; results which were also observed for Tet-V507I-sG. Binding of m102.4 to Tet-HeV/NiV-sGs was not effected by ephrin-B2 binding, but the levels of m102.4 bound to Tet-D582N/V507I-sGs were significantly reduced after ephrin-B2 addition. Interestingly, the levels of bound ephrin-B2 added after m102.4 binding ranged from

60%-100% maximal ephrin-B2 binding for all four Tet-sGs. Considering the four potential binding sites per tetrameric unit, it's reasonable to speculate that neither m102.4 nor ephrin-B2 bind all four possible sites and that multiple ligands are capable of binding simultaneously.

This speculation was further supported by a second ELISA that demonstrated the ability of Tet-HeV/NiV-sGs and Tet-V507I-sG to bind both ephrin-B2 and m102.4 when added concurrently. Furthermore, for Tet-HeV/NiV-sGs the level of ephrin-B2 bound was approximately equal to the maximal ephrin-B2 binding level despite the concentration of m102.4 present.

Tet-D582N-sG clearly favors receptor binding over m102.4, but Tet-V507I-sG will still allow m102.4 to bind even in the presence of receptor. This simultaneous binding of ephrin-B2 and m102.4 was also observed for Tet-HeV/NiV-sGs, suggesting once again that m102.4 has a second neutralization mechanism beyond preventing receptor binding.

Another difference between Tet-HeV/NiV-sGs and Tet-D582N/V507I-sGs occurs upon m102.4 binding after pre-incubation with ephrin-B2. When previously bound to ephrin-B2 Tet-D582N/V507I-sGs are unable to bind m102.4, but Tet-HeV/NiV-sGs bind approximately 50%-60% maximal levels of m102.4 after pre-incubation with ephrin-B2.

Possible escape mechanisms of HeV-G-D582N and NiV-G-V507I

The data presented here indicate that HeV/NiV-G/F association occurs via a provocateur model, in which increased G-F association occurs upon receptor binding. Based on studies with other paramyxoviruses, the receptor-induced conformational changes are most likely a switch from a heads-down conformation to a heads-up

155

conformation, allowing the stalk domain of G to interact with F.   One of the neutralizing

abilities of m102.4 most likely prevents this conformational change, locking G in a

heads-down conformation. This "locking" ability of m102.4 does not prevent receptor

from binding HeV/NiV-Gs, but any bound receptor is unable to remove bound m102.4.

HeV-G-D582N displays a strong preference for receptor over m102.4, such that when

receptor binds it is able to disrupt m102.4 binding. While we have no data to support

how this removal occurs, it is possible that the mutation in HeV-G-D582N causes a

slightly different conformational change in G upon receptor binding that prevents m102.4

from remaining bound. Similarly NiV-G-V507I can bind m102.4 and receptor

simultaneously, but receptor can displace m102.4 and pre-bound receptor prevents

m102.4 from binding. Knowing that Tet-V507I-sG has the highest binding affinity to

m102.4, this suggests that conformational changes are induced upon receptor binding that

disrupt the locking mechanism and binding ability of m102.4. This receptor-induced

conformation in Tet-D582N/V507I-sGs has to be different from that occurring in Tet-

HeV/NiV-sGs. This hypothesis of altered conformation in Tet-D582N/V507I-sG is most

evident in the sequential binding ELISA with ephrin-B2 and m102.4, where m102.4

cannot remain bound to Tet-D582N/V507I-sGs after incubation with ephrin-B2

regardless of which ligand bound Tet-sGs first.

The ability of m102.4 to bind Tet-HeV/NiV-sG even after receptor binding is

remarkable when thinking about G-F association. If G and F do require continual

association during the fusion process, m102.4 may be able to bind HeV/NiV-Gs and

disrupt the fusion process while it is occurring. The m102.4-lock mechanism relies on

the ability of m102.4 to lock HeV/NiV-Gs into a non-receptor-inducible conformation,

inhibiting fusion before it starts. If m102.4 is able to bind after receptor and force

HeV/NiV-G into a non-receptor-inducible conformation, it would be able to not only

prevent fusion from starting but also inhibit it while it is ongoing.

Limitations and Future Directions

While it is certain that receptor but not m102.4 increases G-F association, the

outcome of this association is not fully understood partly due to the limitations of using

Tet-sGs and Tri-sFs. Ephrin-B2 has been shown to cluster on membrane surfaces upon

interaction with its cognate receptor (reviewed in (73)), and preliminary work with

fluorescently tagged HeV/NiV-Gs suggests HeV/NiV-Gs also cluster upon receptor

engagement (data not shown).   However, receptor-induced clustering and its effects

cannot be observed using these soluble constructs. This clustering ability may play an

important role in m102.4 neutralization and escape, not to mention the sporadic G-F

association hypothesized by Porotto *et al*. (153). Further studies need to be conducted

using cell-expressed HeV/NiV-Gs and their m102.4 escape counterparts to determine

how clustering of G and F may influence m102.4 binding. Additionally, more ELISAs

should be conducted to determine the effect of simultaneous addition of receptor and

m102.4 on G-F association. It would be predicted that Tet-HeV/NiV-sGs would be

unable to associate with Tri-sF in the presence of m102.4, but Tet-D582N/V507I-sGs

would still be able to bind Tri-sF.

The present studies also focused on ephrin-B2 and not ephrin-B3 due to the lack

of a reliable antibody for ephrin-B3 detection. It would be interesting to note whether the

results that were obtained with ephrin-B2 would also be observed with ephrin-B3,

especially given the differences in ephrin-B3 usage between HeV and NiV.

One further limitation of our work was the use of m102.4 Fab rather than m102.4 IgG. Studies with antibodies to Influenza A and HIV-1 found that different neutralization mechanisms were used depending on whether the antibody was expressed as a Fab or IgG construct (50; 117). Previous cell-cell fusion assays showed a clear difference between IgG and Fab inhibition of HeV/NiV-Gs (Chapter 4), in which IgG was more potent at neutralizing fusion than Fab. Given that m102.4 IgG has two G binding domains while Fab only has one, the requirement of binding two globular heads to prevent receptor-induced conformational change becomes a tantalizing hypothesis, especially given that higher concentrations of Fab have the same neutralizing effect as IgG.

The hypothesis that Tet-D582N/V507I-sGs undergo different conformational changes than Tet-HeV/NiV-sGs upon receptor binding needs further investigation. As the result of these conformational changes in Tet-sGs is the same (activation of F), it suggests that there are multiple ways to change the conformation of G and/or that the conformational change is a multi-step process where individual steps can be different. Crystal structures of Tet-D582N/V507I-sGs with receptor and m102.4 could provide valuable information on the effects of ligand binding.

Further work also needs to focus on the timing of m102.4 neutralization to determine if m102.4 can prevent and disrupt the fusion process by affecting F activation. One possibility would be to perform a time course cell-cell fusion assay in which m102.4 is added at various times. If m102.4 can only prevent fusion before it starts then there will be a point at which addition of m102.4 will be ineffective. Measuring the levels of bound m106.3 to Tet-sGs can also be determined to identify the conformations of HeV/NiV-Gs following sequential and simultaneous addition of receptor and m102.4. If

m102.4 can force HeV/NiV-Gs into a non-receptor-inducible conformation then m106.3

binding should decrease after m102.4 addition.

Summary

Overall, we have shown that receptor binding increases Tet-sG association with

Tet-sF, but m102.4 addition has no effect on sG-sF association. This suggests that the

neutralization ability of m102.4 occurs by the m102.4-lock mechanism, in which m102.4

binds HeV/NiV-Gs and locks G in a non-receptor-inducible conformation. This

clamping ability does not prevent receptor from binding, but it does prevent receptor-

associated conformational changes which are required for F activation. Possible m102.4

escape mechanisms for HeV-G-D582N and NiV-G-V507I include reduced binding

affinity for m102.4 compared to receptor (HeV-G-D582N) and the ability to still undergo

receptor-induced conformational changes even when m102.4 is already bound (NiV-G-

V507I). These conformational changes are likely different than those observed for

HeV/NiV-Gs, and these changes circumnavigate the locking ability of m102.4 and lead to

the disruption of m102.4 binding.

Chapter 6: Discussion

PREFACE

Hendra and Nipah are highly pathogenic viruses capable of causing severe morbidity and mortality. While presently geographically restricted to Australia and southeast Asia, the detection of henipavirus antibodies and nucleic acid in bats from China and Africa suggest HeV and NiV may be present in a larger geographical area than previously thought. While human HeV infections require the intermediate equine host, yearly outbreaks of NiV in Bangladesh indicate direct bat-human and human-human transmission do occur.

Arguably the greatest advancements in the henipavirus field have been the development of the HeV subunit vaccine and the identification of the human anti-G mAb m102.4. The combined use of these therapeutics has great potential to limit the levels of HeV and NiV infection and mortality. However, one of the hallmarks of RNA viruses is their rapid ability to mutate and render current therapeutics ineffectual. Gaining a better understanding of the mechanics of HeV/NiV fusion will allow us to generate more targeted therapeutics that will also prevent viral escape.

The work presented here represents a detailed study of the effects of receptor and m102.4 binding to HeV/NiV-G, further investigating the mechanism of m102.4 neutralization. This is also the first study to detail the differences between wt and m102.4 escape variants of HeV/NiV-G as we seek to understand how a single mutation in the globular heads leads to escape from m102.4 neutralization.

Previous work by Bossart *et al*. led to the development of soluble HeV/NiV-G glycoproteins that are capable of forming oligomers, binding receptors and inhibiting HeV/NiV infection (15). The greatest limitation of these sGs is their inability to maintain a tetrameric conformation, which is the native conformation of full-length HeV/NiV-Gs. These sGs were capable of forming tetramers, but most of the expressed species were dimeric in nature with limited tetrameric and monomeric expression. While there is no denying the worth of these sGs, they may not completely embody the characteristics of HeV/NiV-Gs that are revealed upon receptor binding, F interaction and/or m102.4 binding and neutralization.

In order to construct a version of HeV/NiV-sGs that more closely resembled the tetrameric nature of HeV/NiV-Gs, the tetramerization motif of GCN4 was appended to the HeV/NiV-sG sequences. The addition of GCN4 resulted in primarily tetrameric conformations of HeV/NiV-sGs. Tet-HeV/NiV-sGs were stable, bound receptors ephrin-B2 and ephrin-B3, bound m102.4, associated with Trimeric HeV/NiV-sF and underwent conformational change upon receptor binding. The ease of large scale production and purification of Tet-sGs created a reliable tool that was used repeatedly to address my two specific aims.

Specific Aim 1 - Develop second-generation m102.4 variants that bind and inhibit wildtype and m102.4 escape variants of HeV and NiV.

The globular head domains of HeV/NiV-Gs contain the binding epitope for receptors ephrin-B2 and ephrin-B3 as well as m102.4, and crystal structures of HeV/NiV-Gs with ephrin-B2 and m102.3, a close variant of m102.4, detail the similarities in binding between these two ligands. Knowing m102.4 binds similarly to ephrin-B2/B3,

we sought to enhance the neutralization ability of m102.4 by making the binding region of m102.4 resemble the binding region of ephrin-B2/B3. Since HeV/NiV-Gs are limited to receptors ephrin-B2 and ephrin-B3 for functional infection, an antibody that closely resembles the receptors may prove more efficacious at inhibiting viral infection with less chance of viral escape. Variants of m102.4 were constructed that replaced the residues of m102.4 with the corresponding residue of ephrin-B2/B3 or alanine, to remove any binding contribution from that specific residue. We predicted that some of these modified m102.4 variants, especially those that more closely resembled receptor, would be able to bind and inhibit HeV/NiV-G mediated fusion with greater efficacy than m102.4. Additionally, the escape variants of HeV/NiV-Gs, HeV-G-D582N and NiV-G-V507I, would also be bound and inhibited by the m102.4 variants that more closely resembled receptor.

Subaim 1 - Mutate m102.4 HeV/NiV-G binding region to more closely resemble ephrin-B2 and -B3 G-H loop

A total of 19 m102.4 variants were constructed that had 1-5 residue changes among a 6-residue span in the binding region of m102.4 considered critical for HeV/NiV-G binding. Ultimately these studies showed that m102.4 remains the most effective antibody at binding HeV/NiV-Gs and preventing receptor binding and cell-cell fusion. The variants were sub-divided into two classes – single mutation and multiple mutations. With the exception of one variant, LD, all of the single mutation variants showed moderate to high levels of Tet-sG binding. The ability of the multiple mutation variants to bind Tet-sGs was dependent upon the conservation of P109. Variants that mutated this residue lost the proline kink, most likely causing a string of downstream tyrosine residues to change their orientation and come into steric conflict with HeV/NiV-Gs. This steric

162

hindrance results in a loss of binding ability. The variants that maintained P109

displayed various abilities to bind Tet-sGs, and the almost fully converted variant SLP

had greater binding to Tet-sGs than the fully converted FSPNLW variant.

m102.4 demonstrated varying abilities to inhibit Tet-HeV/NiV-sG association

with receptors ephrin-B2 and ephrin-B3, but was more effective than any of the m102.4

variants. Two m102.4 variants, LF and HA, demonstrated the highest levels of Tet-sG

binding and the best ability to inhibit Tet-sG and receptor interaction. LF and HA have

single mutations at L105 and H108, respectively, and were able to inhibit HeV/NiV-G

cell-cell fusion. The SLP variant displayed moderate to low levels of Tet-sG binding and

was only able to inhibit Tet-HeV/NiV-sG association with ephrin-B3.

Subaim 2 - Test binding of m102.4 variants to m102.4 escape variants of HeV/NiV-Gs

A majority of the m102.4 variants were unable to bind Tet-D582N-sG, but

binding to Tet-V507I-sG was similar to wild type Tet-NiV-sG. However, none of the

variants, including the parent m102.4, were able to inhibit Tet-D582N/V507I-sGs

association with ephrin-B2, although they proved effective at preventing association with

ephrin-B3. Cell-cell fusion mediated by HeV-G-D582N and NiV-G-V507I were slightly

inhibited by variants LF and HA, but not to the extent of wt HeV/NiV-Gs. Additionally,

when new escape mutants of HeV/NiV-Gs were created using the m102.4 variants, they

tended to cause the same mutations in the same region of HeV/NiV-Gs as m102.4 (D582,

N586 and V507 mutations).

Overall the transformation of the binding region of m102.4 into the binding

region of ephrin-B2/B3 proved ineffective as all of the variants were less effective than

the original m102.4 at binding G, preventing G-receptor interaction and inhibiting G-mediated cell-cell fusion.

Specific Aim 2 - Characterize the interactions of Ephrin-B2, Ephrin-B3 and m102.4 with the attachment glycoproteins of wild type and m102.4 escape variants of HeV and NiV.

My second specific aim sought to further characterize the interactions between HeV/NiV-Gs and -Fs upon receptor binding and to determine how m102.4 may alter this process. Again, the Tet-sGs were used for these studies to address three subaims.

Subaim 1 - Identify conformational changes that occur in HeV/NiV-Gs upon receptor or m102.4 binding

We know that receptor binding to HeV/NiV-Gs induces conformational changes in G that result in F activation. We predicted that these same conformational changes would occur when the Tet-sG constructs bound receptor. Since the Tet-sG constructs are able to bind a conformation-dependent antibody (m106.3) whose epitope is only exposed on G after receptor binding, the Tet-sG constructs do not completely resemble the pre-receptor bound conformation of full-length HeV/NiV-Gs. However, upon addition of ephrin-B2, conformational changes in Tet-sGs were noted as the binding of m106.3 increased. Interestingly, upon addition of m102.4 IgG to Tet-sGs there was no noticeable increase in m106.3 binding, lending support to the theory that m102.4 neutralizes HeV/NiV infection by preventing conformational changes in G that lead to F activation.

Subaim 2 - Determine the interaction between HeV/NiV-Gs and HeV/NiV-Fs

When this study began there were two prevailing models for G-F interaction – the clamp and provocateur models. Work in our laboratory had previously demonstrated the ability of trimeric HeV/NiV-sF glycoproteins to bind Tet-sGs, and we used this capability

to test the effects of receptor and m102.4 binding on G-F association. Upon receptor

addition, be it ephrin-B2 or -B3, increases in Tet-sG and Tri-sF association occurred for

all four Tet-sGs and both Tri-sFs, although receptor preference based on the Tri-sF was

observed. Conversely, addition of m102.4 resulted in no increased association between

Tet-sGs and Tri-sFs. This further supports the hypothesis that the neutralization

mechanism of m102.4 prevents G-F association and thus G activation.

Subaim 3 - Determine how m102.4 neutralizes HeV/NiV infection and how escape variants escape m102.4 neutralization

Almost every assay involving Tet-HeV/NiV-sGs, whether it be receptor binding,

m102.4 binding or G-F association, was repeated with Tet-D582N/V507I-sGs in order to

understand how HeV-G-D582N and NiV-G-V507I escape m102.4 neutralization. The

exact mechanism of m102.4 neutralization remains unclear, but given the binding regions

of receptor and m102.4, it was predicted that m102.4 neutralized HeV/NiV by blocking

receptor binding. Earlier studies in this work have already shown that m102.4 escape

does not occur by an inability of m102.4 to bind HeV-G-D582N and NiV-G-V507I, and

we further established that bound m102.4 does not prevent receptor binding. In fact for

Tet-HeV/NiV-sGs, receptor and m102.4 can bind simultaneously with levels approaching

their maximum binding capability for each ligand. Tet-D582N-sG, however, strongly

favors ephrin-B2 binding over m102.4 and can replace bound m102.4 with ephrin-B2,

and bound ephrin-B2 prevents m102.4 binding. Similar results were seen with Tet-

V507I-sG, but Tet-V507I-sG demonstrated a stronger ability than Tet-D582N-sG to

simultaneously bind ephrin-B2 and m102.4. Taken together these results suggest that the

mutations in HeV-G-D582N and NiV-G-V507I (a) alter the binding affinity of m102.4

165

and/or (b) cause slightly different conformational changes in G upon receptor binding than those observed with HeV/NiV-Gs that results in escape from m102.4 neutralization.

HENDRA AND NIPAH FUSION – WHAT WE'VE LEARNED, LIMITATIONS, UNANSWERED QUESTIONS AND THE EFFECT OF M102.4

HeV/NiV fusion occurs through precise and discrete steps, and inhibition or alteration of any of these steps may prevent membrane fusion and infection. Tetrameric HeV/NiV-Gs and Trimeric HeV/NiV-Fs are expressed on the viral membrane in relatively equal amounts (121), and the presented data suggest that on the viral membrane G and F remain separate. The lack of G and F association is likely due to the conformation of G, particularly the globular heads. We know that the upper region of the stalk domains of HeV/NiV-Gs is responsible for F interaction, and that the globular heads of paramyxoviruses, such as PIV5-HN and MeV-H, switch between a heads-up and a heads-down conformation to either allow or prevent F and G association, respectively (13; 26). Therefore, it seems likely that HeV/NiV-Gs are expressed in a heads-down conformation on the viral membrane.

Both HeV and NiV are capable of binding ephrin-B2 and ephrin-B3, but it seems that NiV has a slight preference for ephrin-B3 likely due to differing residues in HeV/NiV-Gs that result in weaker hydrophobic interactions between HeV-G and ephrin-B3 (205). This preference was especially clear in binding ELISAs where Tri-NiV-sF favored ephrin-B3 addition to increase G-F association. Regardless of which ephrin is used, receptor binds the globular head of HeV/NiV-Gs, resulting in minor conformational changes in both the ephrin receptor and HeV/NiV-Gs. The conformational change in ephrin-B2/B3 is slight with the vast majority of changes centered around the G-H loop with the greatest changes seen at residues F120 and W125 (23). Similarly, the minor

166

conformational changes that occur in HeV/NiV-Gs transpire at the binding pockets for the residues of the ephrin-B2/B3 G-H loop. The greatest structural change appears to occur at the binding pocket for ephrin-B2 F120 and ephrin-B3 Y120 with smaller changes around the conserved proline in the G-H loop (P122) (206).

These minor modifications in HeV/NiV-Gs result in the overall conformational change of G leading to F activation. While the functional stoichiometric binding of HeV/NiV-Gs to receptor remains unknown, it seems unlikely that ephrin-B2/B3 will bind to all four globular heads given the ability of m102.4 and ephrin-B2 to simultaneously bind HeV/NiV-Gs to nearly maximal amounts. Furthermore, it appears that not all four globular heads are required to bind receptor to undergo conformational change induced by receptor. Brindley *et al*. showed that only one of the dimer pairs of MeV-H needs to be activated by receptor binding to initiate fusion, although it remains unclear as whether one globular head or two globular heads of the dimer need to bind receptor (27).

Regardless of which or how many globular heads are bound, the binding of receptor induces a cascade of minor conformational changes in HeV/NiV-Gs that most likely results in the movement of the globular heads from a heads-down to a heads-up position. A recent study with NiV-G showed that sequential conformational changes in two regions (residues 371-392 and177-194, respectively) are responsible for the exposure of the F-activating portion of the Stalk domain (103). Remarkably, neither of these regions is near the epitope for receptor or m102.4, suggesting that additional conformational changes in residues near the binding region may be required to influence residues 371-392 or factors outside of the receptor/m102.4 binding region alter the conformation of G. This would imply that the G-H loop of ephrins and CDRH3 region of

m102.4 serve only to dock receptor and antibody to G, allowing for other interactions to activate G.   Further research will need to clarify exactly how these two regions in NiV-G are influenced and if factors outside of the G-H loop are involved in G activation.

This idea of multiple minor sequential changes in NiV-G, however, is further supported by work showing that mutations in G can alter fusion ability without affecting receptor binding, suggesting that there are multiple steps between receptor binding and F activation that change the conformation of G and disruption of any single step can inhibit fusion (205). Once the globular heads have altered conformation, the exposed Stalk domain can then interact with HeV/NiV-Fs, leading to the activation of F, insertion of the fusion peptide into the target cell membrane and ultimately membrane fusion.

Again this interaction between G and F is not fully understood, but here the data suggest that G and F interaction increases upon receptor binding, following the provocateur model. A particular aspect that the research work here did not address was the effect of receptor clustering on the cellular membranes. Ephrin-B2 is known to cluster when bound to its cognate EPH receptor (reviewed in (73)), but it is unknown whether this same clustering occurs upon HeV/NiV-G binding receptor. Using fluorescent antibodies we've seen evidence of HeV/NiV-Gs clustering on cellular membranes after the addition of ephrin-B2 (data not shown), but the impact of such clustering on G-F association has not been studied. The HeV/NiV glycoproteins are large molecules, and it seems likely that steric clashes would occur if multiple glycoproteins were brought into close proximity. While purely speculation at this point, the clustering of HeV/NiV-Gs may impede association with HeV/NiV-Fs by physically disrupting the binding through steric hindrance, but the revealed stalk domain is continually attempting

to associate with F, which may result in the sporadic association predicted by the third model of G-F association.

The binding of m102.4 to HeV/NiV-Gs disrupts this fusion process, and we propose that m102.4 neutralizes HeV/NiV infection by inhibiting two distinct and critical steps required for fusion (Figure 34). The first proposed neutralization mechanism is prevention of receptor binding. The receptor binding domain of HeV/NiV-Gs also serves as the binding domain for m102.4, and if m102.4 were present in enough abundance it could theoretically bind every available globular head, preventing receptor from binding, which may be the mechanism of m102.4 Fab neutralization. The inability of m102.4 Fab to inhibit HeV/NiV fusion to levels seen in the presence of m102.4 IgG suggests that Fab may not be able to completely lock HeV/NiV-Gs in a non-receptor-inducible conformation and may be more dependent upon blocking receptor binding for neutralization. While it is certain that blocking receptor binding would prevent HeV/NiV infection, this cannot be the only neutralization mechanism of m102.4 as we have repeatedly seen evidence that both receptor and m102.4 can simultaneously bind HeV/NiV-Gs and decreased concentrations of m102.4 Fab results in increased fusion.

A second proposed mechanism for m102.4 neutralization is the "m102.4-lock" mechanism, which was named for the ability of m102.4 to bind and lock HeV/NiV-Gs into a non-receptor-inducible conformation. This neutralization mechanism does not require m102.4 to prevent receptor binding. In fact, receptor can still bind HeV/NiV-Gs but no longer induce conformational changes in HeV/NiV-Gs required for F activation. Exactly how m102.4 locks HeV/NiV-Gs into the pre-receptor-bound conformation is not fully understood. Analysis of crystal structures of HeV-G bound to m102.3 Fab indicate
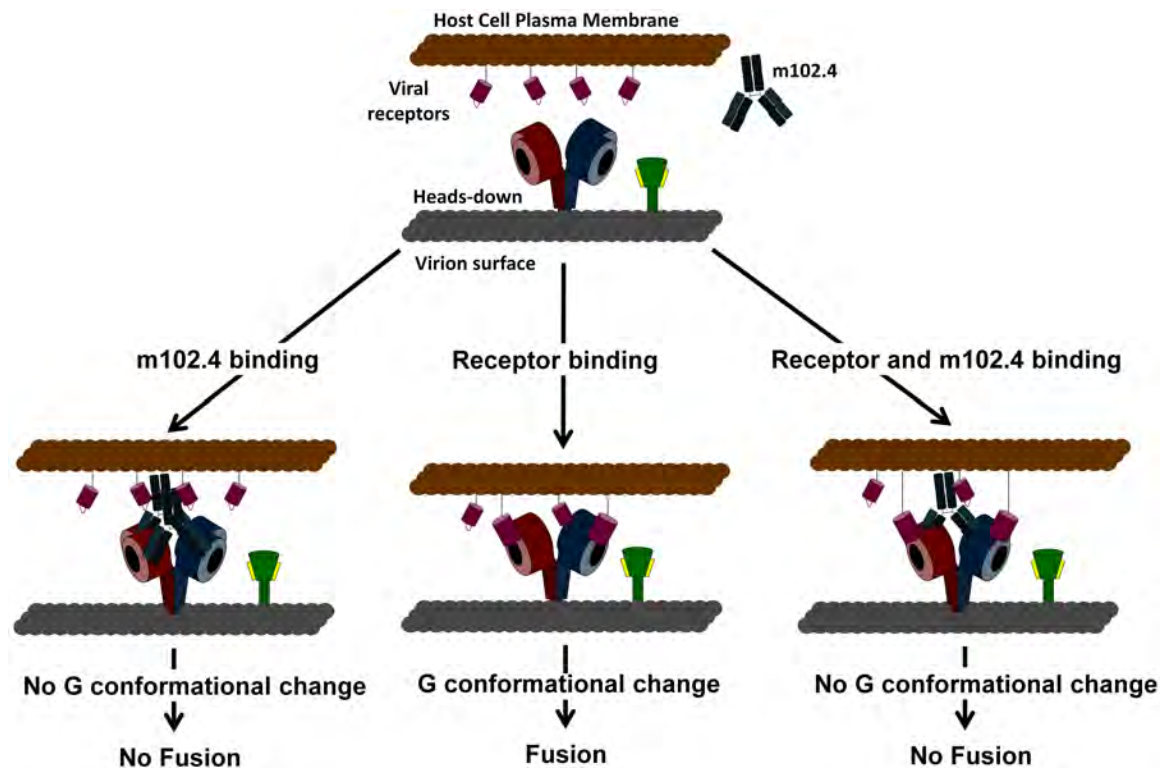
Figure 34: Model of m102.4 neutralization.
The tetrameric attachment (G) glycoprotein (dimers colored red and blue) is shown in the heads-down conformation on the viral membrane with the fusion (F) glycoprotein (green). Receptors ephrin-B2/B3 (maroon) are depicted on a host cell membrane, and m102.4 (blue) is present but unbound to G. The three possible outcomes for G interaction with receptor and m102.4 are shown: **Left** – m102.4 binds all available globular heads and prevents receptor from binding, ultimately inhibiting G conformational changes that lead to F activation and fusion. **Center** – G binds receptor, leading to conformational changes and F activation. **Right** – m102.4 and receptor bind, but receptor can no longer induce conformational changes in G, preventing F interaction and fusion.

there are few conformational changes between unbound and bound G ($C\alpha$ positions

r.m.s.d of 0.257 Å) (207). This contrasts with the changes observed for unbound and

bound HeV/NiV-Gs with ephrin-B2 and ephrin-B3, which are slight but appear to be

greater than the changes observed with m102.3 binding (23; 205; 206). Without the

conformational change that occurs upon receptor binding, F will not be activated and

fusion will not occur.

Theoretically each m102.4 IgG molecule could bind two globular heads, but it

seems unlikely that m102.4 binds every available globular head as maximal levels of

ephrin-B2 could bind Tet-sGs even after pre-incubation with m102.4. Taking into

account that MeV-H only requires activation of one dimer pair of H to initiate fusion, it is

possible that m102.4 binds one globular head from each dimer pair of HeV/NiV-Gs,

locking both dimers into a non-receptor-inducible conformation. While this theory seems

logical and plausible, further work will be needed to ascertain the true nature of m102.4

IgG binding to HeV/NiV-Gs. This work will likely prove difficult as each of the globular

heads in the tetramer must somehow be marked as distinct entities to verify which

globular head(s) m102.4 binds.

Despite the 100% neutralization ability of m102.4 and the lack of HeV/NiV

m102.4 escape variants *in vivo*, it is possible for HeV/NiV to mutate and escape m102.4

neutralization. HeV-G and NiV-G each adapted different mutations to escape m102.4

neutralization, but these mutations are not unique for the individual viruses. The work

with the m102.4 variants suggest that mutation of residue 507 (V507 for NiV and T507

for HeV) can allow either HeV or NiV to escape. Interestingly, mutation of only three

residues was detected in the studies presented here with the m102.4 variants (D582 and

T/V507 for HeV and NiV and N586 for NiV). These three residues cluster around the

binding pockets for L/F/Y and P, which are the two binding pockets in HeV/NiV-G that

undergo the most conformational change upon receptor binding. Therefore these pockets

are also better able to handle mutations that alter interactions with receptor and m102.4.

HeV/NiV-G appear to use multiple mechanisms to disrupt m102.4 neutralization as

different mutations occur at the same or different residues (e.g. D582N, D582E and

N586T).

Interestingly, the most common mutations occurred at residues D582 and N586,

which don't directly affect the binding residues of receptor and m102.4. Rather, these

residues appear to indirectly affect binding by altering the bonds formed by the L/F/Y

binding pocket. This alteration seems to occur through disruption of separate bonds,

indicating the broad potential of HeV/NiV-G to mutate to escape neutralization.

Furthermore the T/V507I mutation is intriguing because it helps form the P binding

pocket and lies directly underneath the conserved P residue in receptors and m102.4.

This mutation, at least in NiV-G-V507I, increases receptor and m102.4 binding affinity

but still allows for escape from m102.4 neutralization, suggesting m102.4 can bind but

not lock NiV-G-V507I in a non-receptor-inducible conformation.

Interestingly, both HeV-G-D582N and NiV-G-V507I, unlike their wt

counterparts, cannot bind m102.4 after having bound ephrin-B2. It therefore seems

possible that the D582N and V507I mutations result in slightly different conformational

changes upon receptor binding that prevent m102.4 from binding. This could explain

why m102.4 variants at low concentrations had differing effects on ephrin-B3 interaction

with Tet-HeV/NiV-sGs and Tet-D582N/V507I-sGs. With recent results showing that

activation of G occurs in sequential steps, it might be possible that multiple pathways could lead to the activation of G, and HeV-G-D582N and NiV-G-V507I are simply using alternative pathways. The ability of HeV/NiV-Gs to escape m102.4 neutralization highlights the flexibility of RNA viruses and the difficulties faced in creating therapeutics to treat infection that won't result in additional mutations and viral escape.

CONTRIBUTION TO PARAMYXOVIRUS FIELD

Many paramyxovirus glycoproteins have been converted into soluble constructs, but this work represents the first time a soluble attachment (HN/H/G) glycoprotein of a paramyxovirus has been constructed that maintains the physiological tetrameric conformation. These tetrameric soluble constructs provide an affordable and fast method for further study of the effects of receptor binding and interaction with the fusion glycoprotein in regards to oligomeric conformation and change. Additionally, as new variants of HeV/NiV-Gs are identified, these variants can quickly be constructed as Tet-sGs and studied to determine the effects of these variations on receptor binding, conformational changes, antibody binding and interaction with F. Furthermore, it may now be possible to obtain crystal structures of HeV/NiV-Gs bound to receptors and/or m102.3 that will contain portions of the HeV/NiV-G stalk domains and perhaps also maintain tetrameric structure, allowing us to further understand the interactions in G that result in the tetrameric oligomerization and how these bonds are changed upon receptor binding.

My work has also helped to further characterize the receptor binding and fusion process of HeV/NiV. The presented data indicate that HeV/NiV association occurs via a provocateur model as receptor binding increases G-F interaction. This does not

completely rule out the possibility that G and F may have a low level of interaction that is enhanced upon receptor binding. However, it is clear that the clamp model is not accurate in detailing the interactions between HeV/NiV-G and -F upon receptor addition.

The neutralization mechanisms of m102.4 have also been further characterized by determining m102.4 must use multiple neutralization mechanisms to inhibit HeV/NiV infection. The first mechanism is outcompeting receptor for binding to HeV/NiV-G. However, we know that m102.4 neutralization cannot occur only through inhibition of receptor binding as m102.4 binding does not necessarily inhibit receptor binding. The second mechanism of m102.4 neutralization appears to be the ability of m102.4 to lock HeV/NiV-Gs into a non-receptor-inducible conformation. Using this information and m102.4 as a starting point, new therapeutics can be developed designed to prevent the receptor-induced conformational changes in G. Additionally, alteration of the m102.4 CDRH3 domain to resemble receptor does not enhance the neutralization ability of m102.4 and that additional binding factors most likely outside of the HeV/NiV-G binding regions, such as the string of tyrosine residues immediately downstream of the m102.4 binding region, must also be considered when attempting to alter m102.4.

Potential Therapeutic Use

The goal of constructing second generation m102.4 antibodies that would be more effective against HeV/NiV and any possible escape variants did not meet with success. Instead the findings led to the identification of two variants that closely mimicked the neutralization ability of m102.4, from binding HeV/NiV-Gs, inhibiting G-receptor binding, decreasing cell-cell fusion and also inducing similar escape mutations in HeV/NiV-Gs. While none of the variants will likely prove effective at neutralizing

174

HeV/NiV escape variants of m102.4, the m102.4 variants may prove beneficial in helping

to specifically direct the mutations that may occur in HeV/NiV escape variants. Since the

two best variants, LF and HA, caused similar mutations in HeV/NiV-G as m102.4, a

therapeutic cocktail of m102.4, LF and HA may prove beneficial in (a) preventing

HeV/NiV infection and (b) guaranteeing that any escape variants of HeV/NiV will be

skewed towards forming D582, N586 and V507 mutations.

In essence a pattern could be generated in which our therapeutics could stay one

step ahead of HeV/NiV infection, although this would require a great amount of time and

cost. Knowing that HeV/NiV will likely produce a D582, N586 or V507 mutation to

escape m102.4 neutralization, treatments that will inhibit these escape variants could be

developed and administered when m102.4 is no longer effective. Additional neutralizing

mAbs could be isolated using Tet-D582N/V507I-sGs, and then used to identify second-

generation HeV/NiV escape variants *in vitro* to determine what additional mutations in

HeV/NiV-G allow escape. While this would not be a permanent solution, having a

therapeutic ready to treat m102.4 escape variants of HeV/NiV-G would allow more time

to develop and license a more permanent therapeutic option, such as a NiV vaccine or an

RNA-dependent RNA polymerase inhibitor that has recently been identified for Measles

virus (130; 196).

UNANSWERED QUESTIONS AND LIMITATIONS

The work presented here has helped answer many of the prevailing questions in

the henipavirus field, but many aspects of HeV/NiV fusion still remain unknown. The

exact nature of HeV/NiV-G and –F interaction still needs to be determined. Studies

continue to provide support of both the clamp and provocateur models, suggesting again

that another model is needed to fully explain G-F association and activation. This interaction may also be better explained when a more detailed understanding of the clustering effects of receptor binding on HeV/NiV-G is available.

Studies have recently determined a two-step conformational change in NiV-G upon receptor binding (103). This work helps explain the slight conformational changes induced in G upon receptor binding that lead to F activation, but more studies are needed to explain the exact mechanics of how changes in these regions alter the overall conformation of G and result in exposure of the upper stalk region. Furthermore, the difference between receptor and m102.4 binding has not fully been elucidated. In part this is due to the uncertainty of the stoichiometric binding of G with receptor or m102.4, which is required for activation or neutralization, respectively. The research work here was limited in this regard through the continual interchange of m102.4 IgG and Fab in the assays. Unfortunately, experimental design was limited as multiple antibodies had to be detected simultaneously. It would be interesting to see if a steady use of m102.4 IgG would result in slightly different results than the use of m102.4 Fab. This could be especially telling for assays involving NiV-G and NiV-G-V507I, since the m102.4-lock mechanism requires m102.4 IgG and neutralizes NiV-G but not NiV-G-V507I.

Another area requiring further study is the ability of HeV-G-D582N and NiV-G-V507I to escape m102.4 neutralization. The present findings suggested two possible escape mechanisms, but these need to be further explored. The ability of m102.4 to bind wild type HeV/NiV-Gs but not HeV-G-D582N/NiV-G-V507I after receptor binding presents an intriguing challenge. A detailed study and comparison of the conformational

changes that occur in all four Gs upon receptor and m102.4 binding may help answer this question.

One final unanswered question from the presented work is whether the results obtained by using ephrin-B2 would also be observed with the use of ephrin-B3. Commercial antibodies to ephrin-B2 and ephrin-B3 are poor and unreliable, and while our laboratory has a highly effective anti-ephrin-B2 antibody, we did not have a readily available ephrin-B3 antibody. In light of the different binding affinities of HeV/NiV-Gs for ephrin-B2 and ephrin-B3 and the differences in G-receptor inhibition by m102.4, it seems worthwhile to repeat the competitive receptor-m102.4 binding ELISAs, sequential and simultaneous, with ephrin-B3.

FUTURE DIRECTIONS

The work presented here sets a foundation for two main areas of work – henipavirus fusion and henipavirus therapeutics. While research into these two areas may start and remain separate, ultimately they will become connected as a better understanding of the henipavirus fusion process will aid in our development of henipavirus therapeutics. Similarly, understanding how HeV/NiV infection can be inhibited may also help explain some of the uncertainties about HeV/NiV fusion.

Henipavirus Fusion

A vast majority of the work presented here relied on the use of Tet-sGs and not full-length HeV/NiV-Gs. Studies have begun that focus on the effects of receptor and m102.4 binding on cell-surface expressed HeV/NiV-Gs and their respective escape variants using fluorescently-tagged antibodies for m102.4 and m106.3. These studies would verify the results obtained with the Tet-sGs and further reveal any contributions of

higher-order oligomerizations on receptor or m102.4 binding. Additionally, they would help reveal the differences between wild type and escape variants of HeV/NiV-Gs as conformational changes in G can be detected and aligned with receptor or m102.4 binding. In fact, preliminary data supports the m102.4-lock mechanism as m102.4 and m106.3 binding have not been observed to occur simultaneously with HeV-G (data not shown).

More studies need to be performed in order to verify that HeV-G-D582N and NiV-G-V507I are able to undergo conformational change in the presence of m102.4. Similar binding ELISAs that were used in this work, such as m106.3 binding and G-F association, should be repeated using simultaneous addition of receptor and m102.4. Additionally, crystal structures of the four Tet-sGs alone and in complex with receptors ephrin-B2, ephrin-B3 and m102.3 could be obtained and compared for differences in binding and globular head conformation. While it would likely take careful work, if a crystal structure of G bound to m102.3 and receptor could be obtained, that would reveal a great amount of information about receptor and m102.4 binding.

Hendra Stalk

Recently, much work has focused on the stalk domains of paramyxovirus attachment glycoproteins (HN/H/G) as they are the F-activating domain. Recently Bose *et al*. demonstrated in PIV5 that the stalk domain is the critical component for F activation and that the globular heads serve as a restraint, preventing premature activation of F by HN (13). Further work has verified that the stalk domain is the F-triggering component for MeV-H and NiV-G (27; 103). In order to determine if this is also true for

Hendra, S-tagged soluble and full-length constructs of HeV-G were constructed that removed the globular head domain while expressing stalk residues 73-190.

So far we have verified expression of soluble and full-length HeV-G-Stalk (Figure 35 A&B) and determined the ability of soluble HeV-G-Stalk to co-precipitate Tri-HeV-sF when co-expressed in mammalian cells (Figure 35C-F). HeV-G-Stalk has also been tested in a cell-cell fusion assay with HeV-F in order to determine the triggering capability of HeV-G-Stalk. Cells expressing HeV-G-Stalk and HeV-F were able to mediate cell-cell fusion, albeit at a level lower than HeV-G-D582N and HeV-F, which served as a positive control (Figure 36). However, when the amount of target and effector cells was doubled (HeV-Stalk/HeV-F double), the level of fusion increased by approximately 50%. While fusion appears to be less robust with HeV-G-Stalk than with a full-length HeV-G, it does allow for fusion to occur, suggesting that the stalk domain is responsible for F activation and the globular heads function in a regulatory role as shown for other paramyxoviruses.

Interestingly it appears that the majority of soluble HeV-G-Stalk is being retained intracellularly as the amount of Stalk detected is much greater in the lysate than the supernatant (Figure 35A). Decreased expression of Stalk in the supernatant, and most likely the membrane surface for full-length Stalk, may contribute to the difficulty in detecting co-precipitated Stalk and F and the low level of cell-cell fusion. Brindley *et al*. recently demonstrated that MeV-H stalk with a shortened GCN4 motif on the C-terminus of the Stalk domain stabilized Stalk expression, allowing for greater cell surface expression, interaction with MeV-F and fusion (26). MeV-H and HeV-G Stalk domains are similarly long, having over 100 residues, and it seems likely that HeV-G-Stalk may

Figure 35: HeV-Stalk expression and association with HeV-F.

(A) Soluble HeV-G-Stalk (sStalk) and (B) full-length HeV-G-Stalk were expressed in USU cells and lysates/supernatants were collected and western blotted to determine Stalk expression. USU cells were also transfected with various concentrations of HeV-sStalk and HeV-sF to determine Stalk-F association. Supernatants and lysates were collected and IP'd for sF then immunoblotted for sF (C) or IP'd for sStalk and immunblotted for sStalk (D). Upon verification of sF and sStalk expression in both the lysates and supernatants the samples IP'd for sStalk were immunoblotted for sF (E), and the samples IP'd for sF were immunoblotted for sStalk (F).
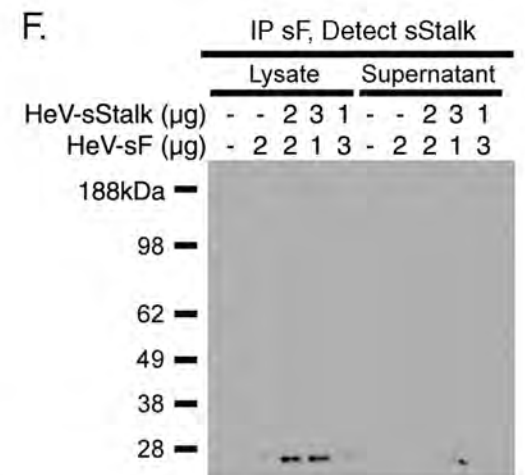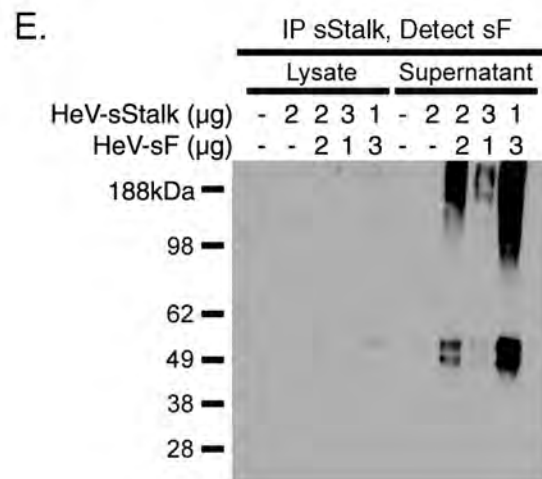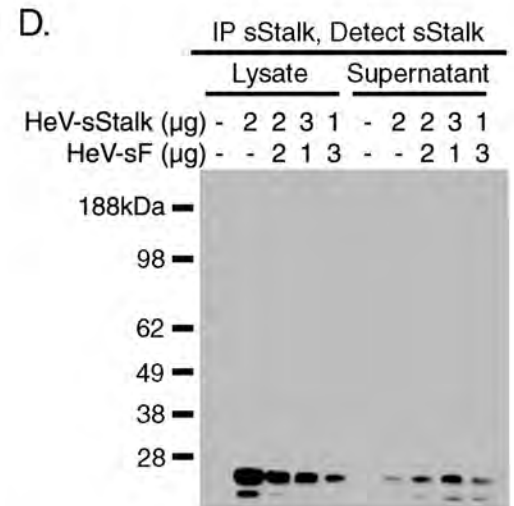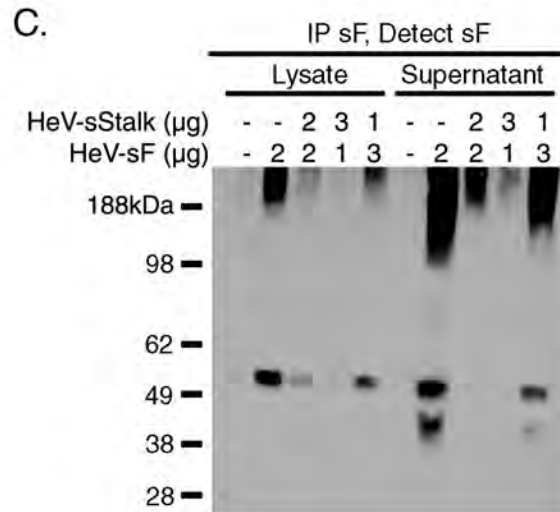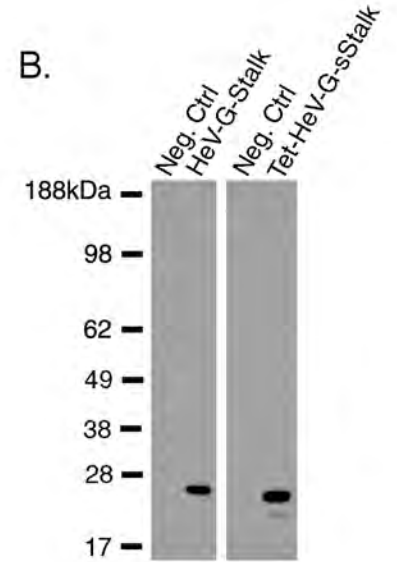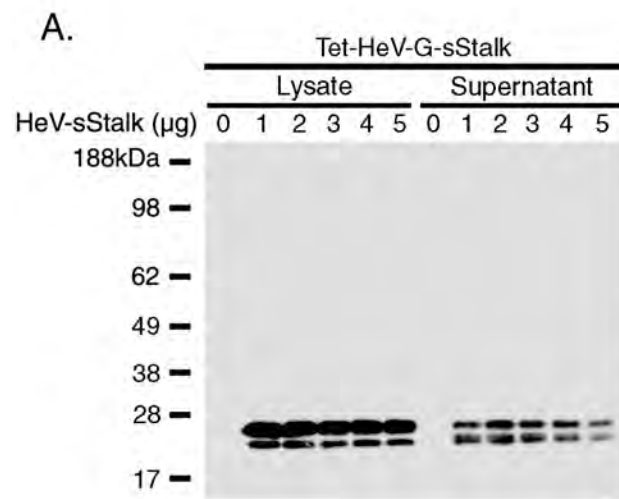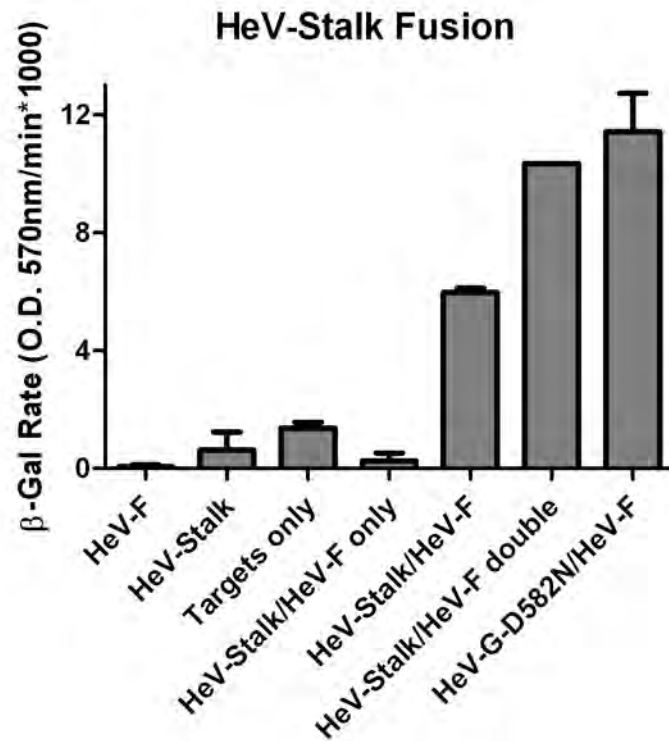
Figure 36: HeV-Stalk mediated cell-cell fusion.
Cells expressing HeV-Stalk or HeV-G-D582N with HeV-F were mixed with receptor-expressing target cells, and the fusion rate was determined. HeV-Stalk/HeV-F double represents fusion that occurred when twice the amount of effector and target cells were mixed.

need additional stabilization for optimal surface expression. Therefore, the HeV-G-Stalk sequence will be amended by adding a truncated GCN4 motif at the C-terminus as was done for MeV-H. Additionally, Stalk constructs of various lengths are being developed, and surface expression of these constructs will be compared in order to determine the best expresser. Once a construct with a high level of surface expression is identified, studies for Stalk-F interaction and Stalk-mediated fusion can continue.

Henipavirus Therapeutics

There are a number of ways that the present findings can help expand the pool of henipavirus therapeutics. While it seems unlikely that m102.4 variants will provide an additional therapeutic on their own, they could be used to generate a cocktail of antibodies that can be administered to infected individuals. Additional mAbs can also be isolated using Tet-D582N/V507I-sGs. These antibodies can then be tested for binding and neutralizing capabilities and compared with m102.4.

The soluble HeV-G-Stalk construct can also be further developed for large-scale production and purification. Soluble HeV-G-Stalk can be tested as a replacement for soluble receptor to inhibit HeV/NiV infection. Furthermore it can be used to identify antibodies that bind the Stalk domain that may also serve as another therapeutic that can block HeV/NiV infection. This is particularly appealing given the high degree of flexibility HeV/NiV possess to mutate and prevent m102.4 neutralization. If a neutralizing, stalk-binding antibody could be isolated, it seems likely drastic changes would have to occur in the stalk domains of HeV/NiV-G to escape neutralization. These changes may also render G-F association impossible, resulting in non-infectious virus.

183

The use of stalk antibodies has already been highly investigated for influenza and shows great promise at neutralizing a broad range of influenza strains and subtypes (90; 112).

SUMMARY

The work presented here provides further insight into the mechanism of HeV/NiV fusion and how m102.4 disrupts this process. Soluble versions of HeV/NiV-G that maintain their tetrameric oligomerization were constructed and used to determine the effect of receptor and m102.4 binding on G conformational change and F association. We have also shown that alteration of the m102.4 binding region to more closely resemble the G-H loops of ephrin-B2 and ephrin-B3 does not provide enhanced neutralization and, depending on the mutation, may abolish m102.4 binding and inhibition. Additionally, m102.4 cannot neutralize HeV/NiV infection by solely preventing receptor binding as m102.4 escape variants of HeV/NiV-Gs are able to bind m102.4 and escape neutralization. We therefore propose that m102.4 neutralizes fusion by two methods – inhibiting receptor binding and locking HeV/NiV-Gs into a non-receptor-inducible conformation. Viral escape from m102.4 occurs by reduced binding affinity to m102.4 or altered m102.4 binding that still allows for receptor-induced conformational changes. My research into the neutralization abilities of m102.4 and how HeV/NiV-Gs escape provides a foundation for continued efforts to characterize these interactions with the goal of further understanding the complexities of henipavirus fusion that will help enhance our current therapeutics for HeV/NiV infection.

Appendix A: Competition ELISAs

Figure 37: Competition ELISAs with Tet-HeV-sG, ephrin-B2, m102.4 and m102.4 variants.

(A) Representative sample of individual competition ELISAs in which Tet-HeV-sG mixed with increasing concentrations of m102.4 and m102.4 variants is incubated with immobilized ephrin-B2. **(B)** Summary of individual competition ELISAs for all 19 variants. All values were normalized to the level of Tet-HeV-sG binding in absence of antibody (100%). Levels of bound Tet-HeV-sG were shown in color for 5 variants of interest (m102.4, LD, LF, HA and SLP), and the data collected using these variants is shown separately in **(C)**. Significance determined by one-way Anova. ***<0.0001, *<0.05

A. Tet-HeV-sG, B2 and m102.4 Variants

B. Tet-HeV-sG & Ephrin-B2 Competition Summary

C. Tet-HeV-sG & Ephrin-B2 Competition Summary
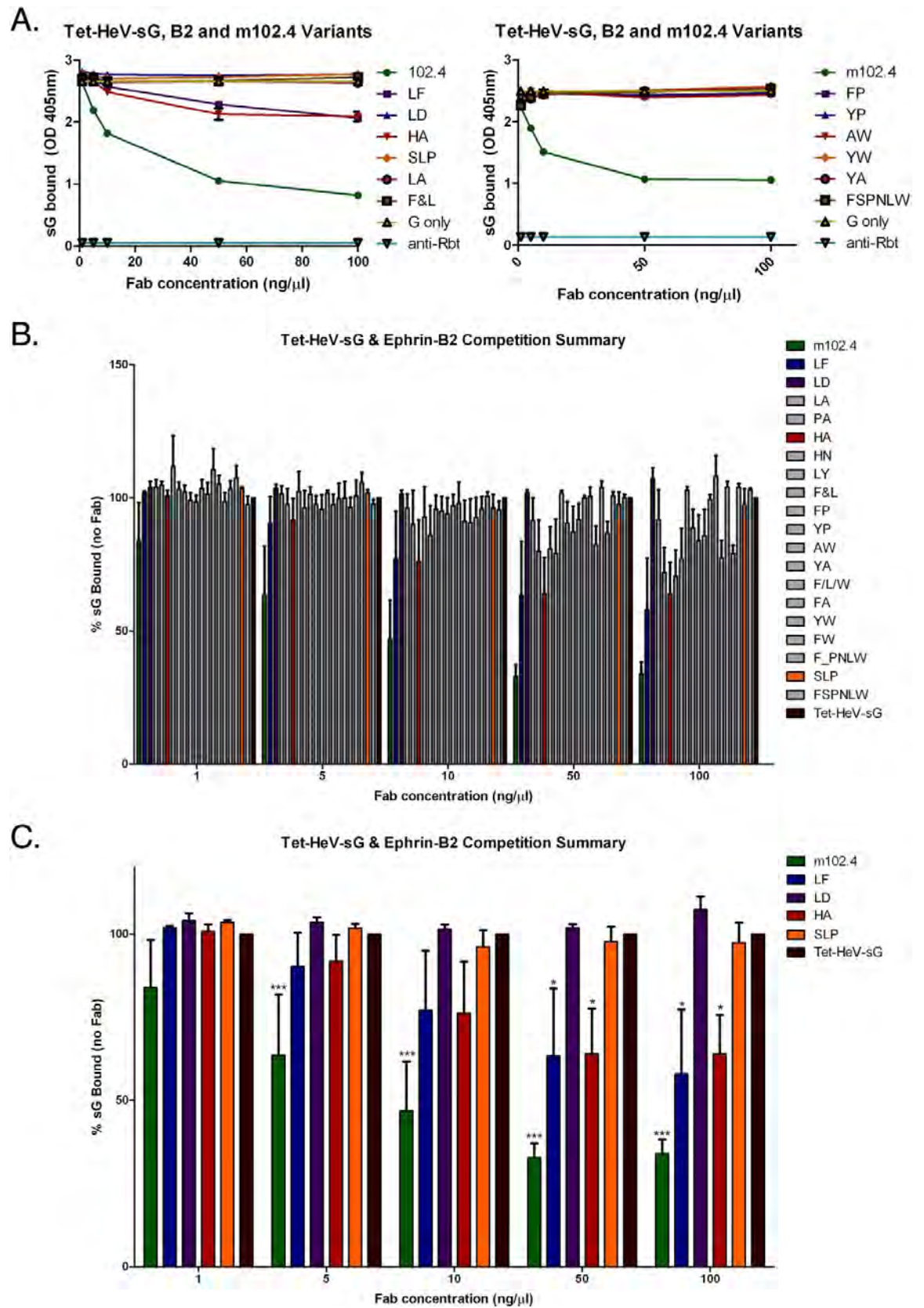
Figure 38: Competition ELISAs with Tet-HeV-sG, ephrin-B3, m102.4 and m102.4 variants.

(A) Representative sample of individual competition ELISA in which Tet-HeV-sG mixed with increasing concentrations of m102.4 and m102.4 variants is incubated with immobilized ephrin-B3. (B) Summary of individual competition ELISAs for all 19 variants. All values were normalized to the level of Tet-HeV-sG binding in absence of antibody (100%). Levels of bound Tet-HeV-sG were shown in color for 5 variants of interest (m102.4, LD, LF, HA and SLP), and the data collected using these variants is shown separately in (C). Significance determined by one-way Anova. ***<0.0001, **<0.001

A.

Tet-HeV-sG, B3 and m102.4 Variants

Tet-HeV-sG, B3 and m102.4 Variants

B.

Tet-HeV-sG & Ephrin-B3 Competition Summary

C.

Tet-HeV-sG & Ephrin-B3 Competition Summary

Figure 39: Competition ELISAs with Tet-NiV-sG, ephrin-B2, m102.4 and m102.4 variants.

(A) Representative sample of individual competition ELISA in which Tet-NiV-sG mixed with increasing concentrations of m102.4 and m102.4 variants is incubated with immobilized ephrin-B2. (B) Summary of individual competition ELISAs for all 19 variants. All values were normalized to the level of Tet-NiV-sG binding in absence of antibody (100%). Levels of bound Tet-NiV-sG were shown in color for 5 variants of interest (m102.4, LD, LF, HA and SLP), and the data collected using these variants is shown separately in (C). Significance determined by one-way Anova. ***<0.0001, **<0.001, *<0.05

A.

Tet-NiV-sG, B2 and m102.4 Variants

Legend: m102.4, LF, PA, HN, F&L, F/L/W, NiV, SVL 11

Tet-NiV-sG, B2 and m102.4 Variants

Legend: m102.4, FP, YP, AW, YW, YA, FSPNLW, G only, anti-Rbt

B.

Tet-NiV-sG & Ephrin-B2 Competition Summary

Legend: m102.4, LF, LD, LA, PA, HA, HN, LY, F&L, FP, YP, AW, YA, F/L/W, FA, YW, FW, F_PNLW, SLP, FSPNLW, Tet-NiV-sG

C.

Tet-NiV-sG & Ephrin-B2 Competition Summary

Legend: m102.4, LF, LD, HA, SLP, Tet-NiV-sG

Figure 40: Competition ELISAs with Tet-NiV-sG, ephrin-B3, m102.4 and m102.4 variants.

(A) Representative sample of individual competition ELISA in which Tet-NiV-sG mixed with increasing concentrations of m102.4 and m102.4 variants is incubated with immobilized ephrin-B3. (B) Summary of individual competition ELISAs for all 19 variants. All values were normalized to the level of Tet-NiV-sG binding in absence of antibody (100%). Levels of bound Tet-NiV-sG were shown in color for 5 variants of interest (m102.4, LD, LF, HA and SLP), and the data collected using these variants is shown separately in (C). Significance determined by one-way Anova. ***<0.0001, **<0.001
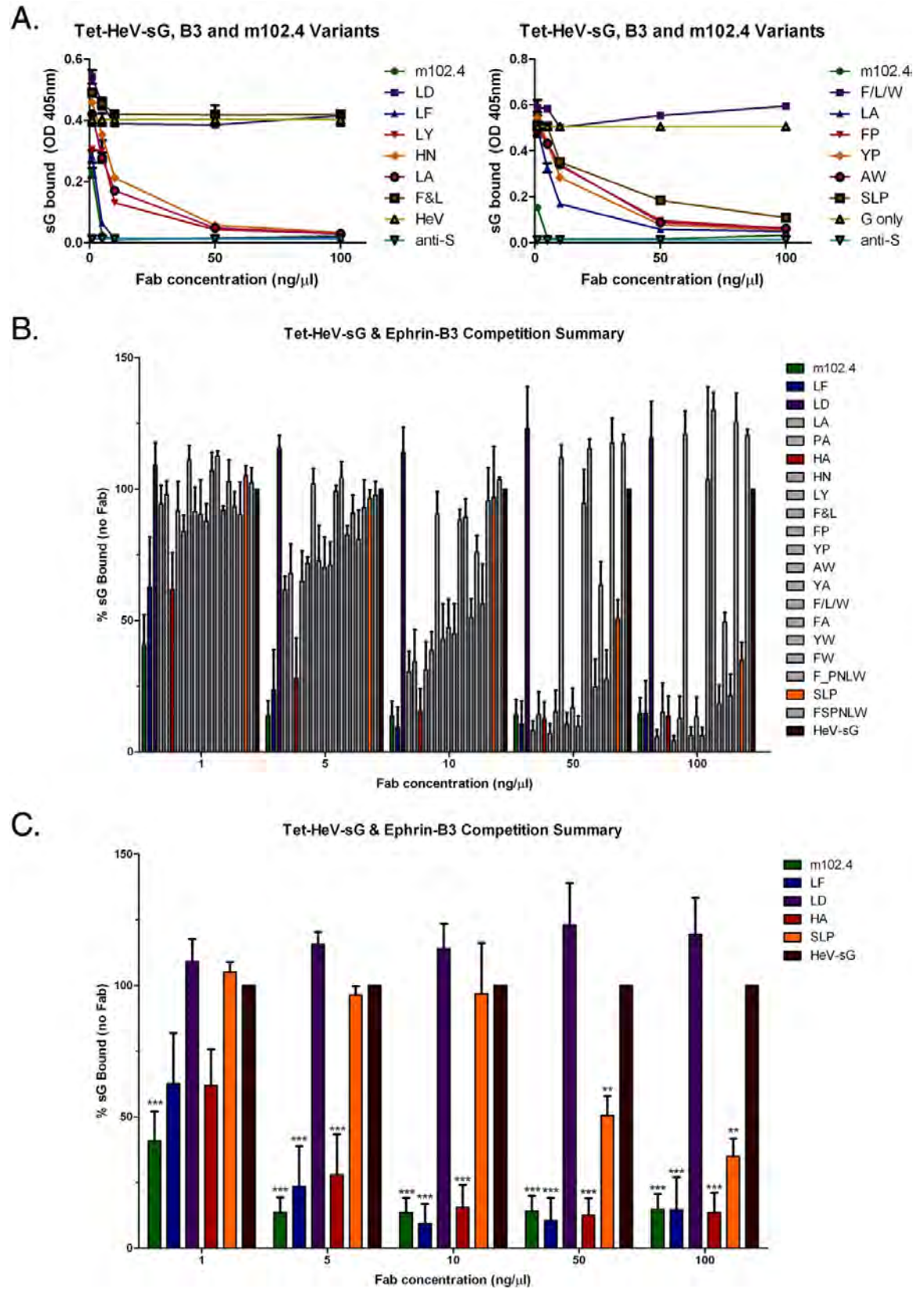
A.

Tet-NiV-sG, B3 and m102.4 variants

Tet-NiV-sG, B3 and m102.4 variants

B.

Tet-NiV-sG & Ephrin-B3 Competition Summary

C.

Tet-NiV-sG & Ephrin-B3 Competition Summary

Figure 41: Competition ELISAs with Tet-D582N-sG, ephrin-B2, m102.4 and m102.4 variants.

(A) Representative sample of individual competition ELISA in which Tet-D582N-sG mixed with increasing concentrations of m102.4 and m102.4 variants is incubated with immobilized ephrin-B2. (B) Summary of individual competition ELISAs for all 19 variants. All values were normalized to the level of Tet-D582N-sG binding in absence of antibody (100%). Levels of bound Tet-D582N-sG were shown in color for 5 variants of interest (m102.4, LD, LF, HA and SLP), and the data collected using these variants is shown separately in (C).

A.

Tet-D582N-sG, B2 and m102.4 Variants

Tet-D582N-sG, B2 and m102.4 variants

B.

Tet-D582N-sG & Ephrin-B2 Competition Summary

C.

Tet-D582N-sG & Ephrin-B2 Competition Summary

194

Figure 42: Competition ELISAs with Tet-D582N-sG, ephrin-B3, m102.4 and m102.4 variants.

(A) Representative sample of individual competition ELISA in which Tet-D582N-sG mixed with increasing concentrations of m102.4 and m102.4 variants is incubated with immobilized ephrin-B3. (B) Summary of individual competition ELISAs for all 19 variants. All values were normalized to the level of Tet-D582N-sG binding in absence of antibody (100%). Levels of bound Tet-D582N-sG were shown in color for 5 variants of interest (m102.4, LD, LF, HA and SLP), and the data collected using these variants is shown separately in (C). Significance determined by one-way Anova. ***<0.0001, **<0.001
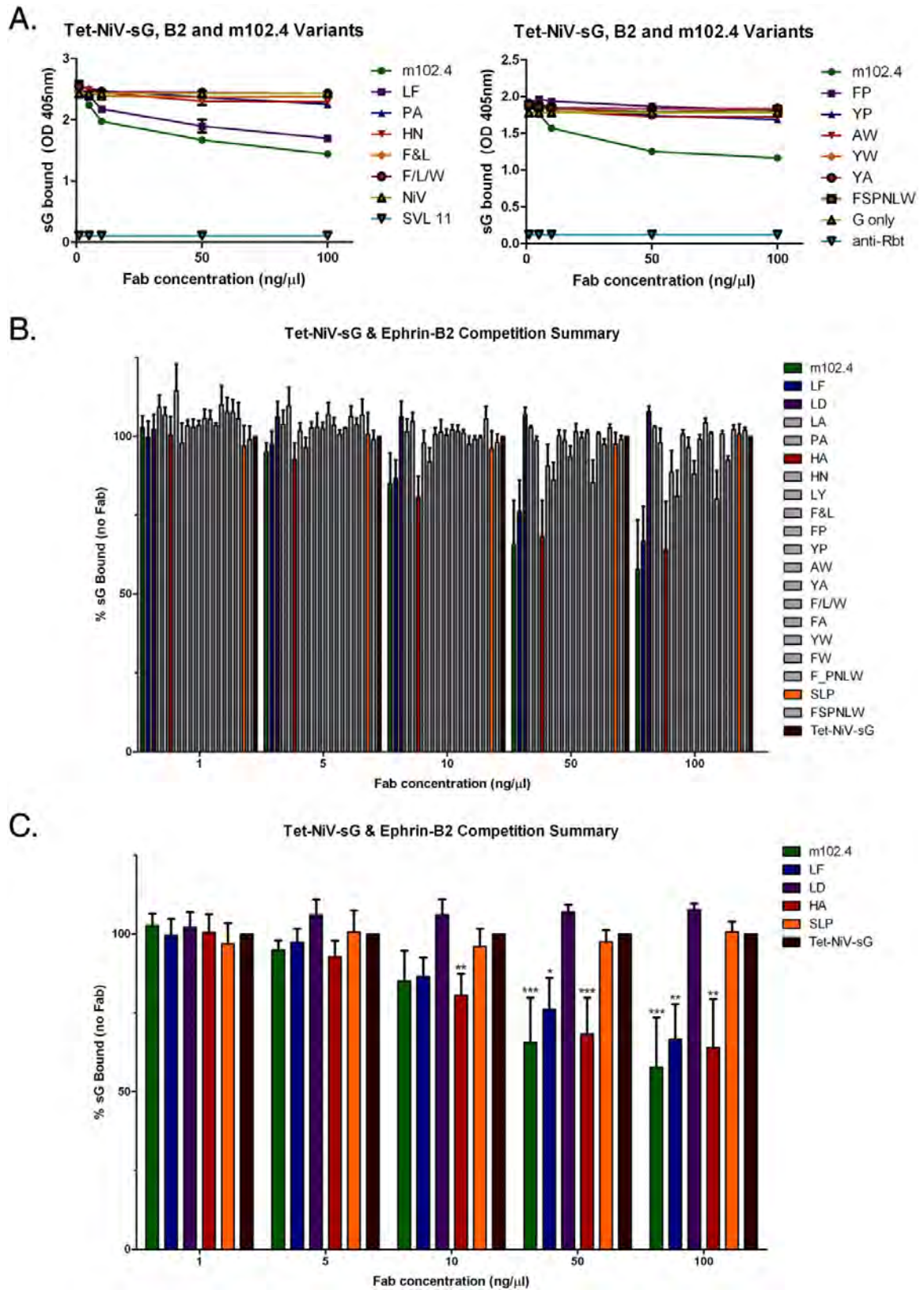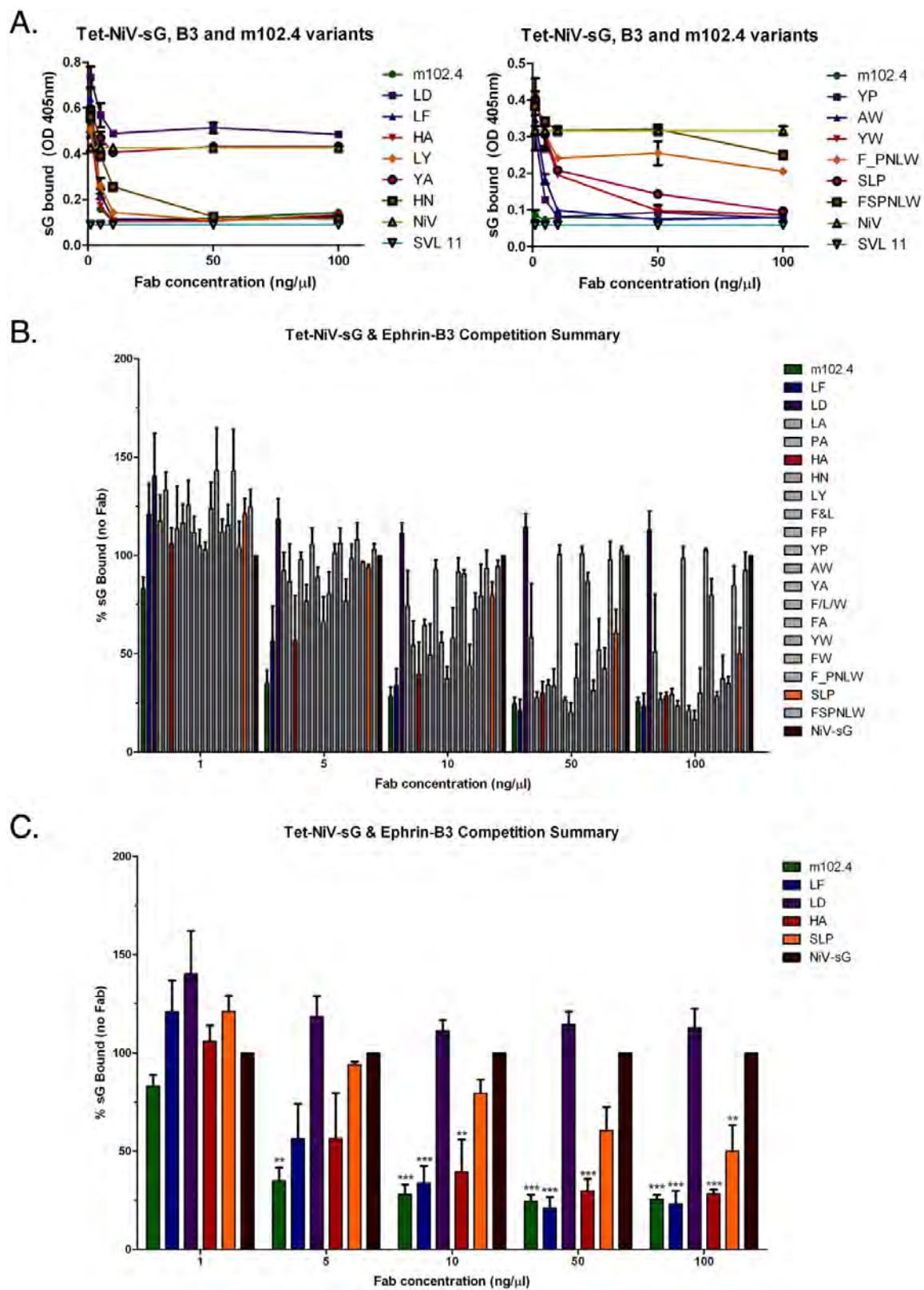
A. Tet-D582NV-sG, B3 and m102.4 variants | Tet-D582N-sG, B3 and m102.4 variants

B. Tet-D582N-sG & Ephrin-B3 Competition Summary

C. Tet-D582N-sG & Ephrin-B3 Competition Summary

196

Figure 43: Competition ELISAs with Tet-V507I-sG, ephrin-B2, m102.4 and m102.4 variants.

(**A**) Representative sample of individual competition ELISA in which Tet-V507I-sG mixed with increasing concentrations of m102.4 and m102.4 variants is incubated with immobilized ephrin-B2. (**B**) Summary of individual competition ELISAs for all 19 variants. All values were normalized to the level of Tet-V507I-sG binding in absence of antibody (100%). Levels of bound Tet-V507I-sG were shown in color for 5 variants of interest (m102.4, LD, LF, HA and SLP), and the data collected using these variants is shown separately in (**C**). Significance determined by one-way Anova. *<0.05

A.

Tet-V507I-sG, B2 and m102.4 Variants

Tet-V507I-sG, B2 and m102.4 Variants

B.

Tet-V507I-sG & Ephrin-B2 Competition Summary

C.

Tet-V507I-sG & Ephrin-B2 Competition Summary
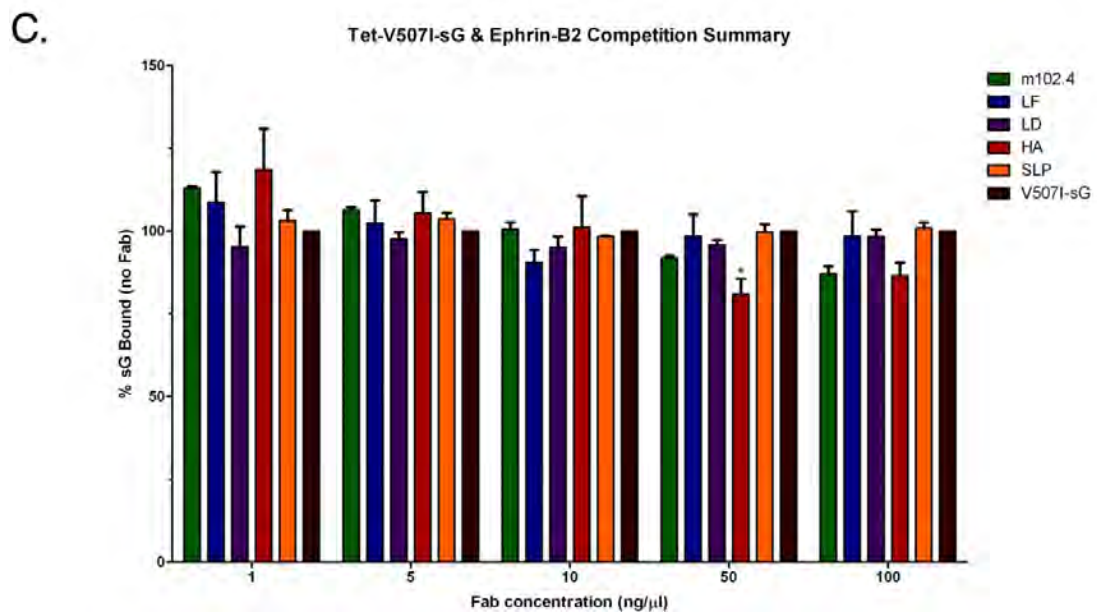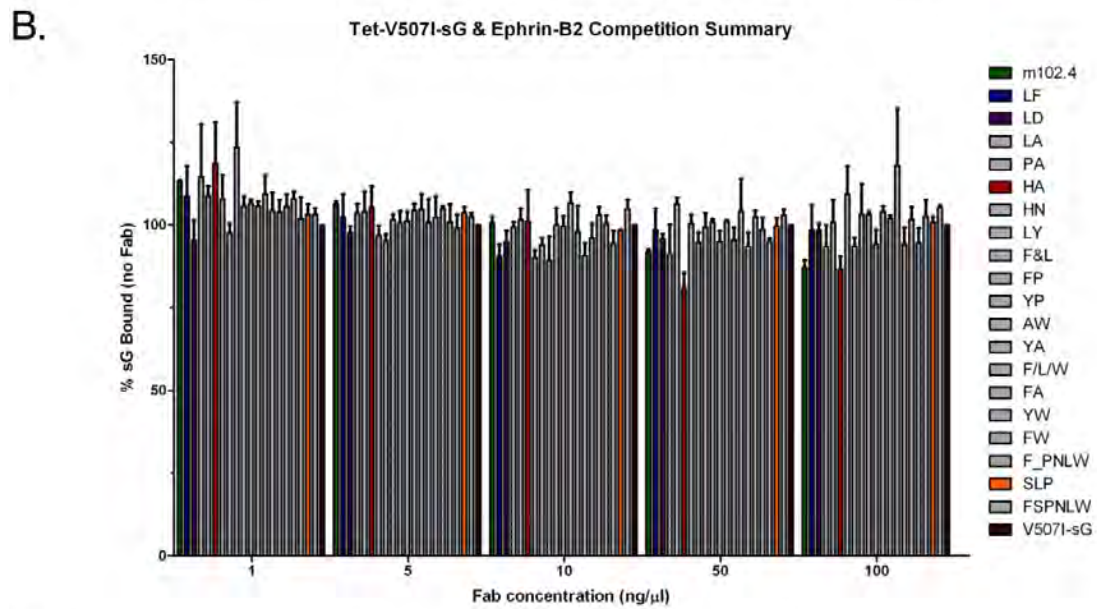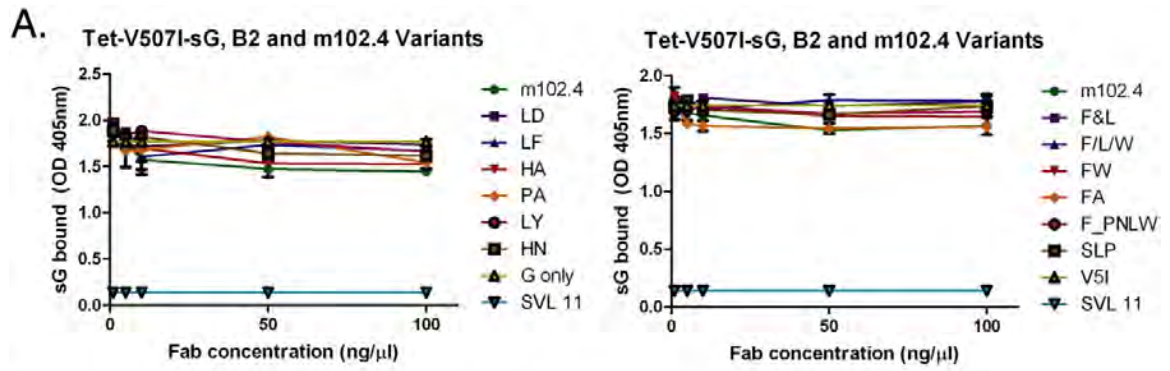
Figure 44: Competition ELISAs with Tet-V507I-sG, ephrin-B3, m102.4 and m102.4 variants.

(A) Representative sample of individual competition ELISA in which Tet-V507I-sG mixed with increasing concentrations of m102.4 and m102.4 variants is incubated with immobilized ephrin-B3. (B) Summary of individual competition ELISAs for all 19 variants. All values were normalized to the level of Tet-V507I-sG binding in absence of antibody (100%). Levels of bound Tet-V507I-sG were shown in color for 5 variants of interest (m102.4, LD, LF, HA and SLP), and the data collected using these variants is shown separately in (C). Significance determined by one-way Anova. *<0.05
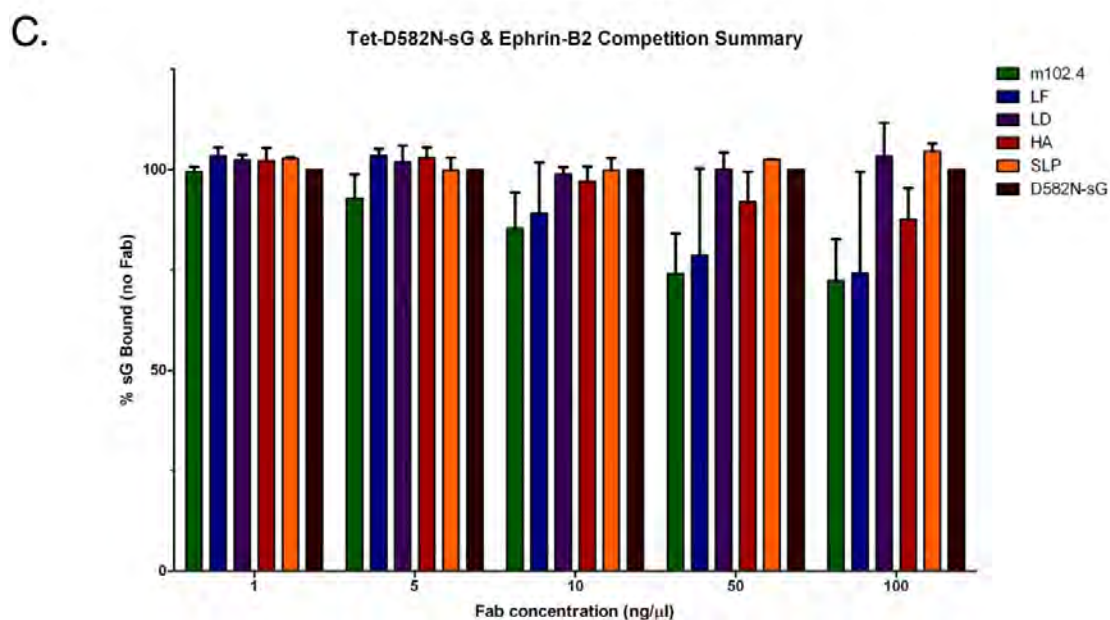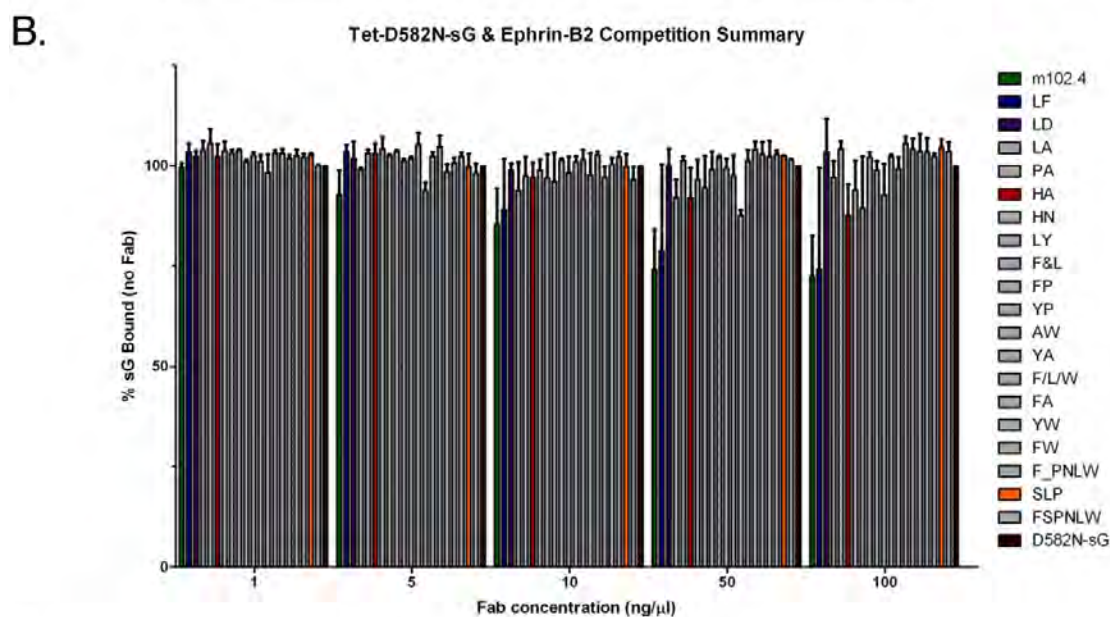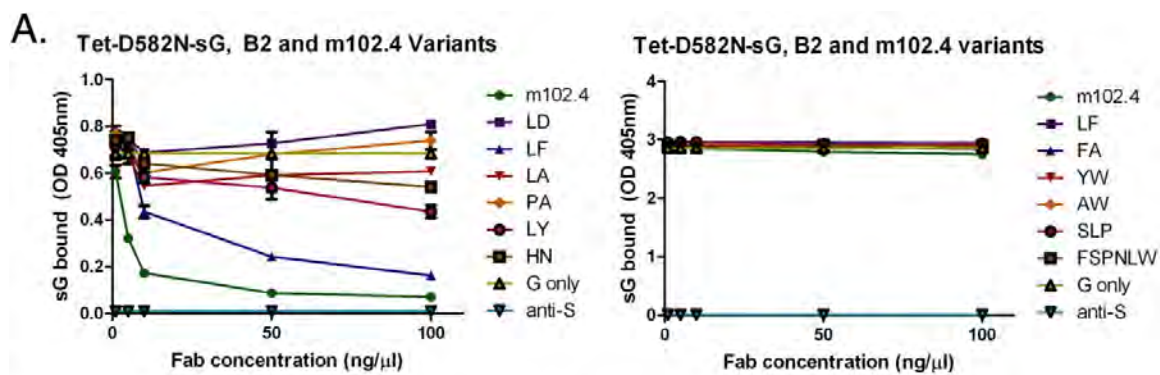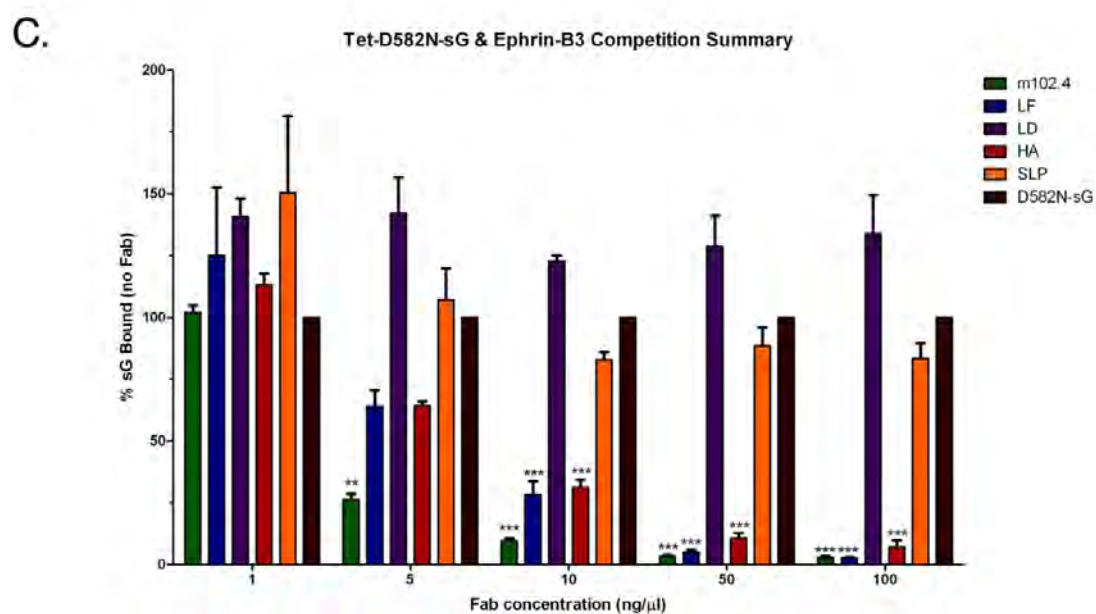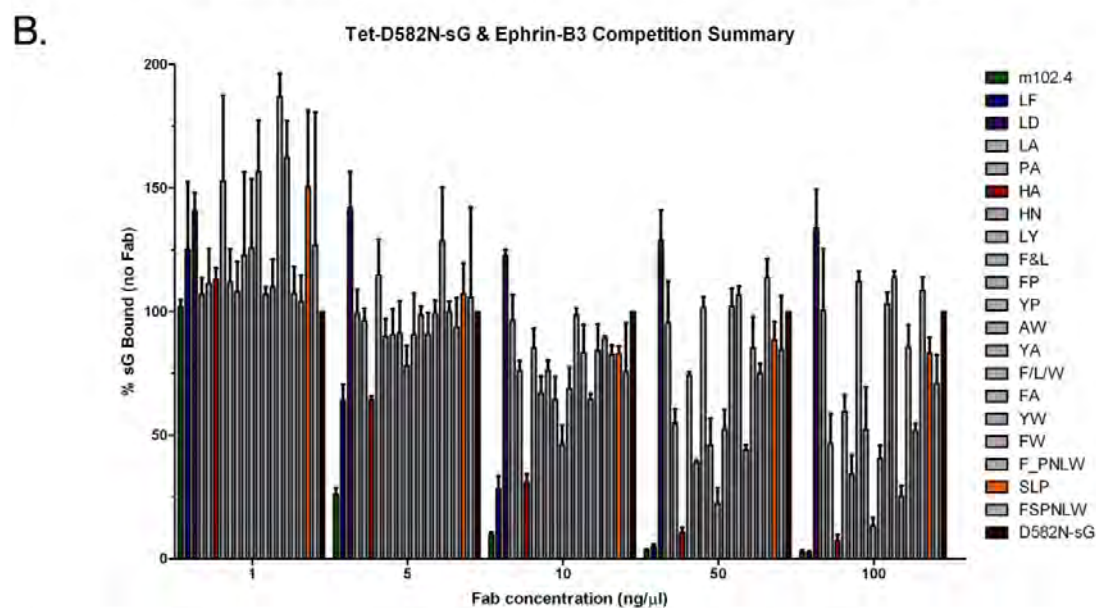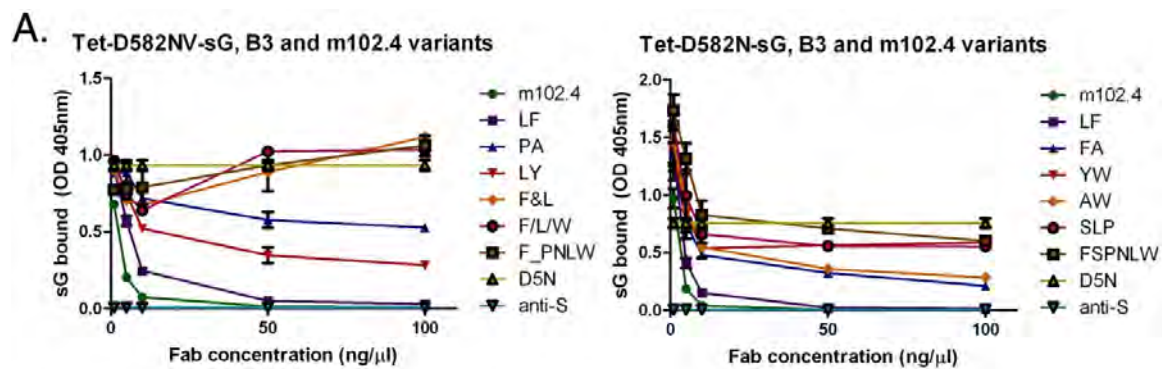
A.

Tet-V507I-sG, B3 and m102.4 variants

Tet-NiV-sG-V507I, B3 and m102.4 Variants

B.

Tet-V507I-sG & Ephrin-B3 Competition Summary

C.

Tet-V507I-sG & Ephrin-B3 Competition Summary
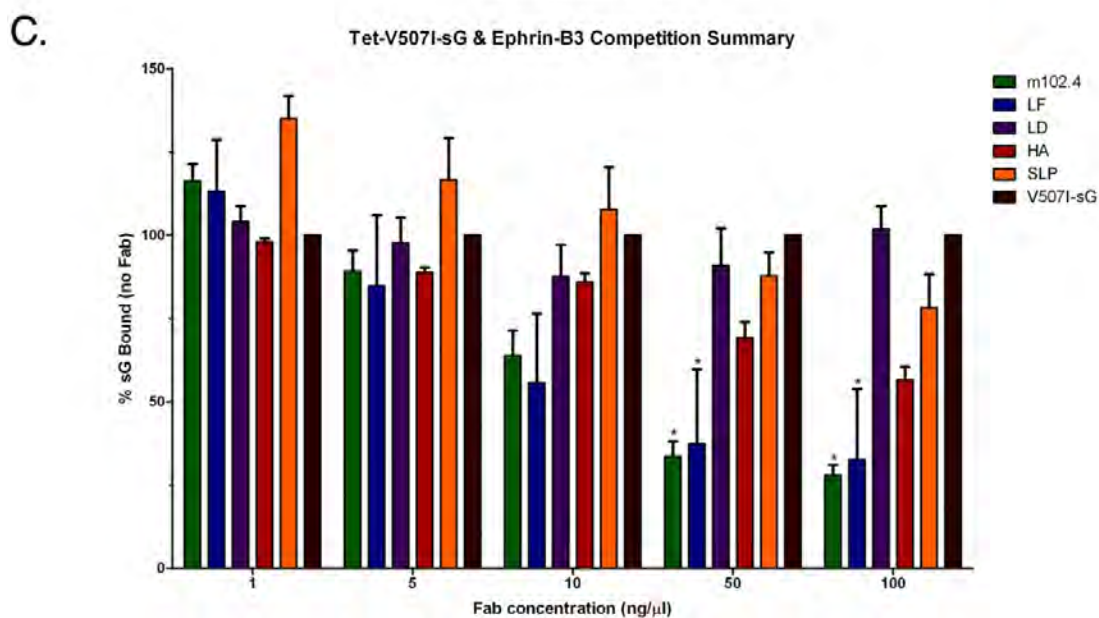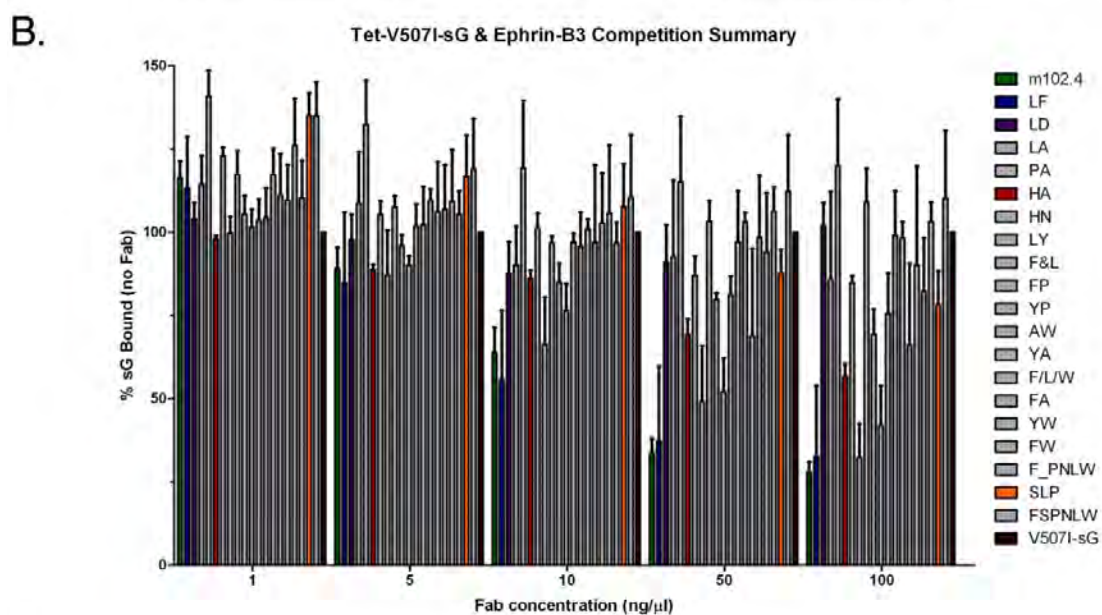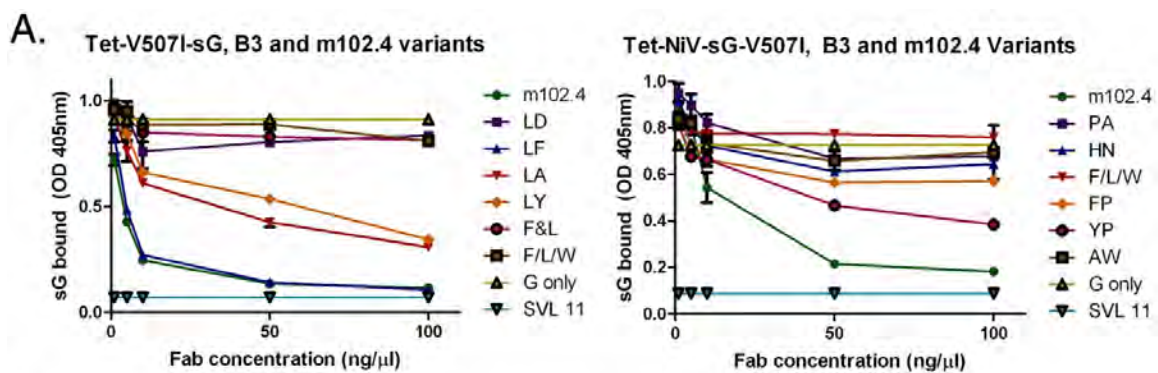
Appendix B: HeV/NiV Mutations that allow for escape from m102.4 variants

Hendra Escape Mutations

Fab	Clone	Mutations
No Fab	1	-
	2	S284L, S309P
	3	G102E
	4	I118T, I545V, I545V
	5	R242K
	6	-
	7	F453L
	8	-

m102.4	1	S175P, I464T, D582S
	2	F50L, Q427R, W519R, D582N
	3	K344E, D582N
	4	D582N
	5	T563A, D582N
	6	D582N

LD	1	I424T, K541R
	2	-
	3	L234P
	4	-
	5	N275D
	6	-

LF	1	Q93R, D423G, D582N
	2	Q93R, D423G, D582N
	3	L126S, D582Y
	4	P535L, D582Y, S604G

HA	1	L47H, N331K, E505G, D582N
	2	L47H, N331K, E505G, D582N
	3	D461G, D582N
	4	N66D, S175P, N226S, D329G, D433N, T507I, V587M
	5	N66D, N186S, F229S, T507I
	6	T507I, I588V
	7	T507I
	8	T507I

SLP	1	E374G
	2	I335V
	3	F148S
	4	G253S
	5	V178M
	6	L413P
	7	K84E, R487G
	8	N210S, I279T
	9	Y334H
	10	G125R, I155V

Nipah Escape Mutations

Fab	Clone	Mutations
No Fab	1	K386E, I401T, I517V
	2	M32K, L57P, G243R, R402G
	3	-
	4	-
	5	I70T, I502V

m102.4

	1	Q196R, N586T
	2	R248G, D582E
	3	C216R, D582E, I588M
	4	I112T, I444T, K560R, N586T
	5	D582E
	6	D582E
	7	A55T, D582E

LD	1	V53A, L97R, N141S, N180S, D379G
	2	N331D
	3	-
	4	S264Y, S457P
	5	I118T, C395Y
	6	K17R, K342E
	7	-
	8	S264F, I502T
	9	-

LF	1	I217V, S307N, D582E
	2	P107S, P167H

3	D582E	
4	L97P, V178A, D582E	

HA	1	A81T, D346G,D582E
	2	P208S, V469A, W479C, N586T
	3	N586T
	4	I20F, M32T, N543S, D582E
	5	L127I, D582E
	6	D582E
	7	S27C, I105V, L294F, D582E, T602A
	8	M32I, D582E

SLP	1	-
	2	-
	3	N269S, A296V, G329D, N378D, T462I
	4	G238E, I249V
	5	K154E, N518D, K560R
	6	K100R
	7	S283N, R516G

REFERENCES

1.   Aguilar HC, Ataman ZA, Aspericueta V, Fang AQ, Stroud M, et al. 2009. A
        novel receptor-induced activation site in the Nipah virus attachment glycoprotein
        (G) involved in triggering the fusion glycoprotein (F). *J Biol Chem* 284:1628-35

2.   Aguilar HC, Matreyek KA, Choi DY, Filone CM, Young S, Lee B. 2007.
        Polybasic KKR Motif in the Cytoplasmic Tail of Nipah Virus Fusion Protein
        Modulates Membrane Fusion by Inside-Out Signaling. *J Virol* 81:4520-32

3.   Aguilar HC, Matreyek KA, Filone CM, Hashimi ST, Levroney EL, et al. 2006. N-
        Glycans on Nipah virus fusion protein protect against neutralization but reduce
        membrane fusion and viral entry. *J Virol* 80:4878-89

4.   Anonymous. 2009. Hendra virus, human, equine - Australia (05): Queensland.
        Rep. 20090910.3189, International Society for Infectious Diseases

5.   Anonymous. 2010. Hendra virus, equine - Australia (05): (QL) human exposure.
        Rep. 20100527.1761, International Society for Infectious Diseases

6.   Anonymous. 2011. HENDRA VIRUS, EQUINE - AUSTRALIA (21):
        (QUEENSLAND) CANINE. *Pro-Med-mail, Archive No. 20110802.2324.
        International Society for Infectious Diseases: Brookline, MA, USA, 2 August
        2011. Available online: http://www.promedmail.org/ (accessed on 10 December
        2013).*

7.   Anonymous. 2011. HENDRA VIRUS, EQUINE - AUSTRALIA (28):
        (QUEENSLAND, NEW SOUTH WALES). *Pro-MED-mail, Archive No.
        20111013.3061. International Society for Infectious Diseases: Brookline, MA,
        USA, 13 October 2011. Available online: http://www.promedmail.org/ (accessed
        on 10 December 2013).*

8.   Barbas C, Burton D, Scott J, Silverman G. 2001. *Phage Display: A Laboratory
        Manual*. Plainview, New York: Cold Spring Harbor Lab. Press

9.   Bellini WJ, Harcourt BH, Bowden N, Rota PA. 2005. Nipah virus: an emergent
        paramyxovirus causing severe encephalitis in humans. *J Neurovirol* 11:481-7

10.   Bishop KA, Hickey AC, Khetawat D, Patch JR, Bossart KN, et al. 2008. Residues
        in the stalk domain of the hendra virus g glycoprotein modulate conformational
        changes associated with receptor binding. *J Virol* 82:11398-409

11.   Bishop KA, Stantchev TS, Hickey AC, Khetawat D, Bossart KN, et al. 2007.
        Identification of hendra virus g glycoprotein residues that are critical for receptor
        binding. *J Virol* 81:5893-901

12. Bonaparte MI, Dimitrov AS, Bossart KN, Crameri G, Mungall BA, et al. 2005. Ephrin-B2 ligand is a functional receptor for Hendra virus and Nipah virus. *Proc Natl Acad Sci U S A* 102:10652-7

13. Bose S, Zokarkar A, Welch BD, Leser GP, Jardetzky TS, Lamb RA. 2012. Fusion activation by a headless parainfluenza virus 5 hemagglutinin-neuraminidase stalk suggests a modular mechanism for triggering. *Proc Natl Acad Sci U S A* 109:E2625-34

14. Bossart KN, Broder CC. 2004. Viral glycoprotein-mediated cell fusion assays using vaccinia virus vectors. *Methods in molecular biology (Clifton, N.J.)* 269:309-32

15. Bossart KN, Crameri G, Dimitrov AS, Mungall BA, Feng YR, et al. 2005. Receptor binding, fusion inhibition, and induction of cross-reactive neutralizing antibodies by a soluble g glycoprotein of hendra virus. *J Virol* 79:6690-702

16. Bossart KN, Fusco DL, Broder CC. 2013. Paramyxovirus entry. *Advances in experimental medicine and biology* 790:95-127

17. Bossart KN, Geisbert TW, Feldmann H, Zhu Z, Feldmann F, et al. 2011. A neutralizing human monoclonal antibody protects african green monkeys from hendra virus challenge. *Science translational medicine* 3:105ra3

18. Bossart KN, McEachern JA, Hickey AC, Choudhry V, Dimitrov DS, et al. 2007. Neutralization assays for differential henipavirus serology using Bio-Plex Protein Array Systems. *Journal of virological methods* 142:29-40

19. Bossart KN, Rockx B, Feldmann F, Brining D, Scott D, et al. 2012. A Hendra virus G glycoprotein subunit vaccine protects African green monkeys from Nipah virus challenge. *Science translational medicine* 4:146ra07

20. Bossart KN, Tachedjian M, McEachern JA, Crameri G, Zhu Z, et al. 2008. Functional studies of host-specific ephrin-B ligands as Henipavirus receptors. *Virology* 372:357-71

21. Bossart KN, Wang LF, Flora MN, Chua KB, Lam SK, et al. 2002. Membrane fusion tropism and heterotypic functional activities of the nipah virus and hendra virus envelope glycoproteins. *J Virol* 76:11186-98.

22. Bossart KN, Zhu Z, Middleton D, Klippel J, Crameri G, et al. 2009. A neutralizing human monoclonal antibody protects against lethal disease in a new ferret model of acute nipah virus infection. *PLoS pathogens* 5:e1000642

23. Bowden TA, Aricescu AR, Gilbert RJ, Grimes JM, Jones EY, Stuart DI. 2008. Structural basis of Nipah and Hendra virus attachment to their cell-surface receptor ephrin-B2. *Nat Struct Mol Biol* 15:567-72

24. Bowden TA, Crispin M, Harvey DJ, Aricescu AR, Grimes JM, et al. 2008. Crystal structure and carbohydrate analysis of Nipah virus attachment glycoprotein: a template for antiviral and vaccine design. *J Virol* 82:11628-36

25. Bowden TA, Crispin M, Harvey DJ, Jones EY, Stuart DI. 2010. Dimeric architecture of the Hendra virus attachment glycoprotein: evidence for a conserved mode of assembly. *J Virol* 84:6208-17

26. Brindley MA, Suter R, Schestak I, Kiss G, Wright ER, Plemper RK. 2013. A stabilized headless measles virus attachment protein stalk efficiently triggers membrane fusion. *J Virol* 87:11693-703

27. Brindley MA, Takeda M, Plattet P, Plemper RK. 2012. Triggering the measles virus membrane fusion machinery. *Proc Natl Acad Sci U S A* 109:E3018-27

28. Broder CC. 2010. Therapeutics and Vaccines against Hendra and Nipah Viruses. In *New Generation Vaccines*, ed. MM Levine, G Dougan, MF Good, MA Liu, GJ Nabel, et al:885-94. New York: Informa Healthcare USA. Number of 885-94 pp.

29. Broder CC, Xu K, Nikolov DB, Zhu Z, Dimitrov DS, et al. 2013. A treatment for and vaccine against the deadly Hendra and Nipah viruses. *Antiviral research*

30. Buchholz CJ, Retzler C, Homann HE, Neubert WJ. 1994. The carboxy-terminal domain of Sendai virus nucleocapsid protein is involved in complex formation between phosphoprotein and nucleocapsid-like particles. *Virology* 204:770-6

31. Calain P, Roux L. 1993. The rule of six, a basic feature for efficient replication of Sendai virus defective interfering RNA. *J Virol* 67:4822-30

32. Calain P, Roux L. 1995. Functional characterisation of the genomic and antigenomic promoters of Sendai virus. *Virology* 212:163-73

33. Chan YP, Lu M, Dutta S, Yan L, Barr J, et al. 2012. Biochemical, conformational, and immunogenic analysis of soluble trimeric forms of henipavirus fusion glycoproteins. *J Virol* 86:11457-71

34. Chan YP, Yan L, Feng YR, Broder CC. 2009. Preparation of recombinant viral glycoproteins for novel and therapeutic antibody discovery. *Methods in molecular biology (Clifton, N.J.)* 525:31-58, xiii

35. Chong HT, Kamarulzaman A, Tan CT, Goh KJ, Thayaparan T, et al. 2001. Treatment of acute Nipah encephalitis with ribavirin. *Ann Neurol* 49:810-3.

36. Chong HT, Kunjapan SR, Thayaparan T, Tong J, Petharunam V, et al. 2002. Nipah encephalitis outbreak in Malaysia, clinical features in patients from Seremban. *Can J Neurol Sci* 29:83-7.

37. Chua KB, Bellini WJ, Rota PA, Harcourt BH, Tamin A, et al. 2000. Nipah virus: a recently emergent deadly paramyxovirus. *Science* 288:1432-5

38. Chua KB, Goh KJ, Wong KT, Kamarulzaman A, Tan PS, et al. 1999. Fatal encephalitis due to Nipah virus among pig-farmers in Malaysia [see comments]. *Lancet* 354:1257-9

39. Chua KB, Lek Koh C, Hooi PS, Wee KF, Khong JH, et al. 2002. Isolation of Nipah virus from Malaysian Island flying-foxes. *Microbes Infect* 4:145-51.

40. Clayton BA, Wang LF, Marsh GA. 2013. Henipaviruses: an updated review focusing on the pteropid reservoir and features of transmission. *Zoonoses and public health* 60:69-83

41. Colgrave ML, Snelling HJ, Shiell BJ, Feng YR, Chan YP, et al. Site occupancy and glycan compositional analysis of two soluble recombinant forms of the attachment glycoprotein of Hendra virus. *Glycobiology*

42. Connolly SA, Leser GP, Jardetzky TS, Lamb RA. 2009. Bimolecular complementation of paramyxovirus fusion and hemagglutinin-neuraminidase proteins enhances fusion: implications for the mechanism of fusion triggering. *J Virol* 83:10857-68

43. Corey EA, Iorio RM. 2007. Mutations in the stalk of the measles virus hemagglutinin protein decrease fusion but do not interfere with virus-specific interaction with the homologous fusion protein. *J Virol* 81:9900-10

44. Corey EA, Iorio RM. 2009. Measles virus attachment proteins with impaired ability to bind CD46 interact more efficiently with the homologous fusion protein. *Virology* 383:1-5

45. Curran J, Marq JB, Kolakofsky D. 1992. The Sendai virus nonstructural C proteins specifically inhibit viral mRNA synthesis. *Virology* 189:647-56

46. Curran J, Pelet T, Kolakofsky D. 1994. An acidic activation-like domain of the Sendai virus P protein is required for RNA synthesis and encapsidation. *Virology* 202:875-84

47. DeBuysscher BL, de Wit E, Munster VJ, Scott D, Feldmann H, Prescott J. 2013. Comparison of the pathogenicity of Nipah virus isolates from Bangladesh and Malaysia in the Syrian hamster. *PLoS neglected tropical diseases* 7:e2024

48. Drexler JF, Corman VM, Gloza-Rausch F, Seebens A, Annan A, et al. 2009. Henipavirus RNA in African bats. *PloS one* 4:e6367

49. Dutch RE, Joshi SB, Lamb RA. 1998. Membrane fusion promoted by increasing surface densities of the paramyxovirus F and HN proteins: comparison of fusion

reactions mediated by simian virus 5 F, human parainfluenza virus type 3 F, and influenza virus HA. *J Virol* 72:7745-53

50. Edwards MJ, Dimmock NJ. 2000. Two influenza A virus-specific Fabs neutralize by inhibiting virus attachment to target cells, while neutralization by their IgGs is complex and occurs simultaneously through fusion inhibition and attachment inhibition. *Virology* 278:423-35

51. Field HE, Mackenzie JS, Daszak P. 2007. Henipaviruses: emerging paramyxoviruses associated with fruit bats. *Curr Top Microbiol Immunol* 315:133-59

52. Freiberg AN, Worthy MN, Lee B, Holbrook MR. 2010. Combined chloroquine and ribavirin treatment does not prevent death in a hamster model of Nipah and Hendra virus infection. *J Gen Virol* 91:765-72

53. Fuentes S, Tran KC, Luthra P, Teng MN, He B. 2007. Function of the respiratory syncytial virus small hydrophobic protein. *J Virol* 81:8361-6

54. Gale NW, Baluk P, Pan L, Kwan M, Holash J, et al. 2001. Ephrin-B2 selectively marks arterial vessels and neovascularization sites in the adult, with expression in both endothelial and smooth-muscle cells. *Dev Biol* 230:151-60

55. Georges-Courbot MC, Contamin H, Faure C, Loth P, Baize S, et al. 2006. Poly(I)-poly(C12U) but not ribavirin prevents death in a hamster model of Nipah virus infection. *Antimicrobial agents and chemotherapy* 50:1768-72

56. Goh KJ, Tan CT, Chew NK, Tan PS, Kamarulzaman A, et al. 2000. Clinical features of Nipah virus encephalitis among pig farmers in Malaysia [see comments]. *N Engl J Med* 342:1229-35

57. Guillaume V, Contamin H, Loth P, Georges-Courbot MC, Lefeuvre A, et al. 2004. Nipah virus: vaccination and passive protection studies in a hamster model. *J Virol* 78:834-40

58. Guillaume V, Contamin H, Loth P, Grosjean I, Courbot MC, et al. 2006. Antibody Prophylaxis and Therapy against Nipah Virus Infection in Hamsters. *J Virol* 80:1972-8

59. Guillaume V, Wong KT, Looi RY, Georges-Courbot MC, Barrot L, et al. 2009. Acute Hendra virus infection: Analysis of the pathogenesis and passive antibody protection in the hamster model. *Virology* 387:459-65

60. Gurley ES, Montgomery JM, Hossain MJ, Bell M, Azad AK, et al. 2007. Person-to-person transmission of Nipah virus in a Bangladeshi community. *Emerging infectious diseases* 13:1031-7

61.   Hahn MB, Gurley ES, Epstein JH, Islam MS, Patz JA, et al. 2013. The Role of Landscape Composition and Configuration on Pteropus giganteus Roosting Ecology and Nipah Virus Spillover Risk in Bangladesh. *The American journal of tropical medicine and hygiene*

62.   Halpin K, Hyatt AD, Fogarty R, Middleton D, Bingham J, et al. 2011. Pteropid bats are confirmed as the reservoir hosts of henipaviruses: a comprehensive experimental study of virus transmission. *The American journal of tropical medicine and hygiene* 85:946-51

63.   Halpin K, Young PL, Field HE, Mackenzie JS. 2000. Isolation of Hendra virus from pteropid bats: a natural reservoir of Hendra virus. *J Gen Virol* 81:1927-32

64.   Harbury PB, Kim PS, Alber T. 1994. Crystal structure of an isoleucine-zipper trimer. *Nature* 371:80-3.

65.   Harbury PB, Zhang T, Kim PS, Alber T. 1993. A switch between two-, three-, and four-stranded coiled coils in GCN4 leucine zipper mutants. *Science* 262:1401-7.

66.   Harcourt BH, Lowe L, Tamin A, Liu X, Bankamp B, et al. 2005. Genetic characterization of Nipah virus, Bangladesh, 2004. *Emerging infectious diseases* 11:1594-7

67.   Harrison MS, Sakaguchi T, Schmitt AP. 2010. Paramyxovirus assembly and budding: Building particles that transmit infections. *Int J Biochem Cell Biol* 42:1416-29

68.   Hashiguchi T, Ose T, Kubota M, Maita N, Kamishikiryo J, et al. 2011. Structure of the measles virus hemagglutinin bound to its cellular receptor SLAM. *Nat Struct Mol Biol* 18:135-41

69.   Hayden MS, Gilliland LK, Ledbetter JA. 1997. Antibody engineering. *Curr Opin Immunol* 9:201-12.

70.   Hayman DT, Wang LF, Barr J, Baker KS, Suu-Ire R, et al. 2011. Antibodies to henipavirus or henipa-like viruses in domestic pigs in ghana, west Africa. *PloS one* 6:e25256

71.   He B, Lin GY, Durbin JE, Durbin RK, Lamb RA. 2001. The SH integral membrane protein of the paramyxovirus simian virus 5 is required to block apoptosis in MDBK cells. *J Virol* 75:4068-79

72.   Hickey A. 2009. *Defining the Antigenic Structure of the Henipavirus Attachment (G) Glycoprotein: Implications for the Fusion Mechanism*. Uniformed Services University of the Health Sciences. 188 pp.

73.   Himanen JP, Nikolov DB. 2003. Eph signaling: a structural view. *Trends Neurosci* 26:46-51

74.   Homaira N, Rahman M, Hossain MJ, Epstein JH, Sultana R, et al. 2010. Nipah virus outbreak with person-to-person transmission in a district of Bangladesh, 2007. *Epidemiol Infect* 138:1630-6

75.   Hooper P, Zaki S, Daniels P, Middleton D. 2001. Comparative pathology of the diseases caused by Hendra and Nipah viruses. *Microbes Infect* 3:315-22.

76.   Horikami SM, Smallwood S, Moyer SA. 1996. The Sendai virus V protein interacts with the NP protein to regulate viral genome RNA replication. *Virology* 222:383-90

77.   Hossain MJ, Gurley ES, Montgomery JM, Bell M, Carroll DS, et al. 2008. Clinical presentation of nipah virus infection in Bangladesh. *Clin Infect Dis* 46:977-84

78.   Hsu VP, Hossain MJ, Parashar UD, Ali MM, Ksiazek TG, et al. 2004. Nipah Virus Encephalitis Reemergence, Bangladesh. *Emerging infectious diseases* 10:2082-7

79.   Hyatt AD, Selleck PW. 1996. Ultrastructure of equine morbillivirus. *Virus Res* 43:1-15

80.   Jack PJ, Anderson DE, Bossart KN, Marsh GA, Yu M, Wang LF. 2008. Expression of novel genes encoded by the paramyxovirus J virus. *J Gen Virol* 89:1434-41

81.   Karron RA, Buonagurio DA, Georgiu AF, Whitehead SS, Adamus JE, et al. 1997. Respiratory syncytial virus (RSV) SH and G proteins are not essential for viral replication in vitro: clinical evaluation and molecular characterization of a cold-passaged, attenuated RSV subgroup B mutant. *Proc Natl Acad Sci U S A* 94:13961-6

82.   Kato A, Kiyotani K, Sakai Y, Yoshida T, Nagai Y. 1997. The paramyxovirus, Sendai virus, V protein encodes a luxury function required for viral pathogenesis. *The EMBO journal* 16:578-87

83.   Kato A, Ohnishi Y, Kohase M, Saito S, Tashiro M, Nagai Y. 2001. Y2, the smallest of the Sendai virus C proteins, is fully capable of both counteracting the antiviral action of interferons and inhibiting viral RNA synthesis. *J Virol* 75:3802-10

84.   Kelley LA, Sternberg MJ. 2009. Protein structure prediction on the Web: a case study using the Phyre server. *Nature protocols* 4:363-71

85.   Khan SU, Gurley ES, Hossain MJ, Nahar N, Sharker MA, Luby SP. 2012. A randomized controlled trial of interventions to impede date palm sap contamination by bats to prevent nipah virus transmission in Bangladesh. *PloS one* 7:e42689

86.   King AM, Viruses ICoTo, Division IUoMSV. 2012. *Virus taxonomy: classification and nomenclature of viruses: ninth report of the International Committee on Taxonomy of Viruses*. Netherlands: Elsevier/Academic Press. 1327 pp.

87.   Kingston RL, Baase WA, Gay LS. 2004. Characterization of nucleocapsid binding by the measles virus and mumps virus phosphoproteins. *J Virol* 78:8630-40

88.   Koolpe M, Burgess R, Dail M, Pasquale EB. 2005. EphB receptor-binding peptides identified by phage display enable design of an antagonist with ephrin-like affinity. *J Biol Chem* 280:17301-11

89.   Krammer F, Margine I, Tan GS, Pica N, Krause JC, Palese P. 2012. A carboxy-terminal trimerization domain stabilizes conformational epitopes on the stalk domain of soluble recombinant hemagglutinin substrates. *PloS one* 7:e43603

90.   Krammer F, Palese P. 2013. Influenza virus hemagglutinin stalk-based antibodies and vaccines. *Current opinion in virology* 3:521-30

91.   Kung N, McLaughlin A, Taylor M, Moloney B, Wright T, Field H. 2013. Hendra virus and horse owners--risk perception and management. *PloS one* 8:e80897

92.   Kurotani A, Kiyotani K, Kato A, Shioda T, Sakai Y, et al. 1998. Sendai virus C proteins are categorically nonessential gene products but silencing their expression severely impairs viral replication and pathogenesis. *Genes to cells : devoted to molecular & cellular mechanisms* 3:111-24

93.   Lackmann M, Boyd AW. 2008. Eph, a protein family coming of age: more confusion, insight, or complexity? *Sci Signal* 1:re2

94.   Lamb RA, Jardetzky TS. 2007. Structural basis of viral invasion: lessons from paramyxovirus F. *Curr Opin Struct Biol* 17:427-36

95.   Lamb RA, Mahy BW, Choppin PW. 1976. The synthesis of sendai virus polypeptides in infected cells. *Virology* 69:116-31

96.   Lamb RA, Parks GD. 2007. Paramyxoviridae: The Viruses and Their Replication. In *Fields Virology*, ed. DM Knipe, PM Howley, 1:1449-96. Philadelphia: Lippincott Williams & Wilkins. Number of 1449-96 pp.

97.   Lee B, Ataman ZA. 2011. Modes of paramyxovirus fusion: a Henipavirus perspective. *Trends in microbiology* 19:389-99

98.	Lee J, Lee HJ, Shin MK, Ryu WS. 2004. Versatile PCR-mediated insertion or deletion mutagenesis. *BioTechniques* 36:398-400

99.	Li J, Quinlan E, Mirza A, Iorio RM. 2004. Mutated form of the Newcastle disease virus hemagglutinin-neuraminidase interacts with the homologous fusion protein despite deficiencies in both receptor recognition and fusion promotion. *J Virol* 78:5299-310

100.	Li Y, Wang J, Hickey AC, Zhang Y, Wu Y, et al. 2008. Antibodies to Nipah or Nipah-like viruses in bats, China. *Emerging infectious diseases* 14:1974-6

101.	Li Z, Xu J, Patel J, Fuentes S, Lin Y, et al. 2011. Function of the small hydrophobic protein of J paramyxovirus. *J Virol* 85:32-42

102.	Lin Y, Horvath F, Aligo JA, Wilson R, He B. 2005. The role of simian virus 5 V protein on viral RNA synthesis. *Virology* 338:270-80

103.	Liu Q, Stone JA, Bradel-Tretheway B, Dabundo J, Benavides Montano JA, et al. 2013. Unraveling a three-step spatiotemporal mechanism of triggering of receptor-induced nipah virus fusion and cell entry. *PLoS pathogens* 9:e1003770

104.	Lo MK, Harcourt BH, Mungall BA, Tamin A, Peeples ME, et al. 2009. Determination of the henipavirus phosphoprotein gene mRNA editing frequencies and detection of the C, V and W proteins of Nipah virus in virus-infected cells. *J Gen Virol* 90:398-404

105.	Lou Z, Xu Y, Xiang K, Su N, Qin L, et al. 2006. Crystal structures of Nipah and Hendra virus fusion core proteins. *Febs J* 273:4538-47

106.	Luby SP. 2013. The pandemic potential of Nipah virus. *Antiviral research* 100:38-43

107.	Luby SP, Gurley ES, Hossain MJ. 2009. Transmission of human infection with Nipah virus. *Clin Infect Dis* 49:1743-8

108.	Luby SP, Hossain MJ, Gurley ES, Ahmed BN, Banu S, et al. 2009. Recurrent zoonotic transmission of Nipah virus into humans, Bangladesh, 2001-2007. *Emerging infectious diseases* 15:1229-35

109.	Luby SP, Rahman M, Hossain MJ, Blum LS, Husain MM, et al. 2006. Foodborne transmission of Nipah virus, Bangladesh. *Emerging infectious diseases* 12:1888-94

110.	Maar D, Harmon B, Chu D, Schulz B, Aguilar HC, et al. 2012. Cysteines in the stalk of the nipah virus G glycoprotein are located in a distinct subdomain critical for fusion activation. *J Virol* 86:6632-42

111. Malur AG, Hoffman MA, Banerjee AK. 2004. The human parainfluenza virus type 3 (HPIV 3) C protein inhibits viral transcription. *Virus Res* 99:199-204

112. Margine I, Krammer F, Hai R, Heaton NS, Tan GS, et al. 2013. Hemagglutinin stalk-based universal vaccine constructs protect against group 2 influenza A viruses. *J Virol* 87:10435-46

113. Marsh GA, de Jong C, Barr JA, Tachedjian M, Smith C, et al. 2012. Cedar virus: a novel Henipavirus isolated from Australian bats. *PLoS pathogens* 8:e1002836

114. Mathieu C, Pohl C, Szecsi J, Trajkovic-Bodennec S, Devergnas S, et al. 2011. Nipah virus uses leukocytes for efficient dissemination within a host. *J Virol* 85:7863-71

115. McEachern JA, Bingham J, Crameri G, Green DJ, Hancock TJ, et al. 2008. A recombinant subunit vaccine formulation protects against lethal Nipah virus challenge in cats. *Vaccine* 26:3842-52

116. McGinnes L, Sergel T, Morrison T. 1993. Mutations in the transmembrane domain of the HN protein of Newcastle disease virus affect the structure and activity of the protein. *Virology* 196:101-10.

117. McInerney TL, McLain L, Armstrong SJ, Dimmock NJ. 1997. A human IgG1 (b12) specific for the CD4 binding site of HIV-1 neutralizes by inhibiting the virus fusion entry process, but b12 Fab neutralizes by inhibiting a postfusion event. *Virology* 233:313-26

118. Melanson VR, Iorio RM. 2004. Amino acid substitutions in the F-specific domain in the stalk of the newcastle disease virus HN protein modulate fusion and interfere with its interaction with the F protein. *J Virol* 78:13053-61

119. Mendez D, Buttner P, Speare R. 2013. Response of Australian veterinarians to the announcement of a Hendra virus vaccine becoming available. *Australian veterinary journal* 91:328-31

120. Meulendyke KA, Wurth MA, McCann RO, Dutch RE. 2005. Endocytosis plays a critical role in proteolytic processing of the hendra virus fusion protein. *J Virol* 79:12643-9

121. Michalski WP, Crameri G, Wang L, Shiell BJ, Eaton B. 2000. The cleavage activation and sites of glycosylation in the fusion protein of Hendra virus. *Virus Res* 69:83-93.

122. Middleton DJ, Morrissy CJ, van der Heide BM, Russell GM, Braun MA, et al. 2007. Experimental Nipah virus infection in pteropid bats (Pteropus poliocephalus). *J Comp Pathol* 136:266-72

123. Moll M, Diederich S, Klenk HD, Czub M, Maisner A. 2004. Ubiquitous activation of the nipah virus fusion protein does not require a basic amino Acid at the cleavage site. *J Virol* 78:9705-12

124. Montgomery JM, Hossain MJ, Gurley E, Carroll GD, Croisier A, et al. 2008. Risk factors for Nipah virus encephalitis in Bangladesh. *Emerging infectious diseases* 14:1526-32

125. Mungall BA, Middleton D, Crameri G, Bingham J, Halpin K, et al. 2006. Feline model of acute nipah virus infection and protection with a soluble glycoprotein-based subunit vaccine. *J Virol* 80:12293-302

126. Murray K, Rogers R, Selvey L, Selleck P, Hyatt A, et al. 1995. A novel morbillivirus pneumonia of horses and its transmission to humans. *Emerging infectious diseases* 1:31-3

127. Murray K, Selleck P, Hooper P, Hyatt A, Gould A, et al. 1995. A morbillivirus that caused fatal disease in horses and humans. *Science* 268:94-7

128. Navaratnarajah CK, Negi S, Braun W, Cattaneo R. 2012. Membrane fusion triggering: three modules with different structure and function in the upper half of the measles virus attachment protein stalk. *J Biol Chem* 287:38543-51

129. Navaratnarajah CK, Oezguen N, Rupp L, Kay L, Leonard VH, et al. 2011. The heads of the measles virus attachment protein move to transmit the fusion-triggering signal. *Nat Struct Mol Biol* 18:128-34

130. Ndungu JM, Krumm SA, Yan D, Arrendale RF, Reddy GP, et al. 2012. Non-nucleoside inhibitors of the measles virus RNA-dependent RNA polymerase: synthesis, structure-activity relationships, and pharmacokinetics. *Journal of medicinal chemistry* 55:4220-30

131. Negrete OA, Chu D, Aguilar HC, Lee B. 2007. Single Amino Acid Changes in the Nipah and Hendra Virus Attachment Glycoproteins Distinguish EphrinB2 from EphrinB3 Usage. *J Virol* 81:10804-14

132. Negrete OA, Levroney EL, Aguilar HC, Bertolotti-Ciarlet A, Nazarian R, et al. 2005. EphrinB2 is the entry receptor for Nipah virus, an emergent deadly paramyxovirus. *Nature* 436:401-5

133. Negrete OA, Wolf MC, Aguilar HC, Enterlein S, Wang W, et al. 2006. Two key residues in ephrinB3 are critical for its use as an alternative receptor for Nipah virus. *PLoS pathogens* 2:e7

134. Nikolov DB, Li C, Barton WA, Himanen JP. 2005. Crystal structure of the ephrin-B1 ectodomain: implications for receptor recognition and signaling. *Biochemistry* 44:10947-53

135. Niwa H, Yamamura K, Miyazaki J. 1991. Efficient selection for high-expression transfectants with a novel eukaryotic vector. *Gene* 108:193-9

136. O'Shea EK, Rutkowski R, Kim PS. 1989. Evidence that the leucine zipper is a coiled coil. *Science* 243:538-42.

137. O'Sullivan JD, Allworth AM, Paterson DL, Snow TM, Boots R, et al. 1997. Fatal encephalitis due to novel paramyxovirus transmitted from horses. *Lancet* 349:93-5

138. Pager CT, Craft WW, Jr., Patch J, Dutch RE. 2006. A mature and fusogenic form of the Nipah virus fusion protein requires proteolytic processing by cathepsin L. *Virology* 346:251-7

139. Pager CT, Dutch RE. 2005. Cathepsin L is involved in proteolytic processing of the hendra virus fusion protein. *J Virol* 79:12714-20

140. Pager CT, Wurth MA, Dutch RE. 2004. Subcellular localization and calcium and pH requirements for proteolytic processing of the Hendra virus fusion protein. *J Virol* 78:9154-63

141. Pallister J, Middleton D, Crameri G, Yamada M, Klein R, et al. 2009. Chloroquine administration does not prevent Nipah virus infection and disease in ferrets. *J Virol* 83:11979-82

142. Pallister J, Middleton D, Wang LF, Klein R, Haining J, et al. 2011. A recombinant Hendra virus G glycoprotein-based subunit vaccine protects ferrets from lethal Hendra virus challenge. *Vaccine* 29:5623-30

143. Parks GD, Lamb RA. 1990. Folding and oligomerization properties of a soluble and secreted form of the paramyxovirus hemagglutinin-neuraminidase glycoprotein. *Virology* 178:498-508

144. Pasquale EB. 2008. Eph-ephrin bidirectional signaling in physiology and disease. *Cell* 133:38-52

145. Pasquale EB. 2010. Eph receptors and ephrins in cancer: bidirectional signalling and beyond. *Nat Rev Cancer* 10:165-80

146. Paterson RG, Johnson ML, Lamb RA. 1997. Paramyxovirus fusion (F) protein and hemagglutinin-neuraminidase (HN) protein interactions: intracellular retention of F and HN does not affect transport of the homotypic HN or F protein. *Virology* 237:1-9

147. Patterson JB, Thomas D, Lewicki H, Billeter MA, Oldstone MB. 2000. V and C proteins of measles virus function as virulence factors in vivo. *Virology* 267:80-9.

148.   Playford EG, McCall B, Smith G, Slinko V, Allen G, et al. 2010. Human Hendra virus encephalitis associated with equine outbreak, Australia, 2008. *Emerging infectious diseases* 16:219-23

149.   Playford G. 2009. Pathology Queensland, Herston, Queensland, Australia. Personal Communication.

150.   Plemper RK, Hammond AL, Cattaneo R. 2001. Measles virus envelope glycoproteins hetero-oligomerize in the endoplasmic reticulum. *J Biol Chem* 276:44239-46.

151.   Plemper RK, Hammond AL, Gerlier D, Fielding AK, Cattaneo R. 2002. Strength of envelope protein interaction modulates cytopathicity of measles virus. *J Virol* 76:5051-61.

152.   Popa A, Pager CT, Dutch RE. 2011. C-terminal tyrosine residues modulate the fusion activity of the Hendra virus fusion protein. *Biochemistry* 50:945-52

153.   Porotto M, Devito I, Palmer SG, Jurgens EM, Yee JL, et al. 2011. Spring-loaded model revisited: paramyxovirus fusion requires engagement of a receptor binding protein beyond initial triggering of the fusion protein. *J Virol* 85:12867-80

154.   Porotto M, Orefice G, Yokoyama CC, Mungall BA, Realubit R, et al. 2009. Simulating henipavirus multicycle replication in a screening assay leads to identification of a promising candidate for therapy. *J Virol* 83:5148-55

155.   Porotto M, Palmer SG, Palermo LM, Moscona A. 2011. Mechanism of Fusion Triggering by Human Parainfluenza Virus Type III: COMMUNICATION BETWEEN VIRAL GLYCOPROTEINS DURING ENTRY. *J Biol Chem* 287:778-93

156.   Portner A, Scroggs RA, Marx PS, Kingsbury DW. 1975. A temperature-sensitive mutant of Sendai virus with an altered hemagglutinin-neuraminidase polypeptide: consequences for virus assembly and cytopathology. *Virology* 67:179-87

157.   Pratap JV, Luisi BF, Calladine CR. 2013. Geometric principles in the assembly of alpha-helical bundles. *Philosophical transactions. Series A, Mathematical, physical, and engineering sciences* 371:20120369

158.   Prescott J, de Wit E, Feldmann H, Munster VJ. 2012. The immune response to Nipah virus infection. *Arch Virol* 157:1635-41

159.   Rader C, Barbas CF, 3rd. 1997. Phage display of combinatorial antibody libraries. *Current opinion in biotechnology* 8:503-8

160.   Ren J, Wang Q, Kolli D, Prusak DJ, Tseng CT, et al. 2012. Human metapneumovirus M2-2 protein inhibits innate cellular signaling by targeting MAVS. *J Virol* 86:13049-61

161. Rockx B, Bossart KN, Feldmann F, Geisbert JB, Hickey AC, et al. 2010. A novel model of lethal Hendra virus infection in African green monkeys and the effectiveness of ribavirin treatment. *J Virol* 84:9831-9

162. Rockx B, Winegar R, Freiberg AN. 2012. Recent progress in henipavirus research: molecular biology, genetic diversity, animal models. *Antiviral research* 95:135-49

163. Rodriguez JJ, Parisien JP, Horvath CM. 2002. Nipah Virus V Protein Evades Alpha and Gamma Interferons by Preventing STAT1 and STAT2 Activation and Nuclear Accumulation. *J Virol* 76:11476-83.

164. Roux L, Waldvogel FA. 1982. Instability of the viral M protein in BHK-21 cells persistently infected with Sendai virus. *Cell* 28:293-302

165. Sanderson CM, McQueen NL, Nayak DP. 1993. Sendai virus assembly: M protein binds to viral glycoproteins in transit through the secretory pathway. *J Virol* 67:651-63

166. Sanderson CM, Wu HH, Nayak DP. 1994. Sendai virus M protein binds independently to either the F or the HN glycoprotein in vivo. *J Virol* 68:69-76

167. Schmitt AP, He B, Lamb RA. 1999. Involvement of the cytoplasmic domain of the hemagglutinin-neuraminidase protein in assembly of the paramyxovirus simian virus 5. *J Virol* 73:8703-12

168. Schmitt AP, Leser GP, Waning DL, Lamb RA. 2002. Requirements for budding of paramyxovirus simian virus 5 virus-like particles. *J Virol* 76:3952-64.

169. Selvey LA, Wells RM, McCormack JG, Ansford AJ, Murray K, et al. 1995. Infection of humans and horses by a newly described morbillivirus [see comments]. *Med J Aust* 162:642-5

170. Sergel T, McGinnes LW, Peeples ME, Morrison TG. 1993. The attachment function of the Newcastle disease virus hemagglutinin-neuraminidase protein can be separated from fusion promotion by mutation. *Virology* 193:717-26.

171. Shaffer JA, Bellini WJ, Rota PA. 2003. The C protein of measles virus inhibits the type I interferon response. *Virology* 315:389-97

172. Shaw ML, Cardenas WB, Zamarin D, Palese P, Basler CF. 2005. Nuclear localization of the Nipah virus W protein allows for inhibition of both virus- and toll-like receptor 3-triggered signaling pathways. *J Virol* 79:6078-88

173. Shaw ML, Garcia-Sastre A, Palese P, Basler CF. 2004. Nipah virus V and W proteins have a common STAT1-binding domain yet inhibit STAT1 activation from the cytoplasmic and nuclear compartments, respectively. *J Virol* 78:5633-41

174. Sissoeff L, Mousli M, England P, Tuffereau C. 2005. Stable trimerization of recombinant rabies virus glycoprotein ectodomain is required for interaction with the p75NTR receptor. *J Gen Virol* 86:2543-52

175. Skiadopoulos MH, Vogel L, Riggs JM, Surman SR, Collins PL, Murphy BR. 2003. The genome length of human parainfluenza virus type 2 follows the rule of six, and recombinant viruses recovered from non-polyhexameric-length antigenomic cDNAs contain a biased distribution of correcting mutations. *J Virol* 77:270-9

176. Smith EC, Popa A, Chang A, Masante C, Dutch RE. 2009. Viral entry mechanisms: the increasing diversity of paramyxovirus entry. *FEBS J* 276:7217-27

177. Smith EC, Smith SE, Carter JR, Webb SR, Gibson KM, et al. 2013. Trimeric transmembrane domain interactions in paramyxovirus fusion proteins: roles in protein folding, stability and function. *J Biol Chem*

178. Smith I, Broos A, de Jong C, Zeddeman A, Smith C, et al. 2011. Identifying hendra virus diversity in pteropid bats. *PloS one* 6:e25275

179. Steffen DL, Xu K, Nikolov DB, Broder CC. 2012. Henipavirus mediated membrane fusion, virus entry and targeted therapeutics. *Viruses* 4:280-308

180. Stone-Hulslander J, Morrison TG. 1997. Detection of an interaction between the HN and F proteins in Newcastle disease virus-infected cells. *J Virol* 71:6287-95.

181. Su AI, Wiltshire T, Batalov S, Lapp H, Ching KA, et al. 2004. A gene atlas of the mouse and human protein-encoding transcriptomes. *Proc Natl Acad Sci U S A* 101:6062-7

182. Tamin A, Harcourt BH, Lo MK, Roth JA, Wolf MC, et al. 2009. Development of a neutralization assay for Nipah virus using pseudotype particles. *Journal of virological methods* 160:1-6

183. Tan CT, Goh KJ, Wong KT, Sarji SA, Chua KB, et al. 2002. Relapsed and late-onset Nipah encephalitis. *Ann Neurol* 51:703-8.

184. Tao Y, Strelkov SV, Mesyanzhinov VV, Rossmann MG. 1997. Structure of bacteriophage T4 fibritin: a segmented coiled coil and the role of the C-terminal domain. *Structure (London, England : 1993)* 5:789-98

185. Techaarpornkul S, Barretto N, Peeples ME. 2001. Functional analysis of recombinant respiratory syncytial virus deletion mutants lacking the small hydrophobic and/or attachment glycoprotein gene. *J Virol* 75:6825-34.

186. Tong S, Compans RW. 1999. Alternative mechanisms of interaction between homotypic and heterotypic parainfluenza virus HN and F proteins. *J Gen Virol* 80:107-15.

187. Toth J, Cutforth T, Gelinas AD, Bethoney KA, Bard J, Harrison CJ. 2001. Crystal structure of an ephrin ectodomain. *Dev Cell* 1:83-92

188. Vanhoof G, Goossens F, De Meester I, Hendriks D, Scharpe S. 1995. Proline motifs in peptides and their biological processing. *FASEB journal : official publication of the Federation of American Societies for Experimental Biology* 9:736-44

189. Virtue ER, Marsh GA, Baker ML, Wang LF. 2011. Interferon production and signaling pathways are antagonized during henipavirus infection of fruit bat cell lines. *PloS one* 6:e22488

190. Virtue ER, Marsh GA, Wang LF. 2011. Interferon signaling remains functional during henipavirus infection of human cell lines. *J Virol*

191. Vogt C, Eickmann M, Diederich S, Moll M, Maisner A. 2005. Endocytosis of the Nipah virus glycoproteins. *J Virol* 79:3865-72

192. Wang LF, Michalski WP, Yu M, Pritchard LI, Crameri G, et al. 1998. A novel P/V/C gene in a new member of the Paramyxoviridae family, which causes lethal infection in humans, horses, and other animals. *J Virol* 72:1482-90

193. Wang LF, Yu M, Hansson E, Pritchard LI, Shiell B, et al. 2000. The exceptionally large genome of Hendra virus: support for creation of a new genus within the family Paramyxoviridae. *J Virol* 74:9972-9.

194. Weise C, Erbar S, Lamp B, Vogt C, Diederich S, Maisner A. 2010. Tyrosine residues in the cytoplasmic domains affect sorting and fusion activity of the Nipah virus glycoproteins in polarized epithelial cells. *J Virol* 84:7634-41

195. Welch BD, Yuan P, Bose S, Kors CA, Lamb RA, Jardetzky TS. 2013. Structure of the parainfluenza virus 5 (PIV5) hemagglutinin-neuraminidase (HN) ectodomain. *PLoS pathogens* 9:e1003534

196. White LK, Yoon JJ, Lee JK, Sun A, Du Y, et al. 2007. Nonnucleoside inhibitor of measles virus RNA-dependent RNA polymerase complex activity. *Antimicrobial agents and chemotherapy* 51:2293-303

197. Whitman SD, Dutch RE. 2007. Surface density of the Hendra G protein modulates Hendra F protein-promoted membrane fusion: role for Hendra G protein trafficking and degradation. *Virology* 363:419-29

198.	Whitman SD, Smith EC, Dutch RE. 2009. Differential rates of protein folding and cellular trafficking for the Hendra virus F and G proteins: implications for F-G complex formation. *J Virol* 83:8998-9001

199.	Williamson MM, Hooper PT, Selleck PW, Gleeson LJ, Daniels PW, et al. 1998. Transmission studies of Hendra virus (equine morbillivirus) in fruit bats, horses and cats. *Australian veterinary journal* 76:813-8

200.	Wong KT. 2010. Emerging epidemic viral encephalitides with a special focus on henipaviruses. *Acta Neuropathol* 120:317-25

201.	Wong KT, Shieh WJ, Kumar S, Norain K, Abdullah W, et al. 2002. Nipah virus infection: pathology and pathogenesis of an emerging paramyxoviral zoonosis. *Am J Pathol* 161:2153-67.

202.	Wong KT, Shieh WJ, Zaki SR, Tan CT. 2002. Nipah virus infection, an emerging paramyxoviral zoonosis. *Springer Semin Immunopathol* 24:215-28

203.	Wong SC, Ooi MH, Wong MN, Tio PH, Solomon T, Cardosa MJ. 2001. Late presentation of Nipah virus encephalitis and kinetics of the humoral immune response. *J Neurol Neurosurg Psychiatry* 71:552-4.

204.	Xu K, Broder CC, Nikolov DB. 2011. Ephrin-B2 and ephrin-B3 as functional henipavirus receptors. *Semin Cell Dev Biol*

205.	Xu K, Chan YP, Rajashankar KR, Khetawat D, Yan L, et al. 2012. New insights into the Hendra virus attachment and entry process from structures of the virus G glycoprotein and its complex with Ephrin-B2. *PloS one* 7:e48742

206.	Xu K, Rajashankar KR, Chan YP, Himanen JP, Broder CC, Nikolov DB. 2008. Host cell recognition by the henipaviruses: crystal structures of the Nipah G attachment glycoprotein and its complex with ephrin-B3. *Proc Natl Acad Sci U S A* 105:9953-8

207.	Xu K, Rockx B, Xie Y, Debuysscher BL, Fusco DL, et al. 2013. Crystal structure of the hendra virus attachment g glycoprotein bound to a potent cross-reactive neutralizing human monoclonal antibody. *PLoS pathogens* 9:e1003684

208.	Yang X, Farzan M, Wyatt R, Sodroski J. 2000. Characterization of stable, soluble trimers containing complete ectodomains of human immunodeficiency virus type 1 envelope glycoproteins. *J Virol* 74:5716-25

209.	Yang X, Lee J, Mahony EM, Kwong PD, Wyatt R, Sodroski J. 2002. Highly Stable Trimers Formed by Human Immunodeficiency Virus Type 1 Envelope Glycoproteins Fused with the Trimeric Motif of T4 Bacteriophage Fibritin. *J Virol* 76:4634-42.

210. Yin HS, Paterson RG, Wen X, Lamb RA, Jardetzky TS. 2005. Structure of the uncleaved ectodomain of the paramyxovirus (hPIV3) fusion protein. *Proc Natl Acad Sci U S A* 102:9288-93

211. Yin HS, Wen X, Paterson RG, Lamb RA, Jardetzky TS. 2006. Structure of the parainfluenza virus 5 F protein in its metastable, prefusion conformation. *Nature* 439:38-44

212. Yob JM, Field H, Rashdi AM, Morrissy C, van der Heide B, et al. 2001. Nipah virus infection in bats (order Chiroptera) in peninsular Malaysia. *Emerging infectious diseases* 7:439-41.

213. Yoneda M, Guillaume V, Sato H, Fujita K, Georges-Courbot MC, et al. 2010. The nonstructural proteins of Nipah virus play a key role in pathogenicity in experimentally infected animals. *PloS one* 5:e12709

214. Young PL, Halpin K, Selleck PW, Field H, Gravel JL, et al. 1996. Serologic evidence for the presence in Pteropus bats of a paramyxovirus related to equine morbillivirus. *Emerging infectious diseases* 2:239-40

215. Yuan P, Swanson KA, Leser GP, Paterson RG, Lamb RA, Jardetzky TS. 2011. Structure of the Newcastle disease virus hemagglutinin-neuraminidase (HN) ectodomain reveals a four-helix bundle stalk. *Proc Natl Acad Sci U S A* 108:14920-5

216. Yuan P, Thompson TB, Wurzburg BA, Paterson RG, Lamb RA, Jardetzky TS. 2005. Structural studies of the parainfluenza virus 5 hemagglutinin-neuraminidase tetramer in complex with its receptor, sialyllactose. *Structure (Camb)* 13:803-15

217. Zhou P, Cowled C, Todd S, Crameri G, Virtue ER, et al. 2011. Type III IFNs in Pteropid Bats: Differential Expression Patterns Provide Evidence for Distinct Roles in Antiviral Immunity. *J Immunol* 186:3138-47

218. Zhu Z, Bossart KN, Bishop KA, Crameri G, Dimitrov AS, et al. 2008. Exceptionally potent cross-reactive neutralization of Nipah and Hendra viruses by a human monoclonal antibody. *J Infect Dis* 197:846-53

219. Zhu Z, Dimitrov AS, Bossart KN, Crameri G, Bishop KA, et al. 2006. Potent neutralization of Hendra and Nipah viruses by human monoclonal antibodies. *J Virol* 80:891-9